

## Journal of Polymer Science

## Part A-1: Polymer Chemistry

## Contents

WALLACE M. PASIKA and SHU-PIN CHEN: Cationic Polymerization of $\alpha$ -Methylstyrene Oxide.....	577
KOZO TSUJI, KOICHIRO HAYASHI, and SEIZO OKAMURA: Electron Spin Resonance Study of Poly-3,3-bis(chloromethyl)oxetane Irradiated with Electron Beams and Ultraviolet Light.....	583
N. A. GAC, G. N. SPOKES, and S. W. BENSON: Thermal Degradation of Nadic Methyl Anhydride-Cured Epoxy Novolac.....	593
R. R. DILEONE: Synthesis of Poly-2-oxazolidones from Diisocyanates and Diepoxides.....	609
TAKAKO TAKAHASHI: Polymerization of Vinylcyclopropanes. IV. Radical Copolymerization of 1,1-Dichloro-2-vinylcyclopropane with Maleic Anhydride..	617
ELIZABETH DYER and RICHARD A. DUNBAR: Phosphorus-Containing Polyurethans.....	629
YOSHITAKA OGIWARA and MASAHIRO UCHIYAMA: Graft Copolymerization of Methyl Methacrylate to Poly(vinyl Alcohol) initiated by Ferric Ion-Hydrogen Peroxide System.....	641
YOSHIMASA HAMA and KENICHI SHINOHARA: Electron Spin Resonance Studies of Polycarbonate Irradiated by $\gamma$ -Rays and Ultraviolet Light.....	651
TOYOKI KUNITAKE and CHUJI ASO: A Proposal on the Steric Course of Propagation in the Homogeneous Cationic Polymerization of Vinyl and Related Monomers.....	665
S. G. HOVENKAMP and J. P. MUNTING: Formation of Diethylene Glycol as a Side Reaction during Production of Polyethylene Terephthalate.....	679
S. TERNEY, J. KEATING, J. ZIELINSKI, J. HAKALA, and H. SHEFFER: Polyamide-Imides.....	683
ECKEHARD SCHAMBERG and JÜRIG HOIGNÉ: Radical and Radiation-Induced Grafting of Some Synthetic High Polymers within the Temperature Range of Their Glass Transition.....	693
JOHN A. HOWELL, MASATSUGU IZU, and KENNETH F. O'DRISCOLL: Copolymerization with Depropagation. III. Composition and Sequence Distribution from Probability Considerations.....	699
H. H. G. JELLINEK and F. FLAJSMAN: Chain Scission of Butyl Rubber by Nitrogen Dioxide in Absence and Presence of Air.....	711
HEIKKI PIETILA, ARTO SIVOLA, and HOWARD SHEFFER: Cationic Polymerization of $\beta$ -Pinene, Styrene and $\alpha$ -Methylstyrene.....	727
TAKAKO TAKAHASHI: Polymerization of Vinylcyclopropanes. V. Radical Copolymerization of 1,1-Dichloro-2-vinylcyclopropane with Monosubstituted Ethylenes.....	739

(continued inside)

# Journal of Polymer Science      Part A-1: Polymer Chemistry

**Board of Editors:** H. Mark • C. G. Overberger • T. G. Fox

**Advisory Editors:**

R. M. Fuoss • J. J. Hermans • H. W. Melville • G. Smets

**Editor:** C. G. Overberger

**Associate Editor:** E. M. Pearce

**Advisory Board:**

T. Alfrey, Jr.	E. M. Fettes	C. S. Marvel	W. H. Sharkey
W. J. Bailey	N. D. Field	F. R. Mayo	W. R. Sorenson
D. S. Ballantine	F. C. Foster	R. B. Mesrobian	V. T. Stannett
M. B. Birenbaum	H. N. Friedlander	H. Morawetz	J. K. Stille
F. A. Bovey	K. C. Frisch	M. Morton	M. Szwarc
J. W. Breitenbach	N. G. Gaylord	S. Murahashi	A. V. Tobolsky
W. J. Burlant	W. E. Gibbs	G. Natta	E. J. Vandenberg
G. B. Butler	A. R. Gilbert	K. F. O'Driscoll	L. A. Wall
S. Bywater	J. E. Guillet	S. Okamura	F. X. Werber
T. W. Campbell	H. C. Haas	P. Pino	O. Wichterle
W. L. Carrick	J. P. Kennedy	C. C. Price	F. H. Winslow
H. W. Coover, Jr.	W. Kern	B. Rånby	M. Wismer
F. Danusso	J. Lal	J. H. Saunders	E. A. Youngman
F. R. Eirich	R. W. Lenz	C. Schuerch	

*Contents (continued), Vol. 8*

AKIRA MATSUMOTO and MASAYOSHI OIWA: Studies of the Polymerization of Diallyl Compounds. VII. Kinetics of the Polymerization of Diallyl Esters of Aliphatic Dicarboxylic Acids.....	751
N. Z. ÉRDY, C. F. FERRARO, and A. V. TOBOLSKY: Preparation of Block Copolymers by Use of Peroxide-Terminated Prepolymer.....	763

**NOTES**

STEPHEN D. BRUCK and PETER F. LIAO: Sorption Behavior of Organic Pyro-polymers in Aqueous Solutions.....	771
O. F. SOLOMON, M. DIMONIE, and C. CIUCIU: Cationic Graft Copolymerization of <i>N</i> -Vinylcarbazole onto (Poly(vinyl Chloride)).....	777
DONALD A. SMITH, ROBERT H. CUNNINGHAM, and BARBARA COULTER: Anomalous Behavior of a Polymeric Amino Ester.....	783

*(continued on inside back cover)*

The Journal of Polymer Science is published in four sections as follows: Part A-1, Polymer Chemistry, monthly; Part A-2, Polymer Physics, monthly; Part B, Polymer Letters, monthly; Part C, Polymer Symposia, irregular.

Published monthly by Interscience Publishers, a Division of John Wiley & Sons, Inc., covering one volume annually. Publication Office at 20th and Northampton Sts., Easton, Pa. 18042. Executive, Editorial, and Circulation Offices at 605 Third Avenue, New York, N. Y. 10016. Second-class postage paid at Easton, Pa. Subscription price, \$325.00 per volume (including Parts A-2, B, and C). Foreign postage \$15.00 per volume (including Parts A-2, B, and C).

Copyright © 1970 by John Wiley & Sons, Inc. All rights reserved. No part of this publication may be reproduced by any means, nor transmitted, nor translated into a machine language without the written permission of the publisher.

## Cationic Polymerization of $\alpha$ -Methylstyrene Oxide

WALLACE M. PASIKA and SHU-PIN CHEN,  
*Polymer Research Center, Chemistry Department,  
Texas A&M University, College Station, Texas 77843*

### Synopsis

The polymerization of  $\alpha$ -Methyl Styrene Oxide initiated by trityl hexachloroantimonate is reported upon. Data is presented on side reactions, percent yield and molecular weight of polymer produced in the polymerization.

It was reported<sup>1</sup> that the low yields and low molecular weight of polymer derived from the reaction of styrene oxide with trityl hexachloroantimonate (THCA) results from the ease with which the  $\alpha$ -hydrogens of styrene oxide are removed as hydride ions and because of side (nonpolymerization) reactions into which the  $\alpha$ -styrene oxide carbonium ion can enter subsequently. If a polymerization mechanism not dependent on the species resulting from the initial  $\alpha$ -abstraction by the THCA were operative, then the hypothesis could be checked by studying the polymerization characteristics of an aromatic oxirane substituted to avoid  $\alpha$  hydrogens. Such an oxirane should give high yields of high molecular weight polymer. Here we report on some polymerization characteristics of  $\alpha$ -methylstyrene oxide with the use of THCA as initiator.

### RESULTS

The yields of polymer as a function of trityl initiator at ice temperature (4°C) and 50°C for bulk and solution polymerizations after 48 hr are shown in Figure 1. The dependence on time of the percentage yield of polymer at two fixed initiator concentrations are shown in Figure 2.

Infrared spectra were obtained on the polymerization mixtures just prior to precipitation of the polymer in methanol. A typical infrared spectrum is represented in Figure 3. Each spectrum reveals that in the polymerizing mixture there exists a substantial concentration of carbonyl function (1720  $\text{cm}^{-1}$ ) and a species with a hydroxyl function (3500  $\text{cm}^{-1}$ ). Infrared spectra on  $\alpha$ -MSO polymerization blanks showed no hydroxyl or carbonyl peaks, indicating that the trityl initiator is responsible for the production of species containing the aldehydic and hydroxylic functions. The infrared spectrum of poly( $\alpha$ -MSO) is shown in Figure 4, from which it is evident that the formed polymer could not be responsible for these ab-

sorptions. A relatively high concentration of some other small molecule species absorbing in the above regions must be present. The molecular weights of the polymers were in the range 500–1000. Another peak of consequence in the polymerization mixtures appears at  $1630\text{ cm}^{-1}$ . This adsorption is characteristic of the double bond stretching vibration.

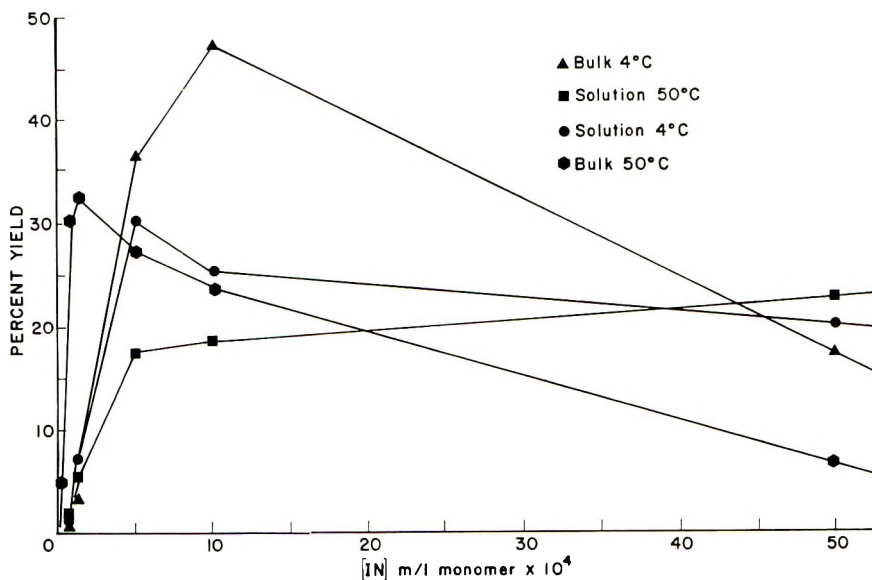


Fig. 1. Yield of methanol-insoluble poly( $\alpha$ -methylstyrene oxide) as a function of trityl initiator concentration. Polymerization period 48 hrs.

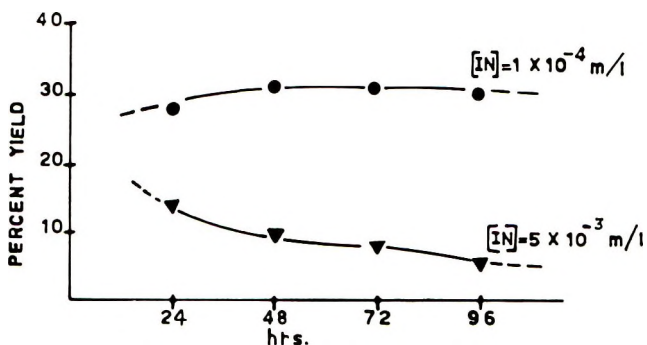


Fig. 2. Percentage yields at fixed trityl initiator concentration for successive bulk polymerization periods of 24 hr.

The infrared spectrum of the mixture resulting when HCl gas was bubbled into  $\alpha$ -methylstyrene oxide is identical to that of the polymerization mixture, except for the absence of peaks at  $1630$  and  $1230\text{ cm}^{-1}$  (ether linkage).

The 2,4-dinitrophenylhydrazone derivative of a compound found in the methanol supernatants was identified as the hydrazone of 2-phenylpropanal.

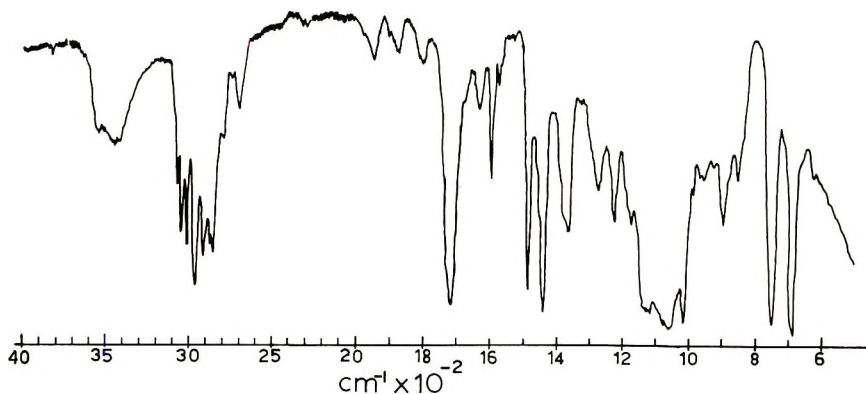


Fig. 3. Representative infrared spectrum of bulk polymerization mixture (trityl initiator  $\alpha$ -methylstyrene oxide) prior to precipitation in methanol.

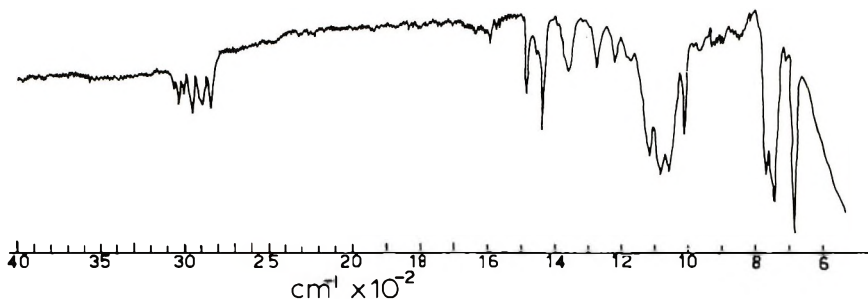


Fig. 4. Infrared spectrum of poly( $\alpha$ -methylstyrene oxide).

## DISCUSSION

From Figure 2 it is evident that the polymerization reaction is a short-lived one and that possibly equilibrium is set up rapidly.

The plots of percentage yield versus initiator concentration curves (Fig. 1) have several interesting features. In the initiator range studied, the yield is higher at the lower temperatures. The difference is considerably more pronounced in the bulk than in the solution polymerizations. In the case of the bulk polymerizations the maximum is at a lower initiator concentration for the higher temperature polymerization series.

The higher yields for the low temperature bulk polymerization and the higher initiator concentration at which the maximum occurs could arise because of decreased transfer and/or decreased isomerization of the carbonium ions to species that do not enter into polymerization reactions.<sup>2</sup>

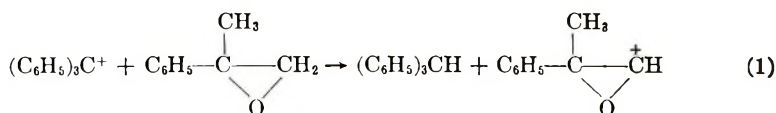
It is expected that in our temperature range the isomerization reaction would be less affected than would the transfer mechanism. This is partially borne out when the results of the solution polymerization series are compared. It would be expected that a diluent would tend to equalize transfer. Therefore any difference between yield-initiator curves would be due to isomerization phenomena. By and large, the curves are near identical. (It may also be that the relatively high dielectric solvent methylene dichloride stabilizes the carbonium ions to roughly the same degree at both these temperatures.) In respect of the bulk polymerizations it is expected that a transfer mechanism would be more dominant at the higher temperatures than at the lower temperatures at any initiator concentration. This would lower the molecular weight of the polymer, giving in the  $\alpha$ -MSO system more methanol-soluble oligomer and the lower yields that are observed.

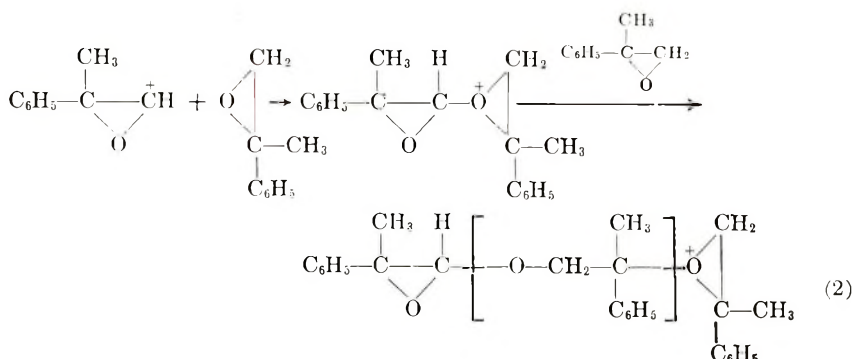
The yields in the bulk polymerizations appear to be dependent on the initiator concentrations in a very complex manner as evidenced by the occurrence of maxima. It is doubtful whether the larger ratio of initiator molecules to monomer molecules at the higher initiator concentrations is the sole reason for the decreasing yields of polymer. The results could be accounted for if disproportionately larger numbers of monomer carbonium ions are formed initially at each succeeding higher initiator concentration and these monomer carbonium ions isomerize and/or transfer the positive center to new monomer molecules, etc. thus robbing the particular system of monomer molecules and preventing the particular system from producing the higher molecular weight polymeric species that are insoluble in methanol. Supporting evidence for part of this argument is found in the fact that the maximum for the 50°C polymerization series is at a lower initiator concentration than that of the 0°C series. A transfer mechanism would become more important at lower initiator concentrations at the higher temperature than at the lower.

Because it is fairly well established<sup>3,4</sup> that trityl hexachloroantimonate abstracts hydride ions in its interactions with cyclic ether and since  $\alpha$ -MSO has no abstractable  $\alpha$  hydrogens, it is not unreasonable to suggest that the  $\beta$  hydrogens of the  $\alpha$ -MSO molecule are abstracted.

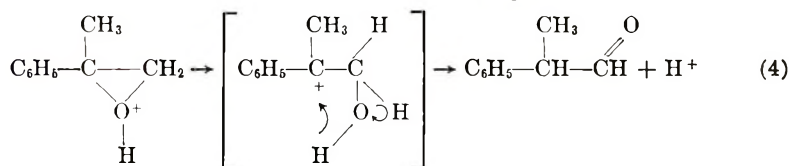
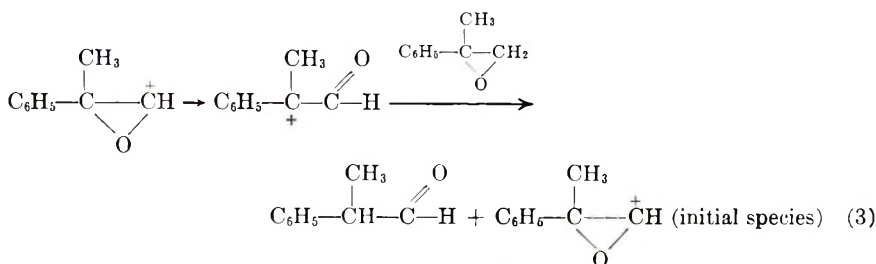
This is an interesting point, since this can only come about if the electronic effects of the phenyl function are strongly transmitted over three bond lengths.

The products of the "side reactions" must be produced via some cyclic mechanism(s) in order that as high a concentration of species be generated as was detected in the infrared spectra. The following mechanism are proposed to explain the observed results. For the polymer formation we have eqs. (1) and (2):

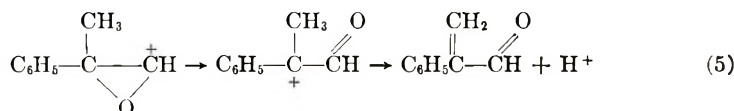




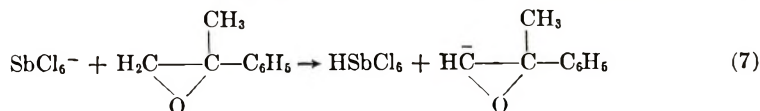
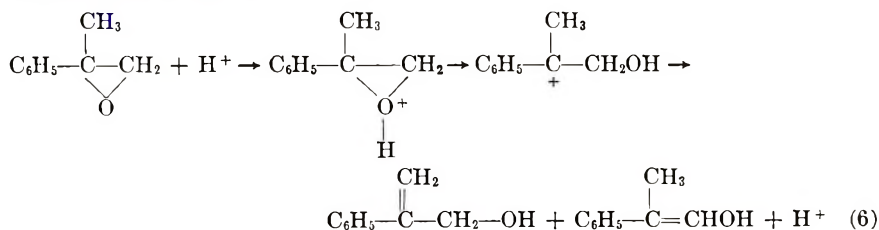
Aldehyde formation may take the path shown in eqs. (3) and (4).



Vinyl (and aldehyde) formation may be described by eq. (5):



Alcohol formation may proceed by eq. (6) or by the alternative mechanism shown in eqs. (7) and (8).



The support extended by The Robert A. Welch Foundation in the form of a research fellowship to S. P. C. and a grant in aid to W. M. P. is gratefully acknowledged.

### References

1. W. M. Pasika, *J. Polym. Sci. A*, **3**, 4287 (1965).
2. J. Heiligmann, *J. Polym. Sci.*, **4**, 183 (1949).
3. M. P. Dreyfuss, J. C. Westfahl, and P. Dreyfuss, *Macromolecules*, **1**, 437 (1968).
4. W. M. Pasika and J. W. Wynn, *J. Polym. Sci., A-1*, **7**, 1489 (1969).

Received April 30, 1969

Revised July 14, 1969



## Electron Spin Resonance Study of Poly-3,3-bis(chloromethyl)oxetane Irradiated with Electron Beams and Ultraviolet Light

KOZO TSUJI,\* KOICHIRO HAYASHI,† and SEIZO OKAMURA,  
*Department of Polymer Chemistry, Faculty of Engineering,  
 Kyoto University, Kyoto, Japan*

### Synopsis

Poly-3,3-bis(chloromethyl)oxetane (poly-BCMO) was irradiated at  $-196^{\circ}\text{C}$  with electron beams and ultraviolet light, and observed ESR spectra were compared. A three-line spectrum (coupling constant of about 21 gauss) and a two-line spectrum (coupling constant of about 18 gauss) were observed after irradiation with electron

beams *in vacuo*. They were attributed to free radicals  $\begin{array}{c} | \\ -\text{C}-\dot{\text{C}}\text{H}_2 \\ | \end{array}$  and  $\begin{array}{c} | \\ -\text{C}-\dot{\text{C}}\text{H}-\text{O}- \\ | \end{array}$ ,

respectively. On the other hand, a three-line spectrum (coupling constant of about 20 gauss) and an asymmetric singlet spectrum were observed after ultraviolet irradiation in

vacuum. They were assigned to free radicals  $\begin{array}{c} | \\ -\text{C}-\dot{\text{C}}\text{H}_2 \\ | \end{array}$  and  $-\text{CH}_2-\text{O}\cdot$ , respectively.

Mechanisms of radical formation were discussed in each case. When poly-BCMO was irradiated with electron beams at  $-196^{\circ}\text{C}$  in the presence of air, peroxy radicals were produced after subsequent treatment at  $-78^{\circ}\text{C}$ . The reaction between alkyl radicals and oxygen molecules was found to be diffusion-controlled.

### INTRODUCTION

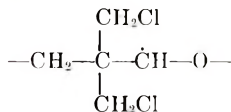
Numerous studies<sup>1-19</sup> have reported electron spin resonance (ESR) spectra of polymers irradiated with ionizing radiation, while several studies<sup>20-24</sup> have been made of ESR spectra of ultraviolet-irradiated polymers. Spectra observed with the two different irradiation methods were not always identical. It is reported,<sup>20-22</sup> for instance, that methyl radicals were observed after ultraviolet irradiation of polypropylene at  $-196^{\circ}\text{C}$ , but not after  $\gamma$ -irradiation. Therefore it seems interesting to compare ESR spectra observed after irradiation of polymers with ionizing radiation and ultraviolet light from the viewpoint of mechanisms of radical formation.

\* Present address: Central Research Laboratory, Sumitomo Chemical Co., Ltd., Takastuki, Osaka, Japan.

† Present address: Faculty of Engineering, Hokkaido University, Sapporo, Japan.

In the case of polyethers, ESR spectra of the polymers irradiated with ionizing radiation have been reported,<sup>15-19,25</sup> but spectra observed after ultraviolet irradiation have not.

In a previous paper<sup>25</sup> we reported that three-line and two-line spectra were observed after irradiation of poly-3,3-bis(chloromethyl)oxetane (poly-BCMO) with electron beams. On analyzing anisotropy of hyperfine structures of the two-line spectrum, it was deduced that the free radical



was responsible for the two-line spectrum.

In the present investigation, ESR spectra of free radicals produced in poly-BCMO irradiated with electron beams and ultraviolet light are compared; the effect of oxygen on the free radicals is also examined.

## EXPERIMENTAL

Poly-BCMO samples were obtained by irradiating BCMO monomer at 0°C with  $\gamma$ -rays from a Co<sup>60</sup> source and by extracting the monomer with methanol from the polymerized BCMO samples. The polymer samples were sealed off after evacuating about to  $10^{-4}$  mm Hg, and were irradiated with electron beams from a Van de Graaff accelerator ( $1.5 \times 10^5$  rad/sec) or ultraviolet light from a high-pressure mercury lamp (Toshiba Electric Co. Ltd.). Some samples were irradiated in the presence of air.

ESR measurements were carried out with an X-band spectrometer with a 100 Kc field modulation mainly at  $-196^\circ\text{C}$ . Measurements at higher temperature were made by the use of variable temperature accessories. In order to evaluate the  $G$  value for radical formation at  $-196^\circ\text{C}$ , the concentrations of the free radicals produced in samples were determined by comparing ESR signal intensity of the sample with that of  $\alpha, \alpha'$ -diphenylpicrylhydrazyl dispersed at known concentration, in poly(methyl methacrylate) film.

## RESULTS

### ESR Spectra of Poly-BCMO Irradiated with Electron Beams

As described in the previous paper,<sup>25</sup> the ESR spectrum at  $-196^\circ\text{C}$  of poly-BCMO irradiated to a dose of  $10^6$  rad consisted of three- and two-line components. The splitting of the former was about 21 gauss. The change in the spectrum shape with increasing temperature is shown in Figure 1. The three-line spectrum observed at  $-196^\circ\text{C}$  gradually decayed out and only the two-line spectrum remained at  $-3^\circ\text{C}$ . The splitting of the latter is about 18 gauss. Change in radical concentration during this warming-up process is shown in Figure 2. It is evident from this figure that the three-

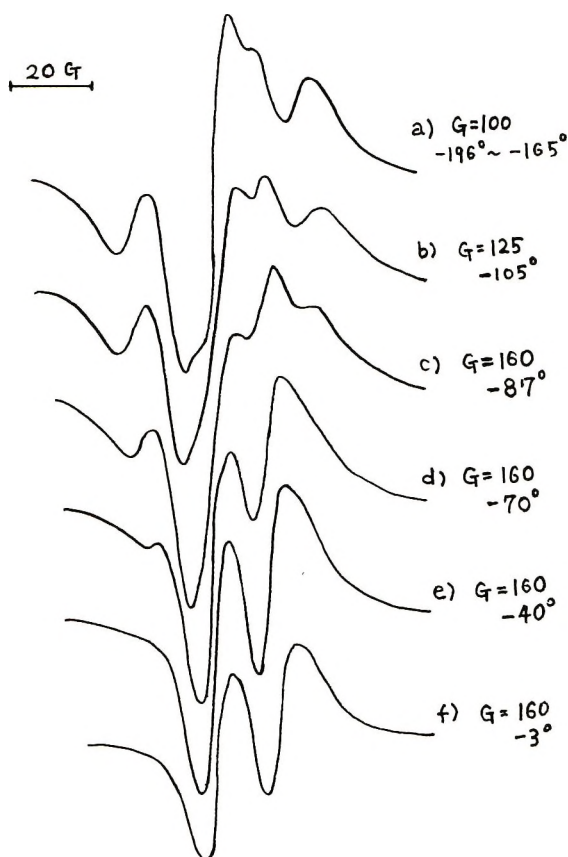


Fig. 1. Change in ESR spectrum of poly-3,3-bis(chloromethyl)-oxetane irradiated with electron beams with increasing temperature. Irradiation dose,  $10^6$  rad; irradiation temperature,  $-196^\circ\text{C}$ ;  $G$  represents an amplifier gain setting.

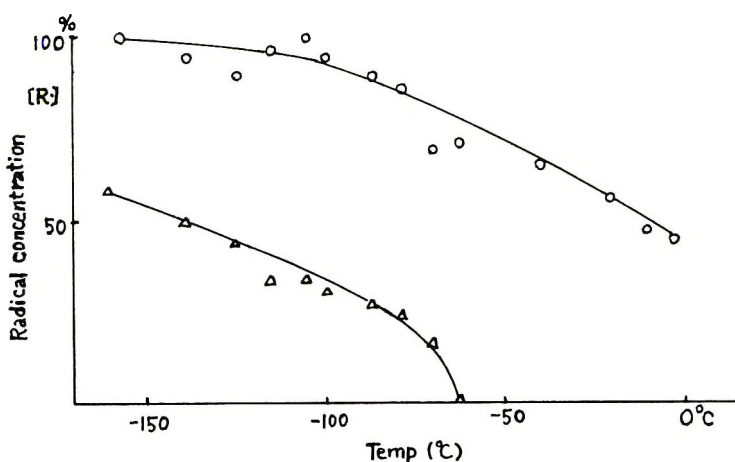


Fig. 2. Decay of radical concentrations in poly-3,3-bis(chloromethyl)oxetane irradiated with electron beams with increasing temperature: (O) total radical concentration; ( $\Delta$ ) concentration of the three-line spectrum. Irradiation dose,  $10^6$  rad.

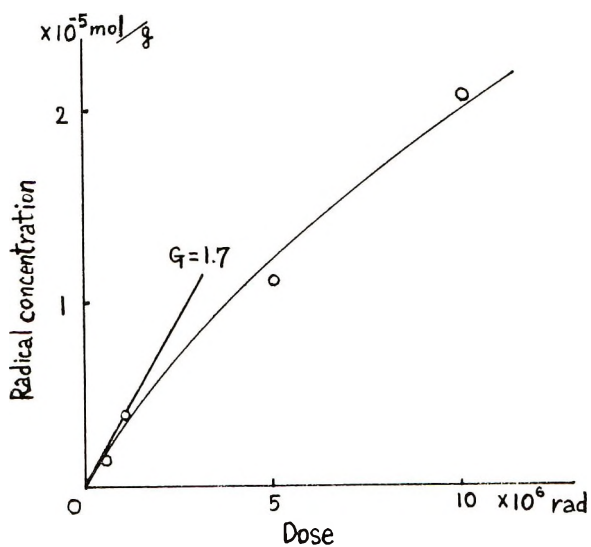


Fig. 3. Dose dependence of radical concentration in poly-3,3-bis(chloromethyl)oxetane irradiated with electron beams at  $-196^{\circ}\text{C}$ .

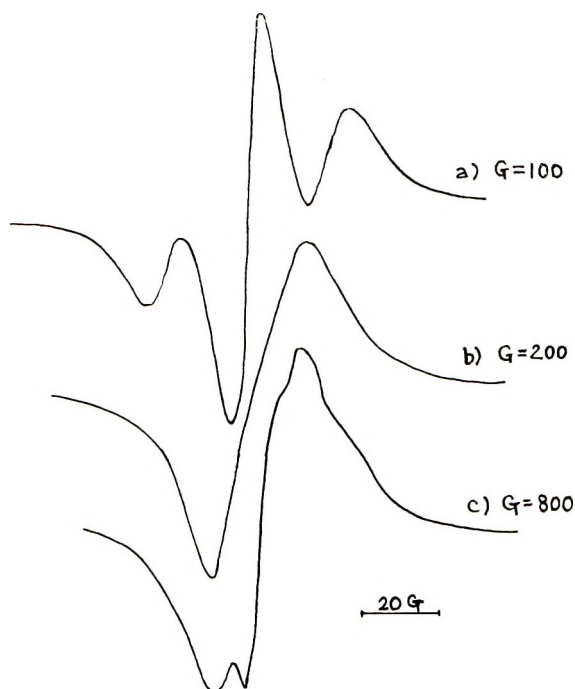


Fig. 4. Change in ESR spectrum of poly-3,3-bis(chloromethyl)oxetane irradiated with ultraviolet light by treatment at  $-78^{\circ}\text{C}$  and  $0^{\circ}\text{C}$ : (a) immediately after ultraviolet irradiation at  $-196^{\circ}\text{C}$  for 150 min; (b) after treatment at  $-78^{\circ}\text{C}$  for 132 min; (c) after subsequent treatment at  $0^{\circ}\text{C}$  for 280 min. ESR measurements were carried out at  $-196^{\circ}\text{C}$ . G represents an amplifier gain setting.

line spectrum disappeared at about  $-63^{\circ}\text{C}$  and that the two-line spectrum also gradually decayed at higher temperature. Dose dependence of total radical concentration at  $-196^{\circ}\text{C}$  is shown in Figure 3. From the initial slope of the curve, the  $G$  value for radical formation is calculated to be 1.7.

### ESR Spectra of Poly-BCMO Irradiated with Ultraviolet Light

When poly-BCMO was irradiated with ultraviolet light at  $-196^{\circ}\text{C}$  for 150 min. from a high-pressure mercury lamp at a sample-source distance of 10 cm, a triplet spectrum with a splitting of about 20 gauss was observed at the same temperature as shown in Figure 4. After subsequent treatment at  $-78^{\circ}\text{C}$  for 132 min, a slightly asymmetric singlet spectrum with  $\Delta H_{msl}$  of about 26 gauss was observed at  $-196^{\circ}\text{C}$ , whose intensity was about half as large as that of the initial spectrum (Fig. 4b). This spectrum changed into an asymmetric singlet spectrum with some shoulders after further treatment at  $0^{\circ}\text{C}$  for 280 min, and the spectrum intensity decreased to about a quarter (Fig. 4c).

### Effect of Oxygen

When poly-BCMO was irradiated at  $-196^{\circ}\text{C}$  with electron beams in the presence of air, the same ESR spectrum was observed at  $-196^{\circ}\text{C}$  as that observed for the sample irradiated *in vacuo*. An ESR spectrum of peroxy radicals, however, appeared in most samples irradiated in the presence of air after treatment at  $-78^{\circ}\text{C}$ , while only the two-line spectrum was observed with the sample irradiated in vacuum after the same treatment. Formation of the peroxy radicals was found to depend upon conversions of polymerization. When the polymer sample of high conversions ( $>80\%$ ) was used, the ESR spectrum due to the peroxy radicals was not observed, only the two-line spectrum after treatment at  $-78^{\circ}\text{C}$  (Fig. 5a). On the other hand, when the samples of low conversions ( $<10\%$ ) was used, an asymmetric spectrum characteristic of the peroxy radicals was observed, as shown in Figure 5c. The  $g$  values of the spectrum were  $g_{\perp} = 2.0019$  and  $g_{\parallel} = 2.0340$ . These values are very close to the values for the peroxy radicals reported in the literature.<sup>26,27</sup> For the intermediate conversions, both the two-line spectrum and a shoulder of the ESR spectrum due to the peroxy radicals were observed (Fig. 5b). After keeping this sample at  $0^{\circ}\text{C}$  for a few days, the shoulder disappeared and the simple two-line spectrum remained. Therefore the peroxy radical seems to be less stable than the free radical responsible for the two-line spectrum.

Similar results were obtained on introducing air at  $-78^{\circ}\text{C}$  into a sample tube irradiated with electron beams at  $-196^{\circ}\text{C}$  in vacuum.

When a crystal polymer sample obtained by polymerizing a BCMO single crystal at  $0^{\circ}\text{C}$  was used, no anisotropy of the ESR spectrum of the peroxy radicals was observed, while the two-line spectrum showed anisotropy.<sup>25</sup> The vanishing of the anisotropy in the spectrum of the peroxy radicals is expected from the facts that poly-BCMO is an unoriented polymer<sup>28</sup> and

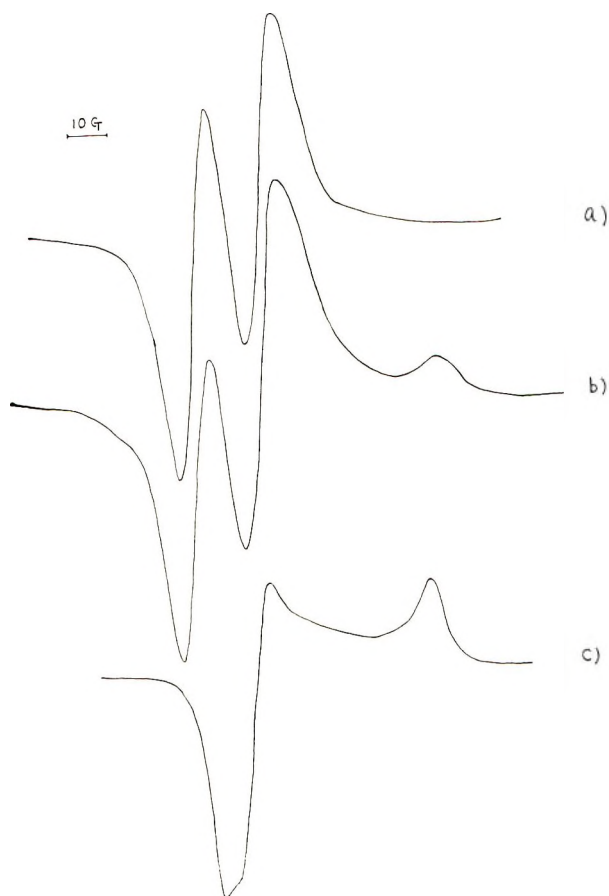
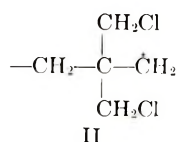
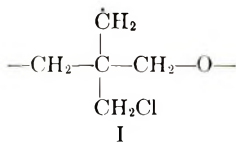


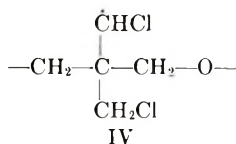
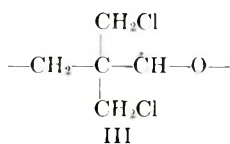
Fig. 5. ESR spectra observed after treatment at  $-78^{\circ}\text{C}$  of poly-3,3-bis(chloromethyl)oxetane irradiated with electron beams at  $-196^{\circ}\text{C}$  in the presence of air: (a) polymer conversion 86%, after treatment for 1 hr; (b) polymer conversion 52%, after treatment for 3 hr; (c) polymer conversion 4%, after treatment for 1 hr. ESR measurements were carried out at  $-196^{\circ}\text{C}$ .

that the direction of the O—O bond of the peroxy radical is almost perpendicular to the main axis of the polymer.<sup>25</sup>

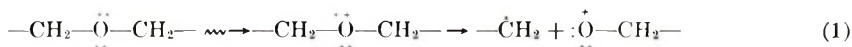
### DISCUSSION

The three-line spectrum with a splitting of about 21 gauss observed after irradiation with electron beams is likely to be caused by unpaired electrons interacting with two protons. From the molecular structure of the polymer, free radicals I and II are thought to be responsible for the three-line spectrum.





The free radical I is produced by elimination of a chlorine atom from the side chain, while the free radical II is produced by main-chain scissions. Golden et al.<sup>29</sup> reported on the basis of viscosity and solubility measurements that random main-chain scissions took place when poly-BCMO was subjected to ionizing radiation. Therefore it will be reasonable to suppose that the free radical II is responsible to some extent for the three-line spectrum. Formation of the free radical II does not seem to be through a homolytic scission of C—O bond, since singlet spectrum expected from free radicals  $-\text{CH}_2-\text{O}\cdot$  was not observed. Therefore it is thought that the free radical II was produced by the mechanism (1) according to the fact that the primary process of radiation is an ionization of unshared electrons in a non-bonding orbital of an oxygen atom.



Gaseous products of radiolysis of poly-BCMO are reported<sup>29</sup> to be mainly  $\text{H}_2$ , CO, and HCl. Therefore elimination of chlorine atoms may be another possible mechanism for formation of free radicals showing the three-line spectrum, although it is reported by Brocklehurst et al.<sup>30</sup> that benzyl chloride in rigid hydrocarbon solvents eliminated a hydrogen atom by gamma radiolysis and a chlorine atom by photolysis.

The two-line spectrum has been attributed to the free radical III by analysis of anisotropy of hyperfine structures, as described in the previous paper.<sup>25</sup> Free radical IV may also be expected to be responsible for the two-line spectrum. This possibility, however, can be excluded from the observation of the smaller coupling constant (18 gauss) which is expected when the free radical has an adjacent oxygen atom. The fact that the two-line spectrum persisted at higher temperature than the three-line spectrum will indicate that the free radicals showing the two-line spectrum are on the main chains, and the free radical III is supported.

The  $G$  value for HCl formation is reported to be about 1.3.<sup>29</sup> If it is assumed that HCl is formed by recombination of hydrogen and chlorine atoms eliminated from the polymer molecules when the free radicals I and III are produced, the minimum  $G$  value for the free radicals I + III is expected to be 2.6. However the  $G$  value for total radical formation obtained at  $-196^\circ\text{C}$  was 1.7. Therefore it may be supposed that radical reactions such as recombination and disproportionation take place to some extent, even at  $-196^\circ\text{C}$ .

The three-line spectrum observed after photolysis of poly-BCMO may be attributed to the free radicals produced by chlorine atom elimination (free radical I) or C—O bond scission (free radical II) or side chain scission

( $\cdot\text{CH}_2\text{Cl}$ ). Bond energies for C—O, C—Cl, C—C, and C—H bonds are 88, 78, 81, and 91 kcal/mole, respectively. Therefore the C—Cl bond is the weakest, and usually chlorine atom elimination takes place in the photolysis of chlorides. The possibility of scission of the C—O bond will be discussed below. It is known, on the other hand, that polypropylene and polyisobutylene show an ESR spectrum of methyl radicals after photolysis at  $-196^\circ\text{C}$ ,<sup>20-22</sup> so it seems natural to expect  $\cdot\text{CH}_2\text{Cl}$  radical formation after photolysis of poly-BCMO. However there is no direct evidence for the observation of this radical, since no narrow line spectra were observed. Moreover the stability of the three-line spectrum observed after photolysis is almost the same as that of the three-line spectrum observed after irradiation with electron beams, although the free radical  $\cdot\text{CH}_2\text{Cl}$  is expected to be less stable.

The asymmetric singlet spectrum observed after subsequent treatment at  $-78^\circ\text{C}$  or  $0^\circ\text{C}$  is thought to be due to  $-\text{CH}_2-\text{O}\cdot$  free radicals produced by main-chain scissions. If this identification is correct, the same number of free radicals of type II should be produced to give the three-line spectrum. Therefore the three-line spectrum is reasonably attributed to the free radicals I and II.

When the polymer was irradiated at  $-196^\circ\text{C}$  in the presence of air, the same spectrum was observed as that *in vacuo*, but the asymmetric spectrum characteristic of the peroxy radicals appeared after the sample was warmed up to  $-78^\circ\text{C}$ . The extent of peroxy radical formation was dependent upon polymer conversions. It should be noticed<sup>25</sup> that alkyl free radicals in irradiated BCMO monomer were not converted into peroxy radicals even in the presence of air; this may be due to close packing of monomer molecules. Poly-BCMO is a crystalline polymer,<sup>28</sup> and molecular packing will vary with polymer conversion. The lower the conversion is, the less perfect is the packing, and the more easily oxygen molecules diffuse into the polymer. Therefore the reaction between the free radicals and oxygen molecules in poly-BCMO is diffusion-controlled. For the poly-BCMO samples irradiated in the presence of air, no conversion was observed from the initial spectrum of alkyl radicals into the asymmetric spectrum due to peroxy radicals, even after prolonged standing at  $-196^\circ\text{C}$ , while peroxy radicals appeared at  $-196^\circ\text{C}$  after ultraviolet irradiation of *n*-hexane,<sup>31</sup> perhaps because of easier diffusion of oxygen molecules into *n*-hexane. It is also reported<sup>32</sup> that the reaction rate of gaseous atomic oxygen with frozen ( $-196^\circ\text{C}$ ) alkenes is determined by diffusion of oxygen atoms in the hydrocarbon layer. In the case of polyoxymethylene, peroxy radicals have been observed only in powder samples and not in pellet samples.<sup>18</sup> This was attributed also to differences in surface area and in ease of diffusion of oxygen molecules into the sample.<sup>18</sup>

That the peroxy radical is less stable than the usual alkyl radicals is apparent from the fact that the asymmetric component originally observed disappeared after storage of the sample of intermediate conversion at  $0^\circ\text{C}$  for a few days and only the two-line spectrum remained. A similar result



has been reported for polyoxymethylene.<sup>18</sup> A faster decay rate of alkyl radicals in polyoxymethylene in the presence of air than that *in vacuo* was explained by formation of peroxy radicals, although no peroxy radicals were observed.<sup>17</sup> This mechanism could be verified by direct observation of the peroxy radicals at lower temperature.<sup>18</sup>

The authors would like to express their thanks to Professor Ichiro Sakurada for his kindness to give them the opportunity to carry out the work at the Osaka Laboratories, Japanese Association for Radiation Research on Polymers which is now known as Osaka Laboratories for Radiation Chemistry, Japan Atomic Energy Research Institute.

### References

1. S. Ohnishi, S. Sugimoto, and I. Nitta, *J. Chem. Phys.*, **37**, 1283 (1962).
2. S. Ohnishi, I. Ikeda, M. Kashiwagi, and I. Nitta, *Polymer*, **2**, 119 (1961).
3. E. J. Lawton, J. S. Balwit, and R. S. Powell, *J. Chem. Phys.*, **33**, 395 (1960).
4. B. Smaller and M. S. Matheson, *J. Chem. Phys.*, **28**, 1169 (1958).
5. H. Yoshida and B. Rånby, *Acta Chem. Scand.*, **19**, 72 (1965).
6. M. Iwasaki, T. Ichikawa, and K. Toriyama, *J. Polym. Sci. B*, **5**, 423 (1967).
7. S. Ohnishi, T. Tanei, and I. Nitta, *J. Chem. Phys.*, **37**, 2402 (1962).
8. H. Fischer, *Kolloid Z.*, **180**, 64 (1962).
9. S. Ogawa, *J. Phys. Soc. Japan*, **16**, 1488 (1961).
10. D. W. Ovenall, *J. Polym. Sci.*, **41**, 199 (1959).
11. M. G. Ormerod and A. Charlesby, *Polymer*, **5**, 67 (1964).
12. M. C. R. Symons, *J. Chem. Soc.*, **1963**, 1186.
13. E. J. Lawton and J. S. Balmit, *J. Phys. Chem.*, **65**, 815 (1961).
14. M. Kashiwagi, *J. Polym. Sci. A*, **1**, 189 (1963).
15. F. C. Thryion and M. D. Baijal, *J. Polym. Sci. A-1*, **6**, 505 (1968).
16. R. Lenk, *Czech. J. Phys.*, **12**, 833 (1962).
17. M. Neiman, T. S. Fedoseeva, G. V. Chubarova, A. L. Buchachenko, and Ya. S. Lebedev, *Vysokomol. Soedin.*, **5**, 1339 (1963).
18. K. Tsuji, T. Okaya, K. Hayashi, and S. Okamura, *Ann. Rept. Japan. Assoc. Rad. Res. Polymers*, **8**, 111 (1966/1967).
19. H. Yoshida and B. Rånby, *J. Polym. Sci. A*, **3**, 2289 (1965).
20. H. L. Browning Jr., H. D. Ackermann, and H. W. Patton, *J. Polym. Sci. A-1*, **4**, 1433 (1966).
21. B. Rånby and H. Yoshida, in *Perspectives in Polymer Science (J. Polym. Sci. C, 12)*, E. S. Proskauer, E. H. Immergut, and C. G. Overberger, Eds., Interscience, New York, 1966, p. 263.
22. B. Rånby and P. Carstensen, *Advan. Chem. Ser.*, **66**, 256 (1967).
23. Y. Kato and A. Nishioka, *Repts. Progr. Polym. Phys. Japan*, **9**, 477 (1966).
24. S. R. Rafikov and Syui Tsz-pin, *Vysokomol. Soedin.*, **3**, 56 (1961).
25. K. Tsuji, T. Iwamoto, K. Hayashi, and H. Yoshida, *J. Polym. Sci. A-1*, **5**, 265 (1967).
26. H. Fischer, K. H. Hellwege, and P. Neudörfl, *J. Polym. Sci. A*, **1**, 2109 (1963).
27. D. W. Ovenall, *J. Phys. Chem. Solids*, **26**, 81 (1965).
28. K. Hayashi, M. Nishii, and S. Okamura, in *Macromolecular Chemistry, Paris 1963 (J. Polym. Sci. C, 4)*, M. Magat, Ed., Interscience, New York, 1963, p. 839.
29. J. H. Golden and E. A. Hazell, *J. Polym. Sci. A*, **2**, 4017 (1964).
30. B. Brocklehurst, G. Porter, and M. I. Savadatti, *Trans. Faraday Soc.*, **60**, 2017 (1964).
31. K. Tsuji and T. Seiki, unpublished data.
32. E. E. Kasimovskaya and A. N. Ponomarev, *Kinetika Kataliz*, **9**, 687 (1968).

Received August 4, 1969

Revised October 13, 1969

## Thermal Degradation of Nadic Methyl Anhydride-Cured Epoxy Novolac

N. A. GAC, G. N. SPOKES, and S. W. BENSON, *Department of Thermochemistry and Chemical Kinetics, Stanford Research Institute, Menlo Park, California 94025*

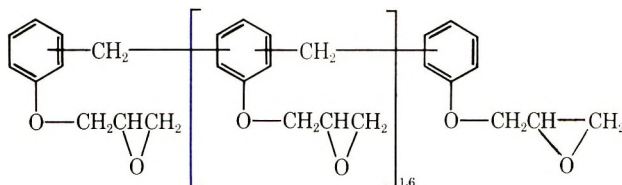
### Synopsis

A DEN438 epoxy novolac-Nadic methyl anhydride-cured polymer was pyrolyzed in vacuum at temperatures to 800°C. Detailed analyses of the products have yielded information on the mechanism of decomposition. Two thirds of the weight loss of the polymer results in formation of relatively involatile high molecular weight gases. Carbon dioxide evolution indicates that at least 50% of the initial anhydride forms diester groups. The degradation of diester sites yields methylcyclopentadiene that is almost entirely decomposed to carbonaceous char.

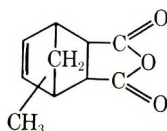
### INTRODUCTION

This study is part of a research program directed at understanding some of the basic phenomena occurring in char-forming ablative heat shields.<sup>1</sup> In an ablating heat shield, gases evolved during pyrolysis of plastics travel through the char layer to the surface of the shield. The high temperatures to which the gases are subjected as they pass to the surface may lead to further pyrolysis and even carbon deposition in the case of high molecular weight molecules.

It was known at the outset of this work that gases such as CO, H<sub>2</sub>, CO<sub>2</sub>, H<sub>2</sub>O, and perhaps methyl cyclopentadiene, were important products of pyrolysis of DEN438-NMA polymers.<sup>2</sup> However, we wanted more de-



Polyglycidyl ether of phenol-formaldehyde novolac (DEN438)



Methylbicyclo[2.2.1]hept-5-ene-2,3-dicarboxylic anhydride (NMA)

tailed information on the natures of the gases evolved during polymer degradation. We have, accordingly, studied the pyrolysis of such a polymeric material and report our conclusions on the natures of the evolved gases and their bearing on the mechanism of degradation of such polymers.

Bishop and Smith<sup>3</sup> have pointed out in a recent review that the thermal degradation mechanisms of epoxide systems are not, as yet, well understood. However, several studies have been made of NMA-cured epoxy systems. Anderson<sup>4</sup> showed that NMA-cured systems decomposed in two stages. The first stage progressed at about 230°C and the second at about 390°C. Sugita and Ito<sup>5</sup> reported that NMA-cured systems eliminated the anhydride in a fairly pure form at temperatures up to about 300°C. Above that temperature, a mixture of products was formed. Lee<sup>6</sup> studied the decomposition of an NMA-cured DEN438 polymer by thermogravimetric analysis and vacuum pyrolysis. He found a two-stage decomposition. The first stage appeared between 260 and 380°C with a 15% weight loss at 350°C. At the highest temperature, 660°C, a 23 wt-% residue remained. The vacuum pyrolysis studies of Lee yielded extensive product analyses of room temperature volatile materials. He found hydrogen, water, carbon monoxide, carbon dioxide, and methyleclopentadiene (MCPD) to be the principal volatiles. No attempt was made quantitatively to relate the amounts of these compounds to the initial polymer composition. Lee<sup>6</sup> pointed out that a tarry residue, consisting mainly of cresols and phenols, was a significant fraction. He proposed several mechanistic schemes to account for the degradation products. He suggested, as did Anderson, that CO<sub>2</sub> and MCPD would arise from diester sites or NMA decomposition. Further, all mechanisms, which included carbon monoxide as a product, showed that CO originated from ether groups.

Carbon monoxide and methane formation from epoxy groups was demonstrated in the pyrolysis of uncured diglycidyl ether of bisphenol A with tagged benzhydryl carbon.<sup>7</sup> CO and CH<sub>4</sub> were the principal products found after pyrolysis between 300 and 400°C. The solid residue contained the tagged atoms, not the gases.

Fleming<sup>8</sup> also investigated the DEN438-NMA thermal degradation. He confirmed that the first stage of decomposition (230–350°C) was elimination of NMA and suggested that NMA arises primarily from monoacid-monoester sites in the polymer. At temperatures greater than 350°C, MCPD was identified by gas chromatography to be a principal degradation product. Permanent gas analysis was not reported. A reverse Diels-Alder mechanism which yielded MCPD and a maleic diester polymer structure was proposed as the mechanism. Therefore, MCPD would only be formed by elimination from diester sites. No quantitative relationships were reported between products and initial polymer composition. Thermogravimetric results showed that at 350°C the weight loss was 15 wt-% and at 700°C about 18 wt-% residue remained in NMA-cured systems. A 24 wt-% residue was found when DEN438-maleic anhydride-cured poly-

mer was pyrolyzed under the same conditions. This result suggested that elimination of MCPD was a constructive degradation process, since the remaining maleic diester structure would enhance char formation.

Taylor<sup>9</sup> has reported a study in which the diester, monoester, and residual NMA contents of NMA-cured DEN438 polymers were determined. He found that approximately 83% of the anhydride forms diester groups, 15% forms monoester groups, and 2% remains unreacted for a formulation in which anhydride is present in an amount equal to 85% of the stoichiometric amount. For a 65% formulation, 83% of the anhydride forms diester groups and 17% forms monoester groups. Virtually all the anhydride reacted; 76% of the stoichiometric amount of anhydride was used in this study.

We have made two detailed vacuum pyrolysis investigations to assess quantitatively the degradation products of the DEN438-NMA polymer. Careful heating of the polymer at temperatures below 350°C for relatively long periods was judged the most convenient way to eliminate anhydride from monoacid-monoester sites. Therefore, at temperatures above 350°C, the amounts of MCPD and CO<sub>2</sub> would be indicative of the number of diester sites initially present.

## EXPERIMENTAL

### Apparatus

A vacuum pyrolysis apparatus was constructed which consisted of a heated quartz reaction tube (25 mm ID × 40 cm long) sealed at one end. The reaction tube was connected to a vacuum manifold (660 cc) through a trap (46 cc) surrounded by liquid nitrogen. The total volume (manifold, trap, and reaction tube) was 960 cc. The sample was introduced inside an open-ended quartz tube (20 mm OD × 6.4 cm).

A 4-in. section of the reaction tube was heated by means of a pair of Nichrome-wound clamshell heaters, which were surrounded by quartz insulation material. Temperature was regulated and changed by a Wheelco 0–800°C temperature controller fitted with a chromel–alumel thermocouple.

The pressure of the noncondensable gases was monitored with a (Pace) pressure transducer–manometer arrangement connected to the vacuum manifold. An oil manometer was used for pressures up to 40 torr (12.5 mm oil = 1 torr) and a mercury manometer at higher pressures.

Collection volumes were prepared as required by the study and attached to the vacuum manifold. Permanent gases (CO, CH<sub>4</sub>, and H<sub>2</sub>) were collected over 90–200 mesh silica gel, previously outgassed for several hours at 100 and 200°C.

The entire system was evacuated to  $5 \times 10^{-5}$  torr at room temperature before starting the experiment.

### Procedure

A disk of polymer was prepared with the use of DEN438 (Dow Chemical), NMA (Allied Chemical), and DB VIII (a tertiary amine catalyst, Argus Chemical) 20:17:1 parts by weight, respectively. The quantity of anhydride corresponds to 76 mole-% of the stoichiometric amount for 1:1 anhydride-to-epoxide group reaction. The cure cycle was 4 hr at 50°C, 4 hr at 150°C, and a post-cure of 12 hr at 205°C. The polymer samples in both studies I and II were taken from the same original disk.

The purities of starting materials were estimated to be about 98%. The infrared spectra of the epoxy novolac and anhydride exhibit weak OH stretching frequencies at 3640 and 3492  $\text{cm}^{-1}$ , respectively, indicating slight hydrolysis. (These spectra are presented below.) Spectra were recorded with a Perkin-Elmer Model 221 spectrometer as thin films on sodium chloride salt plates.

The sample sizes for pyrolyses I and II were 663 and 373 mg, respectively. The total mass was in each case distributed in three small pieces, having a maximum sample thickness of 2 mm. To insure that the particle size did not affect char formation, a thin film (33.8 mg, 10  $\mu$  thickness) of identical composition was pyrolyzed to 800°C. A 23.5 wt-% residue was found.

### Pyrolysis I

In pyrolysis study I, the reaction tube was heated for approximately  $\frac{1}{2}$ -hr time periods, totalling 3 hr, between 250 and 760°C, with temperature steps of 100°C. The period at each temperature was fixed by termination of pressure increase and by visual observation. The heating rate during temperature changes was about 50°C/min. Liquid nitrogen surrounded the product trap during pyrolysis.

The sample was now a charred residue and showed a 77% weight loss. It was further pyrolyzed at 800°C for 2 hr and additional products were eliminated. The total weight loss was 78%.

Products were fractionated into samples: A, permanent gases; B, distillate of Dry Ice temperature; C, room-temperature distillate. *PVT* measurements were made of the expanded samples. A viscous residue which had condensed outside the heated zone was dissolved in 10 ml of benzene. A 2.5 ml aliquot was evaporated to dryness. This high-boiling residue, designated sample D, was weighed. Sample E was the noncondensable fraction from the char pyrolysis at 800°C and sample F was a small amount of condensable material collected in the product trap.

### Pyrolysis II

The procedure outlined above was slightly modified in the second study. The sample was heated as before, except that a 30-min heating period at 400°C was included. Noncondensable gases evolved at 400°C were trapped over silica gel and designated sample A. The pyrolysis was continued for about 3 hr at 450°C, at which point the run was stopped and weighings

made. During pyrolysis, the cooler portion of the reaction tube was heated periodically to achieve partial fractionation of the viscous products. The pyrolysis was stopped and the products were treated as in pyrolysis I. The resulting fractions were: B, noncondensable gases; C, Dry Ice-temperature distillate; D, room temperature distillate; E, trap residue (recovered from benzene); and F, reaction tube residue (recovered from benzene). The charred particles showed a 74% weight loss at this point. Further pyrolysis at 800°C yielded a noncondensable fraction, sample G, and room-temperature volatiles that were designated sample H. The total weight loss was 78%.

### Analyses

Weighings were done with a Mettler microgram balance when possible. Volatile products were analyzed by mass spectrometry. The carbon, hydrogen, and nitrogen contents of the viscous products were determined with an F and M Scientific Model 185 CHN Analyzer. The infrared spectra of these materials were recorded.

## RESULTS AND DISCUSSION

### Time-Temperature-Pressure Histories

Figure 1 summarizes the noncondensable gas pressure increase with time for pyrolysis I. Figures 2 and 3 give this information for pyrolysis II. The pressure increase and visual observations to 450°C are summarized in Figure 2, and the repyrolysis of the same particles to 800°C in Figure 3.

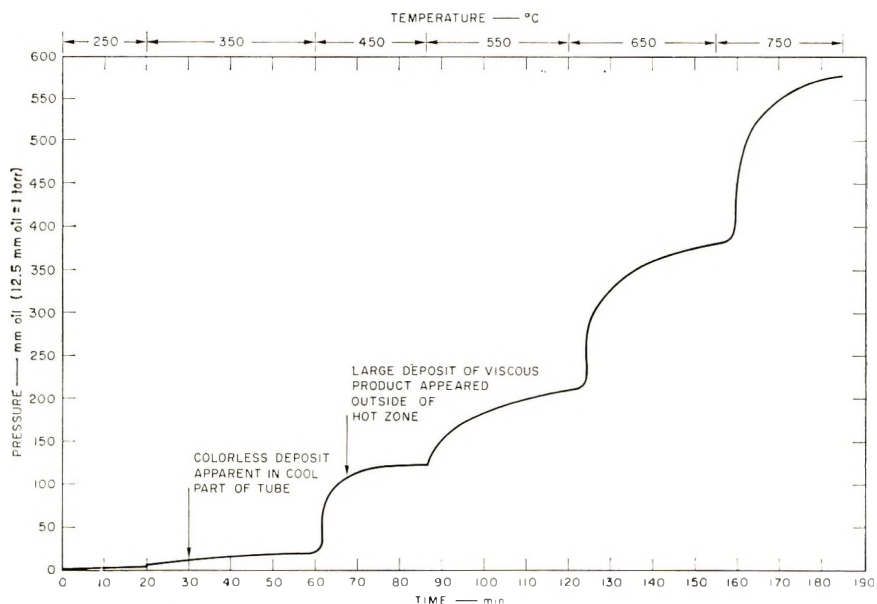


Fig. 1. Time-temperature-pressure history (pyrolysis I).

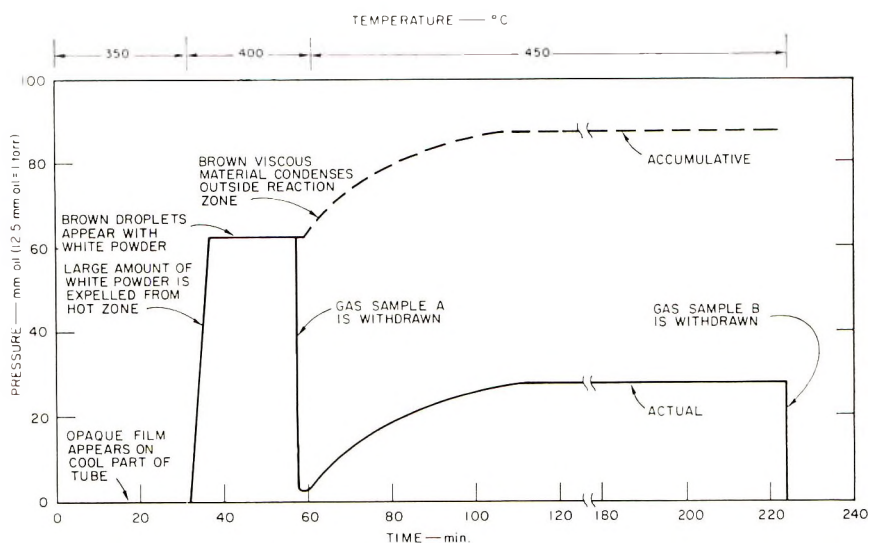


Fig. 2. Time-temperature-pressure history (pyrolysis II).

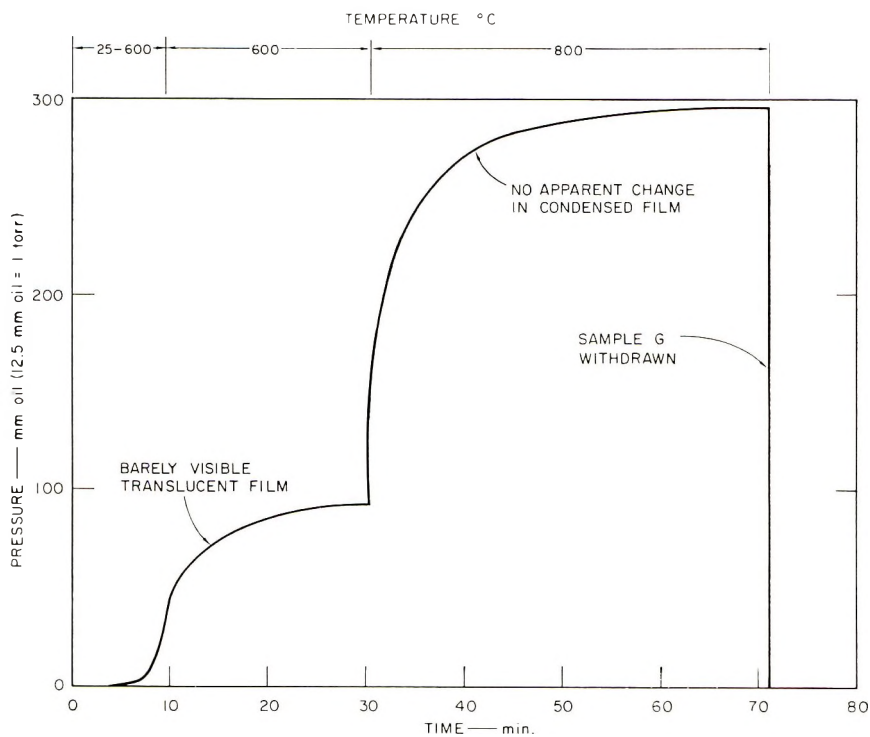


Fig. 3. Time-temperature-pressure history for repyrolysis of charred particles (pyrolysis II).

Relatively nonvolatile, opaque films were observed to form on the cooler portions of the reaction tube with the samples at 350°C. A yellow-brown viscous material subsequently condensed outside the pyrolysis zone at 450°C in both studies. No pressure rise was observed in study II at 350°C. A small pressure increase amounting to about 3% of the total noncondensable pressure rise was observed in study I up to 350°C. In both studies, the elimination of the yellow-brown tarry products followed a rapid pressure rise. Figure 2 shows that this burst of gas evolution occurred after a white material was expelled below 400°C and before the elimination of the highest boiling material at 450°C.

### Mass Spectral Analyses

Table I shows that a total of 7.71 mmole of volatile material was collected in study I (sample size 662.9 mg). The principal volatile materials were H<sub>2</sub>, CO<sub>2</sub>, CH<sub>4</sub>, CO, and H<sub>2</sub>O. No MCPD was found. The principal noncondensable gas evolved at 800°C was H<sub>2</sub> in study I, as shown by the analysis of sample I-E.

Table II lists the analyses of seven gaseous samples collected during pyrolysis II. The total amount of gases evolved was 4.29 mmole (sample size 372.9 mg). The principal volatile products were H<sub>2</sub>, CO<sub>2</sub>, CH<sub>4</sub>, CO, and H<sub>2</sub>O. CO was liberated in two stages. The analysis of fraction A shows that the pressure burst at 400°C (see Fig. 2) was principally due to

TABLE I  
Mass Spectral Analyses: Pyrolysis I

Sam- ple	Origin	Amount of material presented for analysis, mmole	Gas		
			Type	Mole-%	mmole
I-A	Polymer (non- condensibles at liq. N <sub>2</sub> temp.)	2.56	H <sub>2</sub>	48.3	1.24
			CH <sub>4</sub>	28.5	0.73
			CO	20.5	0.52
			N <sub>2</sub>	1.6	0.04
			4 others	1.1	0.03
I-B	Polymer (dis- tillate from T, cooled by Dry Ice)	1.83	CO <sub>2</sub>	79.6	1.46
			C <sub>2</sub> H <sub>4</sub>	7.6	0.14
			C <sub>3</sub> H <sub>6</sub>	2.6	0.05
			10 others	10.2	0.19
I-C	Polymer (room temperature distillate)	2.56 <sup>a</sup>	H <sub>2</sub> O	99 <sup>b</sup>	2.54
			3 others	1	0.02
I-E	Charred particles	0.76	H <sub>2</sub>	88.2	0.670
			CO	7.8	0.059
			CH <sub>4</sub>	0.6	0.005
			6 others	3.4	0.026

<sup>a</sup> Calculated assuming 100% H<sub>2</sub>O; weight liquid collected, 46 mg.

<sup>b</sup> Gas chromatographic analysis shows 1 peak approximately 94% plus four or five small peaks (column DC 550, column temperature 150°C).



TABLE II. Mass Spectral Analyses: Pyrolysis II

Sample	Origin	Amount, mmole	Major constituents		
			Type	Mole-% of sample	mmole
II-A	Gas evolved at 400°C (non- condensable at liq. N <sub>2</sub> temp.)	0.272	CO	57.6	0.157
			CH <sub>4</sub>	34.4	0.094
			N <sub>2</sub>	4.8	0.013
			H <sub>2</sub>	1.3	0.003
			O <sub>2</sub>	1.3	0.003
			3 others (each <1%)	0.6	0.002
			100.0		
II-B	Gas evolved at 450°C (non- condensable at liq. N <sub>2</sub> temp.)	0.125	CH <sub>4</sub>	60.8	0.076
			H <sub>2</sub>	20.4	0.025
			CO	16.5	0.021
			N <sub>2</sub>	1.5	0.002
			4 others (each <1%)	0.8	0.001
			100.0		
II-C	Gas evolved between 350° and 450°C (volatile at Dry Ice temp.)	0.980	CO <sub>2</sub>	77.8	0.762
			CH <sub>4</sub>	1.5	0.015
			C <sub>2</sub> H <sub>6</sub>	7.5	0.073
			C <sub>2</sub> H <sub>4</sub>	3.5	0.034
			C <sub>3</sub> H <sub>6</sub>	3.9	0.038
			CH <sub>3</sub> Cl	1.6	0.016
			7 others (each <1%)	4.2	0.041
II-D	Gas evolved at 350-450°C (volatile at room temp.)	1.44	H <sub>2</sub> O	85.4	1.230
			CH <sub>3</sub> C <sub>5</sub> H <sub>5</sub>	4.7	0.057
			C <sub>3</sub> H <sub>6</sub>	1.5	0.018
			CH <sub>3</sub> COCH <sub>3</sub>	1.2	0.015
			CH <sub>3</sub> OH	1.1	0.014
			C <sub>2</sub> H <sub>5</sub> OH	1.1	0.014
			C <sub>3</sub> -C <sub>6</sub> hydro- carbons	1.9	0.023
			C <sub>7</sub> -C <sub>10</sub> hydro- carbons	0.7	0.009
			4 others <sup>a</sup>	2.4	0.030
II-G	Gas evolved at 450-800°C (noncondensable at liq. N <sub>2</sub> temp.)	1.30	H <sub>2</sub>	72.8	0.947
			CH <sub>4</sub>	14.2	0.185
			CO	11.3	0.147
			5 others	1.7	0.022
II-H	Gas evolved at 450-800°C (volatile at room temp.)	0.158	CO <sub>2</sub>	36.5	0.058
			H <sub>2</sub> O	18.8	0.030
			CH <sub>4</sub>	3.2	0.005
			C <sub>2</sub> H <sub>4</sub>	8.9	0.014
			C <sub>2</sub> H <sub>6</sub>	15.2	0.024
			C <sub>3</sub> H <sub>6</sub>	2.9	0.005
			C <sub>6</sub> H <sub>6</sub>	4.2	0.007
			C <sub>6</sub> H <sub>5</sub> CH <sub>3</sub>	4.2	0.007
			5 others	6.1	0.010
			100.0		

<sup>a</sup> Including approximately 1.8 mg of NMA left as residue.

CO (58%) and CH<sub>4</sub> (34%). (Very little H<sub>2</sub> was collected at 400°C.) Sample II-G (450–800°C) consisted of 0.147 mmole of gas and sample II-A (400°C), 0.157 mmole. The principal noncondensable gas liberated at the higher temperatures was H.

The analysis of sample II-D is of particular interest. It was found to contain 4.7 mole-% MCPD and 85.4 mole-% water. The vapor phase, however, contained 42% MCPD and 6.7% water at room temperature.

### C, H, and N Analyses

Table III gives the C, H, and N analyses for the viscous products. No nitrogen was found, and oxygen weight percentages could be computed by difference. The calculated C, H, and O compositions of NMA, DEN438-cured polymer, phenol, cresol, and (HOC<sub>6</sub>H<sub>4</sub>)<sub>2</sub>CH<sub>2</sub> are given for comparative purposes. These latter compounds were reported by Lee<sup>6</sup> to be the major constituents in the viscous residues. The similar elemental compositions of samples I-D and II-E may indicate poor sampling in the case of D,

TABLE III  
CHN Analyses of Viscous Samples  
Compared with Starting Materials and Expected Products

	C, %	H, %	O, %	N, %
Sample I-D	71.76	6.63	21.61	
Sample II-E	71.87	6.55	21.58	
Sample II-F	76.12	6.45	17.43	
Polymer	70.8	6.3	22.7	0.2
NMA	67.02	5.62	26.96	
Phenol	76.6	6.38	17.0	
Cresols	77.8	7.41	14.8	
(HOC <sub>6</sub> H <sub>4</sub> ) <sub>2</sub> CH <sub>2</sub>	78.0	6.00	16.0	

since only 25% of the total sample was prepared for analysis. Sample I-D was the total viscous residue and its composition would be expected to be intermediate between that of II-E and II-F. The elemental composition of sample II-F (C, 76.12%; H, 6.45%; O, 17.43%) is quite similar to that of phenol (C, 76.6%; H, 6.38%, O, 17.0%).

### Infrared Spectral Analyses

The infrared spectra of the viscous products, II-E and II-F, are given in Figure 4, together with those of NMA and DEN438. A 1.8-mg sample of NMA was isolated from sample II-E and its infrared spectrum was identical with that of commercial NMA. Sample II-E, the collection trap residue, shows prominent NMA carbonyl stretching frequencies at 1842 and 1770 cm<sup>-1</sup>. These bands are barely discernible in the spectrum of II-F. On the other hand, the OH stretching frequency at about 3420 cm<sup>-1</sup> is much more evident in the spectrum of II-F than II-E, which would be indicative of a higher phenol or cresol content in II-F. However, both spectra (F,

TABLE IV  
Mass Balance: Pyrolysis I

Element	Polymer, mg				Products, mg							Recovery	
	DEN438	NMA	DB-VIII	Sample	A	B	C <sup>a</sup>	D <sup>b</sup>	E	F	Char <sup>c</sup>	Amount, mg	%
C	256.0	199.8	14.2	470.0	15.1	21.2	244.0	1.4	1.4		147.8	429.5	91.4
H	22.9	16.7	1.8	41.4	5.4	0.8	4.8	22.6	0.7			34.3	83.0
O	70.0	80.0		150.1	8.4	46.7	38.4	73.4	1.0			167.9	111.8
N			1.4	1.4	1.2							1.2	86
Not identified							2.8			1.5		4.3	
Total	349.0	296.5	17.4	662.9	30.1	68.7	46.0	340.0	3.1	1.5	147.8	637.2	
Wt-%	52.6	44.7	2.7	100.0	4.5	10.4	6.9	51.3	0.5	0.2	22.2	96.0	

<sup>a</sup> Assumed 94% H<sub>2</sub>O.

<sup>b</sup> D designates viscous product.

<sup>c</sup> Assumed 100% carbon.

TABLE V  
Mass Balance: Pyrolysis II

Element	Polymer, mg			Products, mg										Recovery	
	DEN438	NMA	DB-VIII	Sample	A	B	C	D <sup>a</sup>	E	F	G	H	Char <sup>b</sup>	Amount gm	%
C	143.9	112.3	7.97	264.2	3.22	1.19	13.21	12.81	17.77	117.20	4.04	2.28	83.23	254.95	96.6
H	12.8	9.4	1.05	23.3	0.42	0.36	1.32	4.22	1.62	9.91	2.67	0.42		21.03	90.6
O	39.5	45.1		84.6	2.69	0.34	24.40	21.74	5.33	26.81	2.38	2.97		86.66	102.4
N			0.78	0.8											
Not identified															
Total, mg	196.2	166.8	9.8	372.9	6.33	1.89	39.74	38.76	24.72	154.02	9.09	5.67	83.23	363.47	
Wt-%	52.6	44.7	2.6	100.0	1.70	0.51	10.65	10.39	6.52	41.30	2.44	1.51	22.30	97.2	

<sup>a</sup> Including NMA not volatilized for mass spectral analysis. Total NMA isolated as such = 3.6 mg (0.97%).

<sup>b</sup> Assumed to be 100% carbon.

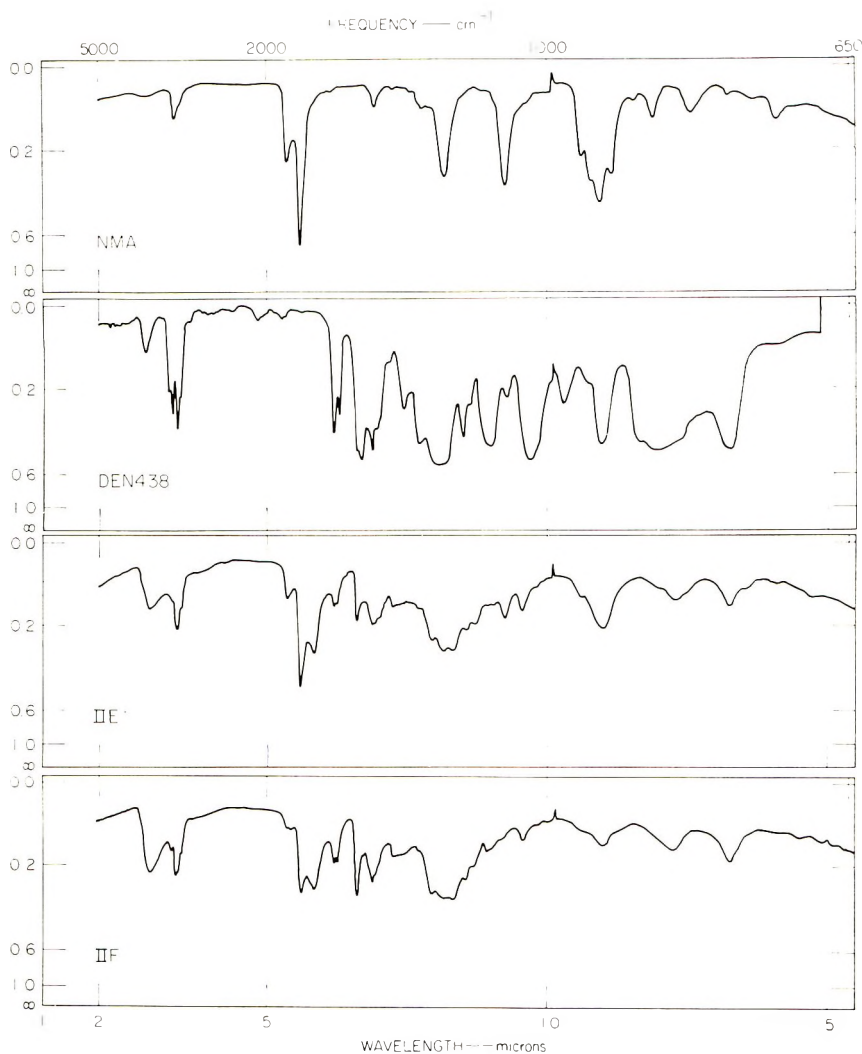


Fig. 4. Infrared spectra of samples of nadic methyl anhydride, DEN 438, and viscous products.

more so than E) show a third band at about  $1707\text{ cm}^{-1}$  indicative of another type of carbonyl group, possibly that of a carboxycyclic acid, or ester.

### Mass Balances

The analytical results given above allowed the computation of the elemental mass balances given in Tables IV and V for studies I and II, respectively. The overall recoveries are seen to be quite good, i.e., 96.0% (Table IV) and 97.2% (Table V). In both cases, the oxygen balance gave percentages greater than 100, and hydrogen balances were low. The high

oxygen contents can be understood, since the starting materials were partially hydrolyzed as indicated by OH stretch (see Fig. 4). It may be that the hydrogen content is low in both cases because the char was not completely dehydrogenated. We have observed H<sub>2</sub> evolution at 1000°C from such char samples.

### Stoichiometric Analysis

A hypothetical initial polymer weight of 100 g was chosen as a basis to compare the results of the two studies. The results reported above are summarized on this basis in Figure 5.

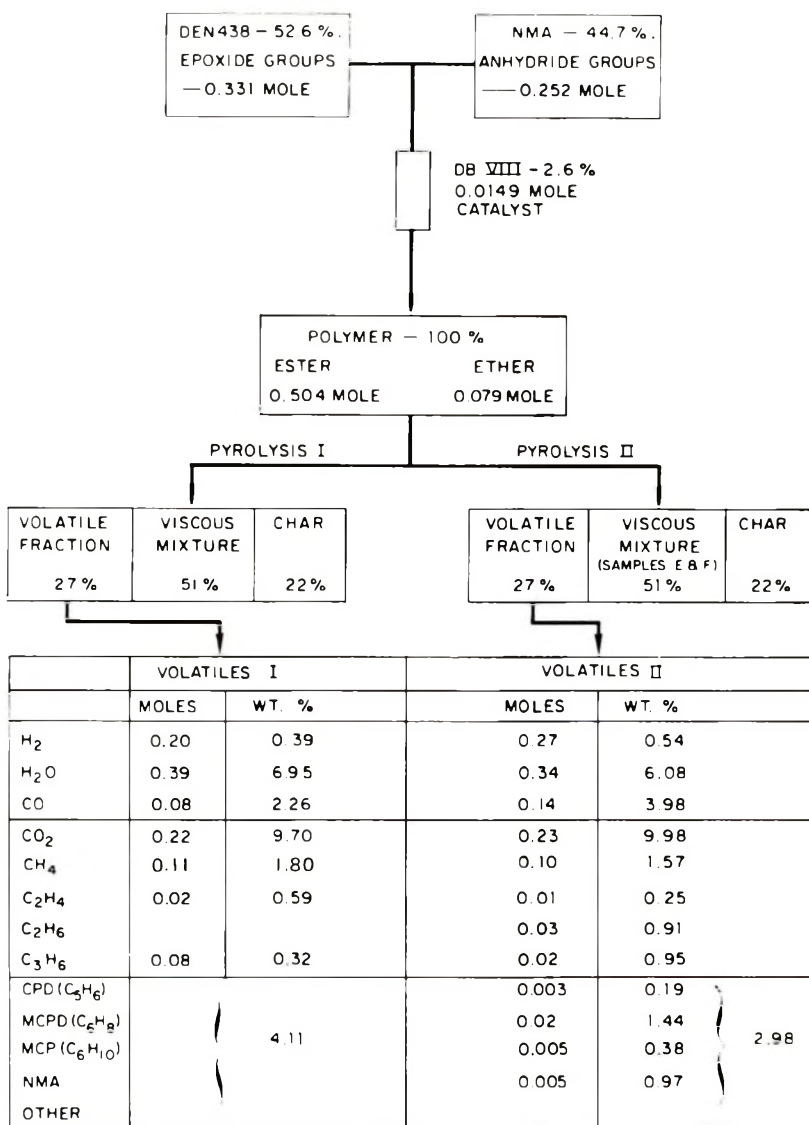


Fig. 5. Partial stoichiometry of DEN 438-NMA polymer pyrolysis.

The polymer composition resulted from 52.6 wt-% of resin (0.331 mole of epoxide group/100 g of polymer), 44.7 wt-% NMA (0.252 mole of anhydride/100 g of polymer), and a small amount of tertiary amine catalyst. If one assumes 100% reaction of the anhydride, 0.504 mole of ester groups with 0.252 mole of diester would result. The remaining 0.079 mole of epoxide groups could react to form ether linkages. These idealized computations assume that DEN438 contains 3.6 mole of epoxide group per mole of resin as reported by the manufacturer.<sup>10</sup>

The results on Figure 5 show that the degradation produces about one fourth volatile products, one half high boiling products, and about one fourth char. Although the two studies followed slightly different procedures, this overall distribution was essentially unchanged.

Considerable detail was derived from the analyses of the volatile products. The amounts of water found, corresponded to slightly more than one mole of water per initial epoxide group. This result suggests that all epoxide groups had reacted during the curing cycle and were subsequently degraded. Lee<sup>6</sup> showed that uncured epoxide resins readily dehydrate on pyrolysis. His observations and the results found in this study suggest that all ester sites are degraded during pyrolysis and that as the degradation continues, an anhydride-cured system behaves like an uncured epoxy system.

It has been shown in other studies<sup>5,8</sup> that NMA is eliminated at temperatures of 350°C and below. Fleming provided evidence that NMA elimination is from monoester sites and that diester sites produce MCPD. CO<sub>2</sub> is the other expected product resulting from the degradation of diester sites following MCPD elimination, i.e., from the breakdown of maleic diester sites. Since 2 moles of CO<sub>2</sub> are expected per diester site, this result shows that a minimum of 50% of the anhydride reacts to form diester linkages. This finding supports Fleming's observation, based on crosslink density measurements, that there is a considerable amount of monoester-monoacid in NMA-cured epoxides. However, Taylor's analysis of cured polymer gave an 83 percent consumption of anhydride to form diester groups. His result is based on ascribing the difference between initial anhydride concentration and that found as unreacted anhydride, plus monoacid-monoester sites. This procedure would tend to introduce a systematic error into his results giving diester contents which are too high. On the other hand, these two results, taken together, indicate that as much as 30% of the maleic diester groups are not degraded during pyrolysis. Some support for this latter view is found in the infrared spectra of the viscous products which show an unidentified carbonyl stretching frequency at 1707 cm<sup>-1</sup>.<sup>11</sup>

On the basis of Lee's analyses,<sup>6</sup> one would predict a large amount of MCPD. The number of moles of MCPD predicted would be equal to one half of the number of CO<sub>2</sub> at a minimum. No MCPD was isolated in pyrolysis I, and only a small amount was isolated in pyrolysis II (17% of the amount expected, based on CO<sub>2</sub>). As was amply demonstrated in this work, erroneous results can be obtained if only the volatile components

are sampled. In Lee's study,<sup>6</sup> the inlet system leading from the pyrolysis system to the spectrometer was not heated and may explain this one discrepancy between his results and ours.

The CO evolution was not the same for pyrolyses I and II. In pyrolysis I, CO was found to be approximately equal to the calculated initial ether linkage content. Approximately twice that amount was found in the second pyrolysis. However, the results of the second study clearly show that CO was evolved in two stages. At 400°C, about 48% of the total was produced. This result indicates that in study I, further etherification did not occur during degradation, since the temperature was raised abruptly from 350 to 450°C. The polymer structure must have been almost completely degraded at 450°C, because the weight loss at this point was so close to the final value. Indeed, the infrared spectrum of the viscous products in study I (not shown) show a much larger 1707  $\text{cm}^{-1}$  peak, relative to the anhydride carbonyl stretching frequencies, than is found in either samples II-E or II-F, supporting this view. (Although these results are consistent with CO evolution from ether sites only, other sources of CO, such as anhydride decomposition, cannot be ruled out.)

The amounts of methane isolated in both studies, 0.11 mole/100 g polymer and 0.10 mole/100 g polymer in studies I and II, respectively, are essentially equal. They are approximately 30% higher than would be predicted if  $\text{CH}_4$  came only from ether groups initially present. This result would be consistent with additional etherification after NMA elimination.

The high boiling materials are the most important fraction on an overall weight loss basis, amounting to about 51 wt-% of the starting materials. These viscous products are difficult to separate and analyze. A small amount of NMA was isolated from these products and a qualitative identification was made. The carbon, hydrogen and oxygen analyses were consistent with a phenolic mixture, including some NMA. If one assumes that all epoxide side chains were degraded to phenolic hydroxyl groups, then 38 wt-% of the 51 wt-% of viscous product would be in the form of phenol, cresols, and  $(\text{HOC}_6\text{H}_4)_2\text{CH}_2$ . The remaining 13 wt-% viscous product would be anhydride (29% of the initial anhydride). This result is in excellent agreement with the 15 wt-% losses at 350°C found in two earlier studies of this polymer.<sup>2,8</sup> Since it is unlikely that the aromatic backbone was degraded, this upper limit of 29% anhydride eliminated would support the earlier contention that Taylor's<sup>9</sup> 15% monoacid-monoester result is too low and his difference calculation of 83% diester is too high.

Fleming<sup>8</sup> found 24 wt-% char residue from MA-cured DEN438, and 18% from NMA-cured DEN438. The  $\text{CO}_2$  results indicate that at least 50% of the diester sites were converted to maleic diester groups. Therefore, in this study 12% char would be predicted as arising from the maleic diester groups generated during degradation. The char yields in this and other studies have been essentially the same, i.e.,  $20 \pm 3\%$ . It is evident that the second source of char lies in the absence of MCPD in the gaseous products. In pyrolysis II, about 83% of the expected MCPD could have been reduced to carbonaceous deposits. This amount would yield an



additional 7% of char. The sum of these two sources gives a char yield of 19%, and this is in excellent agreement with both Fleming's<sup>8</sup> results and those found in this study, namely  $20 \pm 2\%$ . NMA-cured systems thus have high char yields because of reverse Diels-Alder mechanism is operative, producing MCPD, which is pyrolyzed to carbonaceous char.

### CONCLUSIONS

Our conclusions are that the decomposition proceeds in three stages. The first stage is the elimination of NMA from monoacid-monoester sites at temperatures to 350°C. These sites apparently react to form additional ether links not present in the original cured polymer. The second stage is a reverse Diels-Alder elimination of MCPD at about 350 to 400°C. The MCPD does not escape from the polymer, but reacts and thereby enhances carbon formation. About one third of the char comes from the degradation of MCPD. The remaining two thirds comes from a breakdown of the maleic diester groups that are left when MCPD is eliminated. The aromatic backbone is apparently stable at temperatures of 350–400°C. The third stage of decomposition commences at 450°C; the resin backbone structure begins to crack and give phenol-like, high-boiling materials. A significant result of this work is that these high boiling materials that are evolved as gases constitute two thirds of the weight loss of the polymers. The char is almost completely formed at 450°C. Pyrolysis at 800°C led to a further weight loss of only 4%.

The authors wish to thank E. M. McCarthy for CHN analyses and N. McBurney, J. Whittick, and R. F. Muraca for mass spectral analyses.

This work has been supported by Contract NAS 7-472 by the National Aeronautics and Space Administration.

### References

1. G. N. Spokes and S. W. Benson, in *Fundamentals of Gas Surface Interactions*, H. Saltsburg, J. N. Smith, Jr., and M. Rogers, Eds., Academic Press, New York, 1967, p. 318.
2. H. Lee and K. Neville, *Handbook of Epoxy Resins*, McGraw-Hill, New York, 1967, pp. 4–10, 4–11.
3. D. P. Bishop and D. A. Smith, *Ind. Eng. Chem.*, **59** (8) 32 (1967).
4. H. C. Anderson, *J. Appl. Polym. Sci.*, **6**, 484 (1962).
5. T. Sugita and M. Ito, *Bull. Chem. Soc. Japan*, **38**, 1620 (1965).
6. L.-H. Lee, *J. Polymer Sci.*, **A3**, 859 (1965).
7. Molseyev et al., *Plastmassy*, **6**, 11 (1964).
8. G. J. Fleming, *J. Appl. Polym. Sci.*, **10**, 1813 (1966).
9. C. G. Taylor, paper presented to Division of Organic Coatings and Plastics Chemistry, 155th Meeting, American Chemical Society, San Francisco 1968, *Abstracts*, **28**, 251 (1968).
10. Technical Bulletin, *DEN Epoxy Novolac Resins*, Plastics Dept., Dow Chemical Company, Midland, Mich. (1965).
11. L. J. Bellamy, *The Infra-Red Spectra of Complex Molecules*, 2nd Ed., Wiley, New York, 1962, pp. 125, 169.

Received May 20, 1969

Revised September 8, 1969

## Synthesis of Poly-2-oxazolidones From Diisocyanates and Diepoxides\*

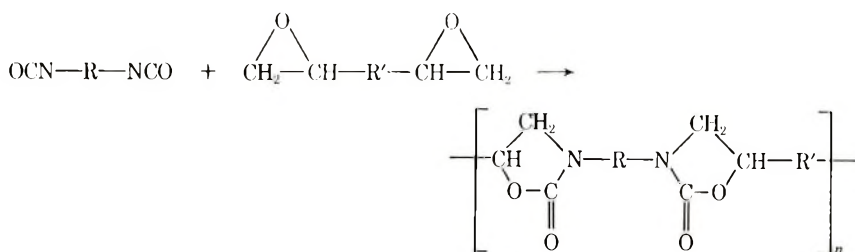
R. R. DILEONE, *Plastics Division, American Cyanamid Co., Stamford, Connecticut 06904*

### Synopsis

Poly-2-oxazolidones of high molecular weight have been synthesized from diisocyanates and diepoxides. The synthetic method was first developed for the model compound 3-phenyl-5-phenoxyethyl-2-oxazolidone prepared from phenyl isocyanate and phenyl glycidyl ether. Conditions found most suitable for a high yield involve slow addition of isocyanate to a solution of epoxide and catalyst, temperatures of 160°C or higher, and a catalytic amount of *n*-butoxylithium in 1-butanol. The same procedure was used to prepare high molecular weight poly-2-oxazolidones. The polymer structure was confirmed by infrared spectroscopy and elemental analysis. All polymers prepared were of sufficient molecular weight to be compression molded. The bulk mechanical properties characterize poly-2-oxazolidones as potentially useful engineering thermoplastics. A mechanism for oxazolidone formation is proposed.

### INTRODUCTION

Speranza and Peppel<sup>1</sup> and later Sandler and co-workers<sup>2</sup> reported the synthesis of poly-2-oxazolidones from diisocyanates and diepoxides using quaternary ammonium halides as catalysts.

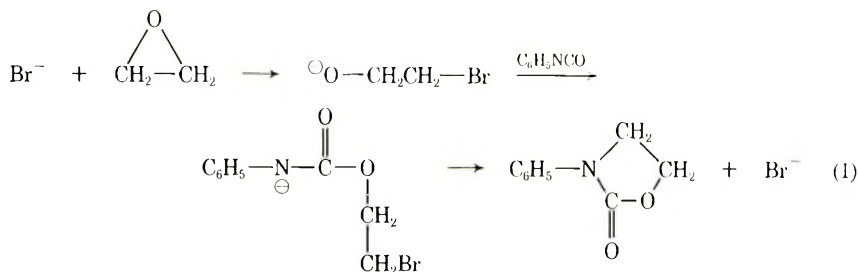


Both reports failed to fully characterize the polymer. We have investigated this synthetic approach and found that quaternary salts do indeed lead to oxazolidone formation but also result in crosslinked or low molecular weight material as was observed by Sandler and co-workers.<sup>2,3</sup> Recently Iwakura and co-workers<sup>4</sup> reported the synthesis of poly-2-oxazolidones from difunctional urethanes and epoxides using tertiary amines as catalysts.

\* Paper presented before the Division of Polymer Chemistry, 155th National Meeting of the American Chemical Society, San Francisco, April 1968.

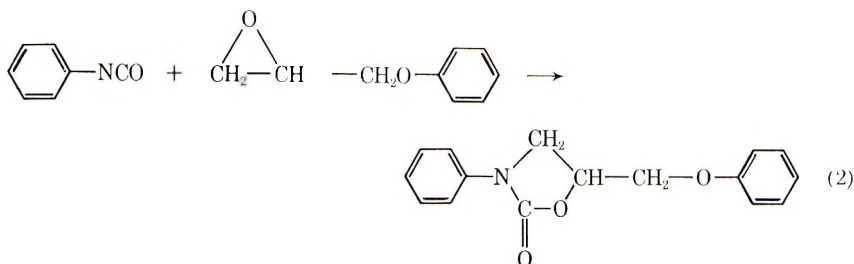
Although Iwakura was able to show the formation of poly-2-oxazolidones, the polymers were all of very low molecular weight, as evidenced by inherent viscosities of less than 0.2 dl/g in DMF.

Speranza and Peppel<sup>1</sup> postulated that opening of the epoxide ring by quaternary halide precedes addition of the isocyanate via the mechanism shown in eq. (1).



If this mechanism is correct, oxazolidone formation competes with homopolymerization of the epoxide, which may be the reason for the formation of crosslinked or low molecular weight polymers.<sup>2-4</sup>

The present work was directed toward finding a catalyst that would permit the synthesis of high molecular weight polyoxazolidones from diepoxides and diisocyanates. To obtain this information, a study was first carried out on the synthesis of the model compound 3-phenyl-5-phenoxy-methyl-2-oxazolidone from phenyl isocyanate and phenyl glycidyl ether [eq. (2)].



## DISCUSSION

### Model Study

The addition condensation of phenyl isocyanate and phenyl glycidyl ether was carried out in *o*-dichlorobenzene as the solvent. Reaction temperature, mode of addition, and catalyst were the three major variables studied. Alkoxides were chosen as catalysts since they are known to be poor nucleophiles for epoxide polymerization.<sup>5</sup> The results of this study are shown in Table I.

Examination of Table I shows *n*-butoxylithium to be the most effective catalyst. The inactivity of the other catalysts was attributed to poor

TABLE I  
Formation of 3-Phenyl-5-phenoxyethyl-2-oxazolidone  
from Phenyl Isocyanate and Phenyl Glycidyl Ether<sup>a</sup>

No.	Mode of addition of reactants	Catalyst (0.5 ml of 0.2 <i>M</i> )	Reaction temp, °C	Yield, %
1	Both mixed	<i>n</i> -BuOLi	150	64
2	" "	<i>t</i> -BuOLi	150	43
3	" "	<i>n</i> -BuONa	150	0
4	" "	<i>n</i> -BuOK	150	0
5	" "	<i>n</i> -BuOLi	120	33
6	" "	<i>n</i> -BuOLi	130	56
7	Phenyl isocyanate added over 2 hr	<i>n</i> -BuOLi	160	95
8	Phenyl isocyanate added over 1/2 hr	<i>n</i> -BuOLi	160	96

<sup>a</sup> With the use of 0.20 mole of each reactant in 50 ml of *o*-dichlorobenzene; reaction period 2 hr.

solubility in the reaction solvent as evidenced by the hazy appearance of the solution. Further, slow addition of the isocyanate to the epoxide at temperatures of 160°C or higher is the preferred procedure. It was also shown in this study that no reaction takes place between the catalyst and the epoxide, or between the isocyanate and the epoxide, under the conditions of the reaction.

### Poly-2-oxazolidones

High molecular weight poly-2-oxazolidones were prepared from diisocyanates and diepoxides by a procedure similar to the one worked out for the model compound (see Experimental).

Polyoxazolidone formation was confirmed by both infrared spectra and elemental analysis. The characteristic absorption band for isocyanate at 2250  $\text{cm}^{-1}$  has entirely disappeared and the band at 1740–1750  $\text{cm}^{-1}$ , characteristic of oxazolidone carbonyl, appears in all the polymers.<sup>3,4,6</sup> Table II summarizes the elemental analysis data as well as inherent viscosities and polymer melt temperatures.


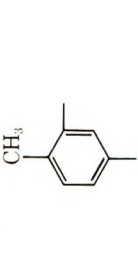
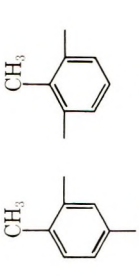
The bulk mechanical properties are shown in Table III. All samples were compression-molded from precipitated polymer.

This is the first time the bulk mechanical properties of polyoxazolidones have been reported. The data reported in Table III characterize these materials as high-temperature engineering thermoplastics.

### Mechanism

Reactions involving nucleophilic displacement by a urethane nitrogen have been reported. For example, Speranza and Peppel<sup>1</sup> proposed a nucleophilic displacement by a urethane anion in their studies on oxazolidone formation [see eq. (1)].

TABLE II  
Polyoxazolidones

R	$\eta_{inh}^a$ dl/g <sup>s</sup>	Softening point, °C	C, %		H, %		N, %	
			Calcd	Found	Calcd	Found	Calcd	Found
	0.41	170	73.22	72.86	5.76	5.92	4.75	5.18
	0.41	195	70.04	70.25	5.84	5.87	5.45	5.42
	0.58	186	70.04	70.14	5.84	5.81	5.45	5.50
80%								
20%								

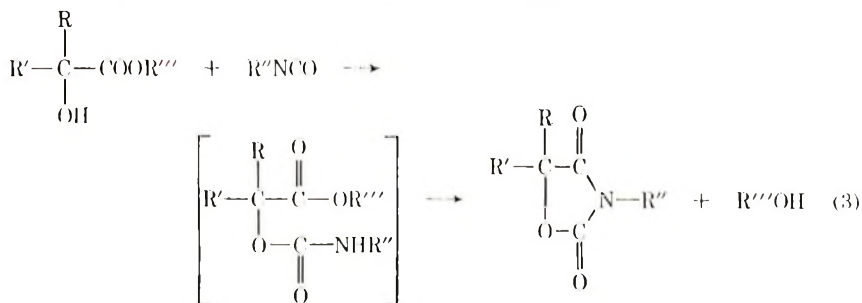
<sup>a</sup> Determined at concentrations of 0.5 g/100 ml in dimethylformamide at 25°C. The highest inherent viscosities previously recorded were generally less than 0.20 dl/g in DMF.<sup>4</sup>

TABLE III  
Physical Properties of Polyoxazolidones

R =

				ASTM test
Flexural strength, psi	14900	16600	12700	D790
Flexural modulus, psi	420000	490000	500000	D790
Tensile strength, psi	9500	8000	10900	D1708
Elongation, %	6.6	3.9	5.9	D1708
Izod impact, ft-lb/in				
Notched	0.6	0.4	0.2	D256
Unnotched	2.5	4.6	2.4	—
Heat distortion temperature (264 psi), °C	143	176	153	D648
Molding temperature, °C	190	210	200	—
Molding pressure (psi)	1000	1000	1000	—

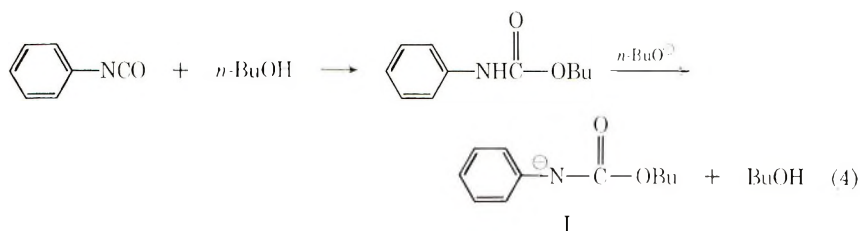
With  $\alpha$ -hydroxyesters, ring closure between the ester and the urethane takes place if a sodium alkoxide catalyst is present.<sup>7</sup>



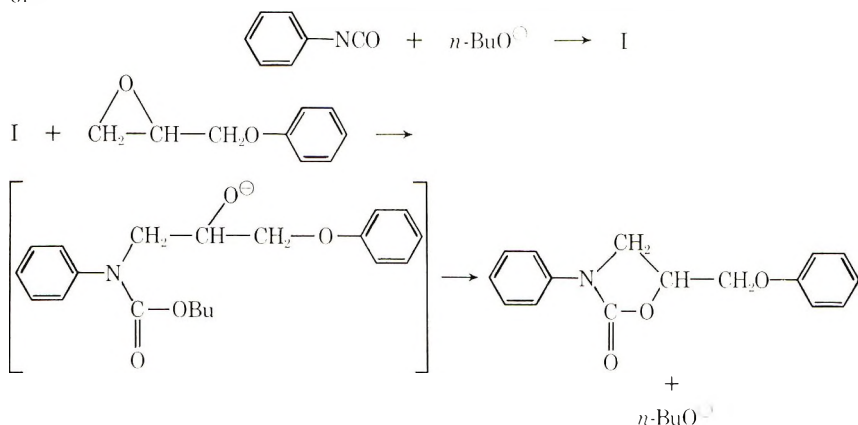
Iwakura and Izawa,<sup>8</sup> in their studies on oxazolidone formation, ruled out any reaction between isocyanates and epoxides. They confirmed that oxazolidone formation could take place only by the addition condensation between urethane and epoxide followed by intramolecular exchange of alcohol to form the oxazolidone ring. They also pointed out that the role

of the tertiary amine catalyst is to enhance the nucleophilicity of the urethane nitrogen. In our studies we found that no reaction takes place between the alkoxide catalyst and the epoxide or between the isocyanate and the epoxide under the conditions of the reaction.

The mechanism consistent with these facts involves, first, the formation of the urethane anion, followed by a nucleophilic attack by the urethane anion on the epoxide ring:



or



## EXPERIMENTAL

### Preparation of Alkali Metal Catalysts

To 1.0 mole of anhydrous *n*-butyl alcohol was added 0.20 mole of the alkali metal. The mixture was stirred at 23°C under nitrogen until all the metal had reacted (usually 24–48 hr.). The catalyst solution was then stored in a glass container sealed with a serum cap. Catalyst was then sampled with a hypodermic syringe.

### Preparation of 3-Phenyl-5-Phenoxymethyl-2-Oxazolidone

A mixture of 0.20 mole of phenyl glycidyl ether and 50 ml of *o*-dichlorobenzene was heated to the desired reaction temperature (see Table I), at which time 0.50 ml of 0.20 M *n*-butoxylithium was added followed by the addition of 0.20 mole of phenyl isocyanate, either all at once or slowly (see Table I for details). Total reaction time was 2 hr. The reaction mixture was then poured into a 5-volume excess of heptane and allowed to crys-

tallize. The product, recrystallized from acetone, melted at 139–140°C (literature,<sup>8</sup> 139–140°C).

### Preparation of Polyoxazolidone

The following procedure was used for all polymer preparations. To an appropriate reaction vessel was added 0.200 mole of 2,2-bis[*p*-(2,3-epoxypropoxy)phenyl]propane, 110 g of *o*-dichlorobenzene, and 30 ml of benzene. The mixture was heated to azeotrope the benzene-water mixture. The heating was continued until a temperature of 180°C was reached. To the dry reactants was then added 0.50 ml of 0.20*M* *n*-butoxylithium solution followed by 0.200 mole of 2,4-toluene diisocyanate over a 60-min period. The reaction was then continued for an additional 30 min at 160°C, the mixture was then cooled to 140°C, diluted with 100 ml dimethylformamide (polymer becomes insoluble in *o*-dichlorobenzene), and cooled to room temperature. The polymer was precipitated in a large volume of methanol in a Waring Blendor. The precipitated polymer was collected by filtration, washed with additional methanol and dried 3 hr. at 80°C. All of the polymers were soluble in dimethylformamide, dimethylacetamide, dimethyl sulfoxide, and methylene chloride.

### References

1. G. P. Speranza and W. J. Poppel, *J. Org. Chem.*, **23**, 1922 (1958).
2. S. R. Sandler, F. Berg, and G. Kitazawa, *J. Appl. Polym. Sci.*, **9**, 1994 (1965).
3. S. R. Sandler, *J. Polym. Sci. A-1*, **5**, 1481 (1967).
4. Y. Iwakura, S. I. Izawa, and F. Hayano, *J. Polym. Sci. A-1*, **4**, 751 (1966).
5. H. Lee and K. Neville, *Handbook of Epoxy Resins*, McGraw-Hill, New York, 1967, Chap. 5.
6. Y. Iwakura, N. Nabeya, F. Hayano, and K. Kurita, *J. Polym. Sci. A-1*, **5**, 1865 (1967).
7. R. F. Rekker, A. C. Faber, D. H. E. Tom, H. Verleur, and W. T. H. Nauta, *Rec. Trav. Chim.*, **70**, 113 (1951).
8. Y. Iwakura and S. Izawa, *J. Org. Chem.*, **29**, 379 (1964).

Received June 9, 1969

Revised September 8, 1969



## Polymerization of Vinylcyclopropanes. IV. Radical Copolymerization of 1,1-Dichloro-2- vinylcyclopropane with Maleic Anhydride

TAKAKO TAKAHASHI, *Government Industrial Research Institute, Osaka Ikeda, Osaka, Japan*

### Synopsis

Radical copolymerization between 1,1-dichloro-2-vinylcyclopropane ( $M_1$ ) and maleic anhydride ( $M_2$ ) was studied. Rearrangement of the radical caused from monomer  $M_1$  and cyclization of growing chain, which was suggested from a consideration of composition and structure of the obtained copolymer, complicate the propagation step in this system. A peculiar copolymer composition equation containing four reactivity ratio parameters was developed, and these parameters were determined.

During the course of our investigations of the radical homopolymerization of vinylcyclopropanes,<sup>1,2</sup> it has become apparent that the propagation consists of two steps: (1) the formation of a substituted cyclopropylcarbinyl radical by addition of the monomer to growing chain end and (2) the rearrangement of this cyclopropylcarbinyl radical by the opening of the cyclopropane ring. The investigations of free-radical addition to vinylcyclopropanes by Huysen et al.<sup>3</sup> and Lishansky et al.<sup>4</sup> also support this mechanism. The rearrangement of cyclopropylcarbinyl radical (the second step) should be in competition with the addition of the monomer to this radical. The latter reaction would give 1,2-type structural units into the polymer. However, the predominance of the rearranged type (1,5-type) in the structural units of the polymers obtained with radical polymerization showed that the rearrangement is faster than the addition of the monomer. In the case of the derivatives which have halogens<sup>2</sup> or a carboethoxy group<sup>5</sup> on the cyclopropane ring, the obtained polymers were selectively of the 1,5-type, since the rearranged radical gains in resonance stability.

In the copolymerization of such compounds with other more active vinyl monomers, a characteristic behavior is expected. It is a matter of course that the reaction might be more complicated than the usual binary copolymerization.

In the first attempted copolymerization of vinylcyclopropanes, 1,1-dichloro-2-vinylcyclopropane (diClVC), which gives selectively 1,5-type polymer, was used. The present work describes the copolymerization of

this compound with maleic anhydride (MAnh) which is known to be difficult to homopolymerize by radical polymerization, but which gives easily 1:1 alternating copolymer with vinyl monomers.

### EXPERIMENTAL AND RESULTS

The monomer, diClVC, was prepared as previously described.<sup>1</sup> The other monomer (MAnh) and other materials were all purified by standard methods.

The copolymerizations were carried out in bulk and in benzene solution. The monomers and  $\alpha,\alpha'$ -azobisisobutyronitrile (AIBN) initiator were weighed into a tube and, in the case of solution copolymerization, diluted with benzene. The tubes were flushed with nitrogen and sealed. The copolymerizations were carried out in a bath at  $60 \pm 0.05^\circ\text{C}$ . The polymers precipitated during the reaction in solution polymerization, though the bulk polymerizations were homogeneous during the reaction. After addition of 1–2 ml of 0.1% diethyl ether solution of hydroquinone, the reactants were poured into diethyl ether and filtered through glass filter funnels. The polymers were repeatedly washed with diethyl ether and dried *in vacuo*. The copolymers were powdery white and soluble in polar solvents, such as tetrahydrofuran and *N,N*-dimethylformamide.

The compositions of the copolymers were calculated from their chlorine contents. The determination of chlorine was carried out by use of a modified combustion flask.<sup>6</sup>

Determination of unsaturation was carried out by a iodine monochloride method similar to that described by Lee et al.,<sup>7</sup> except that a different solvent was used. Since our copolymers were not soluble in chloroform or carbon tetrachloride, they were dissolved in a small quantity of *N,N*-dimethylformamide, enough to prevent the precipitation of the polymer by the addition of the chloroform solution of iodine monochloride. By application of the same method to the homopolymer of diClVC, which has unsaturated structural units, it was ascertained that this method is applicable to determining unsaturation of the copolymers.

The relative composition of the copolymers was determined at low conversions and over a wide range of initial monomer feed compositions. The details of the experimental results of the copolymerizations are summarized in Tables I and II.

### DISCUSSION

Table I shows data for the bulk copolymerization. The variation of the composition of the copolymer with initial monomer feed composition means apparently that MAnh ( $M_2$ ) does not alternate with diClVC ( $M_1$ ). When the composition of MAnh is increased in the monomer feed, the composition of the copolymer approached  $M_1:M_2 = 1:2$ . The results of solution copolymerization are similar to those for bulk copolymerization, though the rate of the former polymerization is much slower (Table II).

TABLE I  
Bulk Copolymerization of 1,1-Dichloro-2-vinylcyclopropane ( $M_1$ ) and Maleic Anhydride ( $M_2$ )<sup>a</sup>

No.	Monomer feed		Polymerization time, hr	Conversion, %	Chlorine content, wt-%	Copolymer		$M_1^*/M_1^b$	$[\eta]^c$
	$M_1$ , mole-%	$M_2$ , mole-%				$M_1$ , mole-%	$M_2$ , mole-%		
1	5.14	94.86	25	1.77	21.11	33.02	66.98		
2	10.44	89.56	25	2.63	21.98	34.57	65.43	0.041	0.06
3	22.38	77.62	25	6.97	23.33	37.01	62.99	0.076	0.07
4	34.96	65.04	25	7.43	24.67	39.47	60.53	0.126	0.07
5	49.65	50.35	25	5.91	26.49	42.87	57.13	0.129	0.07
6	50.43	49.57	20	4.38	26.64	43.16	56.84		0.06
7	66.20	33.80	25	3.09	29.76	49.20	50.80		0.05
8	80.33	19.67	25	0.57	33.50	56.50	43.22		

<sup>a</sup> Polymerization at 60°C with 0.1 mole-% AIBN as catalyst.

<sup>b</sup> Ratio of unsaturated monomer ( $M_1^*$ ) to total monomer ( $M_1$ ) in the copolymer.

<sup>c</sup> Measured with an Ostwald viscometer at 25°C with tetrahydrofuran as solvent.

TABLE II  
 Solution Copolymerization of 1,1-Dichloro-2-vinylcyclopropane ( $M_1$ ) and Maleic Anhydride ( $M_2$ )<sup>a</sup>

No.	Monomer feed		Polymer- ization time, hr	Conversion, %	Chlorine content, wt-%	Copolymer		$M_1^*/M_1$
	$M_1$ , mole-%	$M_2$ , mole-%				$M_1$ , mole-%	$M_2$ , mole-%	
1	16.66	83.34	170	1.57	21.13	33.06	66.94	
2	25.01	74.99	170	1.82	22.49	35.49	64.51	
3	33.34	66.66	170	1.86	22.99	36.39	63.61	
4	41.67	58.33	140	1.95	23.79	37.85	62.15	0.067
5	50.00	50.00	140	1.42	24.42	39.00	61.00	0.092
6	58.34	41.66	140	0.95	25.55	41.10	58.90	0.119
7	66.66	33.34	240	0.42	26.93	43.71	56.29	0.169
8	83.33	16.67	240	trace				

<sup>a</sup> Polymerization at 1.8 mole/l. total initial monomer concentration in benzene at 60°C with 0.1 mole-% AIBN as catalyst.

MANh is a monomer which typically gives alternate copolymers with other vinyl monomers by radical polymerization. In early attempts to explain the alternation, Bartlett and Nozaki<sup>8</sup> proposed the participation of the molecular complex formed between the comonomers, while Walling et al.<sup>9</sup> suggested a charge-transfer interaction between the growing radical and monomer in the transition state of propagation. It is known that these explanations were supported experimentally by many subsequent groups of workers. Recently, Iwatsuki and Yamashita<sup>10</sup> reported the existence of charge-transfer complexes between the comonomers in their series of MANh-*p*-dioxene copolymerizations and concluded that the alternating free-radical copolymerization could be reduced to a homopolymerization of the complexes. Moreover, they showed a classification of charge-transfer copolymerizations with equilibrium constants for complex formation between the comonomers.<sup>11</sup>

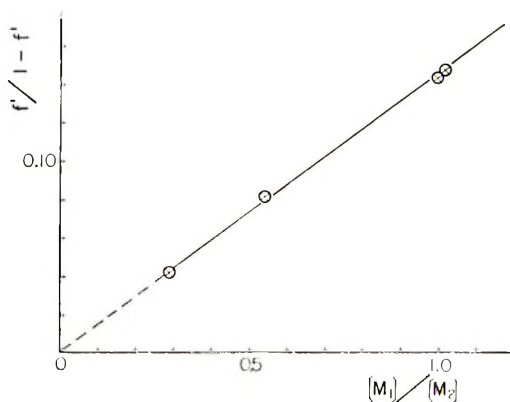
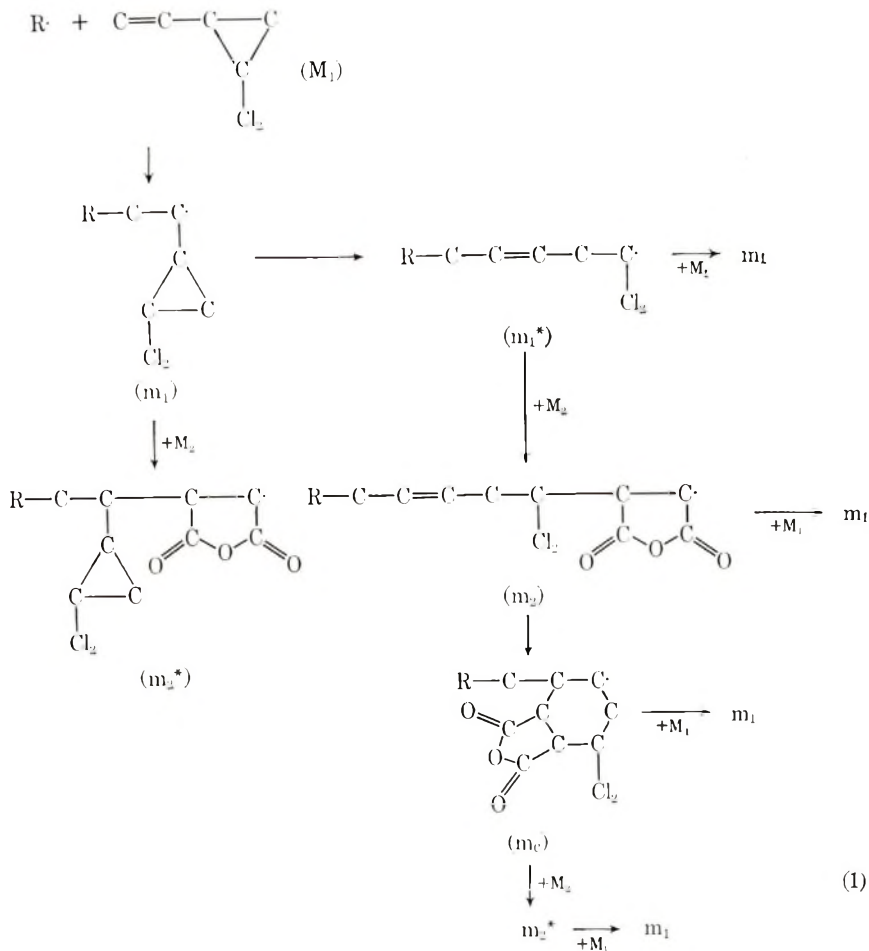


Fig. 1. Plot of  $f'/(1-f')$  vs.  $[M_1]/[M_2]$  (ratio of feed monomers) for bulk copolymerization of 1,1-dichloro-2-vinylcyclopropane ( $M_1$ ) and maleic anhydride ( $M_2$ ).

However, the formation of a molecular complex cannot explain the present results. Moreover, the application of the usual spectroscopic method for confirmation of molecular complex<sup>12</sup> provided no evidence for formation of a complex between diCIVC and MANh. Therefore, the molecular complex between them, if any, must have a very small equilibrium constant value for its formation. This means that, according to the above classification,<sup>11</sup> the present copolymerization pair would give a random copolymer.

Tables I and II show also that the amount of unsaturation in the copolymerized monomer  $M_1$  is small and changes with monomer feed. The small amount of unsaturation might suggest the presence of 1,2-type structural units and/or, because twice as much MANh as diCIVC is capable of copolymerizing, the presence of cyclic structures similar to those in the bimolecular alternating inter-intramolecular copolymerization of divinyl ether with MANh as described by Butler et al.<sup>13,14</sup>

In view of the above, the propagation steps on the copolymerization of diClVC ( $M_1$ ) with MANh ( $M_2$ ) can be illustrated as shown in eqs. (1).



Here  $R\cdot$  denotes an initiator fragment or active polymer end. Addition of monomer  $M_1$  to the radical  $m_1$  is neglected because  $M_1$  gives selectively 1,5-type polymer in the homopolymerization. Additions of monomer  $M_2$  to the radicals  $m_2$  and  $m_2^*$ , which have  $M_2$  in the end, are also neglected. The radical  $m_2$  which has a neighboring unsaturated unit is capable of cyclization as shown.

There are nine propagation steps in this copolymerization [eqs. (2)–(10)].





If the ordinary conditions in the development of copolymer composition equation are assumed, the relative rate of consumption of  $M_1$  and  $M_2$  is given by eq. (11):

$$\frac{d[M_1]}{d[M_2]} = \frac{[M_1]}{[M_2]} \cdot \frac{k_{11}[m_1^*] + k_{21}[m_2] + k_{c1}[m_c] + k_{21'}[m_2^*]}{k_{12}'[m_1] + k_{12}[m_1^*] + k_{c2}[m_c]} \quad (11)$$

Making the stationary-state assumption that the concentrations of radicals  $[m_1^*]$ ,  $[m_2]$ ,  $[m_c]$ , and  $[m_2^*]$  are constant leads to:

$$k_1[m_1] - k_{11}[m_1^*][M_1] - k_{12}[m_1^*][M_2] = 0 \quad (12)$$

$$k_{12}[m_1^*][M_2] - k_c[m_2] - k_{21}[m_2][M_1] = 0 \quad (13)$$

$$k_c[m_2] - k_{c1}[m_c][M_1] - k_{c2}[m_c][M_2] = 0 \quad (14)$$

$$k_{12}'[m_1][M_2] + k_{c2}[m_c][M_2] - k_{21'}[m_2^*][M_1] = 0 \quad (15)$$

Elimination of  $[m_1]$ ,  $[m_1^*]$ ,  $[m_2]$ ,  $[m_c]$ , and  $[m_2^*]$  from eq. (11) by the use of eqs. (12)–(15), gives:

$$\begin{aligned} f &= \frac{d[M_1]}{d[M_2]} \\ &= \frac{1}{[M_2]} \cdot \frac{(1 + a'[M_2])(1 + a[M_1])(r_1[M_1] + [M_2])(r_c[M_1] + [M_2])}{a'(1 + a[M_1])(r_1[M_1] + [M_2])(r_c[M_1] + [M_2]) \\ &\quad + a[M_1](r_c[M_1] + [M_2]) + (r_c[M_1] + 2[M_2])} \end{aligned} \quad (16)$$

where

$$a' = k_{12}'/k_1$$

$$a = k_{21}/k_c$$

$$r_1 = k_{11}/k_{12}$$

$$r_c = k_{c1}/k_{c2}$$

The ratio  $f = d[M_1]/d[M_2]$  denotes by the fractional ratio of monomers combined in the copolymer at low conversions.

A similar equation relating the components of structural units of monomer  $M_1$  in the copolymer can be derived, where  $M_1^*$  is unsaturated (1,5-type) unit in the copolymer:

$$\frac{d[M_1^*]}{d[M_1]} = \frac{[M_1](k_{11}[m_1^*] + k_{21}[m_2])}{[M_1](k_{11}[m_1^*] + k_{21}[m_2] + k_{c1}[m_c] + k_{21}'[m_2^*])} \quad (17)$$

Substituting eqs. (12)–(15) into eq. (17) gives:

$$f' = \frac{d[M_1^*]}{d[M_1]} = \frac{[M_1]\{r_1 + a(r_1[M_1] + [M_2])\}}{(1 + a'[M_2])(1 + a[M_1])(r_1[M_1] + [M_2])} \quad (18)$$

At low conversions, where  $f' = d[M_1^*]/d[M_1] = M_1^*/M_1$ , the ratio of unsaturated monomer  $M_1^*$  to total monomer  $M_1$  in the copolymer, eq. (18) may be applied.

In eq. (16), when the value of  $[M_1]$  is decreased and that of  $[M_2]$  is increased, if the constant  $a'$  equals zero, the equation reduces in the limit to  $f = 1/2$ ; if  $a'$  is not zero, the equation reduces to  $f = 1$ . It seems reasonable to assume that  $a'$  is nearly zero in order to interpret the fact that the composition of the copolymer approaches the value  $M_1:M_2 = 1:2$  in the limiting condition, as shown in Tables I and II. The value  $a' = 0$  suggests that the rearrangement of radical  $m_1$  to  $m_1^*$  is much faster than the attack of  $M_2$  to  $m_1$ . When  $a' = 0$ , eqs. (16) and (18) give eqs. (19) and (20), respectively.

$$f = \frac{1}{[M_2]} \cdot \frac{(1 + a[M_1])(r_1[M_1] + [M_2])(r_c[M_1] + [M_2])}{a[M_1](r_c[M_1] + [M_2]) + (r_c[M_1] + 2[M_2])} \quad (19)$$

$$f' = \frac{[M_1]\{r_1 + a(r_1[M_1] + [M_2])\}}{(1 + a[M_1])(r_1[M_1] + [M_2])} \quad (20)$$

Equation (20) leads to eq. (21):

$$\frac{f'}{1 - f'} = r_1 \frac{[M_1]}{[M_2]} + a \left( r_1 \frac{[M_1]^2}{[M_2]} + [M_1] \right) \quad (21)$$

Figure 1 shows a plot of  $f'/(1 - f')$  against  $[M_1]/[M_2]$  for bulk copolymerization. The plot is a straight line through the origin. It is considered that the constant  $a$  in eq. (21) is nearly zero; therefore,  $r_1$  is obtained from the slope of the straight line in Figure 1 ( $r_1 = 0.15$ ). Values of  $a = 0$  and  $r_1 = 0.10$  were obtained for solution copolymerization in a similar manner. The value  $a = 0$  suggests that predominant reaction of  $m_2$  is cyclization to the radical  $m_c$ .

Equation (19) may be further simplified with  $a = 0$  to give:

$$f = \frac{(r_1[M_1] + [M_2])(r_c[M_1] + [M_2])}{[M_2](r_c[M_1] + 2[M_2])} \quad (22)$$



or

$$f/(r_1F + 1 - f) = r_cF + 1 \quad (23)$$

where  $F = [M_1]/[M_2]$ . A plot of  $f/(r_1F + 1 - f)$  versus  $F$  yields a slope which gives the constant  $r_c$ . The plot was linear as predicted and had a slope  $r_c = 0.90$  and  $0.41$  in bulk and solution copolymerization, respectively. Figure 2 shows the plot in bulk copolymerization.

The copolymer composition curves for bulk and solution copolymerization are shown in Figures 3 and 4. The solid lines are drawn for thus ob-

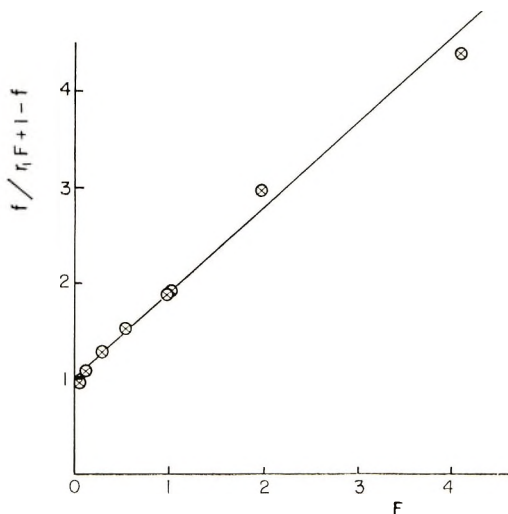


Fig. 2. Plot of  $f/(r_1F + 1 - f)$  vs.  $F$ , where  $F = [M_1]/[M_2]$  (ratio of feed monomers),  $f = d[M_1]/d[M_2]$  (ratio of  $M_1$  to  $M_2$  in copolymer),  $r_1 = 0.15$ , for bulk copolymerization of 1,1-dichloro-2-vinylcyclopropane ( $M_1$ ) and maleic anhydride ( $M_2$ ).

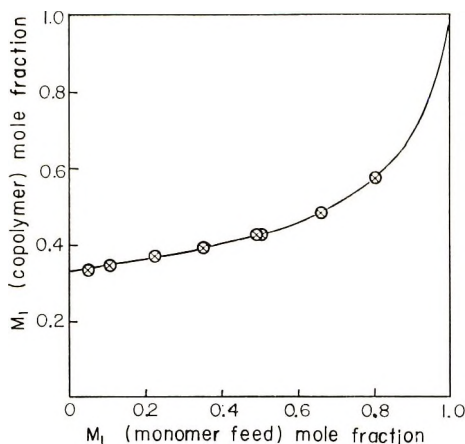


Fig. 3. Bulk copolymerization curve of 1,1-dichloro-2-vinylcyclopropane ( $M_1$ ) and maleic anhydride ( $M_2$ ): (⊗) experimental points; (—) calculated for  $a = a' = 0$ ,  $r_1 = 0.15$ ,  $r_c = 0.90$ .

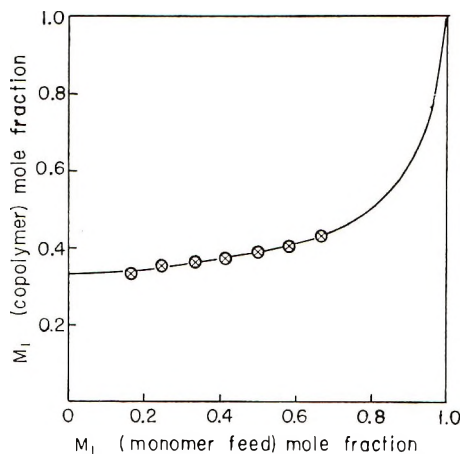


Fig. 4. Solution copolymerization curve of 1,1-dichloro-2-vinylcyclopropane ( $M_1$ ) and maleic anhydride ( $M_2$ ): ( $\otimes$ ) experimental points; (—) calculated for  $a = a' = 0$ ,  $r_1 = 0.10$ ,  $r_c = 0.41$ .

tained constants:  $a = a' = 0$ ,  $r_1 = 0.15$ ,  $r_c = 0.90$ , for bulk copolymerization;  $a = a' = 0$ ,  $r_1 = 0.10$ ,  $r_c = 0.41$ , for solution copolymerization, in eq. (16). They give the best fit to the experimental points.

Constants  $r_1$  and  $r_c$  have the same meaning as monomer reactivity ratios designated in the Mayo-Lewis equation,<sup>15</sup> that is,  $r_1$  is the ratio of the rate constant of monomer  $M_1$  to  $M_2$  for the reaction with radical  $m_1^*$  and  $r_c$  is that for reaction with  $m_c$ . The values obtained for both constants,  $r_1$  and  $r_c$ , were smaller in benzene solution. Similar effects of benzene solvent on radical copolymerization are observed and discussed in terms of the internal dielectric of the reactant molecules,<sup>16</sup> the precipitation of copolymers,<sup>17</sup> and the formation of a complex between the monomer and solvent.<sup>18</sup> In the present case, it seems most reasonable that the increase of the relative reactivity of MAuh by interaction with benzene to form a molecular complex between them<sup>19</sup> influences the copolymerization constants.

## References

1. T. Takahashi and I. Yamashita, *Kogyo Kagaku Zasshi*, **68**, 869 (1965).
2. T. Takahashi, *J. Polym. Sci. A-1*, **6**, 403 (1968).
3. E. S. Huyser and J. D. Taliaferro, *J. Org. Chem.*, **28**, 3442 (1963).
4. I. S. Lishansky, A. M. Guliev, A. G. Zak, O. S. Fomina, and A. S. Khachaturov, *Dokl. Akad. Nauk SSSR*, **170**, 1084 (1966).
5. I. S. Lishansky, A. G. Zak, E. F. Fedorova, and A. S. Khachaturov, *Vysokomol. Soedin.*, **7**, 966 (1965).
6. S. Ota, *Japan Analyst*, **15**, 689 (1966).
7. T. S. Lee, I. M. Kolthoff, and M. A. Maris, *J. Polym. Sci.*, **3**, 66 (1948).
8. P. D. Bartlett and K. Nozaki, *J. Amer. Chem. Soc.*, **68**, 1495 (1946).
9. C. Walling, E. Briggs, K. Wolfstirn, and F. R. Mayo, *J. Amer. Chem. Soc.*, **70**, 1537 (1948).
10. S. Iwatsuki and Y. Yamashita, *Kogyo Kagaku Zasshi*, **67**, 1470 (1964); *ibid.*, **68**, 1138 (1965); *J. Polym. Sci. A-1*, **5**, 1753 (1967).

11. T. Kokubo, S. Iwatsuki, and Y. Yamashita, *Macromolecules*, **1**, 482 (1968).
12. W. C. Vosburgh and G. R. Cooper, *J. Amer. Chem. Soc.*, **63**, 437 (1941).
13. J. M. Barton, G. B. Butler, and E. C. Chapin, *J. Polym. Sci. A*, **3**, 501 (1965).
14. G. B. Butler and K. C. Joyce, in *Macromolecular Chemistry, Brussels-Louvain 1968* (*J. Polym. Sci. C*, **22**), G. Smets, Ed., Interscience, New York, 1968, p. 45.
15. F. R. Mayo and F. M. Lewis, *J. Amer. Chem. Soc.*, **66**, 1594 (1944).
16. C. C. Price and J. G. Walsh, *J. Polym. Sci.*, **6**, 239 (1951).
17. J. Drougas and L. Guile, *J. Polym. Sci.*, **55**, 297 (1961).
18. C. Aso, T. Kunitake, K. Watanabe, paper presented at the 13th Symposium on High Polymers, Tokyo, November 1964.
19. L. J. Andrews and R. M. Keefer, *J. Amer. Chem. Soc.*, **75**, 3776 (1953).

Received September 10, 1969

## Phosphorus-Containing Polyurethans

ELIZABETH DYER and RICHARD A. DUNBAR, *Department of Chemistry, University of Delaware, Newark, Delaware 19711*

### Synopsis

Phosphorus-containing polyurethans of the formula

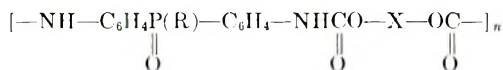


were prepared by interfacial polymerization of 1,4-butanediol and *p*-xylylene- $\alpha,\alpha'$ -bischloroformate with bis(*m*-aminophenyl)alkylphosphine oxides. The polymers had number average molecular weights up to 8600. A test of the stability to alkali of one of the polymers (R=CH<sub>3</sub>, X=1,4-C<sub>6</sub>H<sub>4</sub>) showed it to be as resistant as non-phosphorus analogs, and a film of this polymer exhibited self-extinguishing properties. Thermal degradation of the phosphorus polymers, which began at approximately 230°C, occurred by an initial first-order process, releasing chiefly carbon dioxide. The energies of activation for the maximum rates of weight loss were 31–37 kcal/mole.

### INTRODUCTION

Polyurethans containing phosphorus were previously prepared from phosphorus-containing diisocyanates,<sup>1</sup> triisocyanates,<sup>2,3</sup> or triols,<sup>4</sup> such as RP(O)(NCO)<sub>2</sub>, P(O)(NCO)<sub>3</sub>, P(O)(OC<sub>6</sub>H<sub>4</sub>NCO)<sub>3</sub>, or P(O)(CH<sub>2</sub>OH)<sub>3</sub>. Prepolymers containing hydroxy-terminated phosphonopolyesters have also been used.<sup>5</sup> These polyurethans, which have P—O—C or P—N—C bonds, are susceptible to hydrolysis and subsequent deterioration of the foam or resin.<sup>6</sup>

The object of the present research was to prepare polyurethans with phosphorus-carbon bonds in the backbone; these polymers would be expected to have hydrolytic stability and flame-retardant properties:

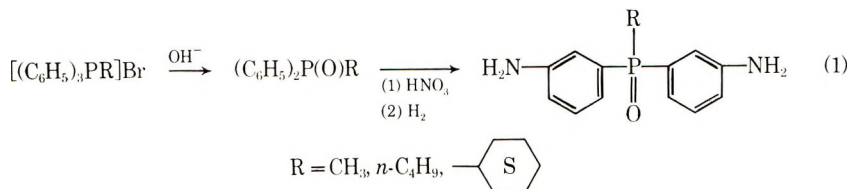


The use of phosphorus-containing diisocyanates was avoided because phosphoryl groups catalyze the formation of carbodiimide units.<sup>7</sup> Hence the reactants chosen were phosphorus-containing diamines and bischloroformates. Phosphorus-containing diamines have been used to prepare polyamides,<sup>8,9</sup> but not polyurethans, so far as the authors are aware.

## RESULTS AND DISCUSSION

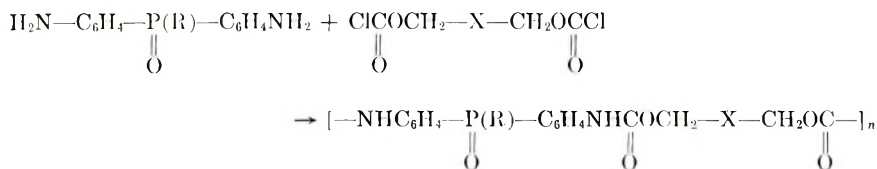
## Preparation of Phosphorus-Containing Polyurethans

The diamine monomers were prepared by nitration and reduction of diaryl phosphine oxides, obtained from decomposition of the corresponding phosphonium salts:



The *n*-butyl bis(*m*-aminophenyl)phosphine oxide is new; the methyl<sup>8</sup> and cyclohexyl<sup>10</sup> derivatives were obtained previously by different initial steps.

The alkyl bis(*m*-aminophenyl) phosphine oxides were polymerized with 1,4-butanediisocyanate or with *p*-xylylene  $\alpha, \alpha'$ -diisocyanate by interfacial methods:



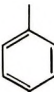
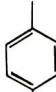
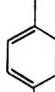
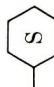
Typical results are shown in Table I. The P-methyl diamines gave polymers I and II by regular interfacial polycondensation<sup>11</sup> procedures; the P-*n*-butyl- and P-cyclohexyldiamines required a modified<sup>12</sup> interfacial technique because of their insolubility in the aqueous phase. With either method, tetrachloroethane gave better yields than dichloroethane, probably because of precipitation of the polymers in the latter solvent.

The polymers were soluble in dimethylformamide, dimethylacetamide, hexamethylphosphoramide, and the fluorinated alcohols. Molecular weights were low, but the highest one (polymer II) is comparable to that of a nonphosphorus polyurethan prepared from 1,6-hexanediamine and 1,6-hexanebiscarbamate.<sup>13</sup>

### Stability of Phosphorus-Containing Polyurethans to Alkaline Hydrolysis

When samples of the phosphorus-containing polymer II were stirred in contact with 1% sodium hydroxide at 50°C for extended periods, practically all of the material was recovered with essentially no change in its viscosity,

TABLE I  
Preparation of Phosphorus-Containing Polyurethans

Polymer No.	R	X	Method <sup>a</sup>	Solvent <sup>b</sup>	Temp., °C		Yield <sup>c</sup> %	$\eta_{inh}^{d,e}$	Method <sup>f</sup>	$\bar{M}_n$	DP <sub>n</sub>
					Initial	Final					
I	CH <sub>3</sub>	(CH <sub>2</sub> ) <sub>2</sub>	I	T	5	6	90	0.23			
I	CH <sub>3</sub>	(CH <sub>2</sub> ) <sub>2</sub>	I	T	25	60	65	0.24			
I	CH <sub>3</sub>	(CH <sub>2</sub> ) <sub>2</sub>	I	D <sup>g</sup>	25	40	44	0.14			
II	CH <sub>3</sub>		I	T	25	60	94	0.89	VPO	8600	20
II	CH <sub>3</sub>		I	D <sup>g</sup>	25	40	76	0.36	BP	3300	8
III	<i>n</i> -C <sub>4</sub> H <sub>9</sub>	(CH <sub>2</sub> ) <sub>2</sub>	MI	T	25	30	70	0.50			
III	<i>n</i> -C <sub>4</sub> H <sub>9</sub>	(CH <sub>2</sub> ) <sub>2</sub>	MI	D <sup>g</sup>	25	40	45	0.11 <sup>h</sup>	VPO	1200	3
IV	<i>n</i> -C <sub>4</sub> H <sub>9</sub>		MI	T	25	60	78	0.50	VPO	4300	9
V		(CH <sub>2</sub> ) <sub>2</sub>	MI	D <sup>g</sup>	25	45	47	0.09 <sup>h</sup>			

<sup>a</sup> I, interfacial method; MI, modified interfacial method; with 0.005–0.008 mole of diamine and of bischloroformate, 0.010–0.016 mole of Na<sub>2</sub>CO<sub>3</sub>, and 0.3–0.6 g. of Duponol ME.

<sup>b</sup> T, tetrachloroethane; D, 1,2-dichloroethane.

<sup>c</sup> After reprecipitation.

<sup>d</sup> In *m*-cresol at 25°C; polymer concentration, 0.5 g./dl.

<sup>e</sup> Dec. temperatures, 225–240°C.

<sup>f</sup> VPO, vapor pressure osmometer with tetrafluoropropanol as solvent; BP, boiling point elevation in hexafluoroisopropanol.

<sup>g</sup> Precipitation of polymer occurred during first 1–2 min of the 5-min reaction time.

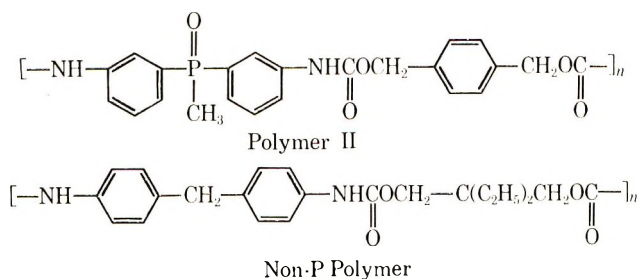
<sup>h</sup> In dimethylformamide at 25°C; polymer concentration, 0.5 g./dl.

TABLE II  
Effect of 1% Sodium Hydroxide at 50°C on Polymer II

Time, hr	Weight recovery, %	Inherent viscosity <sup>a</sup>	
		Original	Recovered
62	97.1	0.42	0.47
105	96.0	0.42	0.44

<sup>a</sup> At a concentration of 0.5 g/dl in *m*-cresol.

as shown in Table II. These results indicate that the resistance of polymer II to base was comparable to that of a nonphosphorus polyurethan previously studied.<sup>14</sup>



### Thermal Stability of Phosphorus-Containing Polyurethans

Data from thermal gravimetric analysis (TGA), given in Table III, shows that the initial temperatures of decomposition of the phosphorus-containing polymers (I-IV) were close to those of analogous nonphosphorus polyurethans. However, the shapes of the TGA curves were somewhat different (Fig. 1). All of the phosphorus polyurethans, illustrated by I and II, showed a region of decreased weight loss after 20-25% decomposition, a behavior not observed with the nonphosphorus polyurethans (VI, VII). This increased stability occurred at a point approaching the theoretical weight loss calculated as carbon dioxide from carbamate groups in polymers II and IV. That this initial decomposition involved breakdown of carbamate groups was confirmed by changes in infrared absorption during the early stages and elementary analyses of the nonvolatile residue (detailed in the Experimental).

The loss of carbon dioxide might occur by a cyclic mechanism (such as postulated<sup>15</sup> for a monomer model) to give a polyamine [eq. (3)].

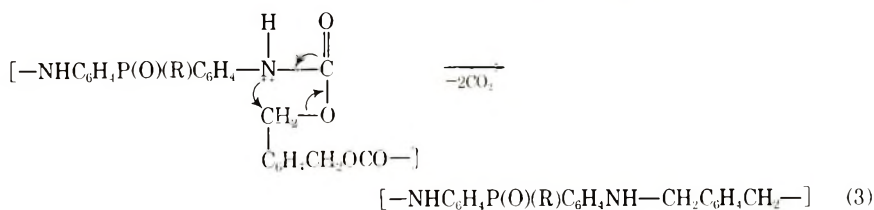


TABLE III  
Thermal Stability of Polyurethans<sup>a</sup>

$$\left[ \text{—NH—Y—NHCOCH}_2\text{—X—CH}_2\text{OC—} \right]_n$$

Polymer no.	Y	X	$\eta_{inh}$	Decomposition temp., °C <sup>b</sup>	$t_{1/2}$ , °C <sup>c</sup>
I		(CH <sub>2</sub> ) <sub>2</sub>	0.24 0.31	230 230	340
II			0.31 0.89 <sup>d</sup> 1.10	230 230 225	450 500 440
III		(CH <sub>2</sub> ) <sub>2</sub>	0.11 0.46	230 230	375
IV			0.50	235	455
VI		(CH <sub>2</sub> ) <sub>2</sub>	0.85	240	325
VII			1.00	230	375

<sup>a</sup> In *m*-cresol at 25°C; polymer concentration, 0.5 g./dl.

<sup>b</sup> Temperature of initial decomposition at a heating rate of 10°C/min under nitrogen.

<sup>c</sup> Temperature of 50% decomposition.

<sup>d</sup> Obtained by fractionation of polymer II having  $\eta_{inh} = 0.89$ .

The phosphorus polyurethans could undergo this type of decomposition somewhat more readily than the nonphosphorus polyurethans because of the possibility of intermolecular hydrogen bonding<sup>16</sup> between the oxygen of the phosphoryl group and the NH hydrogen, thus making the N of the NH more nucleophilic. The ready formation of polyamine groups in the phosphorus polyurethans would explain the subsequent region of slower decomposition in the TGA curves, because polyamines have been shown<sup>17</sup> to decompose more slowly than polyurethans. For example, the polyamine corresponding to polyurethan VII was 50% decomposed<sup>17</sup> at 550°C, whereas the polyurethan VII was 50% decomposed at 375°C (Table III).

#### Activation Energies for Thermal Degradation

Rates of decomposition of the phosphorus and nonphosphorus polyurethans were obtained by using the thermogravimetric analyzer to record weight loss with time at constant temperatures. Again, a difference in the shape of the graphs for the two types of polymers was observed. The phosphorus polymers lost weight in a linear fashion for the first 10% of decomposition and then the rate decreased considerably; the nonphos-



phorus polymers showed an increasing rate of weight loss up to a maximum at 25–35% degradation.

The activation energies were obtained from graphs of the maximum rates of volatilization against the reciprocal of absolute temperature. The  $k$  values for maximum rates of weight loss (conveniently determined from plots of the first derivative<sup>13</sup> of the weight loss versus time) are given in Table IV for polymers I, II, VI, and VII.

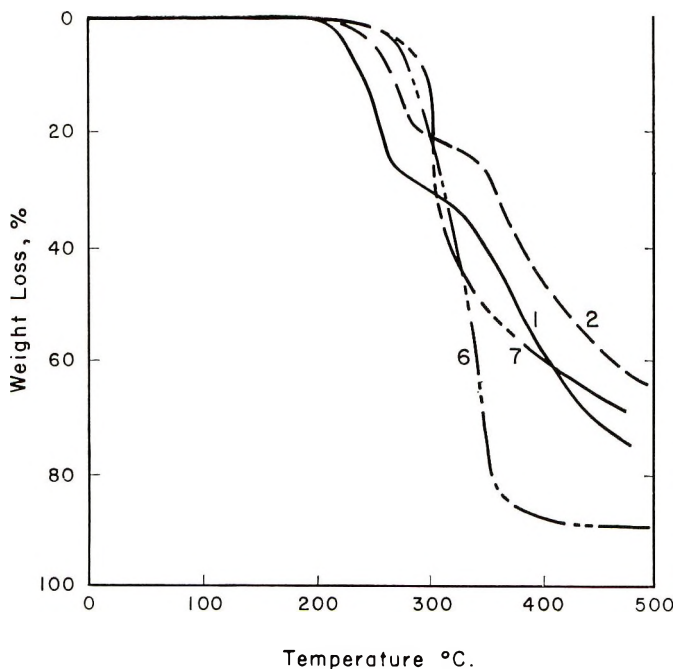


Fig. 1. Thermogravimetric analyses of polyurethans,  $[-\text{NH}-\text{Y}-\text{NHCOCH}_2-\text{X}-$

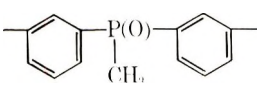

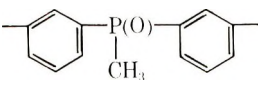
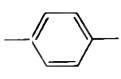
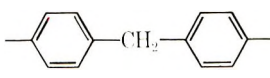
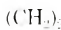
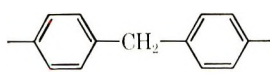
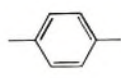
$\text{CH}_2\text{OC}-]_n$ : (1) (—) polymer I,  $\text{Y} = 3,3'-\text{C}_6\text{H}_4\text{P}(\text{O})(\text{CH}_3)-\text{C}_6\text{H}_4$ ,  $\text{X} = (\text{CH}_2)_2$ ;

(2) (---) polymer II,  $\text{Y} = 3,3'-\text{C}_6\text{H}_4\text{P}(\text{O})(\text{CH}_3)-\text{C}_6\text{H}_4$ ,  $\text{X} = 1,4-\text{C}_6\text{H}_4$ ; (6) (- - -) polymer VI,  $\text{Y} = 4,4'-\text{C}_6\text{H}_4\text{CH}_2\text{C}_6\text{H}_4$ ,  $\text{X} = (\text{CH}_2)_2$ ; (7) (- - - -) polymer VII,  $\text{Y} = 4,4'-\text{C}_6\text{H}_4\text{CH}_2\text{C}_6\text{H}_4$ ;  $\text{X} = 1,4-\text{C}_6\text{H}_4$ . Heating rate  $10^\circ\text{C}/\text{min}$  under nitrogen.

Typical Arrhenius plots (for polymers I and II) are shown in Figure 2. The  $E_A$  values for the phosphorus and nonphosphorus polymers were of the same order of magnitude. They were also consistent with the  $E_A$  value found previously<sup>13</sup> by a different method (determination of carbon dioxide) for a similar nonphosphorus polyurethan. This polyurethan, in which  $\text{Y}$  was the same as in polymer VI and  $\text{X}$  was  $(\text{CH}_2)_8$ , had an  $E_A$  value of 34 kcal/mole.<sup>13</sup>

TABLE IV  
Rates of Decomposition and Activation Energies of Polymers

$$\left[ \text{—NH—Y—NHC(=O)CH}_2\text{—X—CH}_2\text{OC(=O)—} \right]_n$$

Polymer no.	Y	X	Temp., °C	k, %/min <sup>a</sup>	E <sub>A</sub> , kcal./mole
I			206	0.078	37
			213	0.173	
			217	0.217	
			217	0.214	
			223	0.306	
			226	0.390	
II			223	0.147	31
			225	0.169	
			230	0.274	
			245	0.605	
			251	0.780	
			255	0.815	
VI			250	0.470	34
			255	0.696	
			257	0.702	
			263	1.04	
			263	1.14	
			267	1.30	
VII			260	0.400	39
			268	0.720	
			268	0.742	
			274	1.14	
			274	1.26	
			284	2.00	

<sup>a</sup> Expressed as maximum per cent volatilization per minute under nitrogen.

## EXPERIMENTAL

### Preparation of Monomers and Model Compounds

#### Diamines

Alkyldiphenylphosphine oxides were prepared by alkaline decomposition<sup>19</sup> of the corresponding alkyltriphenylphosphonium bromides; these were purchased except for the cyclohexyltriphenylphosphonium bromide, made from triphenylphosphine and cyclohexyl bromide.<sup>20</sup> The yields and melting points of R(C<sub>6</sub>H<sub>5</sub>)<sub>2</sub>PO were: R = CH<sub>3</sub> (84%), mp 112°C, lit.<sup>21,22</sup> 110–111°C; R = n-C<sub>4</sub>H<sub>9</sub> (89%), mp 92°C, lit.<sup>23</sup> 95°C; R = C<sub>6</sub>H<sub>11</sub> (75%), mp 168°C, lit.<sup>19</sup> 165–166°C. For the last two substances the literature gives methods different from the one used here.

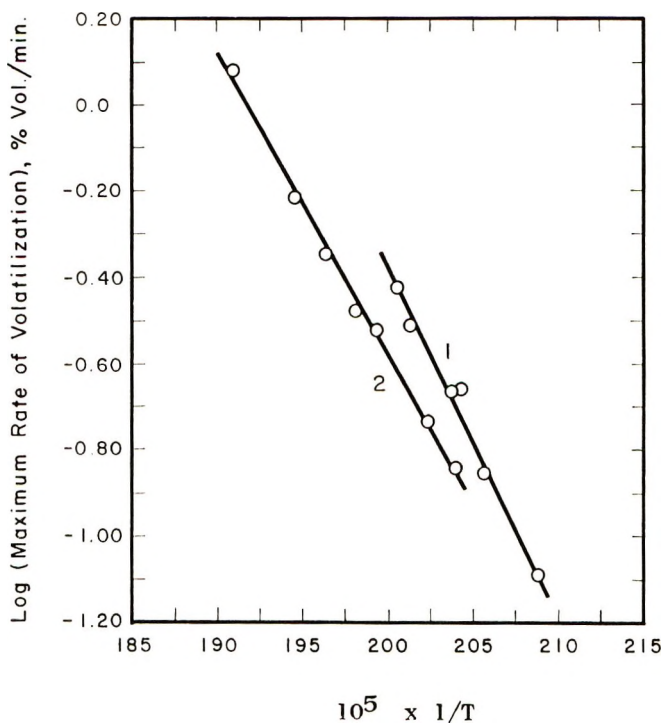


Fig. 2. Plots of log maximum rate of decomposition vs. the reciprocal of the absolute temperature for polymers I and II,  $[-NH-C_6H_4-P(O)(CH_3)-C_6H_4-NHCO_2CH_2-X-CH_2OCO]_n$ : (1) polymer I, X =  $(CH_2)_2$ ; (2) polymer II, X = 1,4- $C_6H_4$ .

Nitration of the alkyldiphenylphosphine oxides according to the method of Bride et al.<sup>24</sup> produced the following alkyldi (*m*-nitrophenyl)phosphine oxides,  $R(m-NO_2C_6H_4)_2PO$ : R =  $CH_3$  (77%), mp 200°C, lit.<sup>24</sup> 205°C; R = *n*- $C_4H_9$  (53%), mp 125°C, lit.<sup>25</sup> 124–125°C; R =  $C_6H_{11}$  (68%), mp 202°C, lit.<sup>10</sup> 200°C.

Catalytic hydrogenation<sup>25</sup> of the alkyldi (*m*-nitrophenyl)phosphine oxides gave the following diamines, which were recrystallized from ethyl acetate and checked for purity by thin layer chromatography.  $R(m-NH_2C_6H_4)_2PO$ : R =  $CH_3$  (79%), mp 145°C, lit.<sup>8</sup> 145–147°C; R =  $C_6H_{11}$  (84%), mp 225–228°C, lit.<sup>10</sup> 222°C; R = *n*- $C_4H_9$  (43%), mp 140°C.

ANAL. Calcd for (R =  $C_4H_9$ ) $C_{16}H_{21}N_2OP$ : C, 66.65%; H, 7.34%; N, 9.72%. Found: C, 66.45%; H, 6.93%; N, 9.55%.

#### Bischloroformates

The usual procedure<sup>26</sup> for phosgenation of the corresponding diols was used to prepare both 1,4-butanebischloroformate and *p*-xylylene- $\alpha,\alpha'$ -bischloroformate. The latter compound, which is new, was obtained in 97% yield (mp 53–55°C from *n*-hexane). It was converted to the bisurethan, mp 216–218°C, with cold concentrated ammonium hydroxide for analysis.

ANAL. Calcd for  $C_{10}H_{12}N_2O_4$ : C, 53.56%; H, 5.40%; N, 12.50%. Found: C, 53.43%; H, 5.46%; N, 12.32%.

### *Biscarbamates (Model Compounds)*

***p*-Xylylenebis(dimethylphosphorylphenyl carbamate).** Nitration of phenyldimethylphosphine oxide,<sup>27</sup> extraction with chloroform, and precipitation with benzene gave *m*-nitrophenyldimethylphosphine oxide in 60% yield, mp 194–195°C.

ANAL. Calcd for  $C_9H_{10}NO_3P$ : C, 48.24%; H, 5.03%; N, 7.03%. Found: C, 48.24%; H, 5.20%; N, 7.21%.

Hydrogenation of this nitro compound with platinum oxide in methanol followed by recrystallization from 20:1 benzene–methanol gave *m*-aminophenyldimethylphosphine oxide in 80% yield, mp 165–167°C.

ANAL. Calcd for  $C_8H_{12}NOP$ : C, 56.79%; H, 7.15%; N, 8.28%. Found: C, 56.43%; H, 7.38%; N, 8.12%.

To a solution of 0.0076 mole of *m*-aminophenyldimethylphosphine oxide in 50 ml of methylene chloride was added a solution of 0.0019 mole of *p*-xylylene- $\alpha,\alpha'$ -bischloroformate in 10 ml of methylene chloride, and the mixture was stirred for 3 hr at 23–25°C. The resulting precipitate, washed with water to remove amine hydrochloride and recrystallized from ethanol–water (1:1), melted at 244–246°C (dec.) (70%).

ANAL. Calcd for  $C_{26}H_{30}N_2O_6P_2$ : C, 59.08%; H, 5.72%; N, 5.30%. Found: C, 58.88%; H, 5.98%; N, 5.37%.

**1,4-Butylenebis(dimethylphosphorylphenyl carbamate).** By a procedure similar to the above, 1,4-butylenebischloroformate<sup>28</sup> gave an 81% yield of this biscarbamate, mp 241–245°C (dec.).

ANAL. Calcd for  $C_{22}H_{32}N_2O_6P_2$ : C, 54.77%; H, 6.68%. Found: C, 55.02%; H, 6.44%.

## Preparation of Polyurethans

### *Interfacial Polymerization*

The procedure used for polymers I, II, VI, and VII is illustrated for polymer II. In a Waring Blender was placed 50 ml of a cold (0–5°C) aqueous solution of 2.0 g (0.008 mole) of methyldi(*m*-aminophenyl)phosphine oxide, 1.73 g (0.016 mole) of sodium carbonate, and 0.6 g of Duponol ME. At maximum speed of stirring a solution of 2.14 g (0.008 mole) of *p*-xylylene- $\alpha,\alpha'$ -bischloroformate in 50 ml of tetrachloroethane was rapidly added. After 5 min the reaction was quenched with cyclohexane. The filtered polymer was washed successively in the blender with water, ethanol, and ether, and dried *in vacuo* at 50–57°C to give 3.3 g of II as a light tan powder which held 0.5 mole of water. A 2.0-g sample was purified by dissolving it in 150 ml of 3:2 dimethylformamide–dimethyl sulfoxide and adding the solution to 2 liters of rapidly stirred distilled water. The fine

TABLE V  
 Analyses of Polyurethans

Polymer no. <sup>a</sup>	Repeating unit	C, %		H, %		N, %	
		Calcd	Found	Calcd	Found	Calcd	Found
I	C <sub>19</sub> H <sub>21</sub> N <sub>3</sub> O <sub>5</sub> P	58.76	59.07	5.45	5.61	7.21	7.37
II	C <sub>23</sub> H <sub>21</sub> N <sub>2</sub> O <sub>5</sub> P	63.30	63.17	4.85	4.73	6.42	6.62
III	C <sub>22</sub> H <sub>27</sub> N <sub>2</sub> O <sub>5</sub> P	61.38	61.41	6.32	6.23	6.51	6.71
IV	C <sub>26</sub> H <sub>27</sub> N <sub>2</sub> O <sub>5</sub> P	65.26	64.95	5.96	5.90		
V	C <sub>24</sub> H <sub>29</sub> N <sub>2</sub> O <sub>5</sub> P	63.14	63.32	6.40	6.62	6.14	6.37
VII	C <sub>23</sub> H <sub>20</sub> N <sub>2</sub> O <sub>4</sub>	71.10	70.69	5.19	5.32	7.21	7.00

<sup>a</sup> Numbers refer to polymers of Tables I, III, and IV.

precipitate, after washing with four 300-ml portions of water and one 300-ml portion of ethanol and drying at 120°C/1–3 mm, gave a 75–90% recovery of pure anhydrous polymer; its properties are summarized in Table I, and analysis is given in Table V.

Polymers VI and VII were obtained in yields of 80% and 90%, respectively, from methylenedianiline and the appropriate bischloroformate. Polymer VI was previously prepared by the isocyanate-diol method.<sup>29</sup> Polymer VII has been recently obtained by the isocyanate method and its thermal decomposition studied.<sup>30</sup>

#### Modified Interfacial Method

The preparation of polymer III is typical of the method used for polymers III, IV, and V. To 50 ml of an aqueous solution containing 1.2 g (0.01 mole) of sodium carbonate and 0.3 g of Duponol ME in a jacketed blender cooled with tap water was added 40 ml of a tetrachloroethane solution containing 1.5 g (0.006 mole) of *n*-butyl-di(*m*-aminophenyl)phosphine oxide. At full speed of stirring 10 ml of a tetrachloroethane solution containing 1.3 g (0.006 mole) of 1,4-butylenebischloroformate<sup>28</sup> was rapidly added, and the stirring continued for 10 min with the inside temperature at 25–30°C. Subsequent isolation and purification as in method A gave 1.6 g (70%) of polymer, described in Tables I and V.

#### Molecular Weights of Polyurethans

A Hewlett-Packard model 301A vapor pressure osmometer was used to determine the molecular weights of polymers II, III, and IV in tetrafluoro-propanol. The instrument and the solvent were calibrated with the model compounds *p*-xylylenebis(dimethylphosphorylphenyl carbamate) and 1,4-butylenebis(dimethylphosphorylphenyl carbamate). For the ebullioscopic molecular weight of polymer II in hexafluoroisopropanol the same model biscarbamates were used to secure the  $K_b$  of the solvent.

#### Thermal Degradation of Polymers

Thermogravimetric data were secured on a duPont model 950 TGA used in conjunction with a 900 DTA in an atmosphere of nitrogen.

In the TGA curves of polymers II and IV, the loss in weight up to the point of decreasing slope could be accounted for as carbon dioxide (calcd 20% for II and 18% for IV; found 18, 19, and 21% for three samples of II and 19% for IV). That this loss of carbon dioxide came from carbamate groups was shown by infrared spectra of polymer II after 0, 14, and 24% degradation, when there was a progressive decrease in the C=O and C—O—C absorption at 1740 and 1220  $\text{cm}^{-1}$ , respectively. In another experiment, a sample of polymer II was degraded to 15.8% weight loss, and the residue analyzed. The calculated composition, on the assumption of 15.8% loss of  $\text{CO}_2$  from carbamate groups was 70.0% C, 5.8% H, 7.8% N, 8.5% P; the found values were 69.0% C, 6.2% H, 7.7% N, 8.5% P.

When a 2.301 g sample of polymer II was heated at 220–230°C under a stream of dry nitrogen for 4 hr, with provision for collection of products in Ascarite and cold traps, the loss in weight of the polymer was 5.8%; 92% of this was due to carbon dioxide, and 4% was due to  $\alpha, \alpha'$ -*p*-xylylenediol, which distilled from the reaction flask. The nonvolatile residue was insoluble in ethanol and in chloroform. Extraction with 1:1 DMSO–formic acid removed 0.45 g of unchanged polymer II; the residual insoluble material was unidentified.

Analyses of products were not done on polymers I and III prepared from butylenebiscarbamate. Data from the TGA curves at the point of decreasing slope indicated that carbon dioxide was not the sole volatile product. (The weight loss calculated was 23% for I and 21% for II; found, 32% and 27%, respectively.)

This paper was abstracted from the Ph.D. dissertation (1967) of Richard A. Dunbar, Armstrong Cork Company Research Fellow, 1964–1967.

## References

1. A. C. Haven, Jr., *J. Amer. Chem. Soc.*, **78**, 842 (1956).
2. H. C. Fielding, Brit. Pat., 982, 931 (1965).
3. H. Holtzschmidt and G. Oertel, *Angew. Chem. Internat. Ed.*, **1**, 617 (1962).
4. L. M. Kendley, H. E. Podall, and N. Filipescu, *SPE Trans.*, 122 (1962).
5. R. L. McConnell and H. W. Coover, Jr., U. S. Pat. 2,926,145 (1960).
6. A. F. Childs and H. Coates, *Kunststoffe*, **54**, 501 (1964).
7. T. W. Campbell, J. J. Monagle, and V. S. Foldi, *J. Amer. Chem. Soc.*, **84**, 3673 (1962).
8. T. Ya. Medved', T. M. Frunze, C.-M. Khu, V. V. Kurashev, V. V. Korshak, and M. I. Kabachnik, *Polymer Sci. USSR*, **5**, 386 (1964).
9. J. Pellon and W. G. Carpenter, *J. Polym. Sci. A*, **1**, 863 (1963).
10. Rhone-Poulenc S. A., Fr. Addn. Pat. 82,481 (1964).
11. E. L. Wittbecker and M. Katz, *J. Polym. Sci.*, **40**, 374 (1959).
12. P. W. Morgan, *Condensation Polymers*, Interscience, New York, 1965, pp. 103, 492.
13. E. Dyer and R. J. Hammond, *J. Polymer Sci. A*, **2**, 1 (1964).
14. E. Dyer and G. W. Bartels, Jr., *J. Amer. Chem. Soc.*, **76**, 591 (1954).
15. E. Dyer and R. E. Read, *J. Org. Chem.*, **26**, 4388 (1961).
16. R. F. Hudson, *Structure and Mechanism in Organo-Phosphorus Chemistry*, Academic Press, New York, 1965, p. 281.
17. E. Dyer and C. C. Anderson, *J. Polym. Sci. A-1*, **5**, 1665 (1967).

18. S. D. Bruck, *Polymer*, **6**, 483 (1965).
19. L. Horner, H. Hoffmann, and H. G. Wippel, *Chem. Ber.*, **91**, 64 (1958).
20. H. J. Bestmann and O. Kratzer, *Chem. Ber.*, **96**, 1899 (1963).
21. A. Michaelis and H. von Soden, *Ann.*, **229**, 316 (1885).
22. G. Wittig and G. Geissler, *Ann.*, **580**, 44 (1953).
23. W. Kuchen and H. Buchwald, *Angew. Chem.*, **69**, 307 (1957).
24. M. H. Bride, W. A. W. Cummings, and W. Pickles, *J. Appl. Chem.*, **11**, 352 (1961).
25. D. C. Morrison, *J. Amer. Chem. Soc.*, **72**, 4820 (1950).
26. W. Sorenson and T. W. Campbell, *Preparative Methods of Polymer Chemistry*, Interscience, New York, 1961, p. 106.
27. G. Aksnes and L. J. Brudvik, *Acta Chem. Scand.*, **17**, 1616 (1963).
28. Y. Iwakura, M. Sakamoto, and H. Yasuda, *Nippon Kagaku Zasshi*, **82**, 606 (1961).
29. E. Dyer and D. W. Osborne, *J. Polymer Sci.*, **47**, 369 (1960).
30. J. K. Backus, D. L. Bernard, W. C. Darr, and J. H. Saunders, *J. Appl. Polym. Sci.*, **12**, 1053 (1968).

Received August 14, 1969

Revised September 10, 1969

## Graft Copolymerization of Methyl Methacrylate to Poly(vinyl Alcohol) Initiated by Ferric Ion-Hydrogen Peroxide System

YOSHITAKA OGIWARA and MASAHIRO UCHIYAMA, *Faculty of Engineering, Gunma University, Kiryu, Japan*

### Synopsis

The reaction occurring on treatment of samples of poly(vinyl alcohol) previously oxidized by sodium hypochlorite with ferric ion and hydrogen peroxide was studied. The graft copolymerization taking place on adding methyl methacrylate to the above system was also studied. Early in the reaction there was a period during which hydrogen peroxide was greatly reduced by the poly(vinyl alcohol), and this corresponded with a rapid cleavage reaction of the main chain of the polymer. Moreover, it was found that the reaction was quantitatively proportional to the formation of carbonyl groups in the sample. On the other hand, very few grafts were scarcely formed during this period; they formed by a mild reaction which took place immediately after this period. It seems that this behavior is quite different from that observed with the ceric ion initiating system. It is presumed that the formation of grafts is due to radicals formed by the cleavage of the main chain, and that the structure of the copolymer so formed is something like a block polymer.

### INTRODUCTION

In a previous paper,<sup>1</sup> we studied the reaction between ceric ion and poly(vinyl alcohol) having carbonyl groups introduced in the main chain by an oxidation treatment and investigated the formation of grafts by an addition of methyl methacrylate. This study indicated that there is cleavage of the main chain with a faster rate in the early stage of the reaction, that the graft copolymerization is initiated by radicals formed at the same time, and that the cleavage reaction depends mostly on the carbonyl groups in the main chain. We presumed that the structure of the copolymer obtained should be something like a block polymer.

We have also examined<sup>2</sup> the reaction between a cellulosic material on which ferric ions had been adsorbed and hydrogen peroxide, and the graft copolymerization by addition of methyl methacrylate. We observed that there is a rapid reduction of the hydrogen peroxide in the early stage of reaction; even though the cellulose chain is cleaved due to such reduction, there is scarcely any formation of grafts from the cellulosic material at this stage of the reaction.



The purpose of this paper is to examine the reaction in the system of ferric ions, hydrogen peroxide, and poly(vinyl alcohol) and to study the graft copolymerization by addition of methyl methacrylate to this system to obtain fundamental information about initiation mechanisms of the graft copolymerization on the cellulosic material.

## EXPERIMENTAL

### Sample

Oxidized poly(vinyl alcohol) was prepared in the same manner as described in the previous paper.<sup>1</sup> Table I shows oxidation conditions, carbonyl contents, and degrees of polymerization. A commercial methyl methacrylate was purified and used. Commercial hydrogen peroxide (30% concentration) was diluted to a certain concentration and used. A reagent grade ferric chloride was employed as ferric ions, and its purity was determined by iodometry.

TABLE I  
Preparation and Analysis of Poly(vinyl Alcohol) Samples

Sample	Amount of sodium hypochlorite for PVA, % <sup>a</sup>	Total carbonyl content, mmole per 100g of PVA	Average degree of polymerization
1	0 <sup>b</sup>	0.0	1230
2	0.59 <sup>c</sup>	7.6	1445
3	0.59 <sup>d</sup>	10.8	1205
4	0.64 <sup>d</sup>	18.8	1490

<sup>a</sup> Values are presented as weight per cent of available chlorine for PVA.

<sup>b</sup> Rinsed with water and acetone.

<sup>c</sup> Oxidation time; 1 hr.

<sup>d</sup> Oxidation time; 2 hr.

### Reaction in the Ferric Ion-Hydrogen Peroxide-Poly(vinyl Alcohol) System

A given amount of aqueous ferric ion solution was added with stirring under nitrogen to 150 ml of aqueous solution in a reaction flask in which 3.00 g of poly(vinyl alcohol) had been dissolved. Then a specified amount of hydrogen peroxide was added, and the total was made up to 240 ml with distilled water. After that, aliquots of 20 ml were taken from the reaction system at each given time for measurement. The reaction in the samples was stopped with 3*N* sulfuric acid, and the unreacted hydrogen peroxide was measured with 0.01*N* potassium permanganate. The reaction temperature was 45°C, the concentration of the ferric ion used in the reaction was 1 mmole/l, and that of hydrogen peroxide 10 mmole/l. The degree of polymerization of poly(vinyl alcohol) was determined in accordance with Nakajima's equation<sup>3</sup> from the viscosity of aqueous solutions.

### Graft Copolymerization

Given amounts of aqueous solution of ferric ion and hydrogen peroxide were in turn added to 25 ml of an aqueous solution containing 0.50 g of poly(vinyl alcohol) and 2.5 ml of methyl methacrylate in a nitrogen substitution system to make a total of 42.5 ml. Then the polymerization was carried out at 45°C and it was stopped by hydroquinone. The separation and determination of the grafts were carried out in the manner described in the previous paper.<sup>1</sup> The number of grafts was indicated as the millimoles of grafts per 100 g of poly(vinyl alcohol) employed.

### RESULTS AND DISCUSSION

Figure 1 shows the changes in the concentration of hydrogen peroxide with time in reactions among poly(vinyl alcohol), ferric ion, and hydrogen peroxide. After about 40 min, almost all the hydrogen peroxide was reduced, and the greater the carbonyl content in the sample, the faster the rate of reduction of the hydrogen peroxide. In the reaction, it may be conceivable that the reduction of hydrogen peroxide occurs simultaneously with the cleavage of the main chain of poly(vinyl alcohol). Thus, the amount of cleavage was calculated from the change in the degree of polymerization; results are shown in Figure 2 with the elapse of time. For each sample there is a sharp cleavage early in the reaction, and the greater the carbonyl content in the sample, the faster the rate of cleavage and the greater the equilibrium value of the amount of cleavage.

With respect to an unoxidized sample, it is found that over a period of several minutes at the beginning, there is an induction period followed by a sharp cleavage. It may be that a new oxidized group introduced by the hydrogen peroxide into the main chain participates in the cleavage. It is

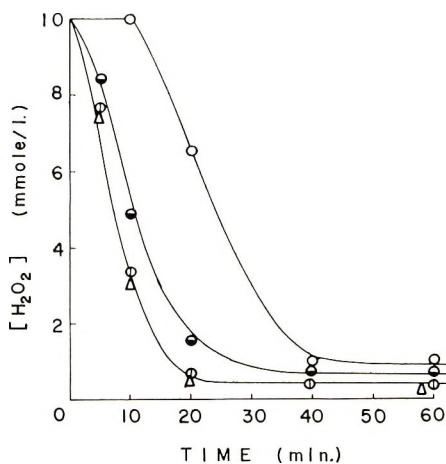


Fig. 1. Changes of the concentration of hydrogen peroxide with time at various total carbonyl contents of PVA (mmole/100 g of PVA): (O) 0; (●) 7.6; (⊙) 10.8; (Δ) 18.8. Reaction temperature, 45°C;  $[Fe^{3+}]$ , 1 mmole/l.;  $[H_2O_2]$ , 10 mmole/l.

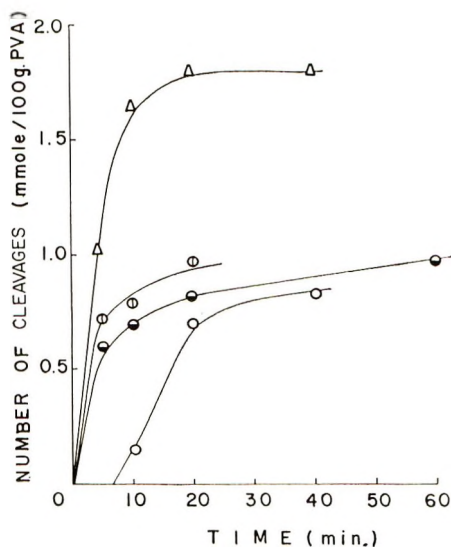


Fig. 2. Changes of the number of cleavages of the PVA chain with time at various total carbonyl contents of PVA (mmole/100 g of PVA): (○) 0; (◐) 7.6; (◑) 10.8; (△) 18.8. Reaction temperature, 45°C;  $[Fe^{3+}]$ , 1 mmole/l.;  $[H_2O_2]$ , 10 mmole/l.

possible also, that this corresponds with the fact that the unoxidized sample shows a only very small reduction in amount of hydrogen peroxide during a period of several minutes at the beginning of the reaction, as may be seen from Figure 1. Sakurada et al.<sup>4</sup> examined the relation between the number of cleavages of the main chain in an oxidative decomposition of the poly(vinyl alcohol) by means of potassium permanganate and the consumption of the potassium permanganate, and reported that the hydroxyl group in the poly(vinyl alcohol) is oxidized to a keto group, where the oxidation cleavage occurs. Shiraishi et al.<sup>5</sup> also reported a cleavage mechanism of poly(vinyl alcohol) samples containing no carbonyl group at all in an alkaline medium, in which the poly(vinyl alcohol) is first oxidized and a carbonyl group is formed in the main chain, and this group is responsible for the cleavage of the main chain.

Methyl methacrylate was added to the above system, and the graft copolymerization to poly(vinyl alcohol) was carried out. The relation between the number of grafts and the time of polymerization is shown in Figure 3. It is found that in the formation reaction of grafts in any sample there exists an induction period of about 10 min after the initiation of the reaction, and that an equilibrium value is reached in about 60 min. Moreover, the greater the carbonyl content, the smaller the equilibrium value. A comparison between Figures 2 and 3 shows that in the oxidized sample there is clearly a time lag between the cleavage of the main chain and the formation reaction of grafts. This is a sharp contrast to the relation in which a violent cleavage of the main chain at the early stage of a reaction initiated by ceric ions has a direct bearing on the formation of grafts.

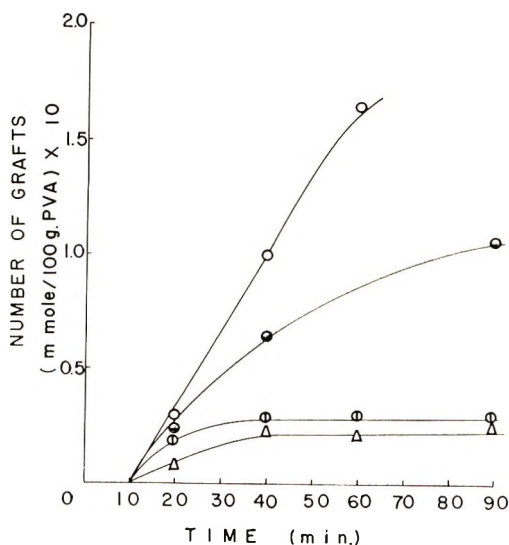


Fig. 3. Changes of the number of grafts with time at various total carbonyl contents of PVA (mmole/100 g of PVA): (○) 0; (●) 7.6; (◻) 10.8; (△) 18.8. Reaction temperature, 45°C;  $[Fe^{3+}]$ , 1 mmole/l.;  $[H_2O_2]$ , 10 mmole/l.

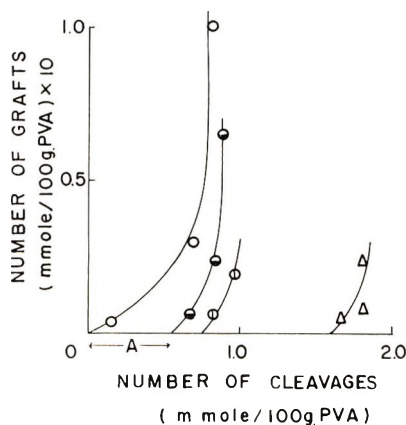


Fig. 4. Relationship of the number of grafts to the number of cleavages at various total carbonyl contents of PVA (mmole/100 g of PVA): (○) 0; (●) 7.6; (◻) 10.8; (△) 18.8. Reaction temperature, 45°C;  $[Fe^{3+}]$ , 1 mmole/l.;  $[H_2O_2]$ , 10 mmole/l.

Figure 4 shows the relation between the amount of cleavage of each sample during various reaction periods and the number of grafts. By extrapolating the curve of the graph of each sample and finding a point at which the extrapolated curve and the abscissa cross each other, it is possible to estimate the amount of cleavage which seems not to be directly connected with the formation of grafts, the amount is indicated as  $A$ .

In Figure 5, it is found that the greater the carbonyl content in each sample, the greater  $A$  is, and that there is approximately a linear relation-

ship between the two. Thus, it is not difficult to presume that cleavage which is unrelated to the formation of grafts of the oxidized sample may occur by the carbonyl groups introduced already into the main chain of

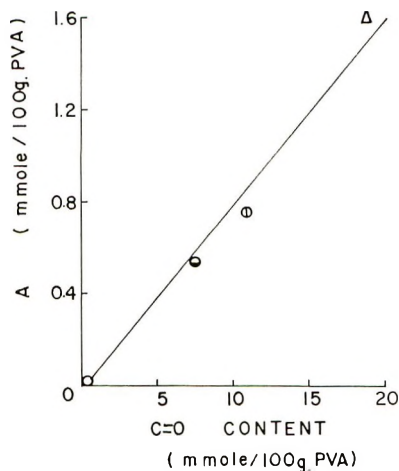


Fig. 5. Relationship of *A* to the total carbonyl contents at various total carbonyl contents of PVA (mmole/100 g of PVA): (○) 0; (●) 7.6; (⊕) 10.8; (Δ) 18.8.

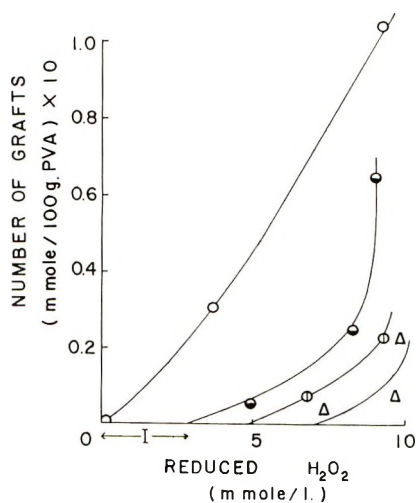


Fig. 6. Relationship of the number of grafts to amount of reduced amount of hydrogen peroxide at various total carbonyl contents of PVA (mmole/100 g of PVA): (○) 0; (●) 7.6; (⊕) 10.8; (Δ) 18.8. Reaction temperature, 45°C; [Fe<sup>3+</sup>], 1 mmole/l.; [H<sub>2</sub>O<sub>2</sub>], 10 mmole/l.

poly(vinyl alcohol), and that such cleavage may occur at the neighboring bond. Takayama<sup>6</sup> reported that in the reaction between hydrogen peroxide and poly(vinyl alcohol) having carbonyl groups in the main chain as

a result of photooxidation, the rate of cleavage is obviously faster than that of unoxidized poly(vinyl alcohol); he also reported that there is a linear relationship between the amount of cleavage and of the carbonyl content,

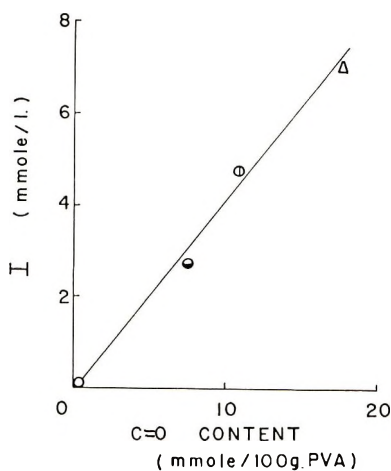


Fig. 7. Relationship of  $I$  to the total carbonyl contents at various total carbonyl contents of PVA (mmole/100 g of PVA): (○) 0; (●) 7.6; (⊕) 10.8; (△) 18.8.

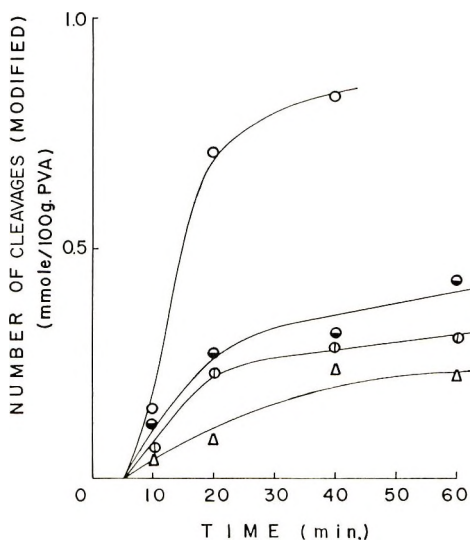


Fig. 8. Changes of the modified number of cleavage with time at various total carbonyl contents of PVA (mmole/100 g of PVA): (○) 0; (●) 7.6; (⊕) 10.8; (△) 18.8.

and that in such a reaction the bond next to the carbonyl group is apt to be cleaved.

In Figure 2, it is shown that the time required for the main chain of the unoxidized sample to begin to cleave is about 5 min, and the amount of

cleavage of each sample during this time agrees roughly with the value of  $A$ . In the unoxidized sample, the induction period of the reaction is scarcely accompanied by the cleavage of the main chain. In the oxidized sample it is presumed that the cleavage reaction of the main chain goes on simultaneously during this period by a previously introduced carbonyl group, and that the sample may be oxidized by the same mechanism as in the unoxidized sample by means of hydrogen peroxide even in the oxidized sample. It seems that the higher the oxidation degree of poly(vinyl alcohol) at the stage of preparing samples, the smaller the proportion of a portion which is subject to such a reaction by hydrogen peroxide, and

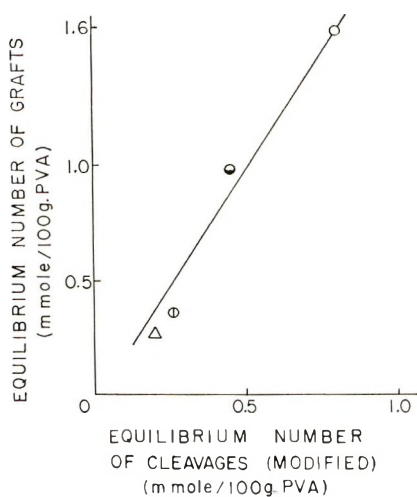


Fig. 9. Relationship of the equilibrium number of grafts to the modified number of cleavage at various total carbonyl contents of PVA (mmole/100 g of PVA: (○) 0; (⊙) 7.6; (⊕) 10.8; (△) 18.8. Reaction temperature, 45°C;  $[Fe^{3+}]$ , 1 mmole/l.;  $[H_2O_2]$ , 10 mmole/l.

consequently that the conditions necessary for the formation of grafts tend to be lost.

Next, in the same manner as  $A$ , the amount of hydrogen peroxide reduced ( $I$ ) not directly as a result of formation of grafts is determined from Figure 6. When  $I$  is compared to carbonyl content, a fairly good linear relationship between the two is obtained, as may be seen in Figure 7. A linear relationship was found between  $A$  and  $I$  too, and about 40 moles of hydrogen peroxide corresponded to 1 mole of cleavage.

Sakurada et al.<sup>7</sup> reported that in the reaction of hydrogen peroxide with poly(vinyl alcohol), 10–20 moles of hydrogen peroxide is required per mole of cleavage. In the present experiment, ferric ions are used, and so it is presumed that the decomposition of hydrogen peroxide accelerated by ferric ions must involve many reactions not related to the cleavage of the main chain.

Figure 8 shows the values obtained by subtraction of  $A$  from the amount of cleavage of each sample, that is, the changes with time in the amount of main-chain cleavage which is thought to take part in the formation of grafts. A comparison of Figure 8 with Figure 3 shows that there is a time correspondence between the cleavage reaction and the formation of grafts. It is found that there is a roughly linear relationship between the equilibrium value of the number of grafts of each sample and the modified cleavage amount. This is shown in Figure 9.

Therefore, it may be that radicals formed by the cleavage of the main chain are certainly concerned in the reaction of graft formation. From Figure 9, about 1 mole of grafts corresponds to 5 moles of the cleavage of the main chain.

### SUMMARY

In a reaction of poly(vinyl alcohol) in a homogeneous solution with ferric ion-hydrogen peroxide, there was considerable reduction of the hydrogen peroxide and cleavage of the main chain of the poly(vinyl alcohol) in the early stage of the reaction, just as was found in the case of ceric ions. Quantitatively, the greater the carbonyl content in the samples, the greater the reduction and also the greater the cleavage. In the graft copolymerization carried out by adding methyl methacrylate, the cleavage of the main chain at the beginning was related with the formation of grafts when ceric ion was used. In contrast, in the initiating system of ferric ion-hydrogen peroxide, an induction period for formation of grafts was found. The formation of grafts was accompanied by cleavage which took place only after an induction period of several minutes. It became clear that the greater carbonyl group content of the main chain that is, the greater the amount of cleavage during the induction period, the smaller the number of grafts formed.

As has been described above, the behavior of the ferric ion-hydrogen peroxide initiating system was quite different behavior from the initiating mechanism of graft copolymerization in the ceric ion initiating system. It seems that this difference is due mainly to a difference in the reactivity of each oxidizing agent with radicals formed by the cleavage of the main chain. That is to say, it seems that the radicals on the trunk polymer are easily attacked by the mobile and reactive hydroxyl radical in the ferric ion-hydrogen peroxide initiating system, and its efficiency of forming grafts is more markedly reduced than in the case of the ceric ion.

If the present study is considered together with the results described in the previous paper, it may be said that in the graft copolymerization of methyl methacrylate to poly(vinyl alcohol), the reaction mechanism differs markedly, depending on the type of oxidizing agent. But it is presumed that the formation of grafts is, in every case, due to radicals formed by the cleavage of the main chain, and that the copolymer formed is something like a block polymer.



### References

1. Y. Ogiwara and M. Uchiyama, *J. Polym. Sci., A-1*, **7**, 1479 (1969).
2. Y. Ogiwara, Y. Ogiwara, and H. Kubota, *J. Appl. Polym. Sci.*, **12**, 2575 (1968).
3. A. Nakajima and K. Furudate, *Kobunshi Kagaku*, **6**, 460 (1949).
4. I. Sakurada and S. Matsuzawa, *Kobunshi Kagaku*, **16**, 633 (1959).
5. M. Shiraishi and S. Matsumoto, *Kobunshi Kagaku*, **19**, 722 (1962).
6. G. Takayama, *Kobunshi Kagaku*, **17**, 698 (1960).
7. I. Sakurada and S. Matsuzawa, *Kobunshi Kagaku*, **16**, 565 (1959).

Received May 6, 1969

Revised September 12, 1969

## Electron Spin Resonance Studies of Polycarbonate Irradiated by $\gamma$ -Rays and Ultraviolet Light

YOSHIMASA HAMA and KENICHI SHINOHARA, *Science and Engineering Research Laboratory, Waseda University, Tokyo, Japan*

### Synopsis

Paramagnetic species produced in polycarbonate (PC) by  $\gamma$ - or ultraviolet irradiation were investigated by ESR. In  $\gamma$ -irradiation, scissions of carbonate groups in the main chain occur. ESR spectra ( $g = 2.0034$ ) composed of a sharp singlet, some broad singlets, and a small signal with hyperfine structure are obtained, and they are assigned to trapped electrons, positive radical ions, phenoxy-type free radicals, phenyl radicals, and  $-\text{O}-\text{C}_6\text{H}_4-\text{C}(\text{CH}_3)_2$  radicals. The  $G$  value for total yields of paramagnetic species at 77°K is 1.8. The percentage of CO and CO<sub>2</sub>, the dominant gases evolved, is 65.4 and 33.8%, respectively. In ultraviolet irradiation, energy is absorbed selectively at the surface region. The surface region becomes insoluble in methylene chloride because of crosslinking of phenyl groups. The ESR spectrum obtained at 77°K is a broad singlet and assigned to phenoxy-type free radicals, phenyl radicals, and polyenyl-type free radicals. Some differences in effects of  $\gamma$ - and ultraviolet irradiation of PC are discussed.

### INTRODUCTION

Electron spin resonance (ESR) studies of free radicals produced in irradiated high polymers have been reported by many authors. In most cases, the free radicals have been produced by high-energy radiation such as  $\gamma$ -rays, electron beams, or x-rays. There have been, however, also some ESR studies on the effect of low-energy radiation such as ultraviolet light on high polymers. Charlesby and Thomas have made a comparison of the effects of ultraviolet and  $\gamma$ -radiation on poly(methyl methacrylate).<sup>1</sup> Browning et al. have reported an ESR study of ultraviolet-irradiated polyolefins.<sup>2</sup> Yoshida and Rånby have found methyl radicals in ultraviolet-irradiated polypropylene.<sup>3</sup>

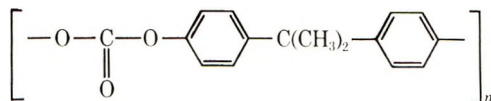
In a previous paper by Hama, Okamoto, and Tamura,<sup>4</sup> a brief description was given of ESR spectrum of polycarbonate and poly(ethylene terephthalate) irradiated by electron beams. These polymers have carbonate and *p*-phenyl groups in a molecule. Observation was also made that the samples acquire reddish-brown color when irradiated at 77°K.

The present paper concerns a more detailed study of the ESR spectra produced by  $\gamma$ - and ultraviolet irradiation on polycarbonate. A comparison of the effects of the two kinds of radiations and a discussion of the origin of the color of the irradiated polycarbonate are also given.

## EXPERIMENTAL

### Preparation of Samples

The polycarbonate (PC) studied was poly(bisphenol-A carbonate),



which was prepared specially for the present investigation by the Research Institute of Mitsubishi Edogawa Chemical Co., Ltd. The crystallinity was 20–30%, and the number-average molecular weight of the polymer was  $3.7 \times 10^4$ . The polymer was of high purity and did not contain any additives such as stabilizers or plasticizers. The polymer was formed in a film of 0.5 mm thickness. Four pieces of rectangular films, 4 mm  $\times$  30 mm, were placed in a quartz tube (Spectrosil, in most cases) which was evacuated to  $10^{-4}$ – $10^{-5}$  mm Hg at room temperature and then sealed.

### Irradiation

The sample was irradiated with  $\gamma$ -rays from a  $^{60}\text{Co}$  source at a dose rate of  $3.3 \times 10^4$  rad/hr or subjected to ultraviolet irradiation from a super high-pressure mercury lamp (USH-250D, Ushio Electric Co., Ltd.), at a distance of 15 cm from the lamp. Predominant wavelengths from this lamp are 3130, 3650, (strongest), and 4350 Å. In all cases of ultraviolet irradiation, the sample was kept in liquid nitrogen.

### ESR Measurement

ESR measurements were carried out by using an X-band spectrometer manufactured by Japan Electron Optics Laboratory Co., Ltd., with 100 KHz field modulation. ESR measurements at 77°K were made by inserting a Dewar vessel with a transparent cylindrical tip into the cavity. The sample was held in the Dewar vessel filled with liquid nitrogen. Heat treatment of the sample was carried out by keeping the sample in a liquid bath of a fixed temperature for 4 min and then returning it quickly to liquid nitrogen.

## RESULTS

### $\gamma$ -Irradiation

**Irradiation and ESR Spectrum at 77°K.** Polycarbonate (PC)  $\gamma$ -irradiated *in vacuo* at 77°K to a dose of 0.7 Mrad became dark green and gave an ESR spectrum as shown in Figure 1 *a*. The spectrum was observed at 77°K. This spectrum consists of superposition of a broad singlet (line-width between points of maximum slope,  $\Delta H_{ms} = 13.0 \pm 0.5$  gauss) and a central sharp singlet ( $\Delta H_{ms} \simeq 4.3$  gauss). There is also a slight indication

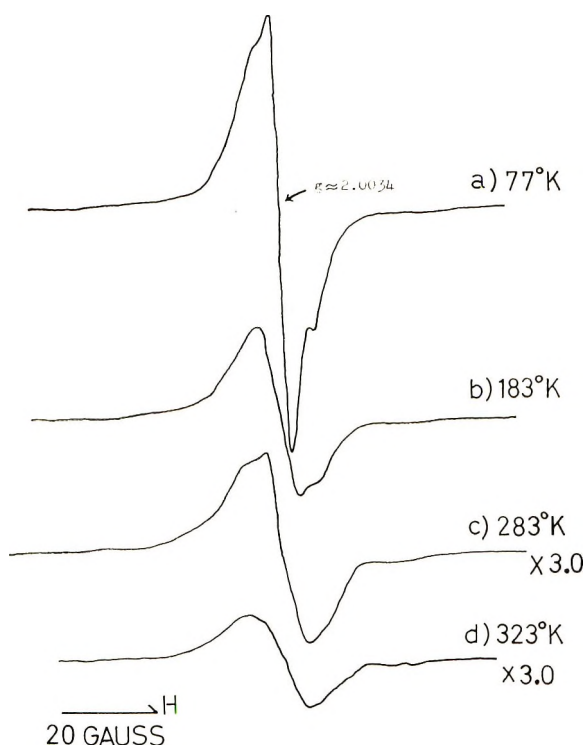


Fig. 1. ESR spectrum of PC  $\gamma$ -irradiated at 77°K to a dose of 0.7 Mrad. Spectra (a); (b); (c) and (d) were obtained at 77°K after heat treatment at indicated temperatures.

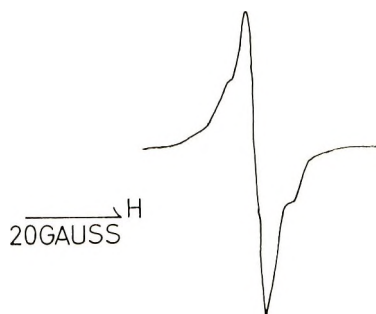


Fig. 2. ESR spectrum decaying in the first decay region, obtained by subtracting (b) from (a) in Fig. 1.

of a weak signal on the outside of the broad singlet. The spectrum was stable in dark at 77°K.

The  $g$  factor of the ESR spectrum which was obtained by comparing with that of  $Mn^{++}$  in  $MgO$  was 2.003<sub>4</sub>.

**Temperature Dependence of the Line Shape and Intensity of the ESR Spectrum.** ESR spectra of PC,  $\gamma$ -irradiated *in vacuo* at 77°K to a dose of 0.7 Mrad and observed at 77°K after heat treatment of the sample at various

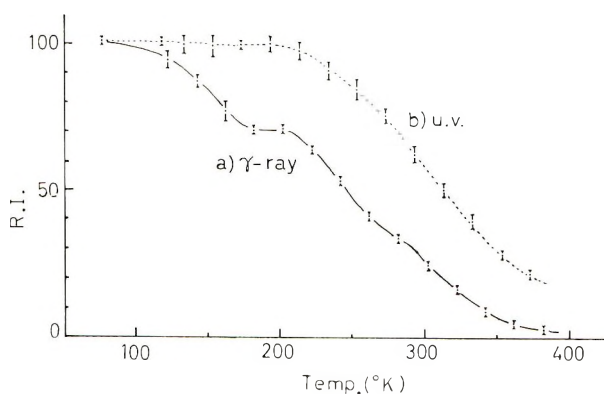


Fig. 3. Relationship between relative intensity R.I. and temperature of heat treatment for PC: (a)  $\gamma$ -irradiated at 77°K; (b) ultraviolet-irradiated at 77°K.

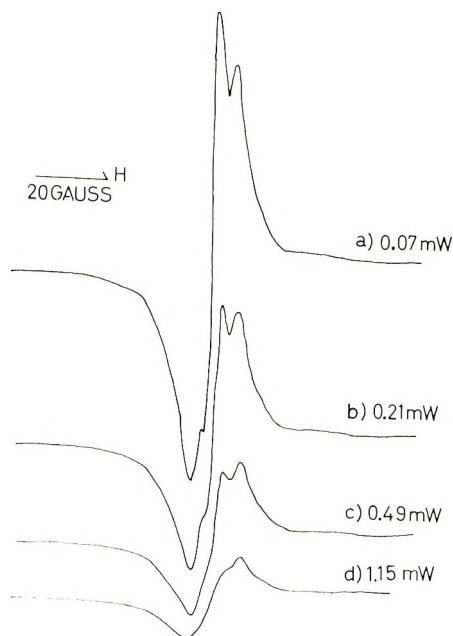


Fig. 4. Change of ESR spectrum with increase of microwave power.

temperatures, are shown in Figure 1. Elevation of the temperature of heat treatment causes the spectrum to vary in both line shape and intensity. The variation of the line shape arises in three regions, i.e., 120–183°K, 203–283°K, and above 283°K. The spectrum obtained in each region consists of a somewhat asymmetric singlet and has no hyperfine structure except a slight indication of the structure in Figure 1*d* observed at high amplification of the spectrometer. In the first decay region, 120–183°K the central sharp singlet disappears rapidly with elevation of temperature

of heat treatment. The ESR spectrum decaying in the first region is shown in Figure 2, which was obtained by subtracting the spectrum of Figure 1*b* from that of Figure 1*a*. This spectrum also consists of the superposition of a broad and a sharp singlet.

The decrease of the relative intensity of the ESR spectrum by heat treatment is shown in Figure 3*a*. A sample irradiated at 77°K was used, and the heat treatment was carried out on this sample at successively higher temperatures. The relative intensity was obtained by comparing the area of the ESR spectrum measured at 77°K after each heat treatment with that measured at 77°K immediately after  $\gamma$ -irradiation at 77°K. The intensity

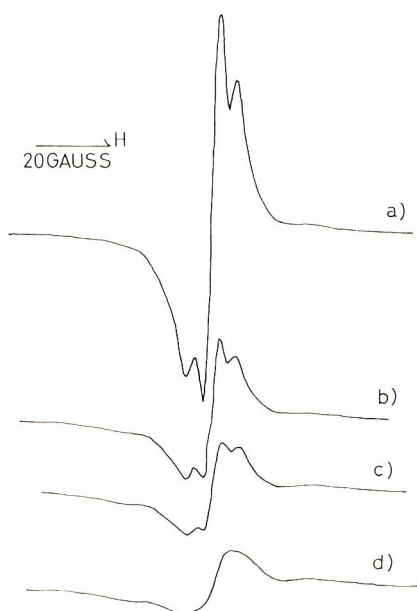


Fig. 5. Change of ESR spectrum caused by illumination with light: (a) before illumination; (b) after illumination for 30 min with light above 7000 Å; (c) after illumination for 60 min with light above 7000 Å; (d) after illumination for 60 min with light above 7000 Å followed by illumination for 5 min with visible light from a tungsten lamp. All the spectra were obtained at 77°K.

of the spectrum apparently decays in two steps with increase of the temperature of the heat treatment. The first decay (120–183°K) corresponds to the first variation of the line shape with the temperature of the heat treatment. At temperatures above 200°K, the intensity decreases monotonously, though the temperature dependence of the line shape suggests the existence of two decay regions, i.e., 203–283°K and above 283°K. This may be attributed to overlap of two decay curves corresponding to the second and third variation of the line shape. The variations of the line shape and the intensity suggest that at least three kinds of paramagnetic species are produced by irradiation at 77°K.

The dark green color observed after irradiation at 77°K fades gradually on raising the temperature of heat treatment and almost disappears at 183°K, till the sample assumes a permanent faint yellow color. It seems probable that the coloration at 77°K is related to the ESR signal decaying in the first region.

**Power Saturation.** The central sharp singlet observed at 77°K in  $\gamma$ -irradiated PC saturates easily at a rather low microwave power. The variation of ESR spectrum with microwave power is shown in Figure 4. With the increase of the power, the central signal decays abruptly and can be hardly observed at microwave power of 1.15 mW. Some deformations of the spectrum due to power saturation seem to be occurring even at the power level of 0.07 mW.

**Photobleaching at 77°K.** The ESR spectrum obtained at 77°K after  $\gamma$ -irradiation at 77°K is stable in the dark at 77°K, but is bleached by exposure to visible light from a tungsten lamp. The remaining signal is similar to that obtained at 77°K after heat treatment at 203°K. The variation of the ESR spectrum by photochemical bleaching is shown in Figure 5. Comparison of Figures 5a and 5b shows that the ESR spectrum at 77°K is bleached to a large extent by 30 min exposure to light of wavelength above 7000 Å. Moreover, the spectral intensity decreased by the photochemical bleaching is nearly equal to that decayed in the first decay region in heat treatment. These results suggest that the part of the signal which disappeared by the photobleaching corresponds to that decayed in the first decay region by heat treatment.

**Yields of Paramagnetic Species and Gases Evolved.** The concentration of the paramagnetic species produced in PC,  $\gamma$ -irradiated at 77°K, was determined by comparing the ESR spectrum with that of 2,2'-diphenylpicrylhydrazyl (DPPH) of a known concentration. The *G* value thus determined for the formation of total paramagnetic species produced in PC  $\gamma$ -irradiated at 77°K was 1.8.

It is known that dominant gases evolved are CO and CO<sub>2</sub> when PC is irradiated.<sup>12</sup> This was confirmed in the present work by results of mass spectrographic analysis. For PC  $\gamma$ -irradiated at room temperature to a dose of 5.4 Mrad, the relative concentrations of CO and CO<sub>2</sub> were 65.4% and 33.8%, respectively. The other 0.8% of the gases was not identified. The absolute yields of gases evolved were not determined.

### Ultraviolet Irradiation

When PC is irradiated by ultraviolet light at 77°K *in vacuo*, it acquires a yellow color. This color is found hardly to fade even at temperatures higher than 383°K.

ESR spectra of PC, ultraviolet-irradiated *in vacuo* at 77°K, for 60 min at 15 cm from the light source, and observed at 77°K after heat treatment of the sample at various temperatures, are shown in Figure 6. These spectra also have no appreciable hyperfine structure and consist of a singlet of  $\Delta H_{ms} \simeq 16$  gauss and having a *g* factor of 2.0045. With elevation of the

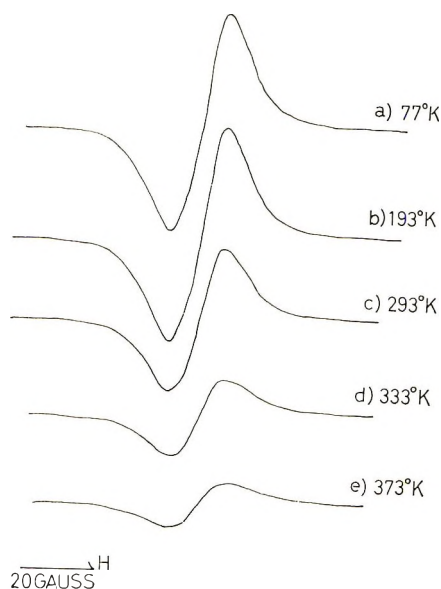


Fig. 6. ESR spectrum of PC ultraviolet-irradiated at 77°K, obtained at 77°K after heat treatment at indicated temperatures.

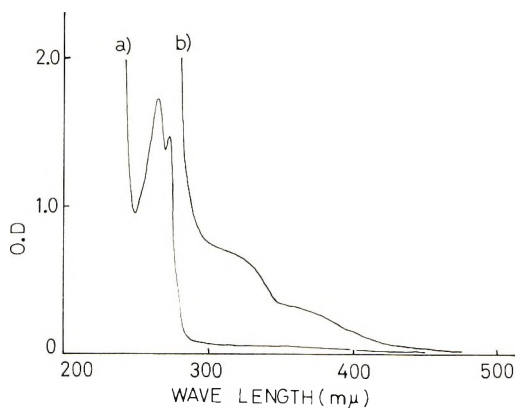


Fig. 7. Electronic absorption spectrum of PC (a) unirradiated; (b) ultraviolet-irradiated for 60 min.

temperature of heat treatment, the intensity of the spectrum changes, but not the shape. The temperature dependence of the relative intensity of this spectrum is shown in Figure 3b. The decrease of the intensity around 140°K found in the decay curve for  $\gamma$ -irradiation was not observed in the case of ultraviolet irradiation. The decay curve at temperatures higher than 203°K is similar to that of  $\gamma$ -irradiation.

The yellow color acquired by ultraviolet irradiation is produced at the surface of the sample. This can be seen by dissolving the sample in methy-



lene chloride, a good solvent for PC. The inner part is completely dissolved, while a thin yellow film coming from the surface remains insoluble.

The electronic absorption spectrum of PC recorded at room temperature before and after ultraviolet irradiation is shown in Figure 7 as function of wavelength. Considerable absorptions are found in the wavelength region shorter than 2500 Å and at 2650 Å before ultraviolet irradiation. After ultraviolet irradiation, two new absorptions appear at wavelengths around 3200 and 3800 Å. The part of the ultraviolet-irradiated sample which is soluble in methylene chloride, however, was found to give an absorption not distinguishable from that of the sample before ultraviolet irradiation. Therefore, the new absorption which appeared after ultraviolet irradiation must be attributed to the insoluble yellow surface.

## DISCUSSION

### Paramagnetic Species Decaying in the First Decay Region in $\gamma$ -Irradiated PC

As described above, at least three kinds of paramagnetic species are produced in PC  $\gamma$ -irradiated at 77°K. These species decay in three regions. The ESR spectrum due to the paramagnetic species decaying in the first region consists of a central sharp singlet and a broad singlet as shown in Figure 2. It has been found that the sharp singlet has following features: (a) the  $g$  factor is near that of the free electron; (b) it is saturated easily at low microwave power; (c) it is bleached by illumination of the light of wavelength above 7000 Å. Moreover, it has been found that the species giving the sharp singlet may be related to the dark green color acquired in the sample  $\gamma$ -irradiated at 77°K.

All these features are those observed for electrons trapped in organic glasses produced by radiolysis,<sup>6-8</sup> and this led us to the conclusion that the sharp singlet arises from trapped electrons in PC.

Shirom et al. have noted, in their ESR study in  $\gamma$ -irradiated 3-methylpentane,<sup>9</sup> that there is some possibility of free electrons being trapped by CO<sub>2</sub> to form CO<sub>2</sub><sup>-</sup> when CO<sub>2</sub> is present.

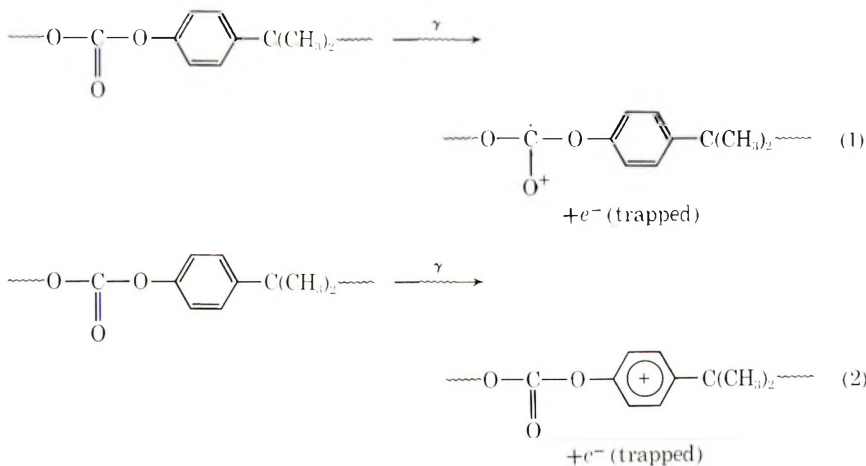
In the present work, an appreciable amount of CO<sub>2</sub> is produced in  $\gamma$ -irradiated PC. Therefore, the production of CO<sub>2</sub><sup>-</sup> is possible. The sharp singlet observed in our experiment, however, was not attributed to CO<sub>2</sub><sup>-</sup> because of the following facts: (a) the sharp singlet is bleached by illumination of the light above 7000 Å, whereas the light of wavelength shorter than 5500 Å is required in bleaching the ESR signal of CO<sub>2</sub><sup>-</sup>; (b) the  $g$  factor of the sharp singlet ( $g \simeq 2.003_4$ ) is different from that of the CO<sub>2</sub><sup>-</sup> signal ( $g \simeq 2.0007$ ).

In polar materials such as PC, there may be an almost infinite number of trapping sites for electrons formed by carbonate groups in neighboring chains. Free electrons may be trapped, at low temperature, at those sites before they reach a CO<sub>2</sub> molecule.

In the first decay region, the sharp singlet always decays along with the broad singlet. This suggests that the species giving the broad singlet combine with trapped electrons in decaying process and that they are probably positive radical ions.

The dark green color acquired by PC in  $\gamma$ -irradiation at 77°K can be attributed to the trapped electrons and positive radical ions. This would allow for the color fading as these charged species disappear by recombination. The dark green color is expected for trapped electrons, and the photobleaching experiment, in which the electron signal was found to be bleached by light above 7000 Å. It may be mentioned, in this connection, that Campbell et al.<sup>5</sup> suggested that the coloration observed by Hama et al.<sup>4</sup> in poly(ethylene terephthalate) irradiated by electron beams at 77°K, may be due to trapped electrons and positive ions.

The production of trapped electrons and positive radical ions can be interpreted as being due to mechanisms (1) and/or (2).



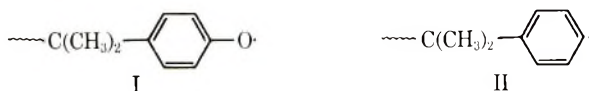
The ESR evidence does not distinguish between (1) and (2).

The traps may be produced by polarization of surrounding carbonate groups by the electric field of the trapped electron. The trapped electrons are liberated from trapping sites on warming or by illumination with visible light. Reding has observed a dynamic mechanical loss peak at 163°K in PC and ascribed this to the motion of carbonate groups.<sup>10</sup> This temperature falls in our first decay region of 120–183°K, which supports our interpretation that, in the neighborhood of this temperature, carbonate groups are set in motion and traps are destroyed liberating trapped electrons. The electrons will then combine with the positive radical ions.

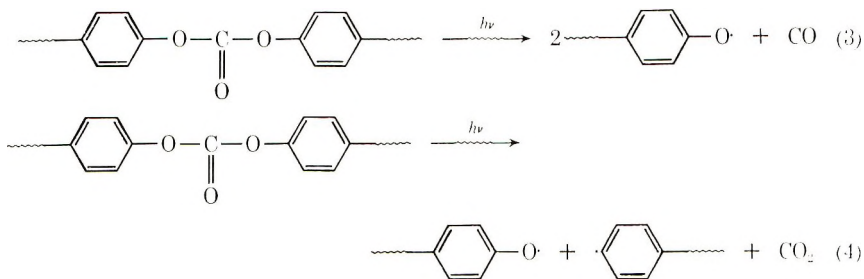
### Species Decaying in the Second Region for $\gamma$ - and Ultraviolet-Irradiated PC

As shown in Figure 3, the relative intensity in two decay curves, i.e., for  $\gamma$ - and ultraviolet irradiation, decreases in a similar way around 220°K.

It is expected that the same kind of free radical decays in this region in  $\gamma$ - and ultraviolet irradiation. It is well known<sup>12</sup> that the dominant gases evolved in  $\gamma$ - and ultraviolet irradiation of PC are CO and CO<sub>2</sub>, as found also in the present work. Considering that ESR spectrum has no appreciable hyperfine structure, free radicals decaying in this region may be assigned to the species I or II.



These free radicals are produced by scission of carbonate groups in main chain, with evolution of CO and CO<sub>2</sub>.



The production of species I may be about five times that of species II since it was found that CO/CO<sub>2</sub>  $\approx$  2.

The decay in the second decay region is either due to the recombination of two phenoxy-type free radicals produced in the process (3) or due to the recombination of the species I and II produced in the process (4). It seems hard to decide immediately which of those two processes to occur in the second decay region. Phenyl radicals are more reactive than phenoxy radicals, but the distance between a phenyl radical and a phenoxy radical is larger than that between two phenoxy radicals produced in the process (3). Moreover, only a small local motion of the chain ends is expected at this temperature in PC. Evidence from ESR spectra favors the interpretation that the decay is due to the recombination of two phenoxy-type radicals, since a small asymmetry observed in the ESR pattern before the decay in the second region, which can be ascribed to the asymmetry of the  $g$ -factor tensor of the phenoxy-type free radicals, almost disappears after the second decay.

#### Species Decaying above 283°K in $\gamma$ - and Ultraviolet-irradiated PC

The ESR spectrum observed at room temperature is comparatively stable, though it decays gradually.

In  $\gamma$ -irradiation, an ESR spectrum with hyperfine structure added to broad singlet is found at higher amplification. The broad singlet may be attributed to superposition of two spectra assigned to the phenoxy-type

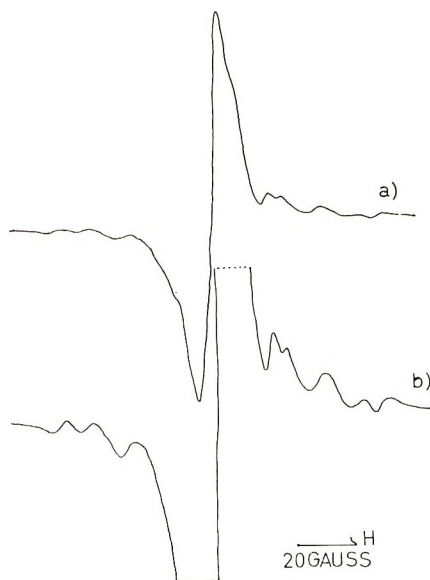
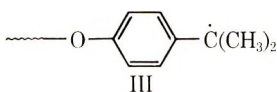


Fig. 8. ESR spectrum of stable radicals at room temperature, measured at 300°K after  $\gamma$ -irradiation at 300°K. Amplification (b) is 3.2 times (a).

free radical and the phenyl radical produced in the process (4), as discussed above.

The ESR spectrum with hyperfine structure becomes more evident in the sample  $\gamma$ -irradiated at room temperature to a dose of 5.5 Mrad, as shown in Figure 8. This spectrum is assigned to a free radical coupling with two methyl groups in the main chain, i.e., probably species III, considering that it has several splittings and the total breadth is about 110 gauss.

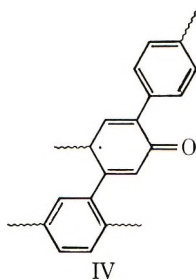


The yield of species III at 77°K is very small compared with the other species.

In ultraviolet irradiation, only a broad singlet was observed at room temperature. No ESR spectrum with hyperfine structure was observed, even at higher amplification. Therefore, no free radicals assigned to the species III are produced in ultraviolet irradiation. Most of the stable free radicals observed at room temperature in ultraviolet irradiation are supposed to be the phenoxy-type free radicals and the phenyl radicals produced in the process (4).

As shown in Figure 3b, however, some free radicals of relative intensity 20% remain after heat treatment of the sample at 370°K. This result indicates that there are still other free radicals which are more stable than the species I and II.

As mentioned above, an insoluble yellow surface is produced by ultraviolet irradiation. This indicates that most of the ultraviolet light is adsorbed in the surface, as expected from the large extinction coefficient of PC, and that crosslinks are formed in the surface, as reported previously<sup>11</sup> in the study of photolysis of poly(ethylene terephthalate). Therefore the more stable free radicals may be polyenyl-type free radicals (IV), produced by crosslinking of the phenyl radicals.



### CONCLUSIONS

The properties of the paramagnetic species produced in PC by  $\gamma$ - and ultraviolet irradiation, and the differences of effects of both radiation on the material were investigated by ESR method.

In  $\gamma$ -irradiation, the energy is absorbed at random in PC and produces several kinds of paramagnetic species, i.e., trapped electrons, positive radical ions, phenoxy-type free radicals, phenyl radicals, and  $-\text{O}-\text{C}_6\text{H}_4-\dot{\text{C}}(\text{CH}_3)_2$  radicals. Although the trapped electrons are stable in dark at 77°K, they are bleached by light of wavelength above 7000 Å. They also decay thermally at temperatures around 140°K by recombining with the positive radical ions. The phenoxy-type free radicals and phenyl radicals decay in two temperature regions, i.e., 203–283°K and above 283°K. These decays may be due to recombination of free radicals as the local motion of chain ends increases. Radicals of the type  $-\text{O}-\text{C}_6\text{H}_4-\dot{\text{C}}(\text{CH}_3)_2$  are produced in a very small quantity. The dark green coloration which is observed at 77°K is attributed to trapped electrons and positive radical ions. The  $G$  value for the formation of paramagnetic species is 1.8 in  $\gamma$ -irradiation at 77°K. The dominant gases evolved are CO and CO<sub>2</sub>, in relative concentrations of 65.4% and 33.8%, respectively.

In the ultraviolet irradiation, the energy is absorbed selectively by carbonate groups in the surface region and produces phenoxy-type free radicals, phenyl radicals, and polyenyl-type free radicals. Trapped electrons, positive radical ions, and  $-\text{O}-\text{C}_6\text{H}_4-\dot{\text{C}}(\text{CH}_3)_2$  radicals are observed on ultraviolet irradiation. The polyenyl-type free radicals are thought to be associated to conjugated double bonds formed by crosslinking of phenyl groups in the surface region by selective energy absorption of carbonate groups. The resulting crosslinked yellow surface is insoluble in methylene chloride.

We wish to thank Professor S. Okamoto and Dr. N. Tamura for helpful discussions and Dr. R. Nakane for mass spectrometric analyses.

### References

1. A. Charlesby and D. K. Thomas, *Proc. Roy. Soc. (London)*, **A269**, 104 (1962).
2. H. L. Browning, Jr., H. D. Ackermann, and H. W. Patton, *J. Polym. Sci. A-1*, **4**, 1433 (1966).
3. B. Rånby and H. Yoshida, in *Perspectives in Polymer Science (J. Polym. Sci. C, 12)*, E. S. Proskauer, E. H. Immergut, and C. G. Overberger, Eds., Interscience, New York, 1966, p. 263.
4. Y. Hama, S. Okamoto, and N. Tamura, *Repts. Progr. Polymer Phys. Japan*, **7**, 351 (1964).
5. D. Campbell, K. Araki, and D. T. Turner, *J. Polym. Sci., A-1*, **4**, 2597 (1966).
6. D. R. Smith and J. J. Pieroni, *Can. J. Chem.*, **43**, 876 (1965).
7. D. R. Smith and J. J. Pieroni, *Can. J. Chem.*, **43**, 2141 (1965).
8. K. Tsuji, H. Yoshida, and K. Hayashi, *J. Chem. Phys.*, **46**, 810 (1967).
9. M. Shirom, R. F. C. Claridge, and J. E. Willard, *J. Chem. Phys.*, **47**, 286 (1967).
10. F. P. Reding, T. A. Fancher, and R. D. Whitman, *J. Polymer Sci.*, **54**, S56 (1961).
11. F. B. Marcotte, D. Campbell, J. A. Cleaveland, and D. T. Turner, *J. Polym. Sci. A-1*, **5**, 481 (1967).
12. R. C. Gilbertson, *Mod. Plastics*, **39**, 143 (April 1962).

Received July 21, 1969

Revised September 12, 1969

## A Proposal on the Steric Course of Propagation in the Homogeneous Cationic Polymerization of Vinyl and Related Monomers\*

TOYOKI KUNITAKE and CHUJI ASO, *Department of Organic Synthesis, Faculty of Engineering, Kyushu University, Fukuoka, Japan*

### Synopsis

A stereochemical scheme of propagation was proposed for polymerizations of vinyl and related monomers by Friedel-Crafts catalysts. For the cationic propagation proceeding via the simple carbonium ion pair, the following two factors were considered to be of primary importance in determining the steric course of propagation: (1) the conformation of the last two units of the propagating polymer segment and the direction of approach of the incoming monomer; (2) the tightness of the growing ion pair. Thus, the front-side (less hindered site) attack to the carbonium ion gives rise to a syndiotactic placement and the back-side attack an isotactic placement. The present model can satisfactorily explain the effects of substituents, catalysts, polymerization media, and polymerization temperature on the steric structure of polymers in cationic polymerization of vinyl ethers. Extension of the scheme to polymerization of the  $\beta$ -substituted vinyl ethers in nonpolar solvents predicts formation of the diisotactic structures consistent with the experimental result. The influences of the polymerization condition on the steric structure of polymer were studied for cationic polymerizations of  $\alpha$ -methylstyrene at low temperatures. Highly syndiotactic polymers were obtained for homogeneous reactions in toluene-rich media. The isotactic unit increased by increasing the content of methylcyclohexane in the solvent mixture. The effect of catalysts, though insignificant in toluene-rich media, was clearly noted in methylcyclohexane-rich media, less active catalysts (e.g.,  $\text{SnCl}_4$ ) yielding higher amounts of the isotactic unit than more active catalysts (e.g.,  $\text{AlCl}_3$ ). These results can be readily accommodated in the present model.

### INTRODUCTION

In recent years it has become increasingly clear that the nature of the propagating carbonium ion pair exerts strong influences on the propagation reaction in Friedel-Crafts polymerizations of vinyl and related monomers. There have been many polymerization studies which related kinetic results with the nature of the propagating carbonium ion pair, though its influence on the polymer structure were not much investigated.

The variation of the monomer reactivity ratio was reported for several monomer pairs in the cationic polymerization<sup>1</sup> and these results were

\* Presented in part at the 16th Discussion Meeting of the Society of Polymer Science, Fukuoka, Japan, October 1967.

partially accounted for in terms of the difference in the nature of the propagating species. We have already reported that the variation of the polymer structure could be correlated with the tightness of the propagating ion pair in polymerizations of cyclopentadiene<sup>2</sup> and of *o*-divinylbenzene<sup>3,4</sup> by Friedel-Crafts catalysts.

The nature of the propagating species similarly plays an important role in deciding the stereochemical course of the cationic polymerization. In particular detailed studies have been made for the stereoregular polymerization of vinyl ethers, since the first synthesis of crystalline poly-(isobutyl vinyl ether) by Schildknecht.<sup>5,6</sup> The steric structures of poly(vinyl ethers) were found to depend on the monomer structure and on the polymerization conditions. For instance, *tert*-butyl vinyl ether<sup>7-9</sup> and trimethylsilyl vinyl ether<sup>10-12</sup> gave isotactic polymers in toluene but syndiotactic polymers in polar solvents, and methyl  $\alpha$ -methylvinyl ether gave a syndiotactic polymer in toluene<sup>13-17</sup> while methyl vinyl ether yielded a somewhat more isotactic polymer under similar polymerization conditions.<sup>18</sup> On the other hand, the steric structure of poly- $\alpha$ -methylstyrene was presumed to depend on the physical state of the polymerization system.<sup>19</sup> Although steric schemes of propagation were proposed by several groups of investigators for explaining the stereochemical results obtained in the cationic polymerization of vinyl ethers,<sup>13,20-22</sup> they appear to be unsatisfactory, as will be discussed below.

In this paper, we present a stereochemical scheme of propagation in the cationic polymerization of vinyl and related monomers, proceeding via simple carbonium ion pairs. The proposed scheme can accommodate the available data on the relation between the steric structure of the polymers and the polymerization condition, in terms of the conformation of the propagating polymer chain and the tightness of the propagating carbonium ion pair.

## EXPERIMENTAL

### Materials

$\alpha$ -Methylstyrene was washed with dilute aqueous alkali and with water, dried over CaCl<sub>2</sub>, and distilled under nitrogen with the use of a 30-cm column packed with glass helices; bp 59.5°C/16 mm Hg. The purified monomer was again distilled before use. Solvents were purified by conventional methods. BF<sub>3</sub>OEt<sub>2</sub>, SnCl<sub>4</sub>, and TiCl<sub>4</sub> were purified by distillation. AlCl<sub>3</sub> was mixed with aluminum powder and sodium chloride and sublimed under nitrogen.

### Polymerization

The polymerization was carried out in a glass-stoppered test tube with a side arm for nitrogen inlet, toluene or methylenecyclohexane or their mixtures being used as solvent. Except for the case of AlCl<sub>3</sub> catalyst, the monomer



(2 ml) and solvents were placed in the vessel. After purging with dry nitrogen, the vessel was cooled to a given polymerization temperature and a catalyst solution was added with a syringe through a self-sealing rubber cap. The amounts of catalyst solutions added were 0.05–0.4 ml (0.02–0.10 mole/l). When  $\text{AlCl}_3$  was used as catalyst, a given amount (about 100 mg) of  $\text{AlCl}_3$  powder was placed in the vessel under dry nitrogen and solvents were added. The mixture was cooled to the polymerization temperature, and 2 ml of the monomer was slowly added under nitrogen. The total reaction volume was 20 ml and the monomer concentration was 10% (v/v).

The polymerization proceeded homogeneously and was fast in toluene-rich media. The rate became slower with increasing content of methylcyclohexane. With  $\text{AlCl}_3$ , no polymer was obtained in the 100% methylcyclohexane medium. In methylcyclohexane-rich media, the polymer precipitated in the reaction mixture. The precipitated polymers were considerably swollen in the 3:7 toluene–methylcyclohexane medium. At  $-30^\circ\text{C}$ , the polymerization systems were homogeneous except for the 100% methylcyclohexane medium. The polymerization was terminated by adding methanol, and the white powdery polymer was obtained by pouring the reaction mixture into excess methanol. The polymer was purified by reprecipitation and dried *in vacuo*.

### NMR Measurements

The NMR measurements were carried out in chlorobenzene at  $120^\circ\text{C}$ . The polymer concentration was usually 20% (w/v). When the solution was too viscous for the measurement, it was diluted to 10 to 15% (w/v). The stereochemistry of the polymer was determined by the cut-and-weigh method of the relative area of the three methyl signals. The experimental error seems to lie within  $\pm 2\%$ .

## RESULTS

### NMR Assignment of Poly- $\alpha$ -methylstyrene

Brownstein and co-workers<sup>23</sup> observed for the first time three methyl signals for poly- $\alpha$ -methylstyrene. From consideration of the probable influences of the paramagnetic shielding of the phenyl ring in the respective steric structure, they assigned the highest-field signal to the syndiotactic methyl group. Consequently, the lowest-field and intermediate-field signals were assigned to the isotactic and heterotactic methyl protons, respectively. On the other hand, Ohsumi et al.<sup>19</sup> adopted the opposite assignment of Sakurada et al.<sup>24</sup> and discussed the influence of the reaction condition on the steric structure. This assignment, i.e., isotactic, heterotactic, and syndiotactic triads in the order of increasing magnetic field, appears untenable, however, for the low-field peak (syndiotactic peak according to their assignment) was small in a free-radical polymer.<sup>23</sup> It is difficult to con-

ceive the formation of a highly isotactic polymer by the free-radical polymerization.

Ramey and Statton<sup>25</sup> gave yet another assignment on the basis of the relative methylene peak area, i.e., syndiotactic, isotactic, and heterotactic triads with increasing field strength. Their assignment was recently preferred to other assignments by Elias et al.<sup>26</sup> on the basis of thermodynamic consideration on the tacticity. However, their assignment is also difficult to adopt from the following reason. In the present investigation as well as in the work of Ohsumi et al.,<sup>19</sup> the low-field peak was always considerably smaller than high-field and middle peaks. This result was also the same with the free-radical polymer obtained by Brownstein et al.<sup>23</sup> On adopting the assignment of Ramey and Statton, these results would indicate low heterotactic contents in spite of high isotactic and syndiotactic contents, and, therefore, require that these poly- $\alpha$ -methylstyrenes are block polymers to a large extent. It is improbable that poly- $\alpha$ -methylstyrene is stereochemically a block polymer, irrespective of whether it was formed by cationic, anionic, or free-radical processes. Furthermore, a recent study by Fujii et al.<sup>27</sup> on the 100 MHz spectrum of poly- $\alpha$ -methylstyrene showed that the lowest-field peak could not be assigned to the heterotactic triad, thus excluding the assignment of Ramey and Statton.

Thus, in this paper we adopted the assignment of Brownstein et al., i.e., isotactic, heterotactic, and syndiotactic triads in the order of increasing field strength.

### Variation of the Steric Structure of Poly- $\alpha$ -methylstyrene with the Polymerization Condition

The steric structures of the polymers obtained under several conditions are given in Table I. Apparently, the steric structure is affected by temperature, solvent, and catalyst. Although conversions differed considerably, it was already shown that the conversion did not affect the steric structure of the resulting polymers.<sup>19</sup>

Ohsumi and co-workers<sup>19</sup> observed that the stereoregularity of poly- $\alpha$ -methylstyrene increased with its solubility in the polymerization medium when *n*-hexane was used as nonsolvent and suggested that the steric structure of the polymer is influenced by the physical state of the system but not by the polarity of solvent. However, variation of the steric structure was noted for the homogeneous polymerization system in the present study as shown in Table I. The polymerization systems were homogeneous at  $-75^{\circ}\text{C}$ , when the amount of toluene was larger than that of methylecyclohexane. At  $-30^{\circ}\text{C}$ , the polymer precipitated only in 100% methylecyclohexane medium. Although the stereochemical variation at  $-78^{\circ}\text{C}$  among the homogeneous systems was small (content of the syndiotactic unit: 96–100%) for  $\text{BF}_3\text{OEt}_2$ ,  $\text{TiCl}_4$ , and  $\text{AlCl}_3$  catalysts, it was undeniably present for  $\text{SnCl}_4$  catalyst, the content of the syndiotactic unit changing from 97% to 86% for No. 9 and No. 10, respectively. These results, together with the gradual decrease in the content of the syndiotactic unit with

TABLE I  
Steric Structure of Poly- $\alpha$ -methylstyrene.

No.	Catalyst	Polymerization temperature, °C	Solvent volume ratio (toluene/methylcyclohexane)	Syndiotactic unit, %	Heterotactic unit, %	Isotactic unit, %	Polymer solubility in mixture
1	BF <sub>3</sub> OEt <sub>2</sub>	-30 ± 2	100/0	87	12	1	Soluble
2	BF <sub>3</sub> OEt <sub>2</sub>	"	70/30	86	13	1	Soluble
3	BF <sub>3</sub> OEt <sub>2</sub>	"	30/70	83	15	2	Soluble
4	BF <sub>3</sub> OEt <sub>2</sub>	"	0/100	73	19	8	Swollen
5	BF <sub>3</sub> OEt <sub>2</sub>	-75 ± 3	100/0	100	0	0	Soluble
6	BF <sub>3</sub> OEt <sub>2</sub>	"	70/30	96	4	0	Soluble
7	BF <sub>3</sub> OEt <sub>2</sub>	"	30/70	72	28	0	Swollen
8	BF <sub>3</sub> OEt <sub>2</sub>	"	0/100	54	34	12	Insoluble
9	SuCl <sub>4</sub>	-75 ± 3	100/0	97	3	0	Soluble
10	SuCl <sub>4</sub>	"	70/30	86	7	7	Soluble
11	SuCl <sub>4</sub>	"	30/70	56	35	10	Swollen
12	SuCl <sub>4</sub>	"	0/100	35	43	22	Insoluble
13	TiCl <sub>4</sub>	-75 ± 3	100/0	100	0	0	Soluble
14	TiCl <sub>4</sub>	"	70/30	96	4	0	Soluble
15	TiCl <sub>4</sub>	"	30/70	71	23	6	Swollen
16	TiCl <sub>4</sub>	"	0/100	50	38	12	Insoluble
17	AlCl <sub>3</sub>	-75 ± 3	100/0	100	0	0	Soluble
18	AlCl <sub>3</sub>	"	70/30	96	4	0	Soluble
19	AlCl <sub>3</sub>	"	30/70	85	15	0	Swollen

increase in the amount of methylecyclohexane, appear to indicate that the steric structure of the polymer was influenced by the nature of solvation rather than by the physical state of the system.

The influence of the variation of the catalytic species on the steric structure was hardly detectable in the 100% toluene medium but increased with the increase in the content of methylecyclohexane, suggesting that the decrease in solvation gave rise to greater influence of the counterions. The order of catalyst for enhancing the syndiotactic content was  $\text{AlCl}_3 > \text{TiCl}_4 \sim \text{BF}_3\text{OEt}_2 > \text{SnCl}_4$ .

An increase in the polymerization temperature resulted in a smaller syndiotactic content in the 100% toluene medium and a smaller variation of the steric structure of the polymer with the solvent composition. Thus, for  $\text{BF}_3\text{OEt}_2$  catalyst the syndiotactic unit varied from 87 to 73% at  $-30^\circ\text{C}$ , but the variation was from 100 to 54% at  $-75^\circ\text{C}$ .

## DISCUSSION

The effects of the polymerization conditions on the stereochemistry of the resulting polymer described in the previous section are similar with those for the polymerization of vinyl ethers. In both types of systems, there is better stereoregulation at lower temperatures and increased isotacticity in less solvating media and with weaker catalysts. It then follows that the factors governing the steric course of the cationic propagation of these monomers may be intrinsically the same.

Models for isotactic propagation in the homogeneous system have been provided only for vinyl ethers by several investigators. Cram and Kopecky<sup>20</sup> and Bawn and Ledwith<sup>21</sup> assumed formation of six-membered rings by the growing chain end; Higashimura et al.<sup>22</sup> postulated the presence of an  $sp^3$ -hybridized carbonium ion. Goodman and Fan<sup>13</sup> modified the mechanism of Cram and Kopecky in order to explain the syndiotactic propagation of methyl  $\alpha$ -methylvinyl ether in toluene. These models possess a common characteristic in that the growing carbonium ion is assumed to be not purely planar but rather tetrahedral.

It is well known that the adjacent ether oxygen stabilizes a carbonium ion to a considerable extent. In order for a growing cation to attain the tetrahedral structure as proposed in these models, it must do so at the expense of stabilization by the ether oxygen. Therefore, it appears difficult to assume a tetrahedral carbonium ion or an oxonium ion as a propagating species without any independent evidence which would support its existence. Furthermore, in the first two models, the influence of the size of the side chain and the role of the counteranion are not clearly stated, and all these models fail to explain the mode of the double bond opening in the polymerization of  $\beta$ -substituted vinyl ethers (see below).

Apparently these models cannot accommodate the available experimental data. In the following is described a new scheme of the steric course of the cationic propagation. Since this model deals with the cationic propaga-

tion of vinyl monomers proceeding via simple carbonium ion pairs, it covers a wide variety of cationic polymerizations of vinyl and related monomers.

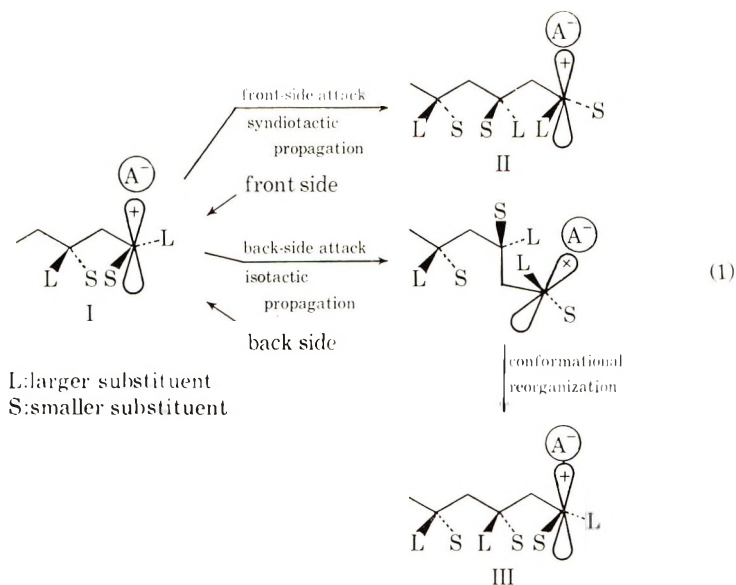
### Steric Course of the Cationic Propagation of Vinyl Monomers

In the present model the following two factors are considered to be of primary importance in determining the steric course of propagation: (a) the conformation of the propagating polymer chain and the spatial arrangement of the counteranion and the incoming monomer, which are largely determined by the steric repulsions; and (b) the direction of monomer attack which is determined by the tightness of the growing ion pair.

The growing carbonium ion is safely assumed to be essentially  $sp^2$ -hybridized and, therefore, the conformation of the least steric repulsion will be that shown by structure I. The substituents at the terminal and penultimate units will be far apart from each other in order to minimize steric crowding. Molecular models indicate that this is especially so in the case of large substituents such as *tert*-butoxy. The position of the counterion may be reasonably assumed to be at the side of the carbonium ion away from the penultimate unit. The stability of this conformation must depend very much on the polymerization temperature and the bulkiness of the substituents. Stereoregular polymers, be they isotactic or syndiotactic, have been obtainable only at low temperatures in the homogeneous cationic polymerization. These results indicate that the fixation of the conformation of the growing chain end is crucial in enhancing the stereoregularity, as is the case with the stereoregular propagation in the free-radical polymerization.<sup>28</sup>

In polar solvents, the counteranion will be only weakly interacting (or not at all if the ion pair is dissociated) with the growing cation, and the steric effect will become a major factor in determining the steric course of propagation. In such a case, the incoming monomer will attack the carbonium ion from the least hindered side (front-side attack), giving rise to a syndiotactic unit (II). This situation is similar to that of the free radical propagation at low temperatures,<sup>21</sup> and this similarity was mentioned in the syndiotactic polymerization of *tert*-butyl vinyl ether in polar solvents.<sup>8</sup> Although the incoming monomer will approach the carbonium ion in the syndiotactic way in order to minimize the steric repulsion between the substituents of the terminal carbon and the monomer, the direction of monomer approach is not relevant for vinyl monomers since the terminal carbonium ion is assumed to be capable of free rotation. The stereochemistry of the terminal carbon in I becomes fixed after the addition is complete, and the tacticity of propagation depends on the relative arrangement of the terminal and penultimate substituents.

In nonpolar solvents, the coulombic interaction between the carbonium ion and the counteranion will be stronger than in polar solvents. The free energy of the ion-pair separation which is necessary for monomer insertion between the ions could reach several kilocalories per mole in nonpolar media (see Appendix). The free energy of the ion-pair separation can be



compensated by the energy ( $\Delta H$ ) released by monomer addition more efficiently in the case of the back-side attack than in the case of the front-side attack, because the ion-pair separation and the bond formation can be simultaneous in the former case. Therefore, if the growing ion pair, I, is tight enough, the incoming monomer may attack the carbonium ion from the back-side. The back-side attack gives rise to an isotactic unit (III), as shown in the scheme. However, if steric hindrance to the back-side attack increases sufficiently because of large penultimate substituents, the front-side attack will ensue, even in nonpolar media. Thus, the incoming monomer will attack the carbonium ion either from the front-side or from the back-side, depending on the tightness (extent of the coulombic interaction) of the ion pair and on the difference in the steric hindrance between the two modes of attack.

In this scheme, the possible interaction of the counteranion and the incoming monomer is ignored. We consider this to be justified because electron-rich monomers such as vinyl ethers, and  $\alpha$ -methylstyrene would interact with the anion only weakly, if at all, and the interaction would not affect the steric course of propagation.

The propagation by the back-side attack is an  $S_N2$ -type reaction. In this connection it is interesting to find a close analogy in the fact that Weiner and Snee<sup>29</sup> observed the bimolecular inverting displacement reaction via ion pairs in the solvolysis of 2-octyl sulfonates.

From the above discussion, it is clear that both of the relative conformation of the penultimate and terminal units, and the direction of the monomer attack (front-side or back-side) must be constant, in order for a highly stereoregular polymer (isotactic or syndiotactic) to be obtainable.

In the above scheme, the growing polymer chain is considered to be in the extended conformation for simplicity. However, it is well known that the isotactic sequence of vinyl polymers cannot assume an extended zigzag conformation. Thus, if an assumption is made that the stable conformation of a polymer segment is fairly close to that in the crystalline state,<sup>30</sup> the conformation of an isotactic segment will be helical, though the helix may not be tight, and that of a syndiotactic segment will be a planar zigzag. Although these conformational differences seem to exert influences on the steric course of propagation of  $\beta$ -substituted vinyl ethers as discussed below and on the presence or absence of the penultimate effect, they will be of secondary importance in the above scheme, as the relative arrangement of the penultimate and terminal substituents and the counteranion will be fairly insensitive to the change in the overall conformation of the polymer chain.

### Interpretation of Experimental Results on the Basis of the Present Model

In the cationic polymerization of vinyl ethers and  $\alpha$ -methylstyrene by Friedel-Crafts catalysts, it was invariably shown that the stereoregularity of the polymer decreased with increase in polymerization temperature. In the radical polymerization of methyl methacrylate, the difference in the activation energies between the isotactic and syndiotactic propagations, approximately 1 kcal/mol,<sup>31</sup> was attributed to the steric difference in the transition state of the monomer addition. Since the conformational energy, *per se*, of this system does not seem to be very different from those of the cationically growing chains, low polymerization temperatures will be similarly necessary for the conformational fixation of the growing terminal segment (the position of the counteranion included) which is presumably required for stereoregular propagations. The loss of stereoregularity with increasing temperature may also be caused by probably small difference in the free energies of activation between the front-side and back-side attacks, apart from the conformational fixation.

That bulky substituents such as *tert*-butyl<sup>7,8</sup> and trimethylsilyl<sup>10,11</sup> were more effective than small substituents like methyl<sup>18</sup> in increasing stereoregularity in vinyl ether polymerizations indicates, according to this theory, that bulky substituents can enhance the conformational stability which is essential for forming stereoregular polymers.

The influences of catalysts and polymerization media on the steric course of propagation can be readily accommodated in the present scheme, taking into account the tightness of the growing ion pair. The effect of catalysts on the stereoregularity was observed for poly(isobutyl vinyl ether),<sup>32</sup> poly(*tert*-butyl vinyl ether),<sup>8</sup> and poly(trimethylsilyl vinyl ether).<sup>10,11</sup> Generally speaking,  $\text{BF}_3\text{OEt}_2$  gave more isotactic units than  $\text{SnCl}_4$  and  $\text{TiCl}_4$  in nonpolar solvents, suggesting that  $\text{BF}_3\text{OEt}_2$  formed tighter ion pairs than  $\text{SnCl}_4$  and  $\text{TiCl}_4$ , although the order of the catalyst effect seems to vary to some extent with the polymerization system used.

The importance of the solvent polarity in the stereoregular propagation has been noticed ever since the preparation of poly(isobutyl vinyl ether).<sup>5,6,32,33</sup> Subsequent investigations showed that vinyl ethers gave isotactic polymers in nonpolar solvents and syndiotactic polymers in highly polar solvents. Typical examples are *tert*-butyl vinyl ether,<sup>8</sup> trimethylsilyl vinyl ether,<sup>10,11</sup> and (though the difference is less pronounced) methyl vinyl ether.<sup>18</sup> Formation of isotactic polymers in nonpolar solvents was also observed for other alkyl vinyl ethers<sup>34-37</sup> and benzyl vinyl ether,<sup>35</sup> although the propagation by simple carbonium ion pairs may not be assumed in some cases.

In the cationic polymerization of  $\alpha$ -methylstyrene, the back-side attack will suffer a considerable disadvantage, since both methyl and phenyl substituents of the penultimate unit will exert steric hindrance toward the back-side attack of the incoming monomer. This may be the reason why  $\alpha$ -methylstyrene gave syndiotactic polymers even in a nonpolar solvent like toluene. However, by increasing the content of methylecyclohexane, which is a poorer solvent, the endgroup ion pair will become tight enough to give rise to the back-side attack in spite of the large steric repulsion. Thus, in the present investigation the isotactic unit increased with the content of methylecyclohexane for any catalyst. The effect of the catalyst will become noticeable only when the two modes of monomer attack coexists, since the overwhelming occurrence of the front-side attack in toluene will render the difference in the counteranion insignificant. The effect of the catalyst observed in methylecyclohexane-rich media supports this view. The order of catalysts for increasing isotacticity ( $\text{SnCl}_4 > \text{BF}_3\text{OEt}_2 \sim \text{TiCl}_4 > \text{AlCl}_3$ ) was somewhat different from those observed in other systems (see above). However, it is probable that the order of the influence of catalysts (i.e., the influence of the counteranions derived therefrom) varies depending on the system studied. The order of potency of Friedel-Crafts catalysts was fairly variable.<sup>3,39,40</sup> Further detailed discussion on the catalyst effect does not seem to be advantageous at this time, since the structure of the counteranion is not clearly defined.

Methyl  $\alpha$ -methylvinyl ether gave a highly syndiotactic polymer in toluene by Friedel-Crafts catalysts.<sup>13-17</sup> Although Goodman and Fan<sup>13</sup> adopted a modified mechanism of Cram and Kopecky for explaining the syndiotactic propagation, their results can be better interpreted in the present model by enhanced steric hindrance to the back-side attack as well as by better conformational fixation, as in the polymerization of  $\alpha$ -methylstyrene.

### Steric Course of Propagation of $\beta$ -Substituted Vinyl Ethers

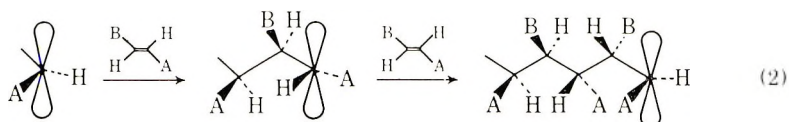
It is interesting to extend the present model to the polymerization of  $\beta$ -substituted vinyl compounds. If the steric effect of the  $\beta$ -substituent is less important as compared with that of the  $\alpha$ -substituent, the same argument as advanced for vinyl monomers should hold as well. On the other hand, since the configuration of the  $\beta$ -carbon of the terminal unit is already fixed, unlike that of the  $\alpha$ -carbon, the direction of monomer approach



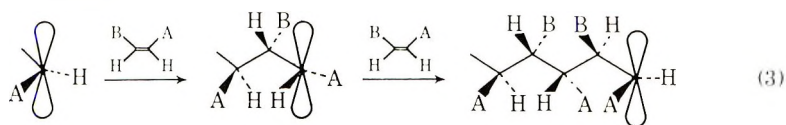
becomes relevant for the stereochemistry of the  $\beta$ -carbon. It would be reasonable to assume a syndiotactic approach of the monomer irrespective of whether it be the front-side or the back-side attack.<sup>41</sup>

In polar solvents, the front-side attack will preferentially occur as shown in eqs. (2) and (3).

*Trans* monomer:



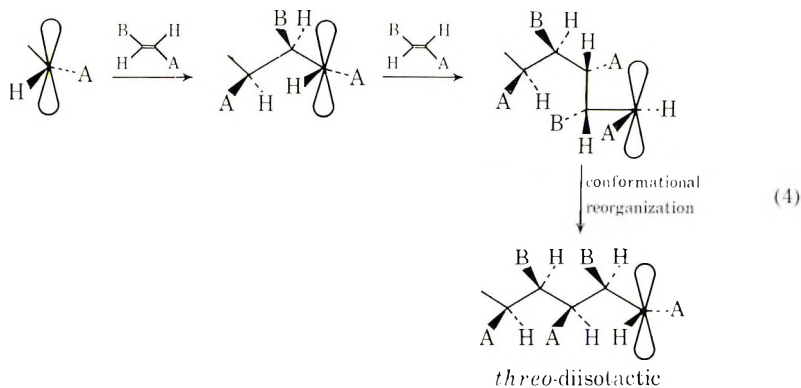
*Cis* monomer:



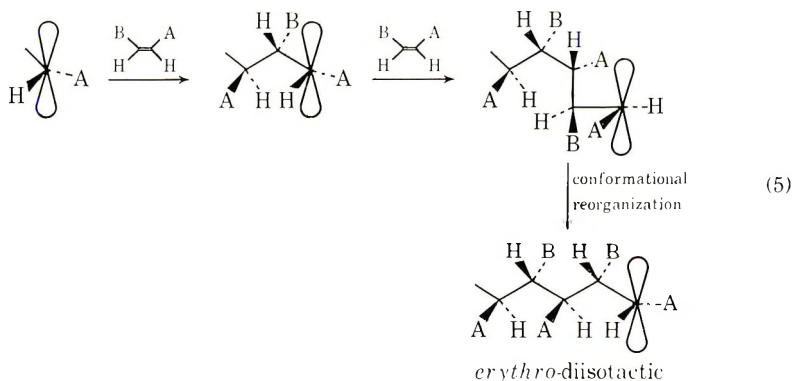
Both monomers give disyndiotactic polymers.

In nonpolar solvents where the back-side attack takes place, the propagation will be as shown in eqs. (4) and (5).

*Trans* monomer:



*Cis* monomer:



A *threo*-diisotactic polymer will be obtained from a *trans*-monomer and a *erythro*-diisotactic polymer from a *cis* monomer.

Natta et al. polymerized *cis*- and *trans*- $\beta$ -chlorovinyl ethers with cationic catalysts in nonpolar solvents.<sup>42</sup> The configuration of the polymers obtained was *erythro*-diisotactic from the *cis* monomer and *threo*-diisotactic from the *trans* monomer, and they formally interpreted the steric relationship between the structures of the monomer and of the polymer to be the *cis* double-bond opening and the constant steric attack. However, their results are in agreement with the prediction based on the present model, and seem to be better understood in terms of the back-side, syndiotactic attack. When the  $\beta$ -substituent is the methyl group, a crystalline *threo*-diisotactic polymer was obtained from *trans* propenyl ether but only amorphous polymer from the *cis* monomer.<sup>37</sup> The latter results were confirmed by Ohsumi et al.<sup>43,44</sup> from the NMR study of the polymer, which showed the exclusive *cis* opening for the *trans* monomer and the *cis* and *trans* opening for the *cis* monomer.

That the mode of the double-bond opening was different between the two isomers of  $\beta$ -methylvinyl ether may suggest that the steric effect of the  $\beta$ -substituent is not negligible in determining the steric course of propagation. Interestingly, the molecular model indicates that the  $\beta$ -substituent of the penultimate unit can or cannot affect sterically the site of monomer attack and the mode of monomer approach, depending on the conformation of the polymer segment. Thus, the difference in the mode of the double-bond opening in the  $\beta$ -substituted vinyl ether as well as the penultimate effect observed in the polymerization of some vinyl ethers<sup>12,18</sup> may be ascribable to the conformational variation of the propagating polymer segment.

## CONCLUSION

In the above discussion, it was shown that the stereoregular propagation in the vinyl polymerization by Friedel-Crafts and related catalysts was explicable on the basis of the physically reasonable assumptions; i.e., the conformational fixation of the last two units of the growing chain and the tightness of the endgroup ion pair affecting the site of monomer attack. Since the contribution of the side chain other than the steric one is not required for maintenance of the stereoregular propagation, the present model should be applicable to the vinyl polymerization in general which proceeds through simple carbonium ion pairs. On the other hand, the cationic propagation accompanied by coordination will not be interpreted by application of the present scheme.

## APPENDIX

The work for separating a contact ion pair to enable monomer insertion can be estimated by the equation:<sup>45</sup>

$$\Delta F = \frac{Ne^2}{D} \left\{ \frac{1}{r_1 + r_2} - \frac{1}{r_1 + r_2 + \Delta} \right\}$$

TABLE II  
Work Required for Separation of an Ion Pair

$D$	$r_1 + r_2, \text{\AA}$	$\Delta, \text{\AA}$	$\Delta F, \text{kcal/mole}$
2	4	1	7.9
2	6	1	3.8
4	4	1	4.0
4	6	1	1.9

where  $N$  is Avogadro's number,  $e$  is the electric charge,  $D$  is the dielectric constant,  $r$  is the ionic radius of ion, and  $\Delta$  is the distance of ion separation.

By substituting appropriate values for nonpolar media, the results given in Table II were obtained.

The authors are grateful to Miss F. Shimada in this department for her capable technical assistance.

### References

1. P. H. Plesch, Ed., *The Chemistry of Cationic Polymerization*, Pergamon Press, London, 1963, p. 558.
2. C. Aso, T. Kunitake, and Y. Ishimoto, *J. Polymer Sci. A-1*, **6**, 1175 (1968).
3. C. Aso, T. Kunitake, and R. Kita, *Makromol. Chem.*, **97**, 31 (1966).
4. C. Aso, T. Kunitake, Y. Matsuguma, and Y. Imaizumi, *J. Polym. Sci. A-1*, **6**, 3049 (1968).
5. C. E. Schildknecht, A. Z. Zoss, and C. McKinley, *Ind. Eng. Chem.*, **39**, 180 (1947).
6. C. E. Schildknecht, *Ind. Eng. Chem.*, **50**, 107 (1958).
7. S. Okamura, T. Kodama, and T. Higashimura, *Makromol. Chem.*, **53**, 180 (1962).
8. T. Higashimura, K. Suzuoki, and S. Okamura, *Makromol. Chem.*, **86**, 259 (1965).
9. I. W. Bassi, C. Dall'Asta, U. Campigli, and E. Strepparola, *Makromol. Chem.*, **60**, 202 (1963).
10. S. Murahashi, S. Nozakura, M. Sumi, H. Yuki, and K. Hatada, *J. Polym. Sci. B*, **4**, 634 (1966).
11. S. Murahashi, S. Nozakura, M. Sumi, S. Fujii, and K. Matsumura, *Kobunshi Kagaku*, **23**, 550 (1966).
12. M. Sumi, S. Nozakura, and S. Murahashi, *Kobunshi Kagaku*, **24**, 424 (1967).
13. M. Goodman, and Y.-L. Fan, *J. Amer. Chem. Soc.*, **86**, 4922, 5712 (1964).
14. K. Matsuzaki, M. Hamada, and K. Arita, *J. Polym. Sci. A-1*, **5**, 1233 (1967).
15. M. Goodman and Y.-L. Fan, *Macromolecules*, **1**, 163 (1968).
16. K.-J. Liu and S. J. Lignowski, *J. Polym. Sci. B*, **6**, 191 (1968).
17. K. Matsuzaki, T. Uryu, and C. Imai, *J. Polym. Sci. B*, **6**, 195 (1968).
18. Y. Ohsumi, T. Higashimura, and S. Okamura, *J. Polym. Sci. A-1*, **5**, 849 (1967).
19. Y. Ohsumi, T. Higashimura, and S. Okamura, *J. Polym. Sci. A-1*, **4**, 923 (1966).
20. D. J. Cram and K. R. Kopecky, *J. Amer. Chem. Soc.*, **81**, 2748 (1959).
21. C. E. H. Bawn and A. Ledwith, *Quart. Rev.*, **16**, 361 (1962).
22. T. Higashimura, T. Yonezawa, S. Okamura, and K. Fukui, *J. Polym. Sci.*, **39**, 487 (1959).
23. S. Brownstein, S. Bywater, and D. J. Worsfold, *Makromol. Chem.*, **48**, 127 (1961).
24. Y. Sakurada, M. Matsumoto, K. Imai, A. Nishioka, and Y. Kato, *J. Polym. Sci. B*, **1**, 633 (1963).
25. K. S. Ramey and G. L. Statton, *Makromol. Chem.*, **85**, 287 (1965).
26. H.-G. Elias, P. Goeldi, and V. S. Kamat, *Makromol. Chem.*, **117**, 269 (1968).

27. K. Fujii, D. J. Worsfold, and S. Bywater, *Makromol. Chem.*, **117**, 275 (1968).
28. B. D. Coleman, *J. Polym. Sci.*, **31**, 155 (1958).
29. H. Weiner and R. A. Snee, *J. Amer. Chem. Soc.*, **87**, 292 (1965).
30. M. V. Volkenstein, *Configurational Statistics of Polymer Chains*, Interscience, New York, 1963, p. 311.
31. F. A. Bovey, *J. Polym. Sci.*, **46**, 59 (1960).
32. S. Okamura, T. Higashimura, and I. Sakurada, *J. Polym. Sci.*, **39**, 507 (1959).
33. T. Higashimura, T. Kodama, and S. Okamura, *Kobunshi Kagaku*, **17**, 163 (1960).
34. S. Okamura, T. Higashimura, and H. Yamamoto, *Kogyo Kagaku Zasshi*, **61**, 1636 (1958).
35. T. Higashimura, Y. Sunaga, and S. Okamura, *Kobunshi Kagaku*, **17**, 257 (1960).
36. T. Kodama, T. Higashimura, and S. Okamura, *Kobunshi Kagaku*, **18**, 267 (1961).
37. G. Natta, *J. Polym. Sci.*, **48**, 219 (1960).
38. S. Murahashi, H. Yûki, T. Sano, U. Yonemera, H. Tadokoro, and Y. Chatani, *J. Polym. Sci.*, **62**, S77 (1962).
39. L. F. Fieser and M. Fieser, *Advanced Organic Chemistry*, Reinhold, New York, 1961, p. 659.
40. O. C. Dermer, D. M. Wilson, F. M. Johnson, and V. H. Dermer, *J. Amer. Chem. Soc.*, **63**, 2881 (1951).
41. L. L. Ferstandig and F. C. Goodrich, *J. Polym. Sci.*, **43**, 373 (1960).
42. G. Natta, M. Peraldo, M. Farina, and F. Bressan, *Makromol. Chem.*, **55**, 139 (1962).
43. Y. Ohsumi, T. Higashimura, S. Okamura, R. Chujo, and T. Kuroda, *J. Polym. Sci. A-1*, **5**, 3009 (1967).
44. Y. Ohsumi, T. Higashimura, and S. Okamura, *J. Polym. Sci. A-1*, **6**, 3015 (1968).
45. M. Szwarc, *Makromol. Chem.*, **89**, 44 (1965).

Received March 10, 1969

Revised September 15, 1969

## Formation of Diethylene Glycol as a Side Reaction during Production of Polyethylene Terephthalate

S. G. HOVENKAMP and J. P. MUNTING, *AKZO Research & Engineering N.V. Arnhem, The Netherlands*

### Synopsis

Polymers of poly(ethylene terephthalate) (PET) always contain a certain amount of incorporated diethylene glycol (DEG), substituting the incorporated glycol. DEG is formed in a side reaction during the ester interchange of dimethyl terephthalate (DMT) with ethylene glycol or during direct esterification of terephthalic acid with ethylene glycol, and to a smaller extent during the polycondensation of the low-molecular material. DEG is formed via an unusual type of reaction: ester + alcohol  $\rightarrow$  ether + acid. Some evidence of this type of reaction is given by the formation of dioxane in low molecular PET and of methyl Cellosolve and methyl carbitol during the ester interchange of DMT with ethylene glycol and diethylene glycol, respectively. The strongest support for this type of reaction, however, was obtained from kinetic data. Polyesters of low molecular weight with OH group contents ranging from 3 to 0.5 mole/kg were heated at 270°C in sealed tubes for 1-7 hr. The kinetic equation for the proposed reaction is:  $d[\text{DEG}]/dt = k[\text{OH}][\text{ester}]$ . With the aid of one rate constant the formation of DEG in all esters could be described.

### INTRODUCTION

Polymers of poly(ethylene terephthalate) (PET) always contain a certain amount of incorporated diethylene glycol (DEG), replacing the incorporated glycol. The amount of DEG influences the physical and chemical properties of the polyester. For instance, the melting point of PET is lowered by about 5°C for every percentage unit (by weight) of DEG content.<sup>1-3</sup> DEG is mainly formed in a side reaction during the interchange of dimethyl terephthalate and ethylene glycol, or during esterification of terephthalic acid with ethylene glycol. To a smaller extent DEG is formed in the subsequent polycondensation step. This paper deals with the kinetics of the formation of DEG as determined by laboratory experiments.

### EXPERIMENTAL AND RESULTS

Five polyesters of low molecular weight with different degrees of polymerization were prepared by esterification of terephthalic acid with glycol according to the method of Kemkes,<sup>4,5</sup> followed by a polycondensation step (removal of glycol by distillation). Catalysts, added after the esterifica-

tion but before polycondensation, were  $\text{Mn}(\text{CH}_3\text{COO})_2 \cdot 4 \text{H}_2\text{O}$ , 0.024%, and  $\text{Sb}_2\text{O}_3$ , 0.04%.

The esters were analyzed for free glycol by reacting the glycol with periodate and subsequent iodometric titration of iodate plus excess periodate.

The number of alcoholic endgroups was determined by NMR analysis of solutions in hot nitrobenzene (150°C) by the method of Heidemann et al.<sup>6</sup> The five esters were heated at 270°C in sealed ampoules, all for 1, 2, 3, 4, 5, 6, and 7 hours. The amounts of DEG in the heated samples were determined by hydrazinolysis of the esters (15 min refluxing with hydrazine), followed by gas chromatographic analysis (column material, Porapak Q; stainless steel column; column temperature, 215°C; carrier gas: wet  $\text{N}_2$ ; flame ionization detector). A similar analysis, but with Carbowax/KOH on Chromosorb-W as column material and with a column temperature of 100°C, permitted the determination of dioxane which proved to be formed during the heating, in amounts not exceeding 10% of the amount of DEG. As DEG is the precursor of dioxane, the amount of dioxane has to be added to the amount of DEG for calculating the total amount of DEG formed. Straight lines were obtained for all esters when the amount of DEG + dioxane was plotted versus the period of heating.

Carboxyl endgroups were determined by photometric titration of solutions of PET in 25 ml *o*-cresol plus 10 ml chloroform with 0.03M alcoholic KOH. (Bromophenol blue indicator).

It was found that the increase in carboxyl endgroups during heating exceeded the increase in DEG by about a factor two.

Particulars about the starting materials and the rate of DEG formation may be found in Table I.

Some screening experiments were performed with pure glycol and with glycol to which small amounts (1–10%) of low molecular weight ester had been added. They showed that DEG formation in pure glycol was almost negligible (Table I), but that the addition of small amounts of ester caused a marked increase in DEG formation. This increase was about proportional to the amount of ester added: about 0.01 mole kg-hr for every per cent of ester.

TABLE I  
Starting Materials and Rate of Formation of DEG and Dioxane

Sample	Glycol, mole/kg	Alcoholic endgroups, mole/kg	DEG + Dioxane formation, mole/kg-hr
1	0.31	2.76	0.037
2	0.05	1.62	0.020
3	0.024	1.24	0.0134
4	—	0.75	0.0084
5	—	0.48	0.0061
Glycol	16.1	—	0.01

### Kinetic Treatment of the Results

From the screening experiments with almost pure glycol it was concluded that ester linkages play the key role in DEG formation. This cannot be concluded from the experiments with the low molecular weight polymer, as the concentration of ester linkages, is almost independent of the degree of polymerization. (Table II.)

TABLE II  
Calculation of Reaction Constant for Ether Formation

Sample	Alcohol groups, mole/kg	Ester groups, mole/kg	$k$ , kg/mole-hr
1	3.38	9	0.0012
2	1.72	10	0.0012
3	1.29	10	0.0011
4	0.75	10	0.0012
5	0.48	10	0.0014
		Avg.	0.0012

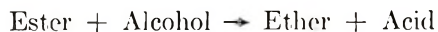
As the concentration of alcoholic groups (sum of endgroups and OH groups of free glycol) seems to be another important parameter, the most simple kinetic equation is

$$d[\text{DEG} + \text{dioxane}]/dt = k [\text{OH}] [\text{ester}]$$

From Table II it appears that application of this equation gives consistent values for  $k$ . The ether formation is not catalyzed by the presence of carboxyl endgroups. In all experiments a marked increase in carboxyl endgroups occurred. The DEG formation, however, proceeded at a constant rate, showing that it was independent of the carboxyl group content. Application of the kinetic equation to the results of the screening experiments with almost pure glycol gives a higher value for  $k$  (about 0.005 kg. mole<sup>-1</sup> hr<sup>-1</sup>). This may be due to the strongly different nature of the reaction medium.

### DISCUSSION

From the kinetic data it follows that in low molecular weight polyester DEG is not formed by a dehydration reaction between two alcoholic groups (as has sometimes been suggested<sup>3</sup>). In that case DEG formation would have been expected to be proportional to the square of the alcoholic group concentration. The formation occurs via an unusual type of reaction:

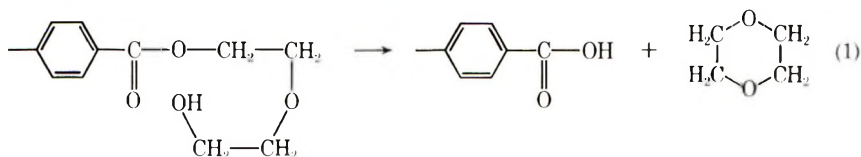


To our knowledge this type of reaction has not been described earlier for esters from weak organic acids and primary alcohols. It has been recognized for a long time, however, that the ether formation through heating of alcohols with concentrated sulfuric acid proceeds in the same way.

It is not surprising that the proposed reaction has not been observed

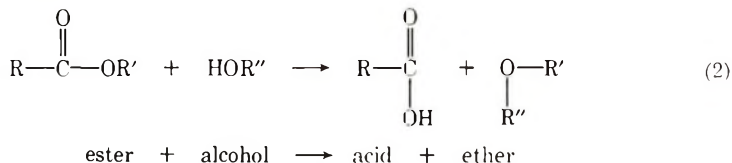
earlier: the temperatures involved in the production of PET are unusual as compared with those in organic reactions.

The following observations give further support to the idea of a reaction between alcohol and ester. The ether, methyl Cellosolve, is formed in small amounts when dimethyl terephthalate is heated with glycol; methyl carbitol is formed when dimethyl terephthalate is heated with DEG. Both reaction products were identified by gas-chromatographic analysis. The formation of dioxane as reported in the experimental part may be explained by an intramolecular reaction of half-esterified DEG:

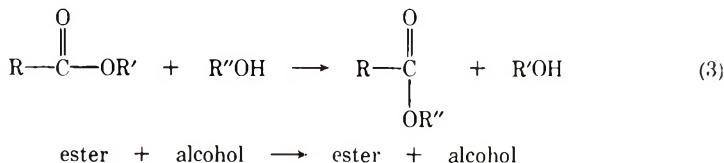


It may be noted that the proposed reaction is analogous to the well-known ester interchange reaction [eqs. (2) and (3)].

Ether formation:



Ester interchange:



DEG formation in low molecular weight polyester is not the only side reaction. From the observed rapid increase of COOH groups it may be concluded that at least one other important reaction occurs. A possible explanation is that glycolic endgroups are degraded at a rather high rate.

### References

1. F. B. Cramer (to E. I. du Pont de Nemours and Co.), U. S. Pat. 3,024,220 (Mar. 6, 1962); U. S. Pat. 3,070,575 (Dec. 25, 1962).
2. R. Janssen, H. Ruysschaert, and R. Vroom, *Makromol. Chem.*, **77**, 153 (1964).
3. J. R. Kirby, A. J. Baldwin, and R. H. Heidner, *Anal. Chem.*, **37**, 1306 (1965).
4. J. F. Kemkes, *Macromolecular Chemistry, Brussels-Louvain, 1967* (*J. Polym. Sci. C*, **22**), G. Smets, Ed., Interscience, New York, in press.
5. Brit. Pat. Spec. 1,001,787.
6. G. Heidemann, P. Kusch, and H. J. Nettelbeck, *Z. Anal. Chem.*, **212**, 401 (1965).

Received June 17, 1969

Revised September 15, 1969



## Polyamide-Imides

S. TERNEY, J. KEATING, and J. ZIELINSKI, *W. H. Wright Research Laboratories, Schenectady Chemical Company, Schenectady, New York*, and J. HAKALA and H. SHEFFER,\* *Technical Institute at Otaniemi, Helsinki, Finland*

### Synopsis

A novel preparation of polyamide-imides from diphenylmethane diisocyanate and trimellitic anhydride in *N*-methylpyrrolidone is described. Partial substitution of trimellitic anhydride with either maleopimaric acid, terephthalic acid, or by various dianhydrides permitted a correlation of structure with solution stability and thermal properties. Heat resistance improved with increasing imide content of the polyamide-imide. Almost all solutions advanced in viscosity on storage at room temperature. The least stable solutions were those that deviated the most from 50-50 amide-imide. However, the viscosity changes depended somewhat on the type of modifying ingredient. For example, polyamide-imides modified by substitution of 10% PMDA (pyromellitic anhydride) or BPDA (benzophenone tetracarboxylic acid dianhydride) were less stable than those modified with 10% (cyclopentanetetracarboxylic acid dianhydride) CPDA or THFDA (tetrahydrofuran-2,3,4,5-tetracarboxylic acid dianhydride). The use of excess reagent and of monofunctional chain stopper was investigated as a means of controlling solution stability.

### INTRODUCTION

The outstanding thermal properties and relatively low cost of aromatic polyamide-imides has led to their use in many fields. This paper describes a new method of synthesis of polyamide-imides from diisocyanates and the anhydride of tribasic acids. This method lends itself readily to modification by partial substitution of other reactive materials for part of the anhydride of the tribasic acid.

An excellent review of aromatic polyamide-imides can be found in the literature.<sup>1</sup> The early method of synthesis of polyamide-imides used acid chlorides and diamines along with a hydrogen chloride acceptor.

Otros<sup>2</sup> showed that isocyanates react with anhydrides to give imides and suggested a mixed anhydride of an *N*-acetylated carbamic acid and a carboxylic acid as the intermediate. This lost carbon dioxide in such a way that its origin could be traced to the carbon of the isocyanate. Müller<sup>3</sup> reacted 1.1-3.0 equivalents of polyisocyanate to every anhydride or acid function to give polyisocyanates containing amide, imide, and excess isocyanate functions. The excess isocyanate functions were masked with

\* Present address: Union College, Schenectady, New York.

cresols. Fetscher<sup>4</sup> claimed, incorrectly, that a 2:1 molar ratio of trimellitic anhydride to isocyanate gave an amide containing dianhydride. There is little doubt that his product had both amide and imide functions in it, since an anhydride functional group reacts with isocyanates at nearly the same rate as a carboxyl function.

In 1966 we investigated the synthesis of polyamide-imides from diisocyanates and trimellitic anhydride at Schenectady Chemical Co. Shortly thereafter a French patent<sup>5</sup> disclosed this same method of polymerization.

Solvents such as dimethylformamide, dimethylacetamide and *N*-methylpyrrolidone were suitable for this synthesis. However, the maximum attainable viscosity was greater for the latter solvent, suggesting that these solvents compete with TMA for the isocyanate function. Weiner<sup>6</sup> has shown that dimethylformamide reacts with phenyl isocyanate to give *N,N*-dimethyl-*N'*-phenylformamidine at 150°C, while Ulrich<sup>7</sup> has shown that the same reagents given pentaphenyl-1,3,6,8,10-pentazospiro-4,5-decane-2,4,7,9-tetrone.

We have found in this investigation that *N*-methylpyrrolidone reacts with phenyl isocyanate at 230°C to give diphenylurea and 1-methyl-2,3-diphenyliminopyrrolidine.

Beck<sup>8</sup> increased the imide content of polyamide-imide by using a mixture of dianhydrides and trimellitic acid chloride to react with a diamine. This method obviously required the use of a scavenger for hydrogen chloride.

## EXPERIMENTAL

### Materials

In general, the solvents were dried by azeotropic distillation with benzene. At first a good deal of water was distilled. When the rate of water collection decreased, the drying process was considered complete, since further heating led to a slow formation of water by interaction of two molecules *N*-methylpyrrolidone. A few batches of polymers were made with solvent dried with Linde molecular sieves, type SA. The chemicals and their sources were: MM [diphenylmethane diisocyanate, (Multrathane M), Mobay Co.]; MDA (methylene dianiline, Fluka A.G.); MPA (maleopimaric acid, Eastman Organic Chemicals); TMA (trimellitic anhydride, Schuchardt, München); PMDA (pyromellitic dianhydride, Schuchardt, München); BPDA (benzophenonetetracarboxylic acid dianhydride, Petroleum Division, Gulf Oil Co.); CPDA (cyclopentane tetracarboxylic acid dianhydride, Copolymer Rubber and Chemical Corp.); THFDA (tetrahydrofuran-2,3,4,5-tetracarboxylic acid dianhydride, Aldrich Chemical Co.); TA (terephthalic acid, Fluka A.G.); NMP (*N*-methylpyrrolidone, Fluka A.G.); PHT (phthalic anhydride, Fluka A.G.); 3,4D (3,4-diaminobenzoic acid, Fluka A.G.); THEI (trihydroxyethyl isocyanurate, Allied Chemical & Dye Corp.).

TABLE I  
Composition and Physical Properties of Polyamide-Imides

Batch no.	Reactant, mole				Other	Viscosity	Solids, %	$\bar{X}_n$	Film
	MDA	MM	TMA						
8-1		0.1	0.1			Z1-Z2	19.6		Flexible
15-1		0.1	0.08	0.02 TA		Z2	29.3		Flexible
52-1		0.1	0.07	0.03 TA		N	25.5		Cloudy, brittle
38-1		0.1	0.09	0.01 PMDA		N-Y	26.9		Flexible
25-1		0.1	0.09	0.01 BPDA		Z2-Z3	28.5		Flexible
65-1		0.1	0.08	0.02 BPDA		Z1	25.0		Flexible
31-1		0.1	0.09	0.01 CPDA		T-U	26.2		Flexible
71-1		0.2	0.08	0.02 CPDA		I	29.0		Brittle
51-1		0.1	0.09	0.01 THFDA		Z-Z1	26.1		Flexible
26-1		0.1		0.1 MPDA		Z2	40.0		Very brittle
39-1		0.05	0.025	0.025 MPDA		Q	26.2		Brittle
44-1		0.05	0.045	0.005 MPDA		N	25.7		Brittle
36-3	0.0505			0.0500 PMDA		V	15.7		Flexible
27-4	0.101			0.105 BPDA		W	17.0		Flexible
53-1		0.1	0.101			Z2	24.3	201	Flexible
74-1		0.1	0.102			Z3	25.3	101	Flexible
56-1		0.1	0.103			Z3-Z4	20.9	68	Flexible
54-1		0.1	0.1	0.001 PHT		Z2	25.5	201	Flexible
68-1		0.1	0.1	0.003 PHT		Z	28.3	68	Flexible
66-1		0.1	0.098	0.004 PHT		L	24.2	101	Brittle
62-1		0.1	0.096	0.008 PHT		O	24.6	51	Brittle
69-1		0.098	0.1	0.004 C <sub>6</sub> H <sub>5</sub> NCO		N	24.2	101	Brittle
55-1		0.1	0.095	0.033 3,4I		Z3	25.4		Flexible
75-1		0.1	0.096	0.033 THEI		W	25.8		Flexible

### Polymer Preparation

All reactants were weighed carefully into a three-necked Pyrex flask with the solvent being added last. The reactants were stirred with a stainless steel paddle while the flask was equipped with a reflux condenser, drying tube, and thermometer. Great care in weighing was essential as the molecular weight and ultimate viscosity was dependent on the molar ratio of reactants. The batches were heated slowly, about 10 hr being required to reach 177°C (the reflux temperature of NMP) from room temperature and held at 177°C until a viscosity of Z2 was obtained at 25% solids. When batches were heated more rapidly than this from room temperature to 177°C a lower ultimate viscosity was achieved. Apparently the rapid heating schedule resulted in the solvent interfering with the desired polyamide-imide formation by reacting with isocyanate functional groups. Those batches that contained maleopimaric acid were made at 121°C and 100% polyimides were made at room temperature. All polyamide-imide batches were prepared at 25% solids in 80/20 NMP-xylol; whereas polyimides were prepared in 100% NMP.

Many batches were discarded as impractical because they were not soluble in the solvent system mentioned above. It is a well known rule that polyamic acid-polyimide resins are insoluble in amide solvents if more than 50% of the polyamic acid is converted to polyimide. We found that if the imide content of the polyamide-imide resins was much over 50%, insoluble polymers were obtained. For example polymers made by reacting 10 mole-% PMDA and 90 mole-% TMA with MM were soluble, whereas those with 20 mole-% PMDA were insoluble. The upper solubility limit was 20 mole-% with BPDA. On the other hand, with CPDA, 50 mole-% of the dianhydride could be included as a replacement for TMA to give a soluble resin.

Also it was noticed that increasing the amide content by inclusion of 20% TA as partial replacement for TMA gave a clear resin solution but 30% TA was cloudy. Apparently deviating very far either way from 50-50 amide-imide leads to insolubility.

A summary of all the formulations appears in Table I. The viscosities are reported as Gardner-Holt numbers and the solids were obtained by heating a 2-g sample of resin solution for 1 hr at 200°C in an aluminum dish. The flexibility of the film depends to a great extent on the degree of polymerization as indicated by the viscosity-solids relationship.

## RESULTS AND DISCUSSION

### Solution Stability

Polyamide-imide polymers dissolved in 80/20 NMP-xylol increased in viscosity on storage at room temperature (Fig. 1). The polymer solution made by partial replacement of TMA with 10 mole-% PMDA changed the most; the ones with 30 and 20 mole-% TA and 10 mole-% BPDA also

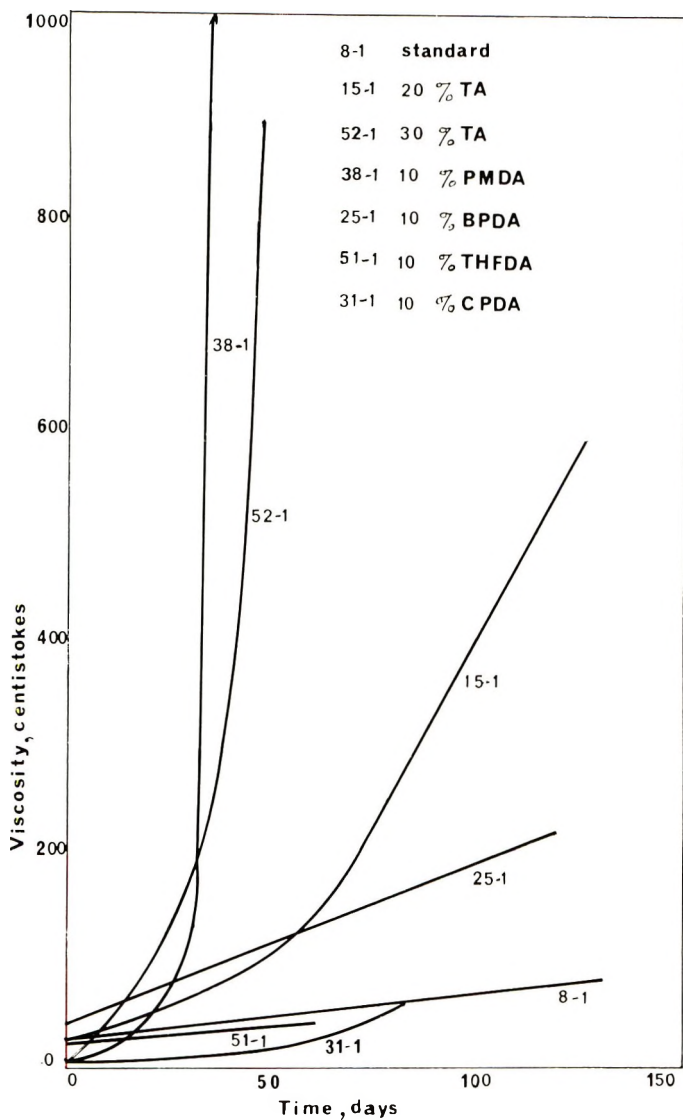


Fig. 1. Solution stability of polyamide-imides.

changed quite rapidly. The ultimate finished polymer solutions were lower in viscosity to begin with and changed less for 10% CPDA, 10% THFDA, and 10% and 50% maleopimaric acid than for those mentioned above. However, the batch with 100% maleopimaric acid gelled on standing.

Further reaction of the free isocyanate with carboxyl and anhydride groups must be responsible for the gradual increase in viscosity observed with formulations containing MM and TMA with isocyanate equivalent to acid plus anhydride, such as 8-1. Analysis has shown that this type of polymer solution has a free isocyanate content of between 0.1–1.0% of the

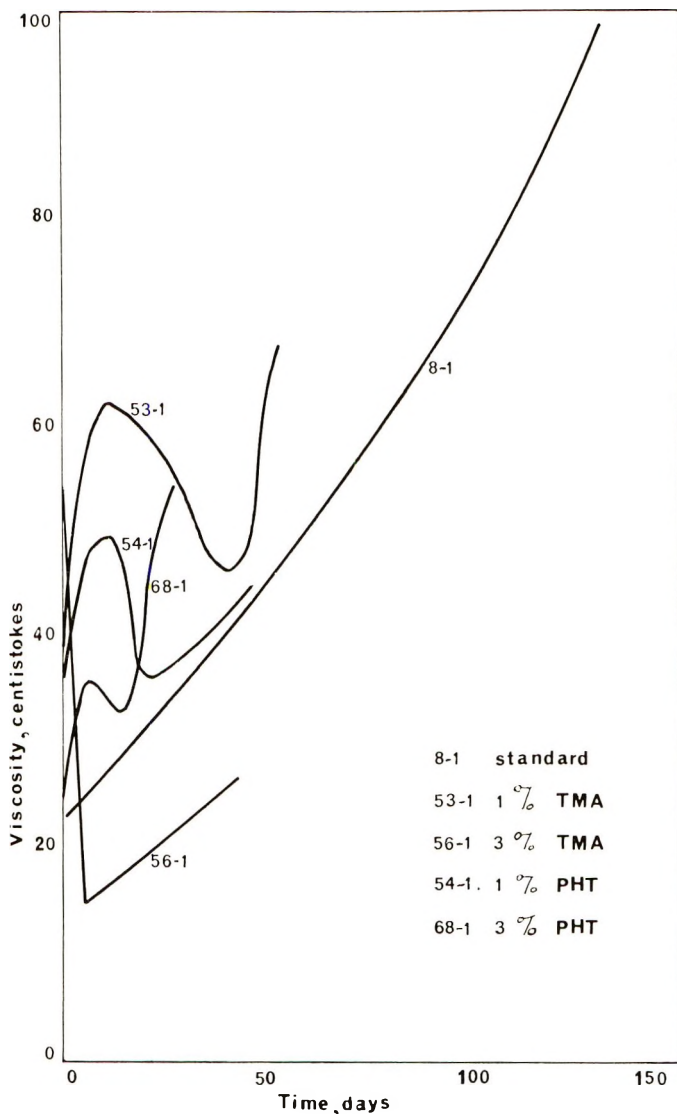


Fig. 2. Solution stability of polyamide-imides with excess anhydride.

initial value prior to polymerization. This free isocyanate is present in spite of polymerizing at 177°C for 10–15 hr.

The large increase in viscosity on standing observed with 10 mole-% PMDA or BPDA formulations may be due to unreacted anhydride combining with amide groups in another polymer chain. If PMDA were partially hydrolyzed before use or during polymerization to a diacid anhydride and only the two carboxyl groups had reacted to form a linear polymer, this would leave a free anhydride group available for crosslinking with amide functions in another polymer chain.

A slow aggregation of the polyamide-imides of high amide content due to hydrogen bonding may account for their increase in viscosity.

### Excess Anhydride and Monofunctional Chain Terminator

In an attempt to overcome the problem of solution instability, between 1 and 3% excess acid and anhydride functions in the form of trimellitic anhydride or phthalic anhydride were reacted with MM. Fairly stable solutions were obtained (Fig. 2), but these polymer solutions became slightly hazy on standing no doubt due to unreacted TMA. These solutions seemed to change viscosity in an erratic fashion.

The two batches with equivalent reactants at 2 or 4 eq-% phthalic anhydride were too low in ultimate viscosity, as was the formulation with 2 eq-% phenyl isocyanate. These formulations all gave brittle films on curing in aluminum dishes and solutions that changed slowly in viscosity on storage (Fig. 3).

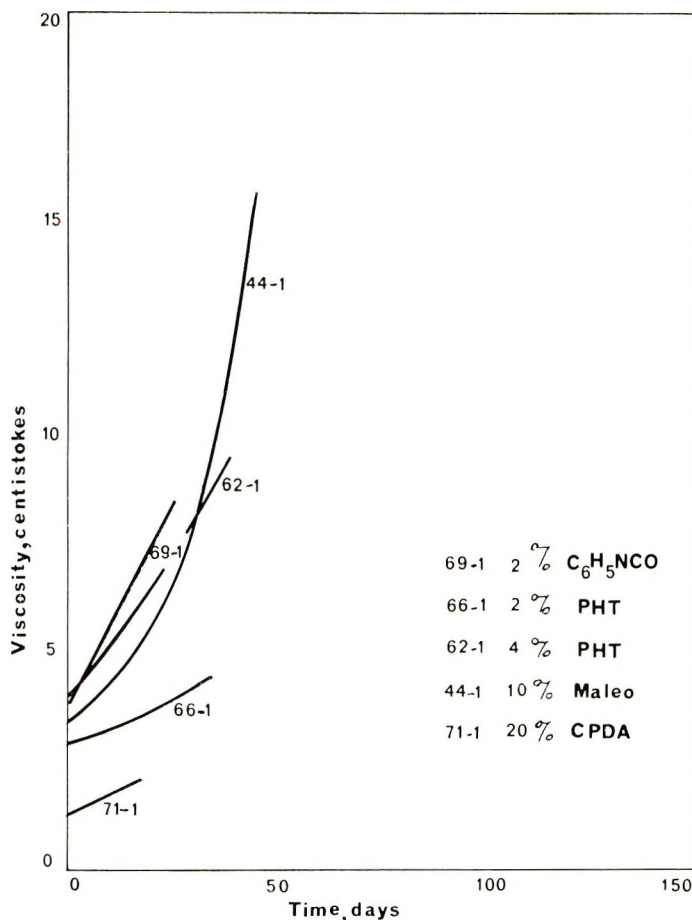


Fig. 3. Solution stability of polyamide-imides.

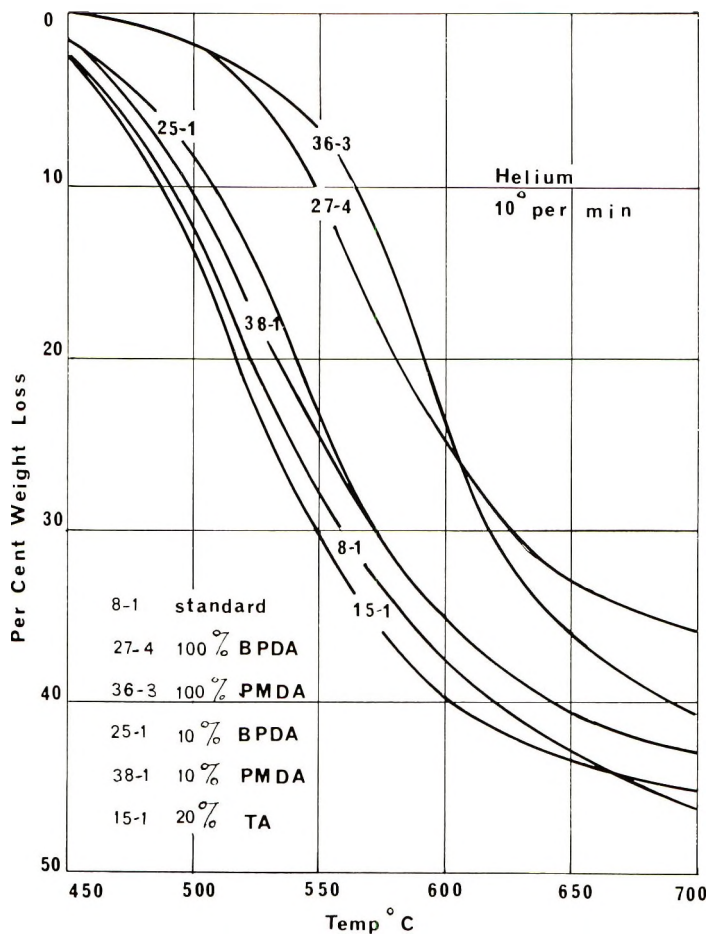


Fig. 4. Thermogravimetric analysis.

A comparison of ultimate viscosity with predicted average degree of polymerization does not show complete correlation due to a lack of purity of the reactants.

The inclusion of 3,4-diaminobenzoic acid (5 eq-%) as a partial replacement for TMA gave a fairly stable solution and a flexible film. In another formulation the inclusion of a small amount of THEI had a similar effect.

### Thermal Stability

Thermal gravimetric analyses were carried out on a Mettler thermoanalyzer no. 26 in helium with a 10°C/min temperature rise. A sample of the film left from solids determination was used for this TGA investigation.

Figure 4 shows that the thermal resistance in helium is directly related to the imide content of the polymer.



Figure 5 shows a more rapid degradation of the polymer as the maleopimaric acid content increased.

It was found that 20% BTDA had lower weight loss than 10% BTDA, but 20% CPDA had higher weight loss than 10% CPDA. The use of either 3,4-diaminobenzoic acid or trishydroxyethyl isocyanurate as partial replacement for TMA reduced the weight loss of polyamide-imides to a small extent.

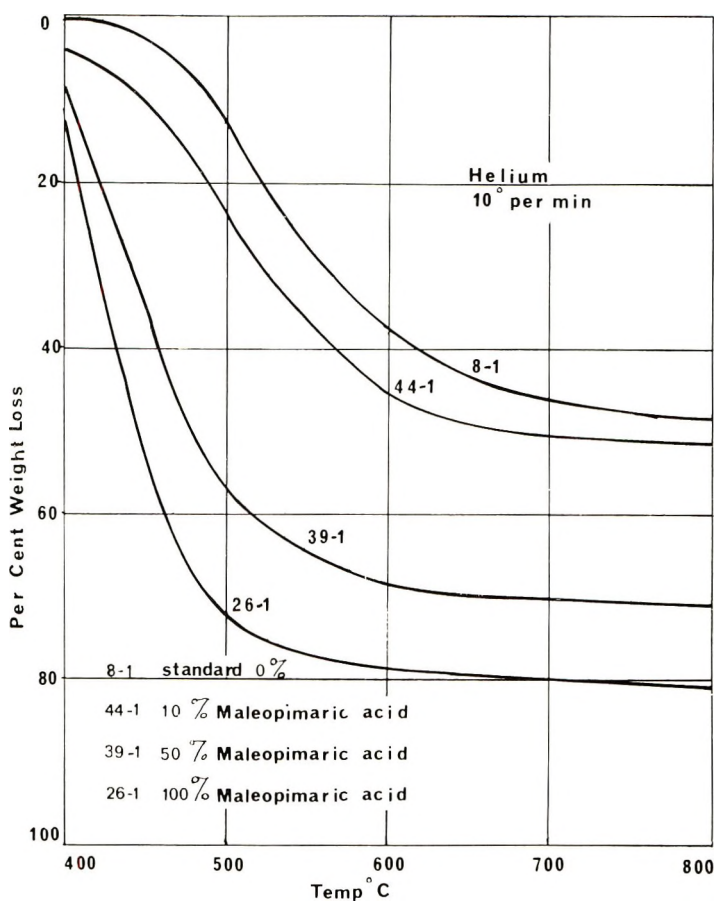


Fig. 5. Thermogravimetric analysis.

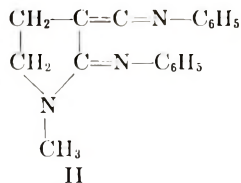
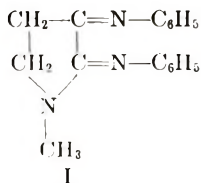
Solvent was found to be present to an extent of 15% in films from 2-g samples (1 hr, 200°C) and to extent of 8% on films from 0.5-g samples (1 hr, 200°C) by TGA analysis. It was assumed that weight loss up to 400°C was due to solvent trapped in the film. Vapor-phase analysis of a sample collected in a liquid air trap proved solvent had been evolved during TGA analysis.

### Reaction of *N*-Methylpyrrolidone with Phenyl Isocyanate

Phenyl isocyanate and *N*-methyl-pyrrolidone (0.1 mole each) were refluxed for 3 hr at 235°C. After standing for several days, 6.0 g of crude crystals was filtered off. On recrystallization from alcohol-water, 1-methyl-2,3-diphenyliminopyrrolidone (I) was obtained; mp 227–228°C; infrared absorptions at 2860–3200 (NCH<sub>3</sub>), 1640 (C=N), 1602, 1597 (amidine), 768, 755, and 700 cm<sup>-1</sup> (monosubstituted benzene); NMR in CF<sub>3</sub>COOH showed  $\delta$  3.18 (s,3), 2.53 (t,2,  $J = 8\text{H}_3$ ), 3.76 (t,2,  $J = 8\text{H}_3$ ), 7.40 (m,6), 7.62 (m,4); NMR in (D<sub>3</sub>C)<sub>2</sub>SO showed  $\delta$  2.97 (s,3), 2.70 (m,2), 2.05 (m,2), 6.7–7.6 (m, 10).

ANAL. Calcd. for C<sub>17</sub>H<sub>17</sub>N<sub>3</sub>: C, 77.6%; H, 6.5%; N, 15.9%. Found: C, 78.9%; H, 6.4%; N, 14.7%.

The absence of ketene imine absorption at 2050–2000 cm<sup>-1</sup> favors structure I over II.



Infrared analysis of the crude crystals established the presence of diphenyl urea as well as I. Distillation of the mother liquor gave 5 g of NMP, bp 122°C/15 mm, and 2.3 g of material having bp 188–196°C/25 mm. This latter fraction crystallized on standing (mp 230°C); recrystallization from alcohol-water increased the melting point to 235°C. Infrared and NMR spectra and mixed melting point proved this material was symmetrical diphenyl urea. Further work to establish the exact yield and other products will be carried out.

### References

1. H. Lee, D. Soffey, and K. Neville, *New Linear Polymers*, McGraw-Hill, New York, 1967, p. 173.
2. L. Otrás, J. Marton, and J. Meisel-Agoston, *Tetrahedron Letters*, **2**, 15 (1960).
3. G. Müller and R. Merten, Brit. Pat. 1,058,236.
4. C. A. Fetsher and E. Schonfeld, U. S. Pat. 3,317,580.
5. Hitachi Chemical Co., French Pat. 1,473,600.
6. M. L. Weiner, *J. Org. Chem.*, **25**, 2245 (1960).
7. R. Ulrich, B. Tucher, F. A. Stuber, and A. A. R. Sayigh, *J. Org. Chem.*, **33**, 3928 (1968).
8. D. Beck, Brit. Pat. 1,075,284.

Received May 20, 1969

Revised September 15, 1969

## Radical and Radiation-Induced Grafting of Some Synthetic High Polymers within the Temperature Range of their Glass Transition\*

ECKEHARD SCHAMBERG and JÜRIG HOIGNÉ, *Inrescovv, AG für industrielle Forschung und Strahlennutzung, Schwerzenbach-Zurich, Switzerland*

### Synopsis

The temperature dependence of radiation-induced grafting onto poly(ethylene terephthalate), polyamides, polyacrylonitrile, and polypropylene has been investigated for several monomers. In all cases a maximum grafting yield is obtained when the reaction is performed in the temperature range of the glass transition  $T_g$  of the polymer used. This maximum yield does not only appear with radiation-induced simultaneous grafting. It also appears when the graft polymerization is induced by pre-irradiation or even by thermal decomposition of organic peroxides. It is assumed that the pronounced maximum of the reactivity at  $T_g$  is obtained because in the glassy state below  $T_g$  the radicals formed cannot react due to a reduced diffusion of the monomer, whereas above  $T_g$  the number of radicals available for polymerization will be reduced with increasing temperature.

### INTRODUCTION

The radiation-induced grafting of polymers depends on the grafting temperature.<sup>1</sup> Some high polymers, however, can be grafted only at higher temperatures.<sup>2,3</sup> Obviously these polymers exist in the glassy state at room temperature. Therefore we investigated the temperature dependence of radical and radiation-induced grafting of some high polymers which are industrially important. Some of the experimental results are reported here.<sup>4</sup>

### EXPERIMENTAL

#### Materials

Poly(ethylene terephthalate) (PET) was in the form of Terylene fabric, warp and weft 50/45 den, no thermal treatment.

The polyamide-6 (PA-6) was Bodanyl yarn, 70/22 den; the polyamide-66 (PA-66) was nylon 66 fabric, warp and weft 70/23 den.

\* Presented by Eckehard Schamberg at the IUPAC-International Symposium on Macromolecular Chemistry, Budapest, August 1969.

A modified polyacrylonitrile (PAN) was used, Dralon fabric, warp-weft 59/39-83/34 den.

The polypropylene fabric (PP) had warp-weft 61/52-111/28 den.

All polymer samples were purified by a 24 hr Soxhlet extraction with methanol and acetone. PET, PAN, and PP samples were, in addition, extracted with water. The chemicals used in these studies were commercially available and were purified by distillation or recrystallization before use.

### Grafting Initiation

**Gamma Irradiation.** Samples (0.5–1.0 g) were irradiated in sealed glass ampoules in the presence of the solution (20–30 ml) and air (Gammacell 220,  $1.2 \times 10^6$  r/hr). All samples were preheated for 1 hr.

**Electron Irradiation.** All samples (0.5–1.0 g) were preheated for 3 min and irradiated to a dose of 1.0 Mrad. For irradiation the samples were transported at a speed of 2.4 cm/sec. under a scanned electron beam (operating at 0.02 mA/cm) at a distance of 3 cm from the window (accelerator: Haefely Basle, 400 keV, 0.25 mA/cm, 1250 cps; scanner width 40 cm).

Grafting induced by dibenzoyl peroxide was performed in the absence of solvents and air. The samples (0.5–1.0 g) were immersed in 20–30 ml solution.

### Sample Measurements

The grafting yield was gravimetrically determined in the absence of moisture. After the irradiation, hydroquinone was added to the samples, which were then extracted with water or toluene until a constant weight was achieved. The experimental error is  $\pm 1\%$ .

## RESULTS AND DISCUSSION

Poly(ethylene terephthalate) (PET) samples (0.5–1.0 g) were irradiated with  $\gamma$ -rays in the presence of an aqueous solution (20–30 ml) of itaconic acid and acrylamide (each 7.5 wt-%) at different temperatures. Up to 75°C, virtually no reaction occurs with the substrate (Fig. 1). Above this temperature the grafting yield increases considerably, and at about 80°C a marked maximum is obtained. In agreement with the literature,<sup>5</sup> DTA measurements<sup>6</sup> of the PET used show that the glass transition occurs between 80 and 85°C. The maximum graft at  $T_g(\text{PET})$  was also obtained by using an aqueous solution of itaconic acid and 4-vinylpyridine (2.4 and 10.0 wt-%). The temperature dependence of the grafting yields ( $\gamma$ -radiation-initiated) of itaconic acid and acrylamide (each 7.5 wt-% in water) onto polyamide-6 (PA-6), polyamide-66 (PA-66), and polyacrylonitrile (PAN) shows maxima at temperatures (40, 50, and 70°C, respectively) which again are in agreement with  $T_g$ -values quoted in the literature<sup>5,7</sup> (Figs. 2 and 3). Even with polypropylene (PP), which has a very low

$T_g$  (about  $-15^\circ\text{C}$ ) the  $\gamma$  radiation-initiated grafting of styrene (50 wt-% in chloroform) shows a maximum in the area of  $T_{g(\text{PP})}$  (Fig. 4).

The pronounced reactivity of the polymers at  $T_g$  is not limited to  $\gamma$ -radiation or a specified grafting method, as is illustrated by the following experi-

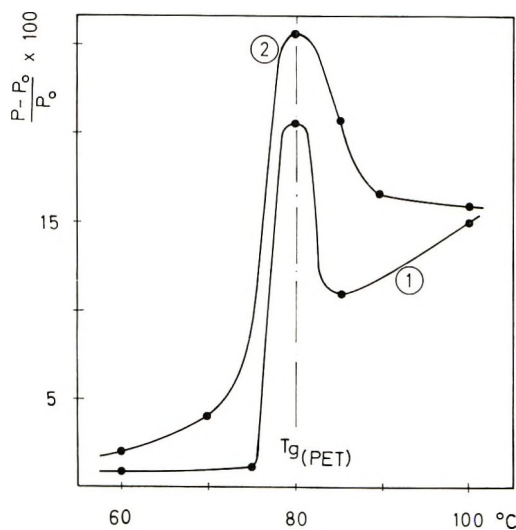


Fig. 1. Temperature dependence of the grafting yield: (1) Simultaneous  $\gamma$ -irradiation of PET and an aqueous solution of 7.5 wt-% itaconic acid and 7.5 wt-% acrylamide, dose 2.0 Mrad; (2) simultaneous  $\gamma$ -irradiation of PET and an aqueous solution of 2.4 wt-% itaconic acid and 10.0 wt-% 4-vinylpyridine, dose 2.0 Mrad.

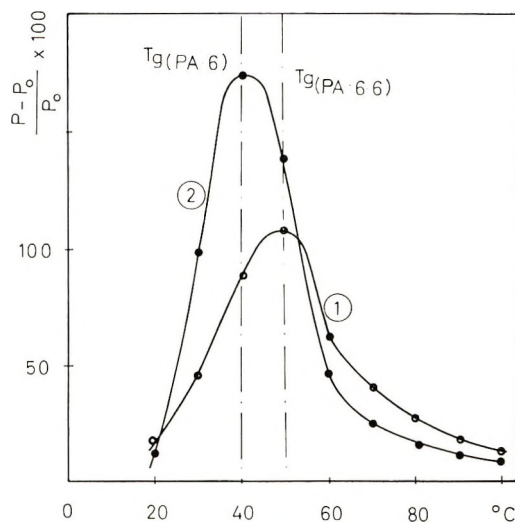


Fig. 2. Temperature dependence of the grafting yield: (1) simultaneous  $\gamma$ -irradiation of PA-66 and an aqueous solution of 7.5 wt-% itaconic acid and 7.5 wt-% acrylamide, dose 1.0 Mrad; (2) simultaneous  $\gamma$ -irradiation of PA-6 and an aqueous solution of 7.5 wt-% itaconic acid and 7.5 wt-% acrylamide, dose 1.0 Mrad.

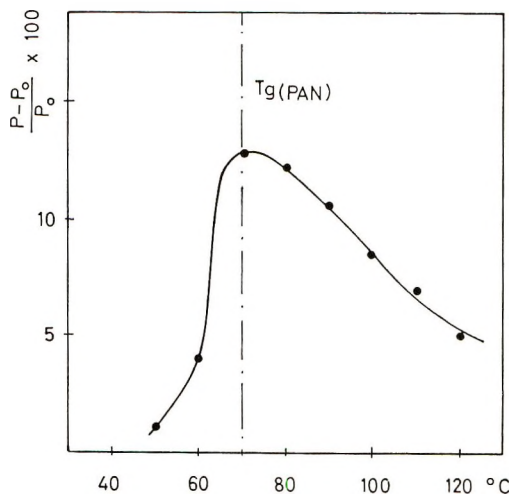


Fig. 3. Temperature dependence of the grafting yield. Simultaneous  $\gamma$ -irradiation of PAN and an aqueous solution of 7.5 wt-% itaconic acid and 7.5 wt-% acrylamide, dose 2.0 Mrad.

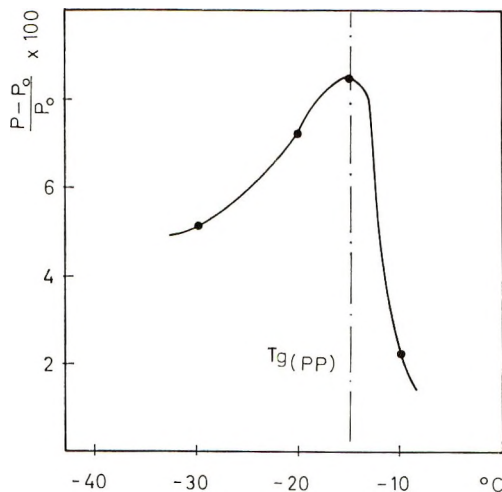


Fig. 4. Temperature dependence of the grafting yield. Simultaneous  $\gamma$ -irradiation of PP and 50% wt-% styrene in chloroform, dose 2.0 Mrad.

ments. Table I shows the yields for grafting itaconic acid and acrylamide (each 7.5 wt-% in water) onto PA-66 by use of the 400-keV accelerator. The maximum yield does not occur only when polyamide and the monomer solution were irradiated simultaneously at 50°C. It also appears when the polymer (0.5–1 g) was pre-irradiated at room temperature and thereafter immersed in the heated monomer solution (50–100 ml) for 15 min. Table II shows the yields for grafting of styrene onto PET with the use of 1.0 wt-% dibenzoyl peroxide as initiator. Dimethylaniline (0.1 wt-%) was

TABLE I  
Yield for the Grafting of Itaconic Acid and Acrylamide onto PA-66<sup>a</sup>

	Yield $[(P - P_0)/P_0] \times 100^b$		
	25°C	50°C	75°C
Samples irradiated in the presence of monomer solution	2.3	10.0	5.4
Samples pre-irradiated in the presence of water	1.4	14.5	7.5

<sup>a</sup> Itaconic acid and acrylamide, each 7.5 wt-% in water; electron irradiation, dose 1.0 Mrad.

<sup>b</sup>  $P_0$  is the original fabric weight;  $P$  is the weight of the grafted fabric.

TABLE II  
Comparison of the Grafting Yield and the Polymerized Material in the Solution for the Grafting of Styrene onto PET with the Use of 1.0 wt-% Dibenzoyl Peroxide and 1.0 wt-% Dimethylamine

	70°C	83°C	92°C	104°C	125°C
Grafting yield $[(P - P_0)/P] \times 100$					
1 hr	—	12.5	18.4	16.7	12.4
2 hr	4.5	22.5	22.5	23.2	15.4
Polymerized material in the solution after 2 hr, wt-% of the employed monomer	15.1	29.5	38.6	53.7	59.0
Grafting yield (2 hr)/polymerized material in the solution	0.30	0.76	0.58	0.43	0.26

added in order to reduce the temperature dependence of the radical formation, which in most cases overrides the pronounced reactivity of the substrate at  $T_g$ . The grafting yield reaches only a flat maximum between 80 and 100°C. On comparing this grafting yield with the polymerized monomer in the solution (by taking the ratio of the grafting yield to the total polymerized material), it is evident that a pronounced maximum in the reactivity occurs even when the radical formation is not initiated by radiation.

One way to explain the experimentally observed effect is the following: When the polymer passes from the glassy state into a highly viscous liquid the ability to undergo radical reactions becomes increased, because at  $T_g$  the polymer chains become more mobile. It can be assumed that with increasing temperature, more and more radicals combine, and therefore they cannot react with the monomer. Additionally, chain termination may be favored due to an increased diffusion rate. This would lead to a lower kinetic chain length. An increase in the rate of chain termination could explain the decrease in the grafting yield above  $T_g$ . But obviously, as shown by grafting PIET (Fig. 1), at temperatures far above  $T_g$  in some cases the grafting yield increases again. No reason can be seen, that chain

termination should suddenly decrease again. Therefore we are inclined to assume, that the decrease of the number of radicals available for the graft polymerization will be overcompensated by an increase of the kinetic chain length causing an increase of the overall grafting yield. The decline in the grafting yield above  $T_g$  is not due to a crystallization process. In the PET samples used, the crystallization occurs only at 140°C, as could be seen from the crystallization peak on the DTA curve. Irradiation of the polymers at very low temperatures leads to the formation of ionic species, but far below  $T_g$  most polymers undergo discoloration, indicating that the ionic species disappear. However, within the temperature range studied, ions will not be present, even below  $T_g$ , and therefore it is not at  $T_g$  where ion-electron-retrapping is occurring.

The authors wish to thank Heberlein & Co. AG, Wattwil, Switzerland, The Sanforized Company, a Division of Cluett-Peabody & Co., Inc., New York, USA, and Hausamman Textil AG, Winterthur, Switzerland, as well as Dr. R. Pfeiffer, Inrescor AG for their permission to publish; Dr. A. Sommerauer, Mettler Instruments, Greifensee-Zürich, Switzerland for performing some DTA measurements and further Mr. H. J. Padrutt and Miss A. Vetter for their help in carrying out the experiments.

### References

1. A. Chapiro, *Pure Appl. Chem.*, **12**, 227 (1966).
2. W. Zielinski, T. Achmatowicz, and A. Robalewski *Proceedings of the 2nd Tihany Symposium on Radiation Chemistry*, 1967, pp. 733-39.
3. A. Ulinska and A. Koscielecka, paper presented at the international conference on Chemical Transformations of Polymers, Bratislava, 1968; Preprint-17.
4. E. Schamberg and J. Hoigné, (Inrescor), Swiss Pat. Appl. 12837/68 and 1665/69.
5. P. V. Papero, R. C. Winckhofer, and H. J. Oswald, *Rubber Chem. Technol.*, **38**, 999 (1965).
6. A. Sommerauer, unpublished results.
7. W. H. Charch and W. W. Moseley, Jr., *Text. Res. J.*, **29**, 525 (1959).

Received July 15, 1969

Revised September 15, 1969



## Copolymerization with Depropagation. III. Composition and Sequence Distribution from Probability Considerations

JOHN A. HOWELL, MASATSUGU IZU,\* and KENNETH F.  
O'DRISCOLL, *Department of Chemical Engineering, State University of  
New York at Buffalo, Buffalo, New York 1424*

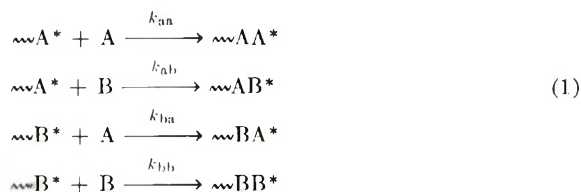
### Synopsis

Elementary probability considerations have been used to derive completely general equations which describe both the sequence distributions and compositions to be expected for copolymerizations which follow kinetic models having complete reversibility for all propagation steps. It is shown that previously derived composition equations for both reversible and irreversible systems are special cases of the general equations derived herein.

### INTRODUCTION

The two previous papers in this series<sup>1,2</sup> as well as papers by Ivin and co-workers<sup>3,4</sup> and by Yamashita<sup>5</sup> have all made use of the pioneering kinetic treatment of Lowry<sup>6</sup> which described the composition behavior to be expected when one of a pair of monomers being copolymerized was capable of depropagating. Lowry explored theoretically the behavior of three different cases, and subsequent experimental work has shown the utility of his Case II<sup>1-5</sup> in describing the variation of copolymer composition with monomer feed, temperature, or concentration for certain monomer systems. The equations Lowry developed are analogous to the well known Mayo-Lewis<sup>7</sup> equation which describes composition for simple binary copolymerization in terms of monomer feed and two reactivity ratios. Lowry's equations require in addition the equilibrium constants for any reversible propagation reactions.

The Mayo-Lewis equation describes the copolymer composition for a system where the composition is determined by four irreversible propagation reactions (1):



\* On leave from Department of Hydrocarbon Chemistry, Kyoto University, Kyoto, Japan.

Lowry considered, in his Case II, the situation when only the last of these reactions was reversible, and that only if the penultimate unit was a monomer B unit:



The approach used by Lowry<sup>6</sup> to solve the kinetics of copolymerization with depropagation was an excellent extension of the steady-state kinetic solution which leads to the Mayo-Lewis equation. However, such an approach does not yield any information about sequence distribution in the copolymer chain, and, of necessity, the equations lack generality and must be rederived in a complex fashion for each specific case. Some years ago, Goldfinger and Kane<sup>8</sup> and, more recently, Price<sup>9</sup> have shown the power of using a probability approach in solving copolymerization problems. Not only does one obtain the composition equations identical to those from the kinetic steady-state approach but as a bonus the sequence distributions are very readily derived. So, for example, it was shown<sup>8</sup> that the relative composition of a copolymer of monomer A and monomer B was given by

$$F_A/F_B = P_{ba}/P_{ab} \quad (2)$$

where  $P_{ab}$  is the conditional probability of a chain ending in monomer A adding on a monomer B. This probability can be expressed in the kinetic terms of the Mayo-Lewis equation as

$$\begin{aligned} P_{ab} &= k_{ab}[\text{B}]/(k_{ab}[\text{B}] + k_{aa}[\text{A}]) \\ &= 1/\{1 + (r_a[\text{A}]/[\text{B}])\} \end{aligned} \quad (3)$$

which gives

$$\frac{F_A}{F_B} = \left(1 + r_a \frac{[\text{A}]}{[\text{B}]}\right) / \left(1 + r_b \frac{[\text{B}]}{[\text{A}]}\right) \quad (4)$$

which is the Mayo-Lewis equation.

The same conditional probabilities can also be used to express sequence distributions; for example, the diad probability in the simplest binary copolymerization without reversibility is given as

$$f_{ab} = f_{ba} = P_{ab}P_{ba}/(P_{ab} + P_{ba}) \quad (5)$$

where  $f_{ab}$  is the probability of finding an —A—B— sequence in a polymer chain compared to the total probability of finding —A—A—, —A—B— and —B—B—. Triad probabilities are readily obtained by multiplying the proper diad probability by the proper conditional probability of addition, e.g.,

$$f_{aba} = f_{ab}P_{ba} \quad (6)$$

and so on for tetrads and higher sequences.

Given the foregoing idea of the power and success of a probability approach to simple, irreversible copolymerization problems, we show in this

paper that a probability approach to copolymerization with depropagation yields composition equations for the most general cases and reduce to ones which are identical to Lowry's, and also give the sequence distributions to be expected.

### SOME ELEMENTARY PROBABILITY CONSIDERATIONS

When a copolymer chain has been formed, the process for each chain is usually so fast that the local composition of any segment of the chain is independent of the position on the chain. The composition can therefore be usefully expressed as probabilities of certain diad combinations. (This holds not only for binary copolymers, but for multicomponent polymers in general. However, this discussion will be restricted to binary copolymers.) The chance of two dissimilar monomer units occurring at any position in the chain in the sequence —A—B— will be noted  $(A_n B_{n+1})$ . Using Bayes' theorem<sup>10</sup> we find that this unconditional diad probability is equal to the unconditional probability of finding an A unit in position  $n$  multiplied by the conditional probability of finding a B unit in position  $n + 1$  given that A is known to be in position  $n$ . Formally stated this is

$$(A_n B_{n+1}) = (A_n)(B_{n+1}|A_n) \quad (7)$$

Similarly we can write

$$(A_n A_{n+1}) = (A_n)(A_{n+1}|A_n) \quad (8)$$

It is important to emphasize that these last two statements do not presume any kinetic model, or random selection of the position, or even any quasi-steady-state polymerization: the statements are always correct. No assumption has been made that a diad conditional probability such as  $(A_{n+1}A_n)$  contains all the kinetic information about the polymerization, and, in general

$$(A_{n+1}|A_n) \neq (A_{n+1}|A_n A_{n-1}) \quad (9)$$

Combining equations 7 and 8 gives

$$\begin{aligned} (A_n B_{n+1}) + (A_n A_{n+1}) &= (A_n)[(A_{n+1} + B_{n+1})|A_n] \\ &= (A_n) \end{aligned} \quad (10)$$

since by the law of total probability the conditional probability of finding an A or a B unit in the  $n + 1$  position given an A in the  $n$  position must be unity in a binary copolymerization.

We can readily write similar statements for another position which we call  $m$ , resulting in

$$(B_m A_{m+1}) + (A_m A_{m+1}) = (A_{m+1}) \quad (11)$$

If positions  $m$  and  $n$  have been randomly chosen, or if the chain was propagated at a quasi-steady state under the mild restraint that both AB and BA sequences are possible, then we may write

$$(\Lambda_{m+1}) = (\Lambda_m) \quad (12)$$

and

$$(\Lambda_n \Lambda_{n+1}) = (\Lambda_m \Lambda_{m+1}) \quad (13)$$

Then without any loss of generality, we set  $m$  equal to  $n$  and obtain from eqs. (10)–(13)

$$(\Lambda_n \Lambda_{n+1}) = (\Lambda_n \Lambda_{n+1}) \quad (14)$$

This not-very-surprising result can be developed by expanding both sides of the statement by Bayes' theorem to give

$$(\Lambda_n)(\Lambda_{n+1}|\Lambda_n) = (\Lambda_n)(\Lambda_{n+1}|\Lambda_n) \quad (15)$$

or

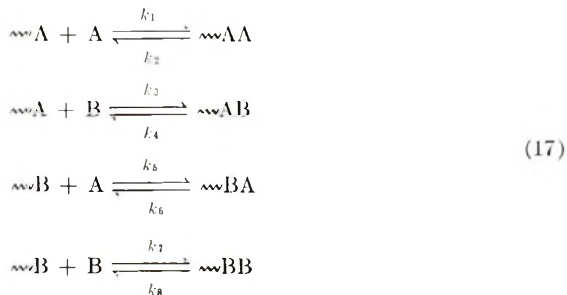
$$\frac{(\Lambda_n)}{(\Lambda_n)} = \frac{(\Lambda_{n+1}|\Lambda_n)}{(\Lambda_{n+1}|\Lambda_n)} \quad (16)$$

This is merely a restatement of eq. (2) in nomenclature which, being slightly different, will prove of further value in this paper.

### CASE I: DEPROPAGATION BY DIAD ENDGROUPS

Suppose that the copolymerization of monomers A and B occurs in such a way that all four of the reactions [eq. (1)] used in deriving the Mayo-Lewis equation are reversible. Suppose further that all reactions are first order in the active polymer and independent of the concentrations of monomer insofar as their variation with time is concerned.

The possible reactions and associated rate constants are then as shown in eqs. (17):



(Note that the propagation rate constants will be treated as pseudo-first order and could more properly be written as  $k_1[\text{A}]$ ,  $k_3[\text{B}]$ , etc., but this is not done here for simplicity of notation.)

To find the concentrations of A and B units in a completed chain, we begin by defining the transient probability that, at time  $t$ , the chance of a chain ending in A,  $(A)_t$ , is given by  $a$ , while that of a chain ending in B,  $(B)_t$ , is given by  $b$ . By the law of total probability

$$a + b = 1 \quad (18)$$

It is also necessary to define some conditional probabilities: if we know that a chain  $n$  units long ends in an A unit at time  $t$  and position  $n$ , the chance that the penultimate unit at position  $n - 1$  is A is defined as a transient probability

$$(A_{n-1}|A_n)_t = \epsilon \quad (19)$$

Then

$$(B_{n-1}|A_n)_t = 1 - \epsilon \quad (20)$$

Similarly, let

$$(B_{n-1}|B_n)_t = \eta \quad (21)$$

$$(A_{n-1}|B_n)_t = 1 - \eta \quad (22)$$

The chance that a chain contains an A unit at any random location within the complete chain is independent of location, if the propagation proceeded in a quasi-steady state manner. Practically, this is satisfied by rapid propagation to a low total conversion so that the monomer concentration does not change while the chains are being formed. For a particular chain let us suppose that the average time for it to increase by one unit is  $\tau$ . The net rate at which A adds to the chain multiplied by  $\tau$  will be the same as the chance of finding an A at a given location in the completed chain. The net rate of A addition will be the rate of adding A minus the rate of depropagation involving ultimate A units:

$$(A_n) = \tau \{ak_1 + bk_5 - a[(1 - \epsilon)k_6 + \epsilon k_2]\} \quad (23)$$

The analogous equation for B units is

$$(B_n) = \tau \{bk_7 + ak_3 - b[(1 - \eta)k_4 + \eta k_8]\} \quad (24)$$

It is also possible to describe the net rate of formation of terminal diads in a similar manner

$$(A_n A_{n+1}) = \tau(ak_1 - a\epsilon k_2) \quad (25)$$

$$(A_n B_{n+1}) = \tau(ak_3 - b(1 - \eta)k_4) \quad (26)$$

$$(B_n A_{n+1}) = \tau(bk_5 - a(1 - \epsilon)k_6) \quad (27)$$

$$(B_n B_{n+1}) = \tau(bk_7 - b\eta k_8) \quad (28)$$

Similarly, the equations for the rate of forming terminal triads take forms such as

$$(A_n A_{n+1} A_{n+2}) = \tau(a\epsilon k_1 - a\epsilon^2 k_2) \quad (29)$$

or

$$(\mathbf{A}_n \mathbf{A}_{n+1} \mathbf{B}_{n+2}) = \tau(a\epsilon k_3 - b\epsilon(1 - \eta)k_4) \quad (30)$$

If we invoke eq. 10, we find from eqs. (25), (26), and (23)

$$a[k_3 + (1 - \epsilon)k_6] = b[k_5 + (1 - \eta)k_4] \quad (31)$$

Similarly, eqs. (25), (29), and (30) may be combined with the statement analogous to eq. (10):

$$(\mathbf{A}_n \mathbf{A}_{n+1}) = (\mathbf{A}_n \mathbf{A}_{n+1} \mathbf{A}_{n+2}) + (\mathbf{A}_n \mathbf{A}_{n+1} \mathbf{B}_{n+2}) \quad (32)$$

to give

$$b\epsilon(1 - \eta)k_4 = a[\epsilon(k_1 + k_2 + k_3) - (k_1 + \epsilon^2 k_2)] \quad (33)$$

The analogous equation for BB diads is

$$a\eta(1 - \epsilon)k_6 = b[\eta(k_7 + k_8 + k_5) - (k_7 + \eta^2 k_8)] \quad (34)$$

Equations (18), (31), (33), and (34) are the set necessary to solve for  $a$ ,  $b$ ,  $\epsilon$ , and  $\eta$  in terms of the eight kinetic rate constants.

We have proven, but do not show, that the transient probabilities,  $\epsilon$  and  $\eta$ , are equal to the nontransient conditional probabilities of finding AA and BB diads within the chain, i.e.,

$$\begin{aligned} \epsilon &\equiv (\mathbf{A}_{n-1} | \mathbf{A}_n)_t = (\mathbf{A}_{n-1} | \mathbf{A}_n) \\ \eta &\equiv (\mathbf{B}_{n-1} | \mathbf{B}_n)_t = (\mathbf{B}_{n-1} | \mathbf{B}_n) \end{aligned} \quad (35)$$

This permits us to write

$$\begin{aligned} (\mathbf{A}_n)(\mathbf{A}_{n-1} | \mathbf{A}_n)_t &= (\mathbf{A}_{n-1} \mathbf{A}_n) \\ (\mathbf{B}_n)(\mathbf{B}_{n-1} | \mathbf{B}_n)_t &= (\mathbf{B}_{n-1} \mathbf{B}_n) \end{aligned} \quad (36)$$

Removal of the transient restraint permits position  $n$  to be any chain position.

Equation (36), in combination with equations (23)–(28) gives the composition equation as

$$\begin{aligned} \frac{(\mathbf{A}_n)}{(\mathbf{B}_n)} &= \frac{(\mathbf{A}_{n-1} \mathbf{A}_n) / \epsilon}{(\mathbf{B}_{n-1} \mathbf{B}_n) / \eta} \\ &= \frac{a\eta(k_1 - \epsilon k_2)}{b\epsilon(k_7 - \eta k_8)} \end{aligned} \quad (37)$$

By letting  $k_2 = k_4 = k_6 = k_8 = 0$ , it is easy to demonstrate that eq. (37) reduces to that of Mayo and Lewis, eq. (4) above.

This last equation can also be shown to reduce to Lowry's Case I which, in terms of our model, occurs when  $k_2 = k_4 = k_6 = 0$ . The next three equations give the equivalence between our notation and Lowry's:

$$\begin{aligned} k_7/k_5 &= [\text{B}]r_2/[\text{A}] \\ k_7/k_8 &= [\text{B}]\rho \\ \eta &\equiv \alpha \end{aligned} \quad (38)$$

Using the notation of the right hand sides of these last three equations, we rewrite eq. (34) as

$$\frac{\alpha^2 r_2}{[\text{A}]\rho} - \alpha \left( 1 + \frac{[\text{B}]}{[\text{A}]} r_2 + \frac{r_2}{[\text{A}]\rho} \right) + \frac{[\text{B}]}{[\text{A}]} r_2 = 0 \quad (39)$$

Upon rearrangement this becomes

$$\alpha^2 - \alpha \left( 1 + [\text{B}]\rho + \frac{\Lambda\rho}{r_2} \right) + [\text{B}]\rho = 0 \quad (40)$$

which is identical to eq. (4) in Lowry's paper.

Furthermore, our eq. (37) becomes

$$(\text{A}_n)/(\text{B}_n) = \alpha(1 + r_2)/[r_2 - (\alpha r_2/\rho)] \quad (41)$$

which is identical to Lowry's eq. (12). Equations (33) and (31) also simplify to

$$\epsilon = k_1/(k_1 + k_3) \quad (42)$$

and

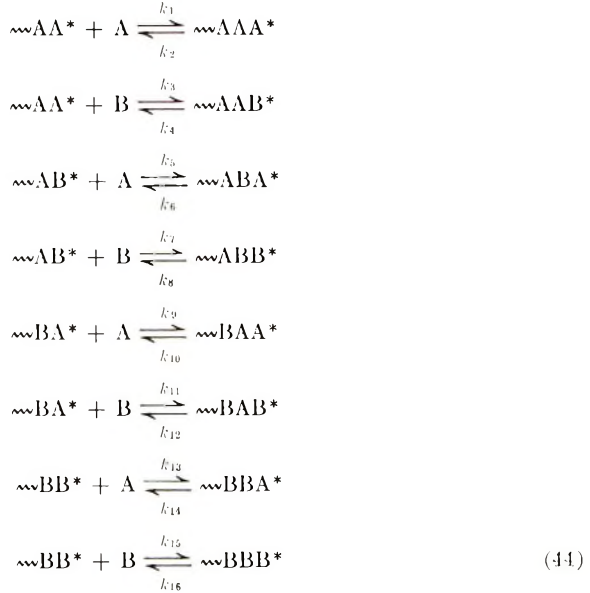
$$bk_3 = ak_3 \quad (43)$$

respectively. The identity of result with respect to composition in our treatment and Lowry's is consistent with expectation. Also, as expected, the probability approach has yielded new sequence distribution equations.

## CASE II. DEPROPAGATION BY TRIAD ENDGROUPS

It will be shown in Part V of this series<sup>11</sup> that our model for Case I is adequate for describing the copolymerization of two monomers such as  $\alpha$ -methylstyrene and methyl methacrylate between their respective ceiling temperatures. However, the utility of Lowry's triad endgroup model has been demonstrated experimentally,<sup>1-4</sup> as mentioned earlier, where only one of the two monomers undergoes depropagation. Therefore it is of value to examine the general results for a triad endgroup model. We do so here only in outline since the details of the derivation are identical in form to that used in our Case I.

Our kinetic notation is expanded to sixteen rate constants, for there are eight reversible reactions to consider:



As in Case I, we define the transient probability that a chain ends in an A unit as  $a$  and that it ends in a B unit as  $b$ . We also retain the transient probabilities defined in eqs. (19)–(22) for penultimate units; we further define the transient probabilities for antipenultimate units as

$$(A_{n-2}|A_{n-1}A_n)_t = \mu \tag{45}$$

$$(B_{n-2}|B_{n-1}B_n)_t = \nu \tag{46}$$

$$(A_{n-2}|A_{n-1}B_n)_t = \psi \tag{47}$$

$$(B_{n-2}|B_{n-1}A_n)_t = \phi \tag{48}$$

Using the same techniques as in Case I, we determine the rates of formation of various end groups and obtain the relations (49)–(56).

$$a + b = 1 \tag{49}$$

$$\eta\nu(1 - \nu)(k_8 - k_{16}) = (1 - \eta)\nu k_7 - \eta(1 - \nu)k_{15} \tag{50}$$

$$\epsilon\mu(1 - \mu)(k_{10} - k_2) = (1 - \epsilon)\mu k_9 - \epsilon(1 - \mu)k_1 \tag{51}$$

$$a(1 - \epsilon)(1 - \phi)\phi(k_{14} - k_6) = b[\phi(1 - \eta)k_5 - \eta(1 - \phi)k_{13}] \tag{52}$$

$$b(1 - \eta)(1 - \psi)\psi(k_4 - k_{12}) = a[\psi(1 - \epsilon)k_{11} - \epsilon(1 - \psi)k_3] \tag{53}$$

$$b\eta[\nu k_{13} - (1 - \nu)k_{15} + \nu(1 - \nu)k_{16}] = a(1 - \epsilon)\phi\nu k_{14} \tag{54}$$

$$a\epsilon[\mu k_3 - (1 - \mu)k_1 + \mu(1 - \mu)k_2] = b(1 - \eta)\psi\mu k_4 \tag{55}$$

$$\begin{aligned}
 b[\eta k_{13} + (1 - \eta)(k_5 + \psi k_4 + (1 - \psi)k_{12})] \\
 = a[\epsilon k_3 + (1 - \epsilon)k_{11} + \phi k_{14} + (1 - \phi)k_6]
 \end{aligned} \tag{56}$$



The sequence distribution probabilities are given by

$$\begin{aligned} (\text{A})/\tau = a\{\epsilon[k_{13} + k_{11} - \mu k_{12} - (1 - \mu)k_{10}] + (1 - \epsilon)(k_9 + k_{11})\} \\ - b(1 - \eta)[\psi k_4 + (1 - \psi)k_{12}] \end{aligned} \quad (57)$$

$$\begin{aligned} (\text{B})/\tau = b\{\eta[k_{13} + k_{15} - \nu k_{16} - (1 - \nu)k_8] \\ + (1 - \eta)[k_5 + k_7 - \psi k_4 - (1 - \phi)k_{12}]\} \end{aligned} \quad (58)$$

where

$$\frac{1}{\tau} = \frac{(\text{A})}{\tau} + \frac{(\text{B})}{\tau} \quad (59)$$

$$\frac{(\text{AA})}{\tau} = \frac{a\epsilon}{\mu} (k_1 - \mu k_2) \quad (60)$$

$$\frac{(\text{BA})}{\tau} = \frac{(\text{AB})}{\tau} = \frac{1}{\phi} (b\eta k_{13} - a(1 - \epsilon)\phi k_{14}) \quad (61)$$

$$\frac{(\text{BB})}{\tau} = \frac{b\eta}{\nu} (k_{15} - \nu k_{16}) \quad (62)$$

$$\frac{(\text{AAA})}{\tau} = a\epsilon(k_1 - \mu k_2) \quad (63)$$

$$\frac{(\text{BAA})}{\tau} = a[(1 - \epsilon)k_9 - \epsilon(1 - \mu)k_{10}] \quad (64)$$

$$\frac{(\text{BBA})}{\tau} = b\eta k_{13} - a(1 - \epsilon)\phi k_{14} \quad (65)$$

$$\frac{(\text{ABA})}{\tau} = b(1 - \eta)k_5 - a(1 - \epsilon)(1 - \phi)k_6 \quad (66)$$

$$\frac{(\text{AAB})}{\tau} = a\epsilon k_3 - b(1 - \eta)\psi k_4 = \frac{(\text{BAA})}{\tau} \quad (67)$$

$$\frac{(\text{BAB})}{\tau} = a(1 - \epsilon)k_{11} - b(1 - \eta)(1 - \psi)k_{12} \quad (68)$$

$$\frac{(\text{ABB})}{\tau} = b(1 - \eta)k_7 - b\eta(1 - \nu)k_8 = \frac{(\text{BBA})}{\tau} \quad (69)$$

$$\frac{(\text{BBB})}{\tau} = b\eta(k_{15} - \nu k_{16}) \quad (70)$$

The copolymer composition equation can be derived as:

$$\frac{(\text{A})}{(\text{B})} = \frac{a\theta\eta\phi(k_1 - \mu k_2) + \mu\nu(b\eta k_{13} - a(1 - \epsilon)\phi k_{14})}{b\eta\mu\phi(k_{15} - \nu k_{16}) + \mu\nu(b\eta k_{13} - a(1 - \epsilon)\phi k_{14})} \quad (71)$$

The foregoing equations can be shown to reduce to Lowry's Case II which, in terms of our kinetic model, eq. (44), assumes

$$\begin{aligned} k_2 &= k_4 = k_6 = k_8 = k_{10} = k_{12} = k_{14} = 0 \\ k_1 &= k_9 \\ k_3 &= k_{11} \\ k_5 &= k_{13} \\ k_7 &= k_{15} \end{aligned} \quad (72)$$

Substituting these values and identities into the appropriate equations gives

$$\phi = \eta = k_7/(k_5 + k_7) \quad (73)$$

$$\psi = \epsilon = \mu = k_1/(k_1 + k_3) \quad (74)$$

$$\nu k_5 - (1 - \nu)k_7 + \nu(1 - \nu)k_{16} = 0 \quad (75)$$

The correspondence between our notation and that of Lowry is given by

$$\begin{aligned} k_1/k_3 &= r_1[\text{A}]/[\text{B}] \\ k_{15}/k_{13} &= r_2[\text{B}]/[\text{A}] \\ \nu &\equiv \beta \\ k_7/k_{16} &= \rho \\ \gamma &= (1 - \eta)/[\eta(1 - \nu)] \end{aligned} \quad (76)$$

Using Lowry's notation, then, eq. (71) becomes

$$(\text{A})/(\text{B}) = (1 + r_1)/[1 + r_2 - (\beta\eta r_2/\rho)] \quad (77)$$

where

$$(\rho\beta/r_2) - (1 - \beta)\rho + \beta(1 - \beta) = 0 \quad (78)$$

and

$$\eta = r_2/(1 + r_2) \quad (79)$$

This expression is easily shown to be equivalent to Lowry's composition equation for his Case II [eq. (25) in ref. 6]:

$$\frac{(\text{A})}{(\text{B})} = \frac{\beta\gamma - 1 + [1/(1 - \beta)]^2}{(r_1[\text{A}]/[\text{B}] + 1)(\beta\gamma + [\beta/(1 - \beta)])} \quad (80)$$

The sequence distribution equations can also be simplified by using the assumptions of Lowry's Case II to give

$$(\text{AA}) = r_1/\{1 + r_1 + [1 + r_2 - (\eta\nu r_2/\rho)]\} \quad (81)$$

$$(\text{BA}) = 1/\{1 + r_1 + [1 + r_2 - (\eta\nu r_2/\rho)]\} \quad (82)$$

$$(\text{BB}) = [r_2 - (\sigma\nu r_3/\rho)]\{1 + r_1 + (1 + r_2 - (\eta\nu r_2/\rho))\} \quad (83)$$

It is of interest to note that, given the postulates of Lowry's Case II, simple expressions for sequence distribution may be obtained in a more direct

fashion. Given that the terminal sequence —AA\* does not depropagate, we can say that in a complete chain

$$\frac{\langle A_n | A_{n-1} \rangle}{\langle B_n | A_{n-1} \rangle} = \frac{k_1}{k_3} = r_1 \frac{[A]}{[B]} \quad (84)$$

Furthermore we can invoke earlier, general results such as eq. (10) to obtain the unconditional probability

$$\langle A_n A_{n-1} \rangle = \langle A_n \rangle \frac{r_1 [A] / [B]}{1 + r_1 [A] / [B]} \quad (85)$$

Using the reversibility of diads previously established as equation 14

$$\langle A_n B_{n-1} \rangle = \langle B_n A_{n-1} \rangle = \langle A \rangle \frac{1}{1 + r_1 [A] / [B]} \quad (86)$$

$$\langle B_n B_{n-1} \rangle = \langle B \rangle - \langle A \rangle \frac{r_1 [A] / [B]}{1 + r_1 [A] / [B]} \quad (87)$$

## DISCUSSION

Equation 71 is the most general copolymer composition equation which has ever been derived. By proper specification of rate constants it may be reduced to any of the following: (a) eq. (35) of this paper; (b) Lowry's Cases I or II; (c) the Mayo-Lewis equation; (d) the "penultimate unit effect" equation of Merz, Alfrey, and Goldfinger.<sup>12</sup> Equation (71) cannot describe antipenultimate unit or higher effects such as Ham<sup>13</sup> has discussed, but it is possible in principle to derive complete equations for cases which, in the nomenclature of this paper, would be tetrad and higher models. Such equations would probably be so cumbersome as to be useless, since a model for depropagation of binary sequences  $n$  units long would require  $(2n)$  independent pieces of kinetic or thermodynamic information.

In addition to being a general description of copolymerization composition, the derivation of eq. (71) has also provided a general description of sequence distribution applicable to those cases (a)–(d) above. The importance of sequence distribution for distinguishing kinetic models has been emphasized by Berger and Kuntz.<sup>14</sup>

Application of the composition and sequence distribution equations derived in this paper is difficult because so many kinetic and/or thermodynamic parameters need specification. For example, the use of eq. (37) demands eight independent rate constants (or four free energies of polymerization plus four propagation rate constants) at any particular temperature. Such an application is possible for real systems and is demonstrated in Part V of this series.<sup>11</sup>

Support of this work by National Science Foundation Grant GK-1878 is gratefully acknowledged.

## References

1. K. F. O'Driscoll and F. P. Gasparro, *J. Macromol. Sci. Chem.*, **A1**, 643 (1967).
2. K. F. O'Driscoll and J. R. Dickson, *J. Macromol. Sci. Chem.*, **A2**, 449 (1968).
3. K. J. Ivin and R. H. Spensley, *J. Macromol. Sci. Chem.*, **A1**, 653 (1967).
4. K. J. Ivin, *Pure Appl. Chem.*, **4**, 271 (1962).
5. Y. Yamashita, H. Kasahara, K. Suyama, and M. Okada, *Makromol. Chem.*, **117**, 242 (1968).
6. G. G. Lowry, *J. Polym. Sci.*, **42**, 463 (1960).
7. F. R. Mayo and F. M. Lewis, *J. Amer. Chem. Soc.*, **66**, 1594 (1944).
8. G. Goldfinger and T. Kane, *J. Polym. Sci.*, **3**, 462 (1948).
9. F. P. Price, *J. Chem. Phys.*, **36**, 209 (1962).
10. H. Cramér, *Elements of Probability Theory*, Wiley, New York, 1955.
11. M. Izu and K. F. O'Driscoll, *J. Polym. Sci. A-1*, in press.
12. E. Merz, T. Alfrey, and G. Goldfinger, *J. Polym. Sci.*, **1**, 75 (1946).
13. G. E. Ham, *Copolymerization*, G. E. Ham, Ed., Interscience, New York, 1964, Chap. 1.
14. M. Berger and I. Kuntz, *J. Polym. Sci. A*, **2**, 1687 (1964).

Received September 17, 1969

## Chain Scission of Butyl Rubber by Nitrogen Dioxide in Absence and Presence of Air

H. H. G. JELLINEK and F. FLAJSMAN,\* *Department of Chemistry,  
Clarkson College of Technology, Potsdam, New York 13676*

### Synopsis

The chain scission reaction suffered by butyl rubber due to  $\text{NO}_2$  (0.01–1 mm Hg) has been studied in the presence and absence of air. It has also been studied as a function of temperature (25–65°C) at constant  $\text{NO}_2$  pressure, again in absence and presence of 1 atm of air. Reaction mechanisms which are in good agreement with the experimental results have been formulated. The synergistic action of  $\text{O}_2$  and  $\text{NO}_2$  has been pointed out.

The effect of relatively high pressures of  $\text{NO}_2$  on polystyrene films was studied from the standpoint of chain scission recently.<sup>1</sup> The main reaction consists of incorporation of nitrate or nitrite groups along the polymer backbone, replacing hydrogen on tertiary carbon atoms; only a small proportion of these groups leads to chain scission. A survey of the effect of  $\text{NO}_2$  and  $\text{SO}_2$ , respectively, on various polymers in presence and absence of air and ultraviolet light has also been given.<sup>2</sup>

The present work deals with an investigation of butyl rubber with respect to chain scission by small amounts of nitrogen dioxide (500–2000 ppm) in the absence and presence of air, respectively, over a temperature range from 25 to 65°C. Only  $\text{NO}_2$  is present as the equilibrium  $2\text{NO}_2 \rightleftharpoons \text{N}_2\text{O}_4$  is almost completely shifted towards  $\text{NO}_2$  at these low pressures.<sup>3</sup> Such small amounts of  $\text{NO}_2$  cause appreciable chain scission, especially in presence of air. The effect may be enhanced if near-ultraviolet radiation were also present. The susceptibility of butyl rubber to oxygen,  $\text{NO}_2$ , and ultraviolet light is due to the isoprene units in this copolymer.

### EXPERIMENTAL

#### Apparatus

The high vacuum apparatus ( $10^{-5}$  mm Hg) was essentially the same as that used for previous work.<sup>1</sup> Only slight modifications in procedure were necessary. These will be described below. Intrinsic viscosities were measured in an Ubbelohde dilution viscometer at 25°C and are expressed in deciliters per gram.

\* Present address: American Cement Technical Center, Riverside, California.

### Materials

Butyl rubber was kindly supplied by Enjay Chemical Corporation (Butyl 268). Its composition is 98.25% by weight of isobutylene and 1.75% by weight of isoprene. The polymer was purified by precipitating twice with methanol from a 2% w/v benzene solution. NO<sub>2</sub> was the same as used previously (Matheson);<sup>1</sup> it was passed through a drying tower and glass wool before being introduced into the high vacuum system. All solvents were of reagent quality.

### Procedure

**Film Preparation.** Films were prepared by pouring 0.95 ml of a 3% w/v solution of the polymer in benzene on to a flat glass plate (ca. 1.8 cm × 6.5 cm). The solvent was evaporated slowly, eventually under vacuum; drying was continued in the high-vacuum apparatus for 25–30 hr at 35°C. The film thickness was ca. 25 μ.

**Control of NO<sub>2</sub> Pressure.** The NO<sub>2</sub> pressure in the reaction system was controlled by means of NO<sub>2</sub> vapor pressures corresponding to several temperatures. The temperature–vapor pressure relationship given by Egerton was used for this purpose.<sup>4</sup> Constant vapor pressure was established by maintaining a trap with liquid NO<sub>2</sub> connected to the apparatus at constant temperature. Acetone–Dry Ice or, for lower temperatures, toluene–liquid nitrogen mixtures were used for this purpose. The following temperatures were chosen for obtaining suitable vapor pressures: –56.2 to –56.5°C, NO<sub>2</sub> 1.0 mm Hg; –61.2 to –61.5°C, 0.5 mm Hg; –68°C, 0.2 mm Hg; –89 to –90°C, 0.01 mm Hg. Temperatures were measured with a calibrated thermometer. Equilibrium pressure was established in the vacuum system including a 3-l. storage vessel; NO<sub>2</sub> was then passed into the thermostated reaction vessel containing the polymer samples on glass plates. After about 30 min, the stopcock to the trap was closed and the reaction continued, while the 3-l. storage bulb remained open to the reaction vessel. Thus, the entire reaction proceeded at a constant NO<sub>2</sub> pressure. The films were degassed at the end of the reaction.

**Experiments in Presence of NO<sub>2</sub> and Air.** Air was introduced via a P<sub>2</sub>O<sub>5</sub> tube after the respective NO<sub>2</sub> pressure had been established. The reaction system was degassed for about 15 min before the polymer samples were removed. This stopped any reaction due to NO<sub>2</sub> absorbed in the films. Intrinsic viscosities of the samples were measured in benzene solutions at 25 ± 0.005°C. The relationship (1) was used for the calculation of the viscosity average molecular weights:<sup>5</sup>

$$[\eta] = 8.3 \times 10^{-4} \bar{M}_v^{0.53} \quad (1)$$

According to the literature,<sup>6</sup> all commercially produced butyl rubber polymers have random molecular size distributions. Hence, a relationship holds,<sup>7</sup> as follows:

$$\bar{M}_v = \bar{M}_n \{ [(\gamma + 1)\Gamma(\gamma + 1)]^{1/\gamma} \} \quad (2)$$

where  $\gamma$  is the exponent in the Mark-Houwink equation. From eqs. (1) and (2), one obtains,

$$[\eta] = 1.13 \times 10^{-3} \bar{M}_n^{0.53} \quad (2a)$$

An average monomer molecular weight of 56.21 was taken for the calculations. A value of  $\bar{M}_n = 2.06 \times 10^5$  was obtained, which corresponds to a number-average chain length of  $\bar{DP}_{n,0} = 3.66 \times 10^3$ . An average chain molecule contains about  $53.8 \cong 54$  isoprene units and 3606 isobutylene units, respectively.

## RESULTS

Figure 1 shows plots of the degree of degradation  $\alpha = (1/\bar{DP}_{n,t}) - (1/\bar{DP}_{n,0})$  versus time for  $\text{NO}_2$  pressures of 1, 0.5, 0.25, and 0.20 mm Hg at  $35^\circ\text{C}$  in absence of air. The curves are calculated on the basis of an assumed mechanism [see Discussion, eq. (7a)], and the points are experimental data. These curves are characterized by an initially fast rate of chain scission, which decreases rather abruptly after about 5–10 hr resulting in straight lines. The rates increase with increasing  $\text{NO}_2$  pressure.

Figure 2 shows similar plots for a range of temperatures from  $25^\circ\text{C}$  to  $65^\circ\text{C}$  at a constant  $\text{NO}_2$  pressure of 0.2 mm Hg. The calculated curves are similar as before; the rates increase with temperature.

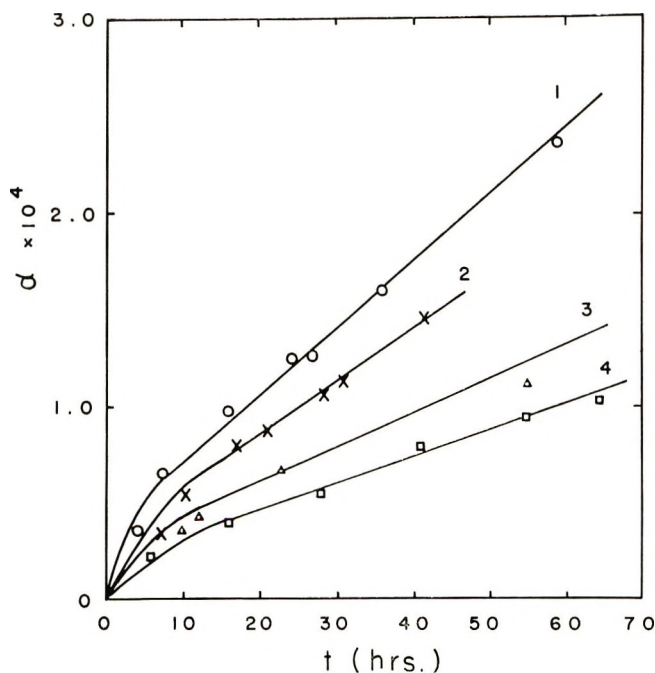


Fig. 1. Degree of degradation  $\alpha$  as a function of time for various  $\text{NO}_2$  pressures in absence of air at  $35^\circ\text{C}$ : (1) 1 mm Hg, (2) 0.5 mm Hg, (3) 0.25 mm Hg, (4) 0.20 mm Hg. The lines are calculated according to eq. (7a), the points are experimental data.

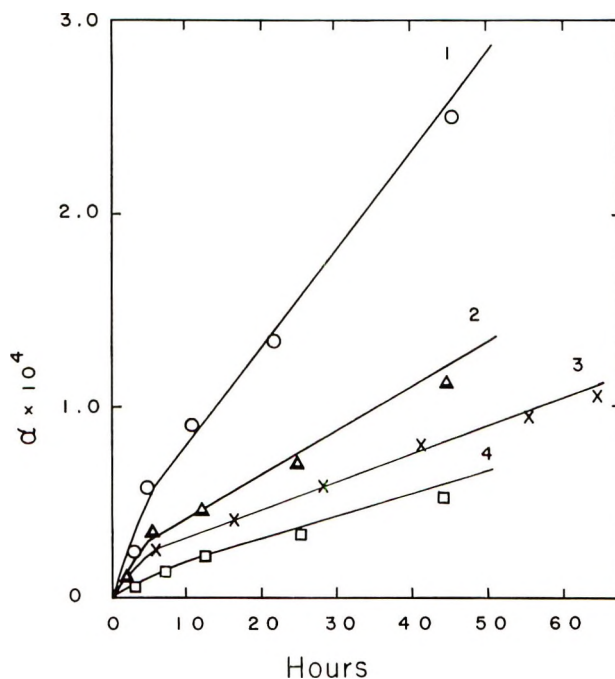


Fig. 2. Degree of degradation  $\alpha$  as a function of temperature for 0.2 mm Hg of  $\text{NO}_2$  (1) 65°C; (2) 45°C; (3) 35°C; (4) 25°C. The lines are calculated by eq. (7a), the points are experimental data.

An interesting observation was made during this investigation. The purified polymer was stored in bulk form in a refrigerator (+4°C) before use. The intrinsic viscosity of the freshly purified polymer was 0.736 dl/g. It decreased to 0.69 dl/g after two months of storage. On exposure of a film prepared from the stored polymer and exposed to 0.5 mm Hg of  $\text{NO}_2$  and 1 atm of air at 35°C, it was found that it degrades slower than a fresh sample (see Fig. 3). Hence, all experiments recorded in this paper were carried out with polymer stored in the refrigerator under nitrogen.

Figure 4 shows plots of  $\alpha$  versus time for experiments at  $\text{NO}_2$  pressures of 1, 0.5, 0.2, and 0.01 mm Hg in the presence of 1 atm of air at 35°C. The curves are quite different from those obtained in absence of air, and the rates of chain scission are about five times those for the experiments in presence of  $\text{NO}_2$  only.

Figure 5 shows the degradation as a function of temperature (25–55°C) in the presence of 0.2 mm Hg of  $\text{NO}_2$  and 1 atm of air, respectively. The rate of chain scission increases with temperature.

Infrared spectra of exposed films mounted on NaCl plates were also investigated. The films were obtained by evaporating benzene solutions; they were finally treated in high vacuum for 24 hr. Butyl rubber shows the same infrared spectra as polyisobutylene except for one sharp peak at 1540  $\text{cm}^{-1}$ . This peak is probably due to the  $\sim\text{HC}=\text{C}$ — double-bond stretch-



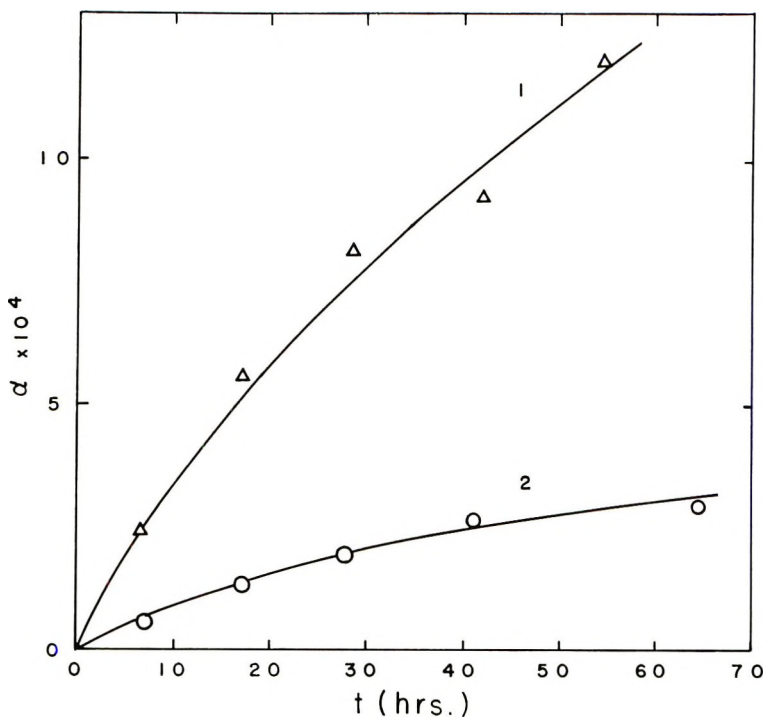
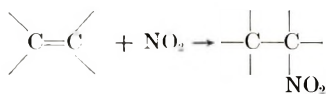


Fig. 3. Effect of storing the polymer at +4°C in presence of air: (1) fresh, purified sample, (2) polymer stored for two months in air. NO<sub>2</sub> pressure 0.5 mm Hg; 1 atm. of air.

ing frequency. After 12 hr exposure to NO<sub>2</sub> (5 mm Hg) at 45°C, a peak appeared at 1550 cm<sup>-1</sup>. This peak can be attributed to the incorporation of NO<sub>2</sub> groups into the polymer,<sup>8</sup>



In presence of air, the peak at 1540 cm<sup>-1</sup> gradually disappears and the appearance of the peak at 1550 cm<sup>-1</sup> becomes more pronounced.

## DISCUSSION

The data shown in Figure 1 indicate that initially some structures degrade, which are more susceptible to chain scission than the normal structures in the polymer molecule. However, these abnormal structures are present only in very small amounts and on degradation become quickly exhausted; only "normal" chain scission proceeds after the kinks in the curves. This is a case which is equivalent to that of "weak links" in a polymer molecule.<sup>9</sup> These "weak links" are assumed to be some oxy-

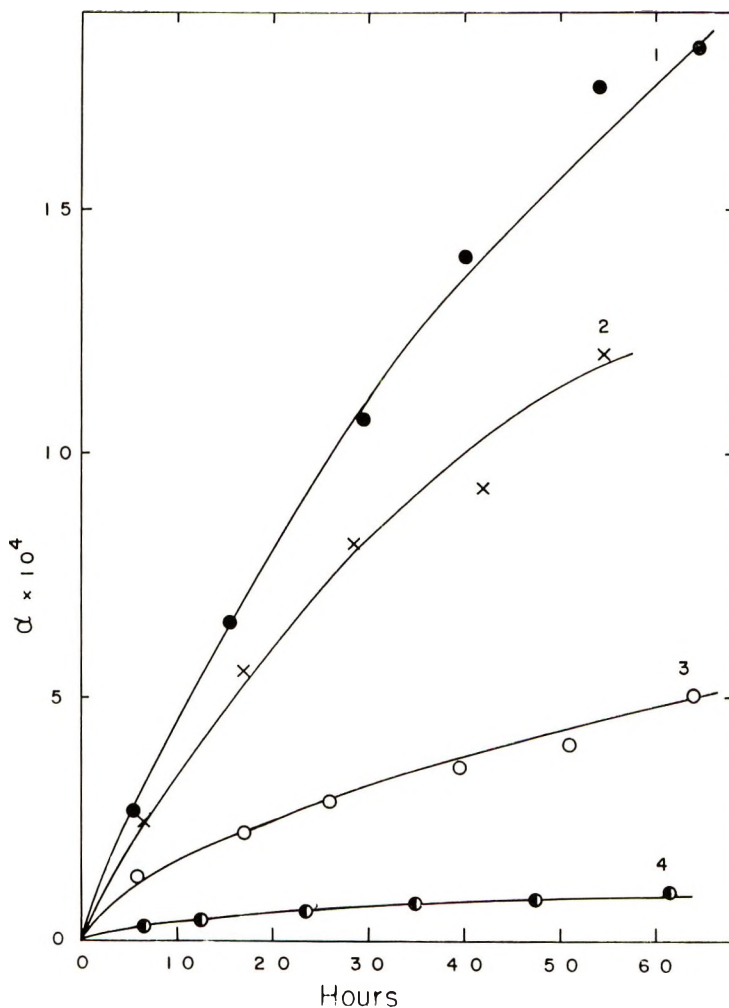
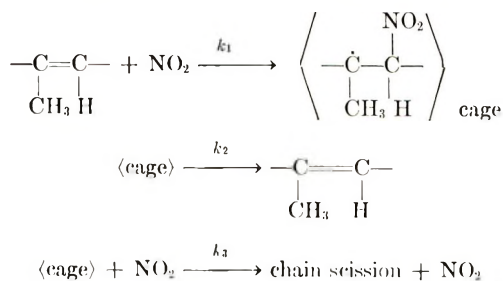


Fig. 4. Degree of degradation in presence of 1 atm. of air at 35°C as a function of  $\text{NO}_2$  pressure and time: (1) 1 mm Hg, (2) 0.5 mm Hg, (3) 0.2 mm Hg, (4) 0.01 mm Hg.

generated structures in the isoprene or some residual catalyst fragments. The "normal" chain scission reaction can be tentatively formulated as



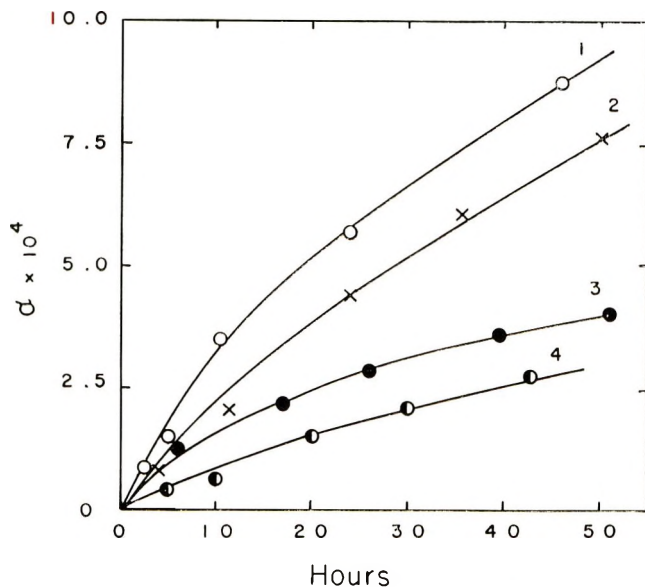


Fig. 5. Degree of degradation at 0.2 mm Hg  $\text{NO}_2$  pressure with 1 atm. of air as a function of temperature and time: (1) 55°C; (2) 45°C; (3) 35°C; (4) 25°C.

The rate of chain scission is then given by

$$-d[n']/dt = k_3[\text{cage}] \quad (3)$$

where  $[n']$  is the concentration of isoprene units in the system at time  $t$ .  $[\text{NO}_2]$  is constant throughout the reaction. The average number of isoprene units in each average chain molecule is 54; the maximum value of  $\bar{s}$ , i.e., the average number of chain scissions in each original chain molecule which occurs at the highest temperature (65°C) in absence of air, is quite small (ca. 1/50 of a break); hence, the total number of isoprene units can be considered constant ( $[n'] \cong [n'_0]$ ).

The steady state concentration of cages is ( $[\text{RH}] = [n'_0]$ )

$$[\text{cage}] = \frac{k_1[n'_0][\text{NO}_2]}{k_2 + k_3[\text{NO}_2]} \quad (4)$$

Hence,

$$-d[n']/dt = k_1k_3[n'_0][\text{NO}_2]/(k_2 + k_3[\text{NO}_2]) \quad (5)$$

Integration of eq. (3) gives,

$$\alpha = \frac{1}{DP_{n,t}} - \frac{1}{DP_{n,0}} = \frac{k_1k_3[n'_0][\text{NO}_2]t}{[n_0](k_2 + k_3[\text{NO}_2])} \quad (6)$$

Here  $\alpha$  is the degree of degradation, i.e.,  $(\overline{DP}_{n,0}/\overline{DP}_{n,t}) - 1 = \bar{s}$ ;  $\overline{DP}_{n,0}$  and  $\overline{DP}_{n,t}$  are the chain lengths at  $t = 0$  and  $t$ , respectively. The ratio  $[n'_0]/[n_0]$  is equal to the average ratio of isoprene units to isobutylene units in an original chain molecule.

Expressed in terms of  $\text{NO}_2$  pressures (mm Hg) eq. (6) becomes,

$$\alpha = \frac{k'_1 k_3 [n'_0] p_{\text{NO}_2} t}{[n_0] (k_2 + k_3'' p_{\text{NO}_2})} \quad (7)$$

or

$$\alpha = \frac{K' p_{\text{NO}_2} t}{K + K''_{\text{III}} p_{\text{NO}_2}} = K_{\text{exp}} t \quad (7a)$$

Thus  $\alpha$  plotted versus time should give a straight line. The straight lines in Figures 1 and 2 were calculated according to eq. (7a); the  $K_{\text{exp}}$  values

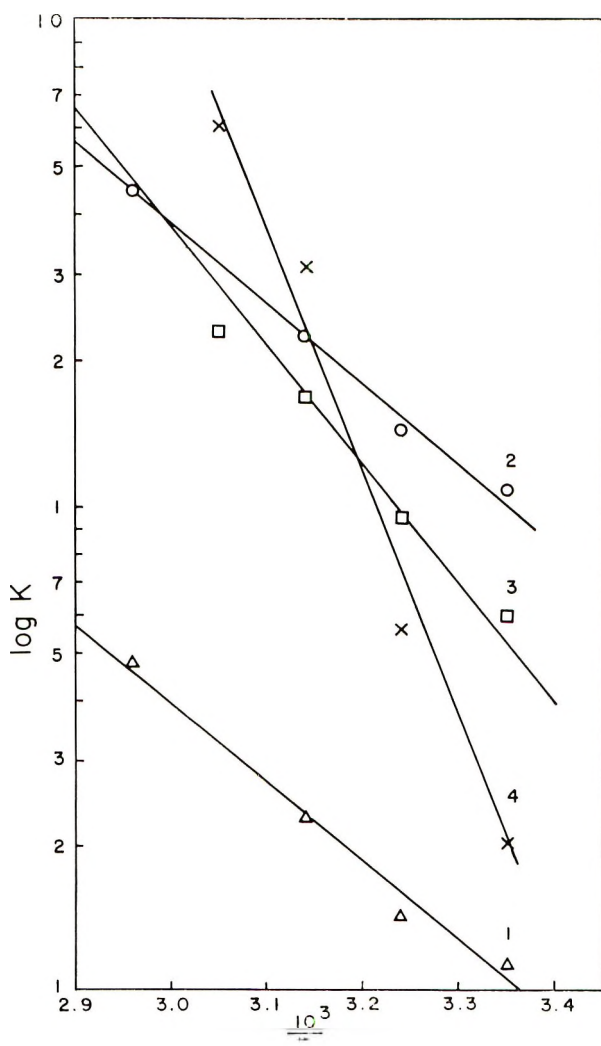


Fig. 6. Arrhenius plots for  $K_{\text{exp}}$ ,  $K'_{\text{exp}}$ ,  $K_{\text{VI}}$ , and  $K''_{\text{exp}}$ : (1)  $10^6 K_{\text{exp}}$ , 7.5 kcal/mole; (2)  $10^7 K'_{\text{exp}}$ , 7.6 kcal/mole; (3)  $10^3 K_{\text{VI}}$ , 11.2 kcal/mole; (4)  $10^3 K''_{\text{exp}}$ , 22.7 kcal/mole.

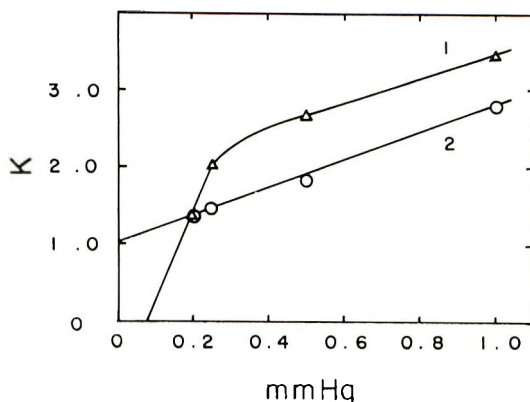


Fig. 7.  $K_{\text{exp}}$  and  $K'_{\text{exp}}$  as a function of  $\text{NO}_2$  pressure at  $35^\circ\text{C}$ .: (1)  $10^6 K_{\text{exp}}$ , (2)  $10 K'_{\text{exp}}$ .

are plotted versus  $\text{NO}_2$  pressure in Figure 7. The dependence on  $\text{NO}_2$  pressure obeys eq. (7a).  $K_{\text{exp}}$  is given by an Arrhenius equation (see Fig. 6):

$$K_{\text{exp}} = 3.8 \times 10^{-2} e^{-7450/RT} \text{ hr}^{-1} \quad (8)$$

The  $K_{\text{exp}}$  values are collected in Table I.

The  $\alpha$  versus time curves (see Figs. 1 and 2) show an accelerated rate of degradation in the very beginning of the reaction (the maximum  $\bar{\alpha}$  at  $65^\circ\text{C}$  equals  $1.8 \times 10^{-2}$  average breaks per original chain or one break on the average in every fiftieth chain). It was pointed out above that this may be due to some oxygenated structures in the chain molecules or possibly to some catalyst residues.

TABLE I  
Rate Constants  $K_{\text{exp}}$  and  $K'_{\text{exp}}$  [Eqs. (7a) and (12)] for Chain  
Scission of Butyl Rubber by Nitrogen Dioxide

$p_{\text{NO}_2}$ , mm Hg	Temp, $^\circ\text{C}$	$K_{\text{exp}} \times 10^6$ , $\text{hr}^{-1}$	$K'_{\text{exp}} \times 10^4$ , $\text{hr}^{-1}$	$m \times 10^2$
1.0	35	3.50	2.88	14.4
0.5	35	2.72	1.84	10.8
0.25	35	2.18	1.49	10.4
0.2	35	1.45	1.44	7.2
0.2	25	1.15	1.09	7.0
0.2	35	1.45	1.44	7.2
0.2	45	2.31	2.28	10.6
0.2	65	4.85	4.50	10.5

The mechanism is the same as before, except for the values of the rate constants. The rate of scission due to "weak links" is given by,<sup>9</sup>

$$-\frac{d[w]}{dt} = \frac{k_{w,1}k_{w,3}}{k_{w,2} + k_{w,3}[\text{NO}_2]} [\text{NO}_2][w] \quad (9)$$

where  $[w]$  is the concentration of "weak links" in the polymer sample;  $[w_0]$  is the "weak link" concentration at  $t = 0$ . Further, let  $m$  be the average number of weak links in each original chain molecule; then eq. (9) gives on integration,

$$\ln \frac{[w_0]}{[w]} = \frac{k_{w,1}k_{w,3}}{k_{w,2} + k_{w,3}[\text{NO}_2]} [\text{NO}_2]t \quad (10)$$

Equation (10) is equal to,<sup>9</sup>

$$-\ln \left( 1 - \frac{\bar{s}_1}{m} \right) = \frac{k_{w,1}k_{w,3}}{k_{w,2} + k_{w,3}[\text{NO}_2]} [\text{NO}_2]t \quad (11)$$

where  $\bar{s}_1$  is the average number of broken weak links in each original chain molecule at time  $t$ .

If  $\bar{s}_1/m = \alpha'$ , one obtains from eq. (11),

$$\begin{aligned} -\ln (1 - \alpha') &= \frac{k_{w,1}k_{w,3}}{k_{w,2} + k_{w,3}[\text{NO}_2]} [\text{NO}_2]t \\ &= \frac{k'_{w,1}k_{w,3}}{k_{w,2} + k'_{w,3}p_{\text{NO}_2}} p_{\text{NO}_2}t = K'_{\text{exp}}t \end{aligned} \quad (12)$$

The rate constants  $K'_{\text{exp}}$  are also given in Table I.

The complete equation for degradation by  $\text{NO}_2$  alone is then,

$$\alpha - \ln (1 - \alpha') = (K_{\text{exp}} + K'_{\text{exp}})t \quad (13)$$

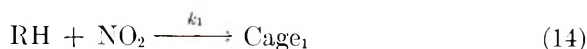
The initial parts of the curves in Figure 1, have been calculated according to eq. (13), the points are experimental data

$$\alpha'/\alpha'' = \text{DP}_{n,0}/m$$

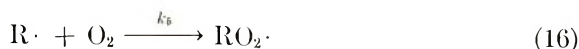
where  $\alpha''$  is the degree of degradation with respect to  $\overline{DP}_{n,0}$  due to breaking of weak links. The energy of activation for breaking weak links is 7.6 kcal (see Fig. 6). Figure 7 shows that the  $K'_{\text{exp}}$  values follow eq. (12).

The experimental results obtained in the presence of  $\text{NO}_2$  and 1 atm of air can be satisfactorily accounted for by a tentative mechanism, given below. Weak links do not play a significant role here, as the chain scission rate is about five times faster than that in the presence of  $\text{NO}_2$  alone.

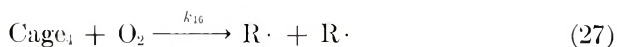
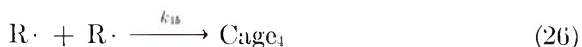
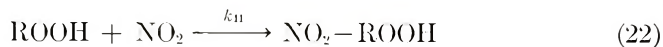
The proposed mechanism is given in eqs. (14)–(28) below; the first part consists of the contribution by the reaction with  $\text{NO}_2$  only,



The second part is the contribution by oxygen alone,



The third part consists of the synergistic reaction of  $\text{NO}_2$  and  $\text{O}_2$ :



The degree of degradation for the whole process is given by eq. (A-12) in the Appendix. The contribution to chain scission by oxygen is quite small, as an extrapolation of the rate constants to zero  $\text{NO}_2$  pressure shows (Fig. 4); hence, the second term in eq. (A-12) can be neglected. The terms containing  $t^2$  and  $t$  are also quite small if  $K_{\text{VI}} \ll 1$ . Hence, this equation reduces to,

$$\alpha = K_{\text{exp}} t + \frac{K''_{\text{exp}}}{K_{\text{VI}}^3} (1 - e^{-K_{\text{VI}} t}) \quad (29)$$

Here

$$K_{\text{exp}} = \frac{k_1 k_3 [n'_0] [\text{NO}_2]}{[n_0] (k_2 + k_3 [\text{NO}_2])} \quad (30)$$

and

$$K''_{\text{exp}} = \frac{k_{11} k_{12} k_{14} [\text{NO}_2] K_{\text{V}}}{(k_{13} + k_{14}) [n_0]} \quad (31)$$

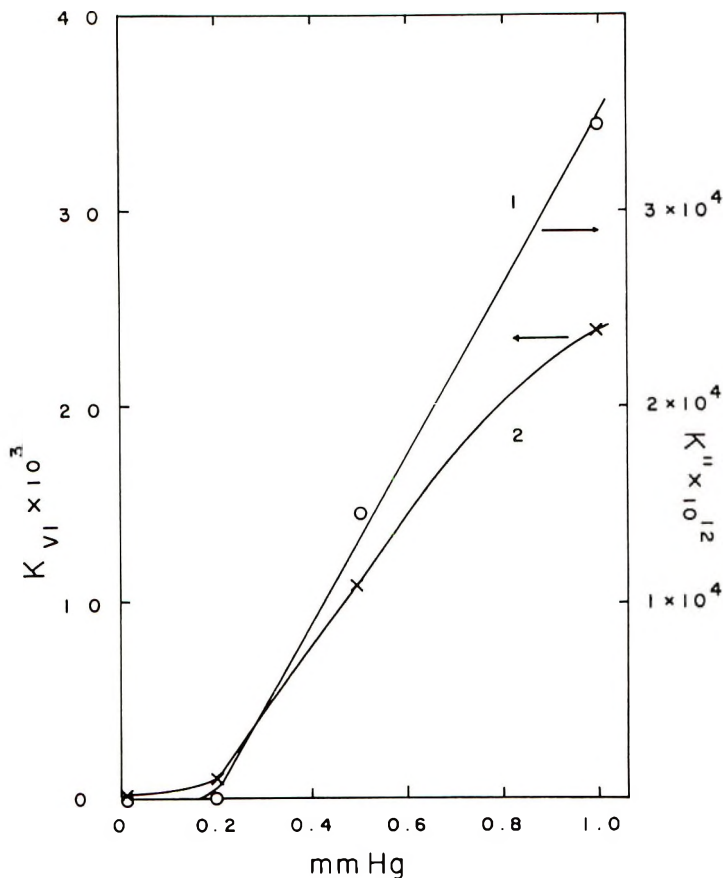


Fig. 8.  $K''_{exp}$  and  $K_{VI}$  as a function of  $\text{NO}_2$  pressure (1 atm. of air) at  $35^\circ\text{C}$ : (1)  $10^{12} K''_{exp}$ ; (2)  $10^3 K_{VI}$ .

The first term in eq. (29) is due to chain scission by  $\text{NO}_2$  alone and the second term represents the synergistic action of  $\text{NO}_2$  and  $\text{O}_2$ .  $K''_{exp}$  and  $K_{VI}$  are functions of  $\text{NO}_2$  and  $\text{O}_2$  (Fig. 8).  $\alpha$  is plotted versus  $(1 - e^{-K_{VI}t})$

TABLE II  
Rate Constants  $K''_{exp}$  and  $K_{VI}$  for Chain Scission of  
Butyl Rubber by  $\text{NO}_2$  in the Presence of Air (1 atm)

$p_{\text{NO}_2}$ , mm Hg	Temp., $^\circ\text{C}$	$K_{VI} \times 10^3$ , $\text{hr}^{-1}$	$K''_{exp} \times 10^{12}$ , $\text{hr}^{-1}$
0.01	35	0.1	0.013
0.20	35	0.95	5.66
0.5	35	11.0	145.50
1.0	35	24.2	34400
0.2	25	0.60	2.05
0.2	35	0.95	5.66
0.2	45	1.7	31.3
0.2	55	2.3	61.0



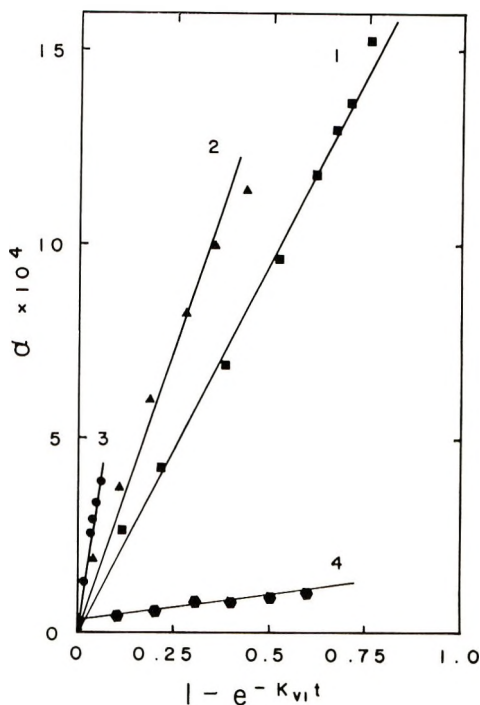
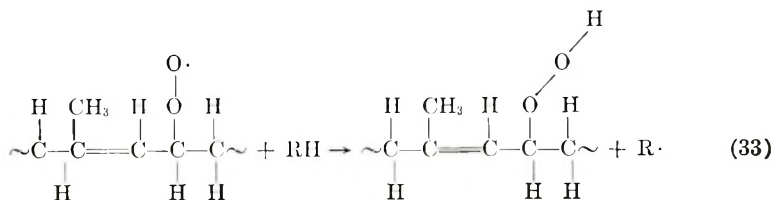
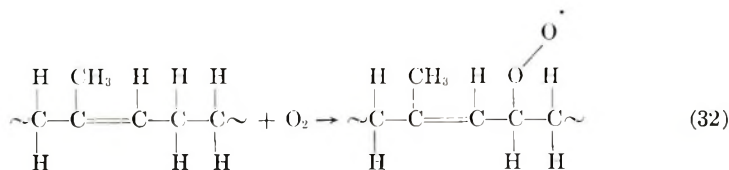


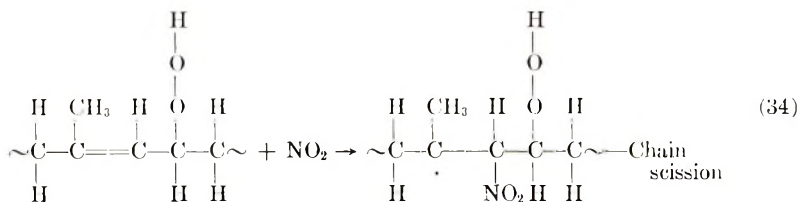
Fig. 9. Degree of degradation  $\alpha$  plotted versus  $(1 - e^{-K_{VI}t})$  according to eq. (29) for various  $\text{NO}_2$  pressures at  $35^\circ\text{C}$  (1 atm. of air): (1) 1 mm Hg; (2) 0.5 mm Hg; (3) 0.2 mm Hg; (4) 0.01 mm (abscissa  $\times 10^2$ ).

in Figure 9. Satisfactory straight lines are obtained as required by eq. (29). The  $K''_{\text{exp}}$  and  $K_{VI}$  values, respectively, are given in Table II. The relevant energies of activation are 11.2 and 22.7 kcal/mole for  $K_{VI}$  and  $K''_{\text{exp}}$ , respectively.

All experimental data are in satisfactory agreement with the proposed mechanisms.

The synergistic action of  $\text{NO}_2$  and  $\text{O}_2$ , i.e., ROOH groups, can be represented as shown by eqs. (32)–(34):





The experimental data do not agree with a kinetic formulation of peroxy-nitrates.

### APPENDIX

The total rate of chain scission is given by,

$$-\frac{d[n']}{dt} = k_3[\text{Cage}_1] + k_{10}[\text{Cage}_2][\text{O}_2] + k_{11}[\text{Cage}_3] \quad (\text{A-1})$$

where  $[n']$  is the concentration of isoprene units in the system.

The steady-state concentrations for the cages are,

$$\begin{aligned}
 [\text{Cage}_1] &= k_1[n'][\text{NO}_2]/(k_2 + k_3[\text{NO}_2]) \\
 [\text{Cage}_2] &= k_8[\text{ROOH}]/(k_9 + k_{10}[\text{O}_2]) \\
 [\text{Cage}_3] &= k_{12}[\text{NO}_2-\text{ROOH}]/(k_{13} + k_{14}) \\
 [\text{Cage}_4] &= k_{15}[\cdot\text{R}]^2/(k_{16} + k_{17}[\text{O}_2])
 \end{aligned} \quad (\text{A-2})$$

Hence, eq. (A-1) becomes,

$$-\frac{d[n']}{dt} = \frac{k_3k_1[n'][\text{NO}_2]}{k_2 + k_3[\text{NO}_2]} + \frac{k_8k_{10}[\text{ROOH}][\text{O}_2]}{k_9 + k_{10}[\text{O}_2]} + \frac{k_{12}k_{11}[\text{NO}_2-\text{ROOH}]}{k_{13} + k_{14}} \quad (\text{A-3})$$

Further,

$$\frac{d[\text{ROOH}]}{dt} = k_6[\cdot\text{RO}_2][n'] - (k_7 + k_8 + k_{11}[\text{NO}_2])[\text{ROOH}] + k_9[\text{Cage}_2] \quad (\text{A-4})$$

and

$$\frac{d[\text{NO}_2-\text{ROOH}]}{dt} = k_{11}[\text{ROOH}][\text{NO}_2] - k_{12}[\text{NO}_2-\text{ROOH}] + k_{13}[\text{Cage}_3] \quad (\text{A-5})$$

The steady-state concentrations of the various radicals are

$$\begin{aligned}
 [\cdot\text{RO}_2] &= \frac{k_5[\text{R}\cdot][\text{O}_2]}{k_6[n']} \\
 [\text{R}\cdot] &= K_{1V}[n']^{1/2}[\text{O}_2]^{1/2}
 \end{aligned} \quad (\text{A-6})$$

where

$$K_{IV} = \{k_4(k_{16}[O_2] + k_{17})/k_{15}k_{17}\}^{1/2}$$

Hence,

$$[\cdot RO_2] = k_5 K_{IV} [O_2]^{3/2} / k_6 [n']^{1/2} \quad (A-7)$$

and

$$d[ROOH]/dt = K_V - K_{VI}[ROOH] \quad (A-8)$$

where

$$K_V = K_{IV} k_5 [n']^{1/2} [O_2]^{3/2}$$

and

$$K_{VI} = k_7 + k_8 + k_{11} [NO_2] - \{k_9 k_8 / (k_9 + k_{10} [O_2])\}$$

It is assumed that  $[n'] \cong [n'_0]$ . The maximum value of  $\bar{s}$  is about 7 for each original chain out of a total of 54.

Integration of eq. (A-8) gives then,

$$[ROOH] = (K_V / K_{VI}) (1 - e^{-K_{VI}t}) \quad (A-9)$$

and

$$[Cage_2] = \{k_8 / (k_9 + k_{10} [O_2])\} (K_V / K_{VI}) (1 - e^{-K_{VI}t}) \quad (A-10)$$

Equation (A-5) can now be integrated:

$$[NO_2-ROOH] = k_{11} [NO_2] (K_V / K_{VI}) [t + (1/K_{VI})(e^{-K_{VI}t} - 1)] \quad (A-11)$$

The term  $-k_{12} \{1 - [k_{13} / (k_{13} + k_{14})]\} [NO_2-ROOH]$  has been neglected, as  $k_{14}$  is small compared with  $k_{13}$ .

Hence eq. (A-3) gives, on integration,

$$\begin{aligned} \alpha &= \frac{1}{DP_{n,t}} - \frac{1}{DP_{n,0}} \\ &= \frac{k_1 k_3 [n'_0] [NO_2] t}{[n_0] (k_2 + k_3 [NO_2])} + \frac{k_8 k_{10} [O_2]}{[n_0] (k_9 + k_{10} [O_2])} \frac{K_V}{K_{VI}} \\ &\quad \times \left[ t + \frac{1}{K_{VI}} (e^{-K_{VI}t} - 1) \right] \\ &+ \frac{k_{11} k_{12} k_{14} [NO_2]}{(k_{13} + k_{14}) [n_0]} \left\{ \left( \frac{K_V}{K_{VI}} \right) \frac{t^2}{2} - \frac{K_V}{K_{VI}^2} \left[ t + \frac{1}{K_{VI}} (e^{-K_{VI}t} - 1) \right] \right\} \quad (A-12) \end{aligned}$$

The authors wish to express their appreciation to the Bureau of State Services, PHS, Division of Air Pollution, 1-RO-1-AP00486 for financial support.

### References

1. H. H. G. Jellinek and E. Flajsman, *J. Polym. Sci. A-1*, **7**, 1153 (1969).
2. H. H. G. Jellinek, F. Flajsman, and F. J. Kryman, *J. Appl. Polym. Sci.*, **13**, 107 (1969).
3. Gmelin's *Handbuch Der Anorganischen Chemie*, System 4, Lieferung 1-4, Verlag Chemie Leipzig, Berlin, 936 (1955), pp. 748.
4. A. C. G. Egerton, *J. Am. Soc.*, **105**, 647 (1914).
5. J. Brandrup and E. H. Immergut, Eds., *Polymer Handbook*, IV-8, Interscience, New York, 1965.
6. D. J. Buckley, *Encyclopedia of Polymer Science and Technology*, H. Mark, N. G. Gaylord and N. M. Bikales, Eds., Wiley, New York, 1965, Vol. 2, p. 772.
7. H. H. G. Jellinek and Y. Toyoshima, *J. Polym. Sci. A-1*, **5**, 3214 (1967).
8. T. Ogishara, S. Tsuchiya, and K. Kuratani, *Bull. Chem. Soc. Japan*, **38**, 978 (1968).
9. H. H. G. Jellinek, *Degradation of Vinyl Polymers*, Academic Press, New York, 1955.

Received July 15, 1969

Revised September 24, 1969

## Cationic Polymerization of $\beta$ -Pinene, Styrene and $\alpha$ -Methylstyrene

HEIKKI PIETILA, ARTO SIVOLA, and HOWARD SHEFFER,\*  
*The Technical University at Otaniemi, Helsinki, Finland*

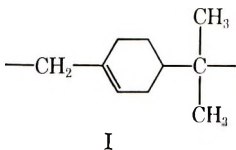
### Synopsis

Molecular weight distributions determined by gel permeation chromatography demonstrate that  $\alpha$ -methylstyrene copolymerizes with both  $\beta$ -pinene and styrene, forming both bi- and terpolymers. The composition of precipitated polymer versus crude polymer, as determined by nuclear magnetic resonance, suggests that  $\beta$ -pinene and styrene also copolymerize. Extraction of the latter bipolymer of  $\beta$ -pinene and styrene with acetone gives only a small amount of insoluble  $\beta$ -pinene homopolymer, confirming that  $\beta$ -pinene and styrene copolymerize in *m*-xylene. GPC analysis shows that each copolymer contains some homopolymer. A comparison of  $\bar{M}_n$  with molecular weight calculated from NMR analysis, assuming chain transfer to solvent, indicates that chain transfer is the predominant method of forming dead polymer. The carbonium ions of the growing chain tend to transfer to solvent with increasing ease in the order  $\beta$ -pinene, styrene, and  $\alpha$ -methylstyrene.

### INTRODUCTION

Fractional precipitation<sup>1</sup> is often used to demonstrate whether a system is a copolymer or a mixture of homopolymers. The number-average molecular weight determined by osmometry is of little value in providing whether a product is a true copolymer or mixture of homopolymers. The molecular distribution as determined by GPC indicates whether a product is a copolymer (in which case a normal distribution is observed) or a mixture of homopolymers (in which case multiple peaks occur). GPC and NMR was used by us to investigate the structure of homopolymers, copolymers, and terpolymers of  $\beta$ -pinene, styrene and  $\alpha$ -methylstyrene.

A literature survey reveals only a single reference to the copolymerization of  $\beta$ -pinene with either styrene or  $\alpha$ -methylstyrene.<sup>2</sup>  $\beta$ -pinene polymerizes to molecular weight 1500 at 50 wt-% in toluene at 40–45°C with the use of 5% Freidel Craft type catalyst. The repeat unit proposed for this polymer<sup>3</sup> has the structure I.



\* Present address: Chemistry Department, Union College, Schenectady, New York

This is confirmed<sup>4</sup> but found not to be the exclusive structure.<sup>5</sup>  $\alpha$ -Methylstyrene at room temperature forms mainly a dimer, but at low temperature yields polymer of higher molecular weight.<sup>6a</sup> Most cationic copolymerizations are ideal,<sup>6b</sup> but in the styrene- $\alpha$ -methylstyrene system  $r_1r_2$  is 0.145. This deviation from an ideal system may be due to a steric effect of the two  $\beta$ -substituents in  $\alpha$ -methylstyrene. Unpublished work<sup>7,8</sup> indicates that  $\beta$ -pinene and styrene do not copolymerize in methylene chloride with aluminum chloride catalyst at 30°C.

### EXPERIMENTAL

Homopolymers, copolymers, and terpolymers of  $\beta$ -pinene, styrene and  $\alpha$ -methylstyrene were prepared at 30°C from a total of 20 g of monomers, 13.3 g *m*-xylene (40% of total weight of batch), and 0.6 g (3%) anhydrous aluminum chloride. No cocatalyst was used other than traces of water found in aluminum chloride, monomers, or solvent. The catalyst was added in four equal portions every 15 min for 1 hr. Then benzene was added to facilitate removal of the catalyst. No special attempt was made to purify the reactants, since the polymerization of the raw materials as supplied gave a more meaningful result from a practical point of view. The composition of the feed is given in Table I along with molecular weights of the polymers.

After diluting with benzene the catalyst was removed by washing with 50 ml of 2% aqueous hydrochloric acid, followed by three 50-ml portions of water. Benzene was evaporated under reduced pressure in order to remove water by azeotropic distillation, and the residue was added to 250 ml of

TABLE I  
Yield and Molecular Weight versus Composition of  
Feed for Precipitated Polymer and Crude Polymer (R)

Batch no.	Weight of reactants, g			$\bar{M}_n$	$\bar{M}_n$ calcd <sup>a</sup>	$k_p/k_{tr}$	Yield, wt-%
	$\beta$ -Pinene	Styrene	$\alpha$ -Methylstyrene				
2	5	10	5	931			30
R2				650			107
4	10	10	—	1100			50
R4				1040			108
5	—	20	—	845	1500	5.8	82
R5				700	750	4.4	111
6	20	—	—	1890	1800	11.8	20
R6				787	2600	5.1	69
7	—	—	20	377	530	2.4	102
10	10	—	10	1050			55
R10				788			62
11-1	—	10	10	753			35
11-2				300			25
R11				469			103

<sup>a</sup> Calcd for chain transfer to solvent.

methanol. The precipitated polymer was redissolved in 50 ml of benzene and reprecipitated with 250 ml of methanol. Final evaporation of the solvents was carried out in a vacuum desiccator for 24 hr. The polymer resulting from this treatment was used for molecular weight determinations, gel permeation chromatography, and NMR analysis. In the case of  $\alpha$ -methylstyrene it was impossible to precipitate the polymer from benzene with methanol. Therefore, a crude polymer was obtained by evaporation of the monomer and solvent for an extended period. Batches 2 and 11 showed a sharp singlet at 2.28 ppm, indicating free *m*-xylene. The presence of rather large amounts of free *m*-xylene in batch 2 may be due to the lack of refinement in the technique of solvent removal for this earlier batch. However, in the case of tacky samples (such as batches 2 and 11) it was difficult to achieve complete solvent removal. In one case, batch 11, the mother liquor after precipitation was evaporated to give 11-2.

A second series of batches was prepared with the same formulas as the first series but with a different procedure for isolation of the polymers (Table I, R batches). These were washed in a manner similar to that of the first series. However, precipitation from methanol was omitted. Instead benzene and unreacted monomer were removed by vacuum distillation. Only in one case, batch R4, were we unsuccessful in removing solvent by this method.

Molecular weights were determined by vapor-pressure osmometry with a model 301A Mechrolab instrument. With benzene as the solvent, molecular weights of 1890 and 845 were obtained for the precipitated homopolymers of  $\beta$ -pinene and styrene, respectively. The corresponding molecular weights for crude homopolymers were 787 and 700.  $\alpha$ -Methylstyrene homopolymer, which could not be precipitated by methanol, had a molecular weight of 377. The molecular weights of all copolymers and terpolymers are given in Table I. Molecular weights of selected fractions

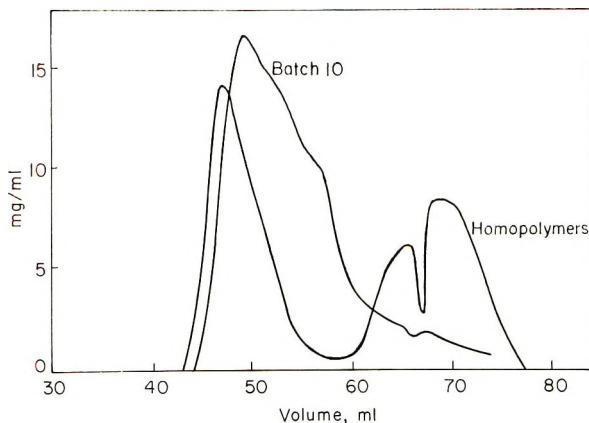


Fig. 1. GPC of 200 mg of batch 10 and 100 mg each of poly- $\beta$ -pinene and poly- $\alpha$ -methylstyrene.

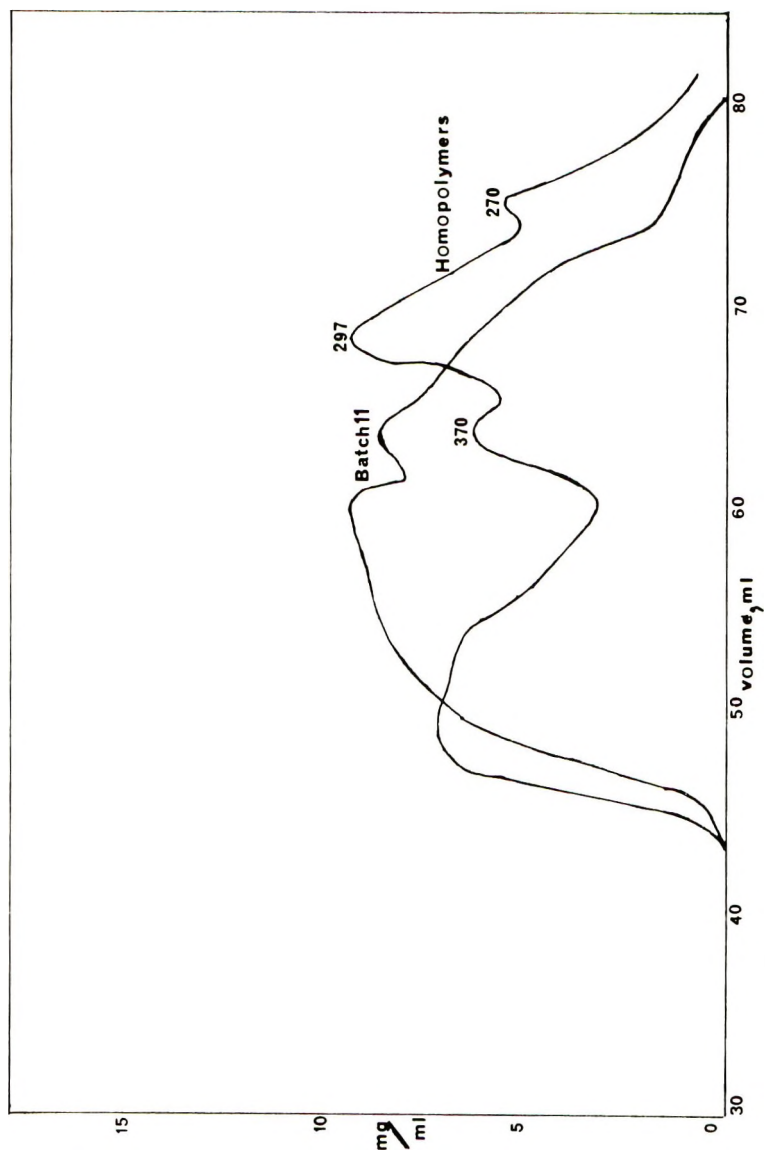


Fig. 2. GPC of 200 mg of batch 11 and 100 mg each of polystyrene and poly- $\alpha$ -methylstyrene.



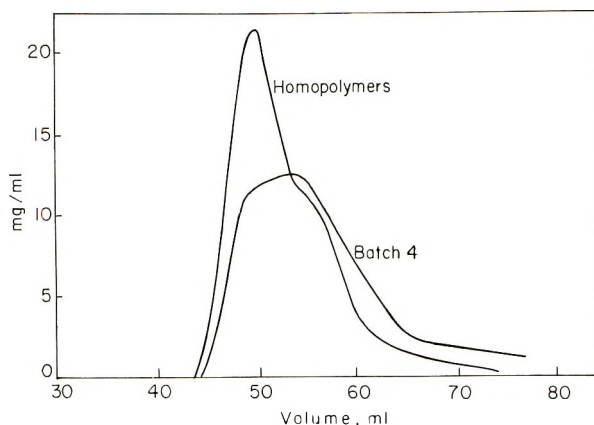


Fig. 3. GPC of 200 mg of batch 4 and 100 mg each of poly- $\beta$ -pinene and polystyrene.

of Batch 2 after GPC are shown in Figure 7 below and molecular weights of selected fractions of the mixture of precipitated homopolymers after GPC in Figures 2 and 7.

Gel permeation chromatography was performed in a glass column (2.5  $\times$  45 cm) fitted with Teflon pistons and packed with 28.5 cm of Sephadex LH-20 (25–100  $\mu$ ) gel in chloroform. This gel is especially designed to separate polymers of low molecular weight. Samples were collected automatically with a RadiRac siphon stand, type 3404B, in test tubes and weighed to a tenth of a milligram on a Mettler balance. A sample size of 200 mg in 1 ml of chloroform and a flow rate of 0.5 ml/min were used.

Analysis was carried out with a Varian A-60 NMR spectrometer with the use of deuteriochloroform as the solvent. Of major interest was the aro-

TABLE II  
NMR Analysis of Polymers

Batch no.	<i>m</i> -xylene, wt-%		Monomer in polymer, wt-%		
	Combined	Free	$\beta$ -Pinene	Styrene	$\alpha$ -Methyl styrene
2	—	17	25.9	49.4	24.7
R2	—	12	25.9	49.4	24.7
4	7	0	42	58	—
R4	—	23	44	56	—
5	6	0	—	100	—
R5	14	0	—	100	—
6	9	0	100	—	—
R6	4	0	100	—	—
7	20	0	—	—	100
10	4	0	45	—	55
R10	7	0	47	—	53
11-1	—	8	—	69	31
11-2	10	0	—	40	60
R11	7	0	—	62	38

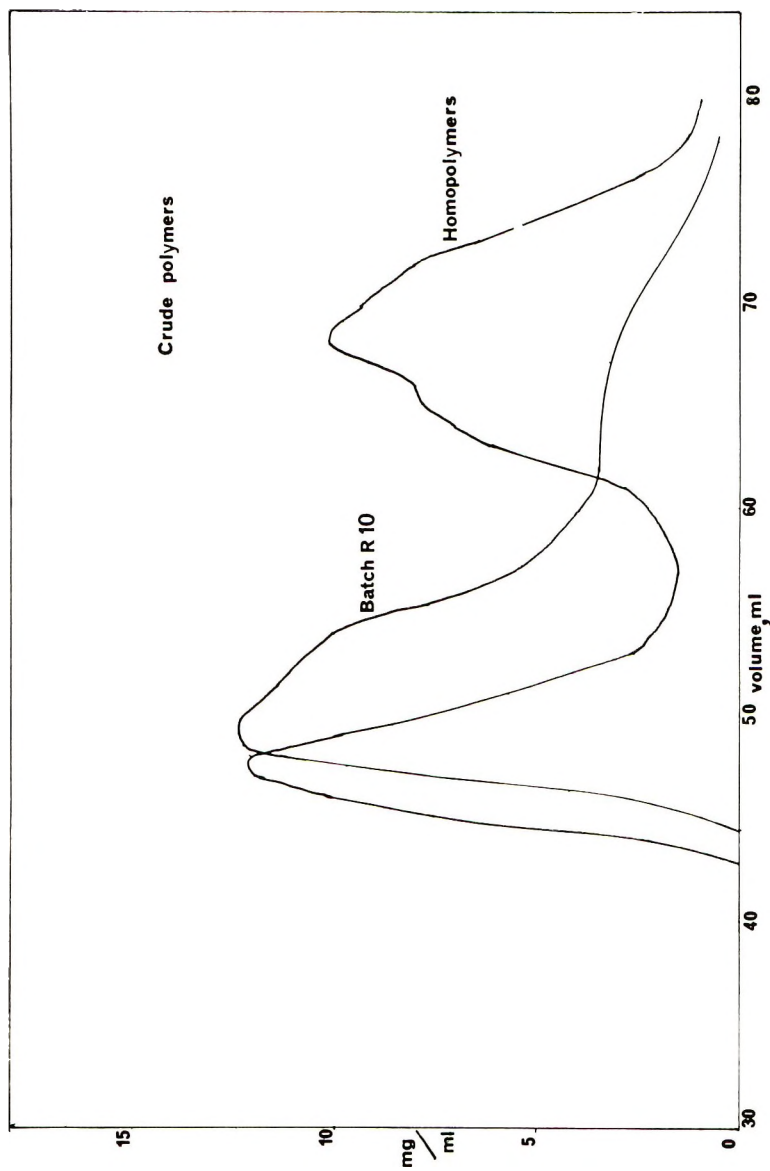


Fig. 4. GPC of 105 mg of batch R10 and 100 mg each of poly- $\beta$ -pinene and poly- $\alpha$ -methylstyrene.

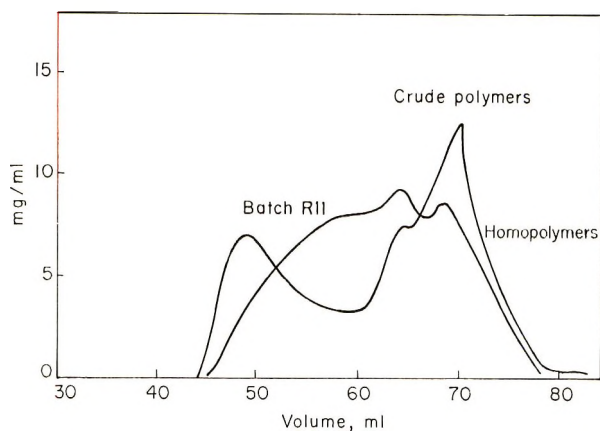


Fig. 5. GPC of 200 mg of batch R11 and 100 mg each of polystyrene and poly- $\alpha$ -methylstyrene.

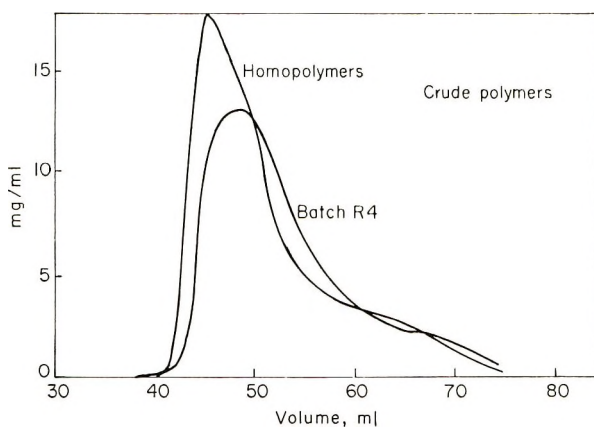


Fig. 6. GPC of 200 mg of batch R4 and 100 mg each of poly- $\beta$ -pinene and polystyrene.

matic-to-aliphatic proton ratio obtained by simple integration. A singlet at 2.28 ppm was assumed to be methyl protons of free *m*-xylene and a broad peak at 2.24 ppm to be combined *m*-xylene. In one instance, the precipitated  $\beta$ -pinene homopolymer, the combined *m*-xylene could be calculated both ways (from aromatic protons and aliphatic protons of solvent), and good agreement was obtained. The magnitude of the absorption at 5.23 ppm in precipitated  $\beta$ -pinene homopolymer suggested the repeat unit I for about half of the polymer. The calculated composition of the precipitated and crude polymers from NMR analysis is given in Table II. In order to confirm that batches 4 and R4 were chiefly copolymers of  $\beta$ -pinene and styrene, 4 g of each were extracted with boiling acetone for 1 hr. The precipitated copolymer yielded 0.61 g and the crude copolymer 0.36 g of insoluble homopolymer of  $\beta$ -pinene. To verify the insolubility of this homopolymer in acetone, 4 g each of batches 6 and R6 was extracted

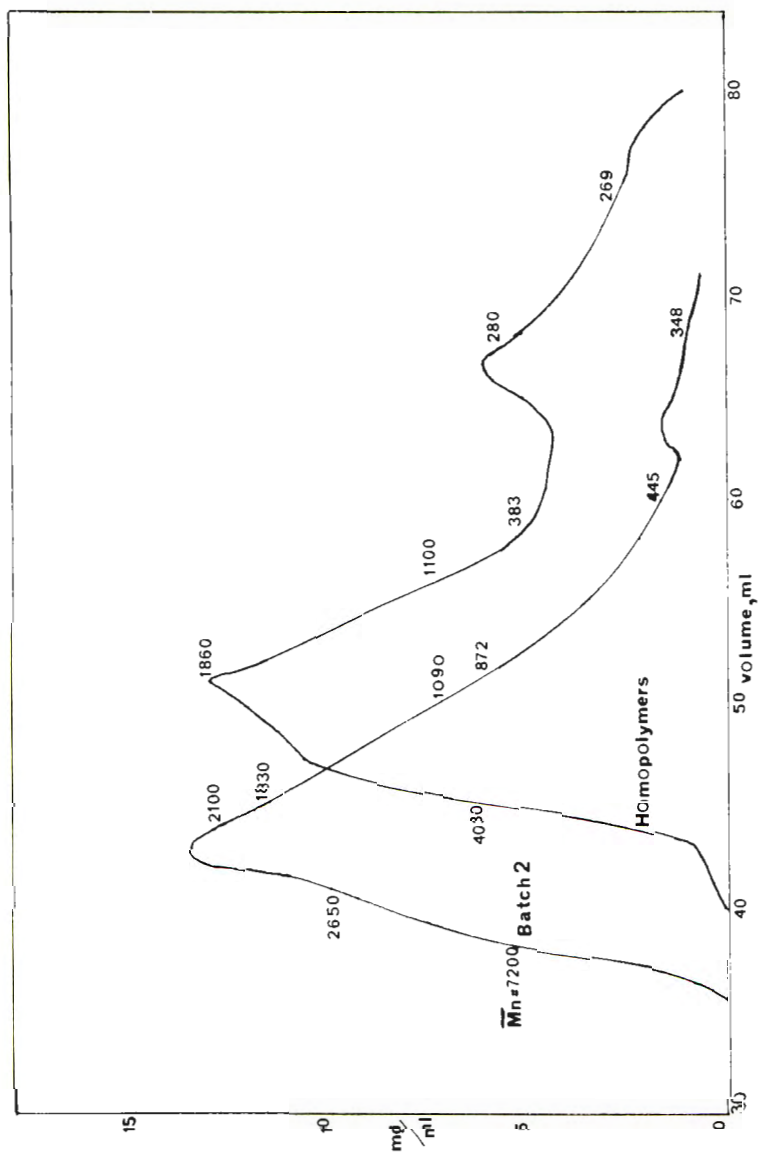


Fig. 7. GPC of 200 mg of batch 2 and 50 mg poly- $\beta$ -pinene, 100 mg polystyrene, and 50 mg poly- $\alpha$ -methylstyrene.

with the same solvent. Only 4% of this precipitated homopolymer of  $\beta$ -pinene and 32% of the crude homopolymer of  $\beta$ -pinene dissolved. In the case of R6 it was suspected that considerable free  $\beta$ -pinene monomer was present in this crude polymer.

The chemicals used in this work and their sources are listed below: aluminum chloride (waterfree, sublimed, 97% min.), E. Merck A.G., Germany;  $\beta$ -pinene (pract. 95%), Fluka A.G., Switzerland; styrene (technical), Ab Syntes, Sweden;  $\alpha$ -methylstyrene (> 98% pure), Fluka A.G.; chloroform, (99–99.4%, ethanol 0.6–1.0%), E. Merck A.G.; *m*-xylene (>99.5% pure), Fluka A.G.; benzene (min. 99.5%), E. Merck A.G.; methanol (min. 99%), E. Merck A.G.; Sephadex LH-20 (25–100 $\mu$ ), Pharmacia, Sweden.

## DISCUSSION

### Copolymerization

The molecular weights of bipolymers and terpolymers correlate very well with those of homopolymers. The molecular weights of the polymers depend on the type of feed, with  $\beta$ -pinene tending to give higher molecular weights and  $\alpha$ -methylstyrene lower molecular weights in general. Precipitated polymers are always higher in molecular weight than crude polymers. The much higher molecular weight of precipitated polymer compared to crude polymer suggests either better fractionation in the case of  $\beta$ -pinene homopolymer or the presence of considerable monomer in the crude product. Because solvent reacts with the growing chain, crude yields greater than one hundred per cent are sometimes obtained. The 69% crude yield for  $\beta$ -pinene homopolymer and 62% crude yield for the copolymer of  $\beta$ -pinene and  $\alpha$ -methylstyrene suggests a lower polymerization rate for  $\beta$ -pinene.

The molecular weights for selected samples from GPC of homopolymer mixture of polystyrene and poly- $\alpha$ -methylstyrene correspond roughly to dimer and trimer.

The compositions of the crude copolymers and terpolymers agree fairly well with the feeds. Since the monomer reactivity ratios in these systems are probably not unity, the final polymers must consist of a copolymer-homopolymer mixture when the yields approach 100%. When the composition of the copolymer deviate much from that of the feed it is in favor of styrene and opposed to either  $\beta$ -pinene or  $\alpha$ -methylstyrene. Styrene must have a higher polymerization rate than the other two monomers. The compositions of the precipitated and crude copolymers are in good agreement indicating, that all three bipolymers may be copolymers. One would expect fractionation if these were mixtures of homopolymers. Batch 11-2 obtained from the mother liquor of methanol precipitation of the copolymer of styrene and  $\alpha$ -methylstyrene is richer in  $\alpha$ -methylstyrene. This is expected, since  $\alpha$ -methylstyrene homopolymer is more soluble because of its low molecular weight.

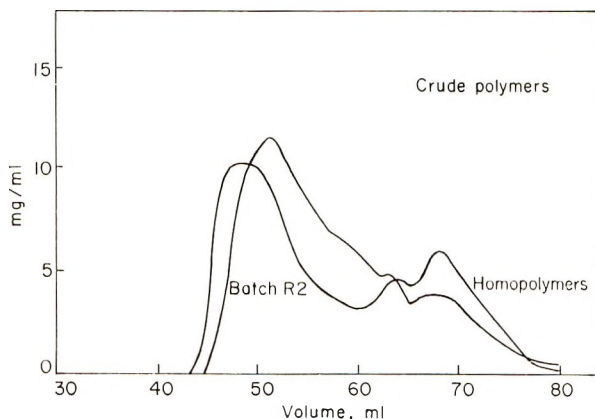


Fig. 8. GPC of 200 mg of batch R2 and 50 mg poly- $\beta$ -pinene, 100 mg polystyrene, and 50 mg poly- $\alpha$ -methylstyrene.

A comparison of GPC of bipolymers with the mixtures of homopolymers for precipitated samples of  $\beta$ -pinene and  $\alpha$ -methylstyrene (Fig. 1) and styrene and  $\alpha$ -methylstyrene (Fig. 2) shows that the bipolymers are copolymers, since the molecular weight distribution of the bipolymers differs considerably from the molecular weight distribution of the mixtures of homopolymers. In the case of  $\beta$ -pinene and styrene (Fig. 3) a decision cannot be made.

Because of the possibility that methanol precipitation of the bipolymers may have left  $\alpha$ -methylstyrene homopolymer in the mother liquor, vacuum distilled samples of a new series of polymers are analyzed. The chromatographs of the crude bipolymers of  $\beta$ -pinene and  $\alpha$ -methylstyrene (Fig. 4) and styrene and  $\alpha$ -methylstyrene (Fig. 5) demonstrate conclusively that these bipolymers are copolymers. In  $\beta$ -pinene and styrene bipolymer, again, a decision from GPC cannot be made (Fig. 6).

A comparison of GPC of the terpolymers with a mixture of homopolymers for both precipitated (Fig. 7) and vacuum-distilled (Fig. 8) samples reveals that  $\alpha$ -methylstyrene is copolymerizing in these systems. A decision about the other two monomers cannot be obtained from GPC alone.

A close examination of the GPC of binary and ternary polymers indicates the presence of a small amount of  $\alpha$ -methylstyrene homopolymer in these batches.

Because GPC is unable to demonstrate that  $\beta$ -pinene and styrene copolymerize, extraction of the bipolymer with acetone was carried out.  $\beta$ -Pinene homopolymer is found to be quite insoluble in this solvent while styrene homopolymer is soluble. The copolymer is also assumed to be soluble. Since only 9% of the crude bipolymer and 17% of the precipitated bipolymer is insoluble in acetone, it is concluded that the major portion of this bipolymer is a copolymer. The fact that  $\beta$ -pinene and styrene copolymerize in *m*-xylene but not in methylene chloride may be due to a change in monomer reactivity ratios with change of solvent. An alternate ex-

planation of the different behavior of  $\beta$ -pinene and styrene in xylene compared to methylene chloride is as follows. *m*-Xylene may have functioned as a bridging agent, terminating both a growing styryl carbonium ion and a  $\beta$ -pinene carbonium ion. This explanation seems less likely for steric reasons.

### Termination

The mechanism of termination by aromatic compounds in the cationic polymerization of styrene is known to be a Friedel-Crafts alkylation.<sup>9</sup> Dead polymers may be formed by termination of growing carbonium ion by release of a proton to reform the catalyst complex, by chain transfer to monomer, or by chain transfer to solvent. If molecular weights are controlled by catalyst concentration and termination is the only mechanism, a molecular weight of several thousand is expected for the homopolymers.

From the combined *m*-xylene content of both precipitated and crude homopolymers it is possible to calculate molecular weights assuming chain transfer to solvent as only mechanism of forming dead polymers (Table I). A comparison of calculated and observed molecular weights demonstrates that chain transfer is the dominant mechanism of forming dead polymers.

From the expression  $\bar{X}_n = (k_p/k_{trs})[M]/[S]$  for chain transfer to solvent, an estimate of  $k_p/k_{trs}$  is obtained (Table I). Further work will be carried out at lower conversion to verify these values. The values of 5.8 and 4.4 for  $k_p/k_{trs}$  for styrene in *m*-xylene with the use of aluminum chloride catalyst are smaller than the value of 95.2 for  $k_p/k_r$  (reciprocal molecular termination constant) for styrene in *p*-xylene with stannic chloride catalyst.<sup>9</sup> This is understandable, since *m*-xylene is expected to be a better chain-transfer agent than *p*-xylene.

$\alpha$ -Methylstyrylcarbonium ion shows the most chain transfer to solvent, followed by styrylcarbonium ion. The carbonium ion derived from  $\beta$ -pinene undergoes the Friedel-Craft chain transfer with *m*-xylene less readily than the other two carbonium ions.

### References

1. F. R. Mayo and F. M. Lewis, *J. Amer. Chem. Soc.*, **66**, 1394 (1944).
2. Neth. Appl. 6,611,789; *Chem. Abstr.*, **67**, 10075X (1967).
3. W. J. Roberts and A. R. Day, *J. Amer. Chem. Soc.*, **72**, 1226 (1950).
4. C. S. Marvel, J. R. Hanley, Jr., and D. T. Longone, *J. Polym. Sci.*, **40**, 551 (1959).
5. W. J. Roberts and A. L. Ward, in *Encyclopedia of Chemical Technology*, R. E. Kirk and D. F. Othmer, Eds., Interscience, New York, 1954, Vol. 13, p. 700.
6. P. H. Plesch, *The Chemistry of Cationic Polymerization*, Pergamon Press, New York, 1963, (a) p. 311; (b) p. 559.
7. A. Sivola and O. Harva, unpublished data.
8. A. Sivola, thesis, Technical University of Helsinki at Otaniemi, 1969.
9. C. G. Overberger and G. F. Endres, *J. Polym. Sci.*, **16**, 283 (1955).

Received June 10, 1969

Revised September 24, 1969

## Polymerization of Vinylcyclopropanes. V. Radical Copolymerization of 1,1-Dichloro-2-vinylcyclopropane with Monosubstituted Ethylenes

TAKAKO TAKAHASHI, *Government Industrial Research Institute, Osaka, Ikeda, Osaka, Japan*

### Synopsis

A peculiar copolymer composition equation applicable to the radical copolymerization of 1,1-dichloro-2-vinylcyclopropane with monosubstituted ethylenes was developed. The theory was applied to such ethylenes as methyl acrylate, methyl methacrylate, and styrene. The reactivity ratio parameters which give the best fit to the experimental data were determined.

In the preceding paper of this series,<sup>1</sup> radical copolymerization of 1,1-dichloro-2-vinylcyclopropane (diClVC) with maleic anhydride (MAnh) was described. From the considerations that diClVC rearranges by opening the ring in the propagation step of homopolymerization and that cyclization of the growing chain is possible in the copolymerization of diClVC with MAnh, a peculiar copolymer composition equation containing four reactivity ratio parameters was developed. It was shown, from the experimental results, that two parameters are nearly zero. These values suggest that the opening of the cyclopropyl ring of diClVC is rapid in copolymerization as well as in homopolymerization and that the cyclization [eq. (1)] is independent of the presence of monomers. The general course of the propagation can be more simply illustrated as shown in eq. (1).

Here R· denotes initiator fragment or active polymer end.

In the present paper, a copolymer composition equation applicable to the copolymerization of diClVC with monosubstituted ethylenes is derived on the basis of the behavior of diClVC in copolymerization with MAnh and its applicability is demonstrated experimentally for methyl acrylate (MA), methyl methacrylate (MMA), and styrene (St), as monosubstituted ethylenes.

### COPOLYMER COMPOSITION EQUATION

The propagation steps of the copolymerization of diClVC ( $M_1$ ) with monosubstituted ethylenes ( $M_2$ ) can be illustrated by the general scheme shown as eq. (2).





This propagation is based on the simplifying assumption that the rearrangement of radical  $m_1$  to  $m_1^*$  and the cyclization of  $m_2$  to  $m_c$  are very much faster than addition of monomers to them, as observed in the copolymerization with MAnh.

Propagation steps and their rate constant in this copolymerization are given in eqs. (3)–(10).



If the ordinary conditions in the development of copolymer composition equation are assumed, the relative rate of consumption of  $M_1$  and  $M_2$  is given by eq. (11):

$$\frac{d[M_1]}{d[M_2]} = \frac{[M_1]}{[M_2]} \cdot \frac{k_{11}[m_1^*] + k_{c1}[m_c] + k_{21}[m_2^*]}{k_{12}[m_1^*] + k_{c2}[m_c] + k_{22}[m_2^*]} \quad (11)$$

Making the stationary-state assumption that the concentrations of radicals  $[m_2]$ ,  $[m_c]$ , and  $[m_2^*]$  are constant leads to:

$$k_{12}[m_1^*][M_2] - k_c[m_2] = 0 \quad (12)$$

$$k_c[m_2] - k_{c1}[m_c][M_1] - k_{c2}[m_c][M_2] = 0 \quad (13)$$

$$k_{c2}[m_c][M_2] - k_{21}[m_2^*][M_1] = 0 \quad (14)$$

Elimination of  $[m_1^*]$ ,  $[m_c]$  and  $[m_2^*]$  from eq. (11), by the use of eqs. (12)–(14), gives:

$$\frac{d[M_1]}{d[M_2]} = \frac{[M_1]}{[M_2]} \cdot \frac{(r_1[M_1] + [M_2])(r_c[M_1] + [M_2])}{[M_1](r_c[M_1] + [M_2]) + [M_2]([M_1] + r_2[M_2])} \quad (15)$$

where

$$r_1 = k_{11}/k_{12}$$

$$r_c = k_{c1}/k_{c2}$$

$$r_2 = k_{22}/k_{21}$$

Equation (15) relates the copolymer composition to the monomer concentrations.

A similar equation relating the amount of unsaturated units (1,5-type units) of diClVC,  $M_1^*$ , to the total amount of diClVC in the copolymer can also be derived:

$$d[M_1^*]/d[M_1] = r_1[M_1]/(r_1[M_1] + [M_2]) \quad (16)$$

By putting

$$\begin{aligned} d[M_1]/d[M_2] &= f \\ d[M_1^*]/d[M_1] &= f' \\ [M_1]/[M_2] &= F \end{aligned}$$

eqs. (15) and (16) can be rewritten:

$$-(F/f)(r_1F + 1 - 2f) = (F^2/f)(r_1F + 1 - f)r_c - r_2 \quad (17)$$

$$f'/(1 - f') = r_1F \quad (18)$$

At low conversions, the value  $f$  will be given by the fractional ratio of monomers combined in the copolymer and  $f'$  given by determination of unsaturation in the copolymer. Therefore, eqs. (17) and (18) permit a graphic evaluation of parameters  $r_1$ ,  $r_c$ , and  $r_2$ .

## EXPERIMENTAL

The monomer, diClVC, was prepared as previously described.<sup>2</sup> Other materials were all purified by standard method.

The monomers and benzoyl peroxide (BPO) initiator were weighed into glass tubes, and the tubes were flushed with nitrogen and sealed. The tubes were agitated in a bath held at  $60 \pm 0.05^\circ\text{C}$  for sufficient time to give a copolymer at low conversion. The reactants were poured into methanol and filtered through glass filter funnels. The polymers were purified by repeated precipitation from benzene solution with methanol and dried *in vacuo*.

The copolymer compositions were calculated from the chlorine contents. The method was as previously described.<sup>1</sup>

Determination of unsaturation was carried out by the iodine monochloride method given in the literature.<sup>3</sup>

## RESULTS AND DISCUSSION

The experimental results of the copolymerization of diClVC with MA are summarized in Table I. It is shown that the amount of unsaturated monomer unit in the copolymerized monomer  $M_1$  is small and changes with monomer feed.

TABLE I  
 Copolymerization of 1,1-Dichloro-2-vinylcyclopropane ( $M_1$ ) and Methyl Acrylate ( $M_2$ )<sup>a</sup>

No.	Monomer feed		Polymerization time, hr	Conversion, %	Chlorine content, wt-%	Copolymer		$f^b$
	$M_1$ , mole-%	$M_2$ , mole-%				$M_1$ , mole-%	$M_2$ , mole-%	
1	12.11	87.89	3.5	5.56	3.24	4.02	95.98	0.037
2	13.22	86.78	2	1.63	3.53	4.39	95.61	0.038
3	27.48	72.52	15	9.04	7.81	10.05	89.95	0.125
4	51.39	48.61	50	6.59	16.36	22.51	77.49	0.267
5	79.21	20.79	113	1.66	31.50	49.42	50.58	
6	79.38	20.62	165	2.03	31.69	49.81	50.19	
7	12.03	87.97	8	15.80	3.35	4.17	95.83	
8	27.63	72.37	25	12.81	7.87	10.13	89.87	
9	50.79	49.21	70	9.93	16.74	23.10	76.90	0.247
10	50.91	49.09	70	9.77	15.53	21.22	78.78	0.250

<sup>a</sup> Polymerization at 60°C with 0.1 mole-% BPO as catalyst.

<sup>b</sup> Ratio of unsaturated monomer unit to total monomer ( $M_1$ ) in the copolymer.

TABLE II  
 Copolymerization of 1,1-Dichloro-2-vinylcyclopropane ( $M_1$ ) and Methyl Methacrylate ( $M_2$ )<sup>a</sup>

No.	Monomer feed		Poly- merization time, hr	Conversion, %	Chlorine content, wt-%	Copolymer		$f'$	$[\eta]^b$
	$M_1$ , mole-%	$M_2$ , mole-%				$M_1$ , mole-%	$M_2$ , mole-%		
1	18.10	81.90	3	9.49	1.38	1.97	98.03		0.43
2	36.82	63.18	7	8.72	3.39	4.87	95.13		0.20
3	50.24	49.76	16	8.31	5.58	8.12	91.88	0.065	0.13
4	57.31	42.69	36	9.45	7.23	10.60	89.40	0.082	0.08
5	78.19	21.81	48	0.37	14.79	22.62	77.38	0.203	
6	18.18	81.82	7	20.81	1.60	2.28	97.72		0.40
7	36.92	63.08	24	23.76	3.83	5.52	94.48		0.21
8	47.27	52.73	32	17.31	5.43	7.89	92.11		0.18
9	57.61	42.39	48	13.19	7.49	11.00	89.00		

<sup>a</sup> Polymerization at 60°C with 0.1 mole-% BPO as catalyst.

<sup>b</sup> Measured in a Ostwald viscometer at 25°C with acetone as solvent.

TABLE III  
 Copolymerization of 1,1-Dichloro-2-vinylcyclopropane ( $M_1$ ) and Styrene ( $M_2$ )<sup>a</sup>

No.	Monomer feed		Polymerization time, hr	Conversion, %	Chlorine content, wt-%	Copolymer		$f'$	$[\eta]^b$
	$M_1$ , mole-%	$M_2$ , mole-%				$M_1$ , mole-%	$M_2$ , mole-%		
1	14.21	85.79	3	4.30	0.64	0.94	99.06	0.58	
2	19.92	80.08	5	6.24	0.94	1.39	98.61	0.50	
3	50.22	49.78	16	6.96	3.53	5.27	94.73	0.15	
4	59.76	40.24	20	5.47	5.03	7.56	92.44	0.12	
5	75.06	24.94	70	4.81	8.76	13.41	86.59	0.128	
6	79.63	20.37	33	2.22	10.95	16.94	83.06	0.158	

<sup>a</sup> Polymerization at 60°C with 0.1 mole-% BPO as catalyst.

<sup>b</sup> Measured in a Ostwald viscometer at 25°C with benzene as solvent.

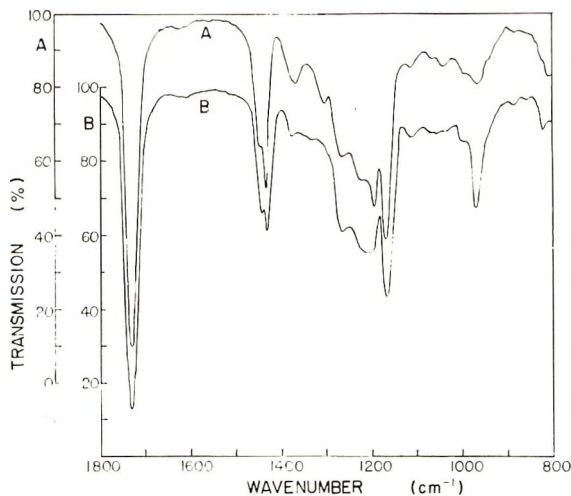


Fig. 1. Copolymerization of 1,1-dichloro-2-vinylcyclopropane ( $M_1$ ) and methyl acrylate ( $M_2$ ). Infrared spectra of copolymer and polymer blend: (A) chloroform solution (0.5 mole/l.) of copolymer containing 50 mole-% each of  $M_1$  and  $M_2$ ; (B) chloroform solution (0.5 mole/l.) of a mixture of homopolymers of  $M_1$  and  $M_2$ , each 50 mole-%.

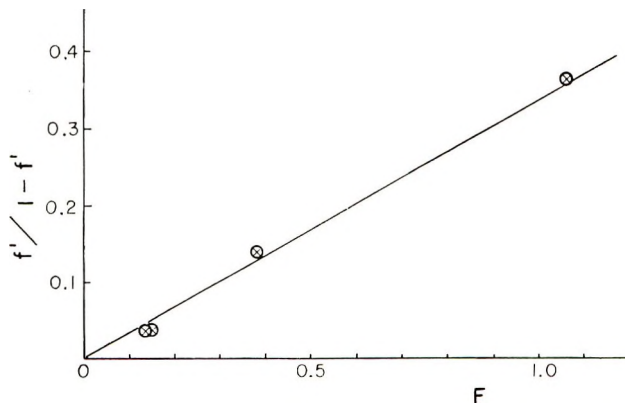


Fig. 2. Copolymerization of 1,1-dichloro-2-vinylcyclopropane ( $M_1$ ) and methyl acrylate ( $M_2$ ). Evaluation of copolymerization parameter  $r_1$  according to eq. (18).

The infrared spectra of the equimolar chloroform solutions of the copolymer containing 50 mole-%  $M_1$  and  $M_2$  (obtained in experiment 6) and of the 50:50 mixture of homopolymers (poly-diCIVC-poly-MA) are shown in Figure 1. The absorption band at  $965\text{ cm}^{-1}$  for homopolymer mixture (Fig. 1B) is assigned to the *trans*-double bond of poly-diCIVC whose structural units are all of the unsaturated 1,5-type.<sup>2</sup> This peak for the unsaturated 1,5-type units in  $M_1$  is remarkably decreased in the copolymer. Since there is a weak absorption of poly(methyl acrylate) in the same region, determination of unsaturation by using this peak was not carried out. The ratio of unsaturated monomer unit to total monomer  $M_1$  combined in

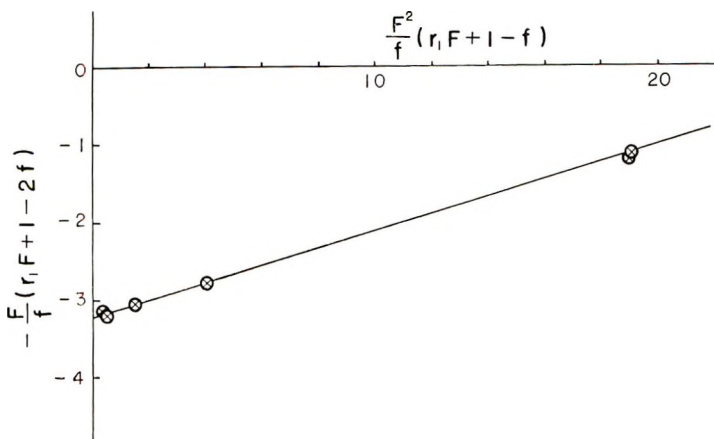


Fig. 3. Copolymerization of 1,1-dichloro-2-vinylcyclopropane ( $M_1$ ) and methyl acrylate ( $M_2$ ). Evaluation of copolymerization parameters  $r_c$  and  $r_2$  according to eq. (17);  $r_1 = 0.33$ .

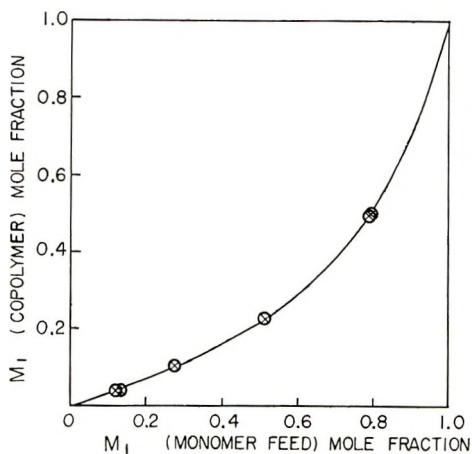


Fig. 4. Copolymerization of 1,1-dichloro-2-vinylcyclopropane ( $M_1$ ) and methyl acrylate ( $M_2$ ): (⊗) experimental points; (—) calculated for  $r_1 = 0.33$ ,  $r_c = 0.11$ ,  $r_2 = 3.2$ .

the copolymer was calculated from the value obtained by the iodine monochloride method. In Figure 1, it is also observed that there is no pronounced difference between curves *A* and *B* in the region  $1000\text{--}1100\text{ cm}^{-1}$ , where, if any cyclopropyl group exists, sharp peaks assigned to it usually appear. Therefore, it is unlikely that the paucity of unsaturation in copolymerized  $M_1$  results from the residue of cyclopropane ring. These facts support the propagation of copolymerization illustrated above.

In Figure 2, a plot of  $f'/(1 - f')$  against  $F$  is shown. The plot is linear as predicted and has a slope of  $r_1 = 0.33$  following eq. (18). Figure 3 shows the plot of  $-F(r_1F + 1 - 2f)/f$  against  $F^2(r_1F + 1 - f)/f$ , where  $r_1$



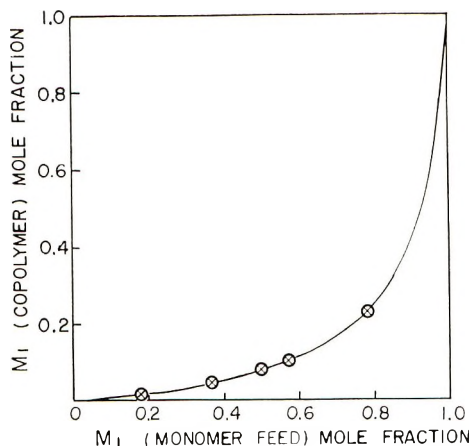


Fig. 5. Copolymerization of 1,1-dichloro-2-vinylcyclopropane ( $M_1$ ) and methyl methacrylate ( $M_2$ ): ( $\otimes$ ) experimental points; (—) calculated for  $r_1 = 0.07$ ,  $r_c = 0.07$ ,  $r_2 = 11.0$ .

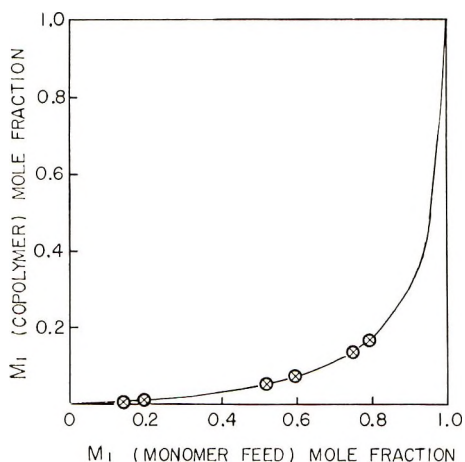


Fig. 6. Copolymerization of 1,1-dichloro-2-vinylcyclopropane ( $M_1$ ) and styrene ( $M_2$ ): ( $\otimes$ ) experimental points; (—) calculated for  $r_1 = 0.05$ ,  $r_c = 0.03$ ,  $r_2 = 17.4$ .

$= 0.33$ . The plot is linear; parameters  $r_c$  and  $r_2$  are found to be 0.11 and 3.2 from the slope and the intercept, respectively, following eq. (17). The copolymer composition curve for this system, calculated from these  $r_1$ ,  $r_c$ , and  $r_2$  values, is shown in Figure 4. It gives the best fit to the experimental data. These operations were carried out by using the experimental data of the upper column (experiments 1-6) in Table I, they were obtained at lower conversions.

Tables II and III show data for the copolymerizations of diCIVC with MMA and St. Parameters  $r_1$ ,  $r_c$ , and  $r_2$  could be determined graphically in the same manner as for the diCIVC-MA system. They are for diCIVC-MMA,  $r_1 = 0.07$ ,  $r_c = 0.07$ ,  $r_2 = 11.0$ ; for diCIVC-St,  $r_1 = 0.05$ ,  $r_c =$

0.03,  $r_2 = 17.4$ . The composition curves for these systems calculated from these values agree exactly with the experimental results (Figs. 5 and 6).

Thus, the results of the studies on the copolymerization of diCIVC support the introduction of a six-membered ring into the polymer chain. In a previous paper,<sup>4</sup> it was reported that some polymers produced by radical homopolymerization of vinylcyclopropanes have some unknown saturated structural units, which may be cyclobutanes. The possibility of the presence of six-membered rings will also have to be considered.

### References

1. T. Takahashi, *J. Polym. Sci. A-1*, in press.
2. T. Takahashi and I. Yamashita, *Kogyo Kagaku Zasshi*, **68**, 869 (1965).
3. T. S. Lee, I. M. Kolthoff, and M. A. Maris, *J. Polym. Sci.*, **3**, 66 (1948).
4. T. Takahashi, *J. Polym. Sci. A-1*, **6**, 403 (1968).

Received September 24, 1969

## Studies of the Polymerization of Diallyl Compounds. VII. Kinetics of the Polymerization of Diallyl Esters of Aliphatic Dicarboxylic Acids

AKIRA MATSUMOTO and MASAYOSHI OIWA, *Department of Applied Chemistry, Faculty of Engineering, Kansai University, Senriyama, Suita-shi, Osaka, Japan*

### Synopsis

Radical polymerization studies on diallyl oxalate (DAO), diallyl malonate (DAM), diallyl succinate (DASu), diallyl adipate (DAA), and diallyl sebacate (DAS) have been conducted kinetically from the standpoint of cyclopolymerization. Benzoyl peroxide was employed as the initiator. The initial overall rate of polymerization,  $R_p$ , was not proportional to the square root or the first power of the initiator concentration,  $[I]$ . But  $R_p/[I]^{1/2}$  and  $[I]^{1/2}$  bore a linear relationship, provided the monomer concentration was kept constant. The residual unsaturation of the polymers decreased with decreasing monomer concentration. The ratio of the rate constant of the unimolecular cyclization reaction to that of the bimolecular propagation reaction of the uncyclized radical,  $K_c$ , was evaluated from the above relationship between the residual unsaturation and the monomer concentration at 60°C. The  $K_c$  values obtained were 3.6, 3.2, 2.8, 2.5, and 1.2 mole/l. for DAO, DAM, DASu, DAA, and DAS, respectively.

The overall activation energies of polymerization were found to be 21.1 (DAO), 24.2 (DAM), 21.7 (DASu), 22.0 (DAA), and 22.2 (DAS) kcal/mole.

### INTRODUCTION

It is well known that diallyl compounds undergo cyclopolymerization.<sup>1-9</sup> The polymerization of diallyl quaternary ammonium salts by Butler<sup>2,3</sup> and of various diallyl esters of dicarboxylic acids by Simpson<sup>1</sup> were the first cyclopolymerizations reported.

It seems, however, that there have been few detailed studies on the kinetics of cyclopolymerization for diallyl compounds.

Simpson<sup>1</sup> studied the polymerization of various diallyl esters from the standpoint of gelation using benzoyl peroxide as initiator and found that the conversion at the gelation point was greater than would be calculated for the formation of networks from tetrafunctional monomers. This divergence from theory could be explained to some extent as resulting from a loss of unsaturation by cyclization; this was also supported by measurements of unsaturation and degree of polymerization. In his report, Simpson also proposed a reaction scheme for the polymerization of the diallyl esters, but the kinetics based on the scheme were not established. It has been assumed that the reactivities of the uncyclized radical with an

adjacent pendant double bond and of the cyclized radical are equivalent. Thus, the dependence of the residual unsaturation and the degree of polymerization on the monomer concentration can not be explained quantitatively by using the kinetic equations derived from Simpson's scheme.

Gibbs<sup>10</sup> has proposed general kinetics of cyclopolymerization which include two types of termination reaction, one by the reaction of pairs of radicals, and the second type involving a degradative chain transfer. The polymerization of diallyl esters is of the second type. The kinetics derived a dependence of the rate on the first power of the initiator concentration, whereas Simpson<sup>1</sup> did not find an exact proportional correlation between the rate of monomer consumption and the first power of the initiator concentration for diallyl phthalate. In the other equation derived to evaluate the cyclization constant,  $k_c/k_{11}$ , the fit of the experimental data by Simpson for a linear relationship was excellent, but, unfortunately, the intercept of the line was higher than the value predicted, 1.25 as opposed to 1.00.

On the other hand, we reported detailed kinetics on the polymerization of diallyl phthalate<sup>11</sup> and diallyl carbonate<sup>12</sup> in previous papers, in which the uncyclized and cyclized radicals were treated individually. The agreement between the kinetics and the experimental data was excellent.

In this paper, the polymerization of diallyl esters of several aliphatic dicarboxylic acids was carried out; by employing the equation derived in previous papers, we will kinetically discuss our results in terms of cyclopolymerization.

## EXPERIMENTAL

### Materials

Diallyl oxalate (DAO), diallyl malonate (DAM), diallyl succinate (DASu), diallyl adipate (DAA), and diallyl sebacate (DAS) were prepared by esterification of the corresponding aliphatic dicarboxylic acids with allyl alcohol according to the method described in the literature.<sup>13</sup> Monomers were purified by distillation *in vacuo* before use.

Benzoyl peroxide (BPO) was purified by the repeated precipitation from a chloroform solution with methanol.

Benzene was washed thoroughly with concentrated sulfuric acid, then washed with distilled water until it became neutral, dried on calcium chloride, and distilled over metallic sodium.

### Polymerization Procedure

Polymerizations were carried out in glass ampoules (10–50 ml capacity), with the use of benzene as the solvent and BPO as the initiator. Measured amounts of diallyl ester, BPO, and benzene were placed in a glass ampoule which was then evacuated under reduced pressure and flushed twice with nitrogen. The ampoule was then sealed under vacuum and put into a thermostat regulated at the desired temperature.

After a definite period of reaction time, the polymer produced was precipitated by pouring the reaction mixture into more than tenfold volume of cooled methanol containing hydroquinone and separated by centrifugation. The polymer thus obtained was then washed repeatedly with methanol and dried *in vacuo* until a constant weight was obtained. The percentage conversion was calculated from the weight of polymer isolated. The polymer was then purified by dissolving it in acetone and by subsequent reprecipitation with methanol.

### Analysis

The unreacted pendant allyl groups of the purified polymer were determined by the method of Simpson et al.<sup>14</sup> The residual unsaturation of the polymer was then expressed as percentage of the corresponding pure diallyl ester.

The number-average molecular weight of the polymer was measured with a Hewlett Packard 302 vapor-pressure osmometer.

## RESULTS AND DISCUSSION

### Kinetics of Polymerization of the Diallyl Esters

Holt and Simpson<sup>1</sup> studied the polymerization of a number of diallyl esters and proposed the reaction scheme shown in eqs. (1)–(6),

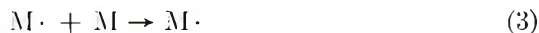
Initiation:



Cyclization:



Propagation:



Chain termination:



Re-initiation:



Radical termination:

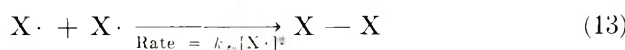
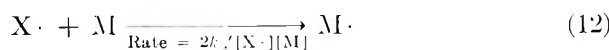
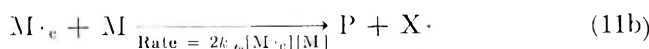
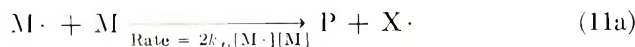
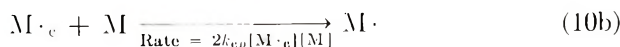
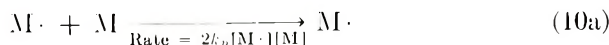
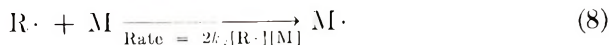


where I is initiator; M is the diallyl ester monomer; P is polymer produced;  $M\cdot$  is a growing chain radical; and  $X\cdot$  is a degraded radical.

It should be noted, however, that in this reaction scheme the uncyclized and cyclized radicals were not differentiated, and so the dependence of the residual unsaturation on the monomer concentration could not be explained quantitatively by using the kinetic equations derived from the above

scheme, as the cyclized radical can cyclized further according to this reaction scheme.

In order to improve the above scheme, it seems reasonable to treat the uncyclized and cyclized radicals individually [eqs. (7)–(13)].



Here  $R\cdot$  denotes an initiator radical,  $M\cdot$  is the initial radical derived from the attack of a radical on  $M$ , and  $M\cdot_c$  is the radical formed by the intramolecular cyclization of  $M\cdot$ .

From these points of view, we derived the kinetic equations by assuming steady-state conditions in the previous papers,<sup>11,12</sup> in which two cases were discussed. In the first case, where the loss of monomer by initiation, chain termination, and re-initiation reactions is not negligible compared with that by the propagation, the kinetic chain length is small. In the other case, where the propagation reaction is predominant, the kinetic chain length is sufficiently large, and the simplified kinetic equations can be, therefore, used instead of the more elaborate ones.

In the polymerization of diallyl phthalate,<sup>11</sup> the degree of polymerization became considerably smaller with a decrease in the monomer concentration, and therefore, it was necessary to apply the elaborate kinetic equations.

On the other hand, in the polymerization of diallyl carbonate,<sup>12</sup> where the degree of polymerization was quite large, we could use the simplified kinetic equations.

In the polymerizations of diallyl esters of aliphatic dicarboxylic acids investigated in this paper, the degree of polymerization was quite large,\* and therefore, the simplified kinetic equations could be applied as for diallyl carbonate.

\* For example, in the bulk polymerization of the diallyl esters, the initial degree of polymerization was 85 (DAO), 70 (DAM), 71 (DASu), 61 (DAA), and 54 (DAS).

The simplified kinetic equations were derived as follows; if a steady-state is assumed for the different types of radicals based on the reaction scheme mentioned above, eqs. (14)–(17) can be obtained.

$$[R\cdot] = fk_d[I]/k_i[M] \quad (14)$$

$$[M\cdot] = \frac{2fk_d[I] + 2k_i'(2fk_d[I]/k_{t3})^{1/2}[M]}{2k_{t1}[M] + k_c k_{t2}/(k_{cp} + k_{t2})} \quad (15)$$

$$[M\cdot_c] = \frac{\{k_c/2(k_{cp} + k_{t2})[M]\} \{2fk_d[I] + 2k_i'(2fk_d[I]/k_{t3})^{1/2}[M]\}}{2k_{t1}[M] + k_c k_{t2}/(k_{cp} + k_{t2})} \quad (16)$$

$$[X\cdot] = (2fk_d[I]/k_{t3})^{1/2} \quad (17)$$

Here  $f$  denotes the efficiency of initiation of chain radicals by  $R\cdot$ .

The rate of polymerization is given by

$$R_p = 2k_p[M\cdot][M] + 2k_{cp}[M\cdot_c][M] \quad (18)$$

On substituting for  $M\cdot$  and  $M\cdot_c$  by using eqs. (15) and (16) we have:

$$R_p = \{2fk_d[I] + 2k_i'(2fk_d[I]/k_{t3})^{1/2}[M]\} \times \left\{ \frac{2k_p[M] + k_c k_{cp}/(k_{cp} + k_{t2})}{2k_{t1}[M] + k_c k_{t2}/(k_{cp} + k_{t2})} \right\} \quad (19)$$

The degree of polymerization is also given by

$$\bar{P}_{n,0} = R_p / \{2k_{t1}[M\cdot][M] + 2k_{t2}[M\cdot_c][M]\} \quad (20)$$

On substituting for  $M\cdot$  and  $M\cdot_c$  by using eqs. (15) and (16) we obtain:

$$\bar{P}_{n,0} = \frac{2k_p[M] + k_c k_{cp}/(k_{cp} + k_{t2})}{2k_{t1}[M] + k_c k_{t2}/(k_{cp} + k_{t2})} \quad (21)$$

On the other hand, the rate of formation of the pendant double bonds in the polymer is given by

$$dm/dt = 2k_p[M\cdot][M] - k_c[M\cdot] + 2k_{cp}[M\cdot_c][M] \quad (22)$$

This equation is true in the absence of crosslinking reactions, since these reactions will consume double bonds in the polymer. However, in the early stage of polymerization, the loss of double bonds by the crosslinking reaction should be small compared with the loss during propagation.

By using eqs. (15) and (16) we obtain:

$$dm/dt = \{2fk_d[I] + 2k_i'(2fk_d[I]/k_{t3})^{1/2}[M]\} \times \left\{ \frac{2k_p[M] - k_c k_{t2}/(k_{cp} + k_{t2})}{2k_{t1}[M] + k_c k_{t2}/(k_{cp} + k_{t2})} \right\} \quad (23)$$

Equations (19) and (23) give:

$$\frac{dm}{dM} = \frac{2k_p[M] - k_c k_{t2}/(k_{cp} + k_{t2})}{2k_p[M] + k_c k_{cp}/(k_{cp} + k_{t2})} \quad (24)$$

which on rearrangement gives:

$$(1 - P)^{-1} = 1/(1 + \beta) + (2/K_c)[M] \quad (25)$$

where  $P$  is the ratio of residual pendant double bonds in the polymer to that of the polymerized diallyl ester monomer,  $dm/dM$ , while  $\beta$  and  $K_c$  are  $k_{t2}/k_{cp}$  and  $k_c/k_p$ , respectively.

Combination of eqs. (19) and (21) gives:

$$R_p/\bar{P}_{n,0} = 2fk_d[I] + 2k_t'(2fk_d[I]/k_{t2})^{1/2}[M] \quad (26)$$

### Effect of the Initiator Concentration on the Initial Rate of Polymerization

The bulk polymerizations of DAO, DAM, DASu, DAA, and DAS were investigated under different initiator concentrations at 60°C. The time-conversion curves for the polymerization of DAO are shown in Figure 1.

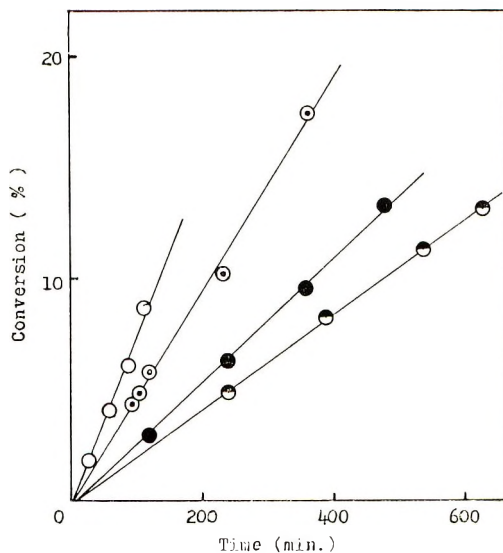


Fig. 1. Time-conversion curves in the bulk polymerization of diallyl oxalate at 60°C: (○)  $[I] = 0.4$  mole/l.; (⊙)  $[I] = 0.2$  mole/l.; (●)  $[I] = 0.1$  mole/l.; (◐)  $[I] = 0.06$  mole/l.

The initial rates of polymerization  $R_p$  of DAO as calculated from the slope of the straight lines are shown in Table I. Those of other diallyl esters are also summarized in Table I. They are not proportional to the square root or to the first power of the initiator concentration, as had been expected from eq. (19). However, when the monomer concentration is kept constant and the initiator concentration is varied, it may be on the



TABLE I  
Effect of the Initiator Concentration on the Polymerizations  
of Diallyl Esters of Aliphatic Dicarboxylic Acids<sup>a</sup>

Monomer	[Initiator], mole/l.	$R_p \times 10^5$ , mole/l.-sec	$(R_p/[I]^{1/2})$ $\times 10^5$ (mole/l.) <sup>1/2</sup> /sec	$(R_p/[I])$ $\times 10^5$ , sec <sup>-1</sup>
DAO	0.40	8.05	12.72	20.1
DAO	0.20	5.29	11.84	26.5
DAO	0.10	3.14	9.93	31.4
DAO	0.06	2.31	9.42	38.5
DAM	0.40	7.42	11.73	18.5
DAM	0.20	4.42	9.87	22.1
DAM	0.10	2.86	9.06	28.6
DAM	0.06	2.06	8.41	34.3
DASu	0.40	5.15	8.14	12.9
DASu	0.20	2.96	6.61	14.8
DASu	0.10	1.88	5.95	18.8
DASu	0.06	1.28	5.22	21.3
DAA	0.40	4.27	6.74	10.7
DAA	0.20	2.28	5.09	11.4
DAA	0.10	1.38	4.37	13.8
DAA	0.06	1.01	4.11	16.8
DAS	0.40	3.45	5.46	8.6
DAS	0.20	1.95	4.36	9.8
DAS	0.10	1.22	3.85	12.2
DAS	0.06	0.83	3.40	13.9

<sup>a</sup> Polymerized in bulk at 60°C with benzoyl peroxide as initiator.

basis of kinetics expected from eq. (19) that  $R_p/[I]^{1/2}$  versus  $[I]^{1/2}$  will be a straight line.\*

From this standpoint, the relationships between  $R_p/[I]^{1/2}$  and  $[I]^{1/2}$  obtained from Table I are plotted in Figure 2. The fit of the experimental data for the linear relationship is fairly good, as observed in the previous works for the polymerizations of diallyl phthalate<sup>11</sup> and diallyl carbonate.<sup>12</sup>

### Dependence of the Degree of Polymerization on the Initiator and Monomer Concentration

From eq. (21) it may be kinetically expected that the degree of polymerization will be independent of the initiator concentration but dependent on the monomer concentration.

This was already confirmed in the polymerizations of diallyl phthalate<sup>11</sup> and diallyl carbonate.<sup>12</sup> Therefore, it may be true in the polymerizations of diallyl esters of aliphatic dicarboxylic acids concerned with in the present paper.

\* Equation (19) can be written as follows:

$$\frac{R_p}{[I]^{1/2}} = 2\{fk_d[I]^{1/2} + 2k_t'(2fk_d/k_t)^{1/2}(M)\} \left\{ \frac{2k_p[M] + k_c k_{cp}/(k_{cp} + k_{ct})}{2k_t[M] + k_c k_{ct}/(k_{cp} + k_{ct})} \right\}$$

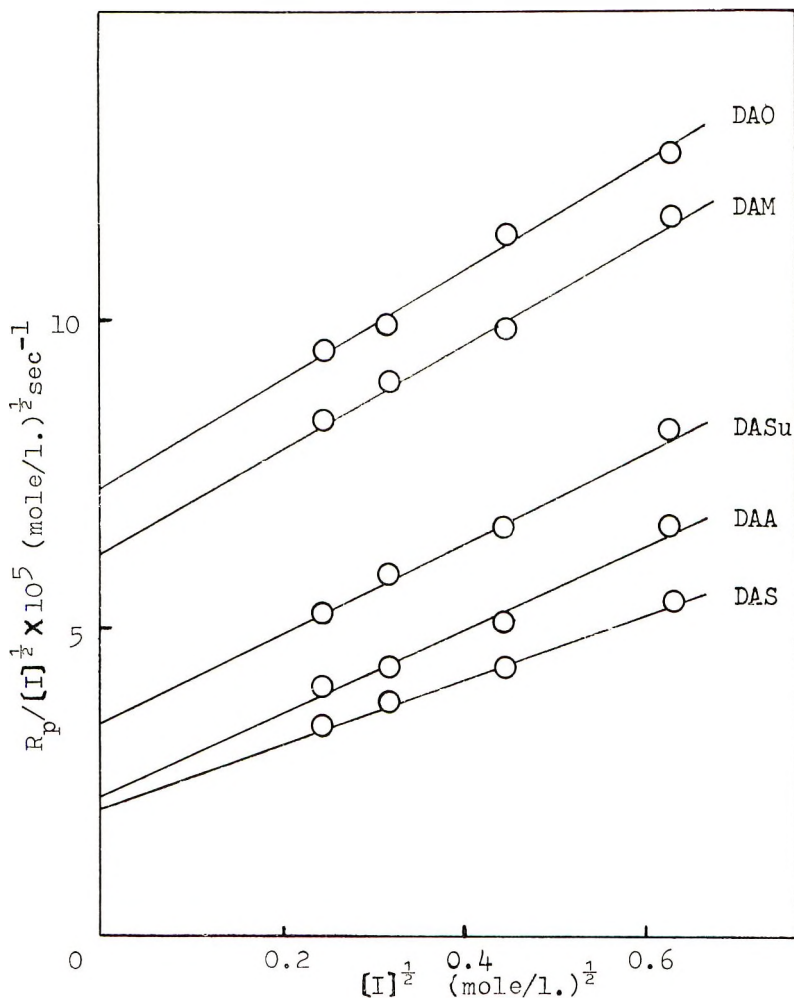


Fig. 2. Plots of  $R_p/[I]^{1/2}$  vs.  $[I]^{1/2}$  in bulk, polymerization temperature 60°C.

### Activation Energy

To determine the overall activation energies, the polymerizations were carried out in bulk at 60, 70, and 80°C, using 0.06 mole/l. of BPO as initiator. The plots of the logarithm of  $R_p$  versus  $1/T$  are shown in Figure 3. The overall activation energies of polymerization calculated from the slope of the curves were 21.1 (DAO), 24.2 (DAM), 21.7 (DASu), 22.0 (DAA), and 22.2 (DAS) kcal/mole.

### Estimation of $K_c$

In cyclopolymerization the intramolecular cyclization reaction is unimolecular and the usual propagation reaction is bimolecular; therefore, the residual unsaturation of the polymer,  $R_{ns}$ , may be expected to decrease

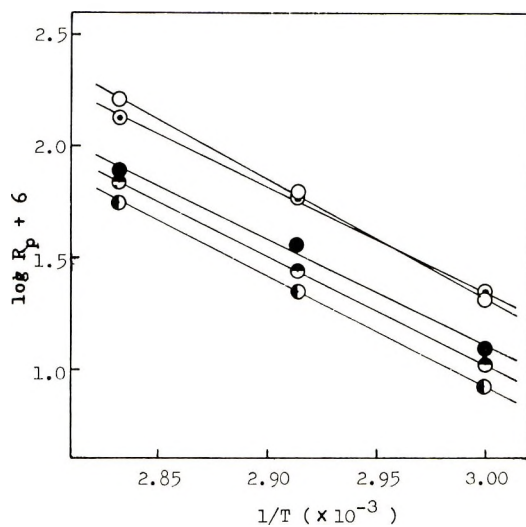


Fig. 3. Plots of  $\log R_p$  vs.  $1/T$ : ( $\odot$ ) DAO; ( $\circ$ ) DAM; ( $\bullet$ ) DASu; ( $\ominus$ ) DAA; ( $\bullet$ ) DAS. Polymerization in bulk,  $[I] = 0.06$  mole/l.

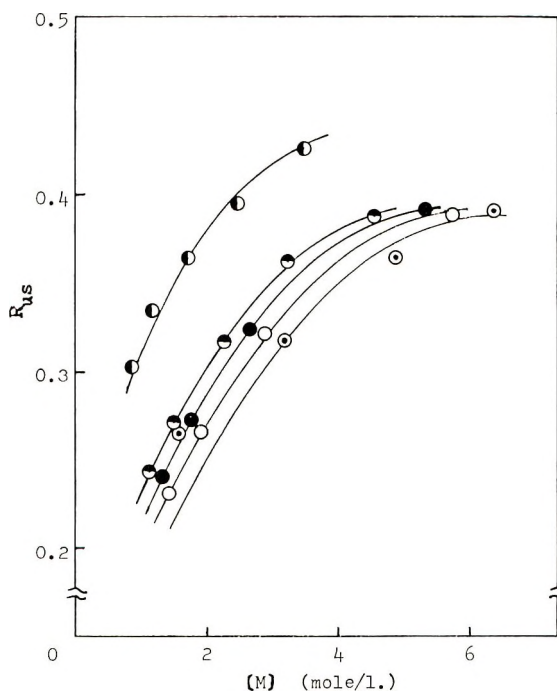


Fig. 4. Relations between the residual unsaturation and the monomer concentration: ( $\odot$ ) DAO; ( $\circ$ ) DAM; ( $\bullet$ ) DASu; ( $\ominus$ ) DAA; ( $\bullet$ ) DAS. Polymerization temperature,  $60^\circ\text{C}$ ;  $[I] = 0.2$  mole/l.

with a decrease in the monomer concentration. From such a standpoint, polymerizations were carried out under different monomer concentrations at 60°C, with the use of 0.2 mole/l. of BPO as initiator and benzene as solvent. The results obtained are given in Table II and plotted in Figure 4.

TABLE II  
Effect of the Monomer Concentration on the Residual  
Unsaturation of the Polymers<sup>a</sup>

Monomer	[M], mole/l.	$R_{us}$ <sup>b</sup>
DAO	6.38 <sup>c</sup>	0.391
DAO	4.95	0.363
DAO	3.19	0.319
DAO	1.59	0.265
DAM	5.76 <sup>c</sup>	0.387
DAM	2.88	0.322
DAM	1.92	0.267
DAM	1.44	0.232
DASu	5.33 <sup>c</sup>	0.392
DASu	2.66	0.324
DASu	1.78	0.272
DASu	1.33	0.242
DAA	4.53 <sup>c</sup>	0.388
DAA	3.23	0.362
DAA	2.26	0.317
DAA	1.51	0.272
DAA	1.13	0.244
DAS	3.47 <sup>c</sup>	0.426
DAS	2.48	0.395
DAS	1.73	0.363
DAS	1.16	0.335
DAS	0.87	0.303

<sup>a</sup> Polymerizations were carried out at 60°C, with 0.2 mole/l. of benzoyl peroxide as initiator.

<sup>b</sup> The residual unsaturation is the degree of unsaturation of the polymer expressed as a percentage of the corresponding pure diallyl ester monomer and was obtained by the analysis of the polymer less than 10% conversion.

<sup>c</sup> These are bulk polymerizations and all other experiments are solution polymerizations using benzene as solvent.

$R_{us}$  decreased with a decrease in the monomer concentration as we would have expected. It should be noted that  $R_{us}$  must be 0.5 if no cyclization and crosslinking reactions occur. On the other hand, in the early stage of polymerization the crosslinking reaction should be negligible. The deviation of  $R_{us}$  from 0.5 may be, therefore, attributed predominantly to the intramolecular cyclization reaction. The ratio of the rate constant of the unimolecular cyclization reaction to that of the bimolecular propagation of the uncyclized radical,  $K_c$ , was evaluated by applying eq. (25) to the results shown in Table II. The plots of  $(1 - F)^{-1}$  versus  $[M]$  are shown in Figure 5. They have a good linear relationship, as was predicted by eq. (25). From the slope of the straight lines,  $K_c$  was estimated to be 3.6,

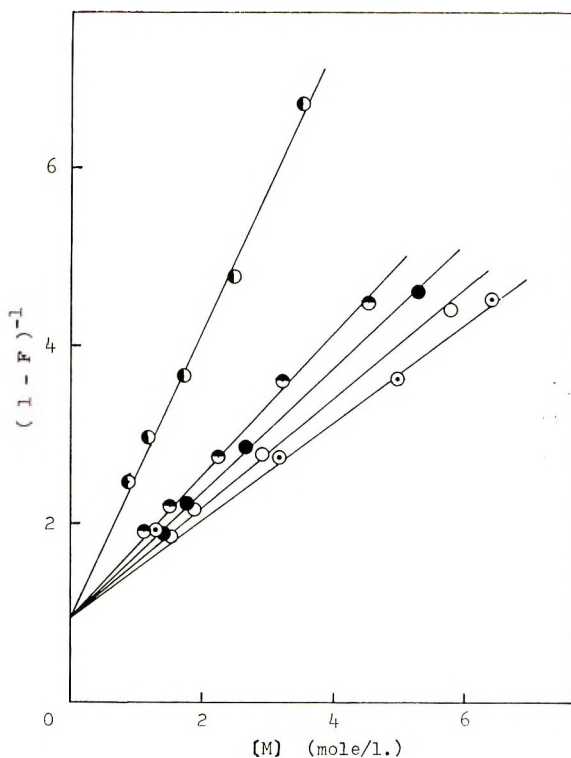


Fig. 5. Plots of  $(1 - F)^{-1}$  vs.  $[M]$ : ( $\odot$ ) DAO; ( $\circ$ ) DAM; ( $\bullet$ ) DASu; ( $\ominus$ ) DAA; ( $\bullet$ ) DAS. Polymerization temperature,  $60^{\circ}\text{C}$ ;  $[I] = 0.2$  mole/l.

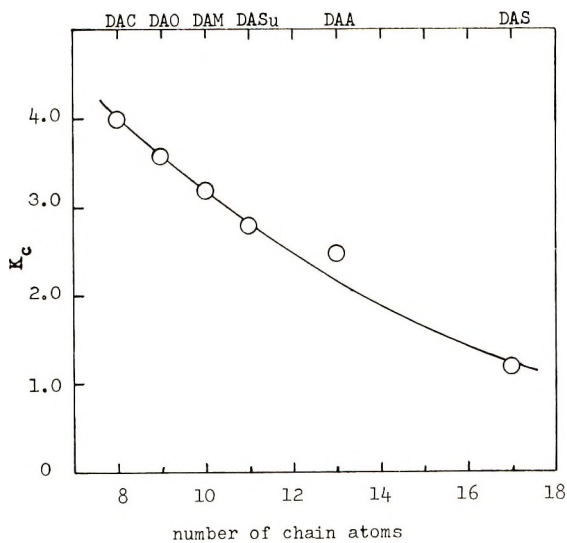


Fig. 6. Relation between  $K_c$  and the number of chain atoms in the consecutive addition.

3.2, 2.8, 2.5, and 1.2, mole/l. for DAO, DAM, DASu, DAA, and DAS, respectively.

The relationship between  $K_c$  and the number of chain atoms in the consecutive addition are plotted in Figure 6, where the number of chain atoms in the consecutive addition structures varies from 8 in the case of diallyl carbonate to 17 in diallyl sebacate, assuming a head-to-tail configuration. As is evident from Figure 6, a good correlation was observed between the monomer structure and its tendency to cyclize during polymerization.

In cyclopolymerization,  $K_c$  is the critical factor determining the microstructure of the polymer. It may be interpreted as twice the monomer concentration necessary for the rate of the bimolecular propagation reaction to equal that of the unimolecular cyclization. Thus, the monomer concentrations of DAO, DAM, DASu, DAA, and DAS required for the two processes to proceed at an equal rate are 1.8, 1.6, 1.4, 1.25, and 0.6 mole/l., respectively.

### References

1. T. Holt and W. Simpson, *Proc. Roy. Soc. (London)*, **A238**, 154 (1956).
2. G. B. Butler and F. L. Ingley, *J. Amer. Chem. Soc.*, **73**, 895 (1951).
3. G. B. Butler and R. J. Angelo, *J. Amer. Chem. Soc.*, **79**, 3128 (1957).
4. S. G. Matsoyan, G. M. Pogosyan, R. N. Skripnikova, and A. V. Mushegyan, *Vysokomol. Soedin.*, **5**, 183 (1963).
5. S. G. Matsoyan, G. M. Pogosyan, A. O. Dzhagalyan, and A. V. Mushegyan, *Vysokomol. Soedin.*, **5**, 854 (1963).
6. V. G. Ostroverkhov, L. A. Brumorskaya, and A. A. Korniyenko, *Vysokomol. Soedin.*, **6**, 1020 (1964).
7. G. B. Butler, A. Crawshaw, and W. L. Miller, *J. Amer. Chem. Soc.*, **80**, 3615 (1958).
8. G. B. Butler, *J. Polym. Sci.*, **48**, 279 (1960).
9. C. S. Marvel, *J. Polym. Sci.*, **48**, 101 (1960).
10. W. E. Gibbs, *J. Polym. Sci. A*, **2**, 4815 (1964).
11. A. Matsumoto, K. Asano, and M. Oiwa, *Nippon Kagaku Zasshi*, **90**, 290 (1969).
12. A. Matsumoto, K. Takashima, and M. Oiwa, *Bull. Chem. Soc. Japan*, **42**, 1959 (1969).
13. D. M. Vinokurov and M. B. Khaikina, *Izv. Vysshikh. Uchebn. Zavedenii, Khim. Khim. Tekhnol.*, **6**, 83 (1963); *Chem. Abstr.*, **59**, 6250 (1963).
14. W. Simpson, T. Holt, and R. J. Zetie, *J. Polym. Sci.*, **10**, 489 (1953).

Received July 30, 1969

Revised October 10, 1969

## Preparation of Block Copolymers by Use of Peroxide-Terminated Prepolymer

N. Z. ÉRDY\* and C. F. FERRARO, *Central Research Department, FMC Corporation, Princeton, New Jersey 08540* and A. V. TOBOLSKY, *Department of Chemistry, Princeton University, Princeton, New Jersey 08540*

### Synopsis

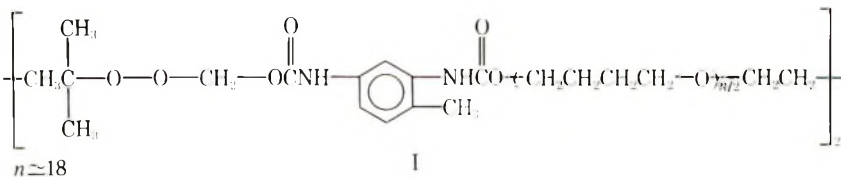
Block copolymers containing poly(tetramethylene oxide) and poly(methyl methacrylate) segments were prepared. A commercially available poly(tetramethylene oxide) terminated with tolylene diisocyanate was capped with *tert*-butyl hydroxymethyl peroxide and the resulting prepolymer peroxide was used as a free-radical initiator of vinyl polymerization. Block copolymers formed in temperature-programmed vinyl polymerizations possessed improved impact strengths over poly(methyl methacrylate) from 0.35 to 1.18 for a fixed (nonoptimized) block length of poly(tetramethylene oxide).

### INTRODUCTION

The preparation of block copolymers containing both rubbery and glassy segments has resulted in materials possessing a combination of the characteristic properties of each of these segments within the same molecular chains. The purpose of the work presented in this paper was to synthesize block copolymers of this type containing poly(tetramethylene oxide) and poly(methyl methacrylate). Several workers have utilized stirred poly(ethylene oxide),<sup>1</sup> polyethers and polyesters terminated with peroxycarbamate groups,<sup>2</sup> and poly(ethylene oxide) containing azonitrile groups<sup>3</sup> as sources of free radicals to initiate polymerization of many vinyl and di-vinyl monomers and prepare block copolymers. Anionic polymerization techniques have also been used to prepare block copolymers of poly(ethylene oxide) and polystyrene.<sup>4</sup>

For this paper a commercially available poly(tetramethylene oxide) terminated on both ends with tolylene diisocyanate was combined with *tert*-butyl hydroxymethyl peroxide. The bis(*tert*-butyl peroxymethyl carbamate) polyether prepolymer (*t*-BuPP) formed may be represented by the structure I on the following page.

\* Present address: Stauffer Chemical Company, Eastern Research Center, Dobbs Ferry, N. Y. 10522.



Some decomposition studies of the *t*-BuPP and its polymerization of methyl methacrylate at different temperatures are discussed. Information from these experiments was utilized to predict the course of temperature programmed block copolymerizations.

The impact strengths of the block copolymers are compared with the values obtained for poly(methyl methacrylate).

## EXPERIMENTAL

### Materials

Benzene (spectral grade) was dried over sodium wire. Methyl methacrylate was freed from inhibitor by fractional distillation. Poly(tetramethylene oxide) capped with tolylene diisocyanate (Adiprene L-100, du Pont de Nemours & Co., Inc., MW 1680, amine equivalent 950)<sup>5,6</sup> was used as received. *tert*-butyl hydroxymethyl peroxide was prepared from formaldehyde, and *tert*-butyl hydroperoxide.<sup>7</sup>

*t*-BuPP was prepared from the reaction of tolylene diisocyanate-capped poly(tetramethylene oxide) (500 g) with an excess of *tert*-butyl hydroxymethyl peroxide (120 g) at room temperature, under anhydrous conditions, in benzene (500 g) using triethylamine (2 g) as catalyst. The product was isolated and purified by precipitation and reprecipitation from benzene into petroleum ether; MW 1950; peroxygen content 3.25 wt-%.

### Analyses

Peroxygen contents of polymers were determined by mixing sodium iodide (6 g), water (3 ml), glacial acetic acid (50 ml), sample (about 0.25 g in 10 ml benzene solution) and concentrated hydrochloric acid (2 ml) in the order given. After stirring (20–30 min) at room temperature, a water–isopropanol mixture (1:1 by volume, 100 ml) was added. The liberated iodine was titrated against aqueous sodium thiosulfate (0.05*N*). Water (50 ml) was added immediately before the completion of the titration to facilitate observation of the endpoint. An electrometric dead-stop device was also used to aid determination of the endpoint. Blank titrations consumed less than 0.02 meq of titrant. All titrations were carried out with rigorous exclusion of air achieved by continual addition of Dry Ice to the titration flask and to the reactants before mixing.

Amine equivalents were determined by a method developed in these laboratories.<sup>8</sup>

Number-average molecular weights were determined in benzene at 39°C by means of a Mechrolab vapor-phase osmometer Model 301. Viscosity-



average molecular weights can be calculated from intrinsic viscosities measured at 25°C in benzene by using the relationship:<sup>9</sup>

$$[\eta] = 0.57 \times 10^{-4} M_v^{0.76}$$

Determination of melt viscosities was based essentially on the ASTM Committee D-20 method.<sup>10</sup> Measurements were performed at 230°C.

Impact strengths were measured by using the ASTM Izod impact procedure.<sup>11</sup>

### Decomposition of *t*-BuPP and Block Copolymerization

For decomposition kinetics, benzene solutions (10 ml) of *t*-BuPP were added to Carius tubes, degassed twice, and sealed under vacuum. After specific time intervals in an oil bath the contents of each tube were analyzed iodometrically to determine the concentration of undecomposed *t*-BuPP. All solutions turned progressively yellow during the decomposition.

In high conversion block copolymerizations, the required amounts of *t*-BuPP and methyl methacrylate were degassed twice and sealed off in Carius tubes. After polymerization for two days at the required temperature in an oil bath, conversions were generally greater than 95%. The samples were used for impact strength measurements without further purification. Some experiments were carried out over the whole range of polymerization to obtain complete conversion-time curves. Polymers were recovered at specific time intervals, and the degrees of conversion were determined gravimetrically by precipitating the polymers from benzene into a sevenfold excess of hexane, filtering and drying under vacuum to constant weight.

## RESULTS AND DISCUSSION

### Decomposition of *t*-BuPP

The rate of decomposition of *t*-BuPP in benzene was studied at three temperatures. The data are presented on a plot for first-order decomposition kinetics (Fig. 1). It appears that the decompositions at 80 and 100°C follow quite closely the first-order kinetics over the examined range of decomposition. The deviation from linearity at 115°C suggests the presence of competing reactions with higher kinetic order, and these are complicating the decomposition kinetics. It can be shown from the data presented in Figure 1 that the decomposition kinetics of *t*-BuPP may follow more closely to an overall order of 3/2. Bartlett and Nozaki<sup>12</sup> have shown that for benzoyl peroxide decomposition in several solvents, induced decomposition can lead to modified first-order kinetics resulting in a higher overall order. Further experiments would be necessary to determine whether *t*-BuPP exhibits this behavior.

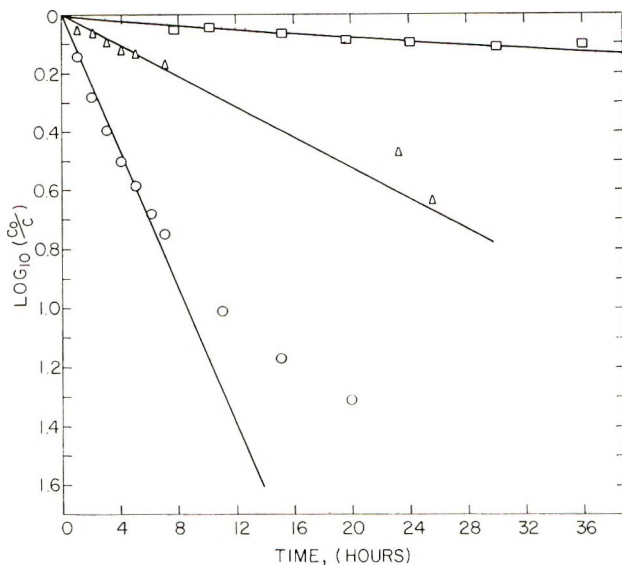


Fig. 1. Decomposition of *t*-BuPP in benzene at several temperatures and various initial molar peroxygen concentrations: (□) at 80°C, 8.92; (△) at 100°C, 2.46; (○) at 115°C, 2.46.

### Conversion-Time Curves for Polymerization of Methyl Methacrylate by *t*-BuPP

The polymerization of methyl methacrylate was investigated over a wide range of conversion. Kinetic curves at 80 and 100°C are shown in Figure

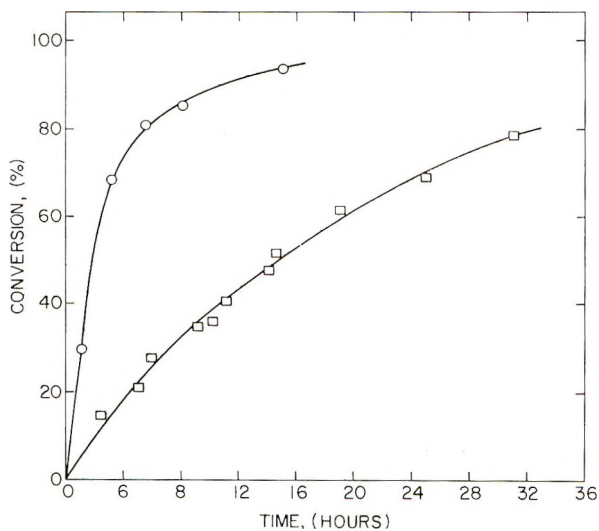


Fig. 2. Variation of the degree of conversion of methyl methacrylate with the time of polymerization with *t*-BuPP (10 wt-%) as initiator: (□) 80°C; (○) 100°C.

2. An unexpected feature of these plots is the absence of a Trommsdorff effect.<sup>13</sup> In most other cases unless methyl methacrylate is diluted with solvent to below about 40% monomer concentration an acceleration in rate of polymerization is observed at higher conversions and rapid gelation occurs.

### Effect of Polymerization Variables on the Impact Strength of the Poly(tetramethylene Oxide)-Poly(methyl Methacrylate) Block Copolymers

Methyl methacrylate was polymerized in bulk for 48 hr at 80°C with the use of *t*-BuPP as initiator at concentrations of 5, 10 and 15% by weight. Similar experiments were performed at 100 and 115°C. The Izod impact strengths, intrinsic viscosities  $[\eta]$ , and melt viscosities  $\eta_m$  of the block copolymers are shown in Table I. Polymerization for longer times did not

TABLE I  
Effect of *t*-BuPP Concentration and Temperature of  
Polymerization on the Properties of Block Copolymers

Temp, °C	<i>t</i> -BuPP, wt-%	Impact strength, ft × lb/in. of notch	$[\eta]$ , dl/g	$\eta_m \times 10^{-5}$ , poise (230°C)
80	5	0.50	1.7	19.7
80	10	0.76	—	8.9
80	15	1.18	1.0	6.1
100	5	0.51	1.3	—
100	10	0.56	1.0	6.3
100	15	—	—	—
115	5	0.36	1.0	—
115	10	—	0.6	1.1
115	15	—	—	—

lead to further improvement of impact strength. Table I shows that for a given concentration of *t*-BuPP an increase in temperature of polymerization produces block copolymers with lower impact strengths. These lower values correspond to the expected decrease in molecular weights shown by the lower intrinsic and melt viscosities. At a fixed temperature of polymerization an increase in the concentration of *t*-BuPP leads also to expected lower intrinsic and melt viscosities. Impact strengths increase however in this case. Poly(methyl methacrylate) homopolymer (Rohm and Haas, Plexiglas) had a measured impact strength of 0.37.

It is expected that polymerization at low temperatures would lead to a few prepolymer molecules adding long blocks of methyl methacrylate. In addition there would be long-chain methyl methacrylate homopolymer and an appreciable amount of unreacted peroxide terminated prepolymer.

Polymerization at high temperatures would lead to short vinyl polymer blocks attached to the polyether segments and homopolymer with no unreacted peroxy-terminated prepolymer (dead-end conditions).<sup>14</sup>

A programmed polymerization starting at low temperatures and ending up at high temperatures would give a wide chain length distribution for vinyl blocks and homopolymer, with no unreacted prepolymer. Several such polymerizations were carried out on the basis of the kinetic data and resulted in impact strength values close to 1.0.

The problem of the relative amount of block copolymer and homopolymer actually present in these samples is a very challenging one, but at the time of these studies we did not find the opportunity to develop a satisfactory fractionation. It should be pointed out that all these structures had a fixed chain length of poly(tetramethylene oxide). It has been demonstrated very recently by Meier,<sup>15</sup> Morton and co-workers<sup>16</sup> and by Cooper and Tobolsky<sup>17</sup> that the physical properties of styrene-butadiene-styrene block copolymers are inherent upon the presence of molecular domains. The formation and strength of these domains is dependent upon the chain length and molecular weight distribution of the blocks. The chain length of the soft segment in our system was far from optimum.

We wish to express our appreciation to Dr. B. F. Landrum for his consultations and guidance, to Dr. W. Riedeman and C. A. Erickson for carrying out the synthesis of the peroxy prepolymer and to F. D. Petke for completing the melt viscosity measurements. We also wish to acknowledge the valuable assistance of Dr. F. C. Baines in preparing this manuscript.

## References

1. Y. Minoura, T. Kasuya, S. Kawamura, and A. Nakano, *J. Polym. Sci. A-1*, **5**, 43 (1967).
2. A. V. Tobolsky and A. Rembaum, *J. Appl. Polym. Sci.* **8**, 307 (1964).
3. J. Furukawa, S. Takamori, and S. Yamashira, *Angew. Makromol. Chem.*, **1**, 92 (1967).
4. M. Baer, *J. Appl. Polym. Sci.*, **2**, 417 (1964).
5. R. J. Athey, *Rubber Age*, **85**, No. 7, 77 (1959).
6. R. J. Athey, *Ind. Eng. Chem.*, **52**, 611 (1960).
7. F. H. Dickey, F. F. Rust, and W. G. Vaughan, *J. Amer. Chem. Soc.*, **71**, 1432 (1949).
8. Analytical Method CA-177, Central Research Department, FMC Corporation.
9. P. J. Flory, *Principles of Polymer Chemistry*, Cornell Univ. Press, Ithaca, N. Y., 1953, p. 312.
10. Melt Viscosities, ASTM Committee D-20, Method D 1238-62T.
11. Impact Strengths, ASTM Committee D-20, Method D 256-56 (Methods A and C).
12. P. D. Bartlett and K. Nozaki, *J. Amer. Chem. Soc.*, **68**, 1686 (1946); *ibid.*, **69**, 2299 (1947).
13. E. Trommsdorff, H. Köhle, and P. Lagally, *Makromol. Chem.*, **1**, 169 (1948).
14. A. V. Tobolsky, *J. Amer. Chem. Soc.*, **80**, 5927 (1958); *ibid.*, **82**, 1277 (1960).
15. D. J. Meier, in *Block Copolymers (J. Polym. Sci. C, 26)*, J. Moacanin, G. Holden, and N. W. Tschoegl, Eds., Interscience, New York, 1969, p. 81.

16. M. Morton, J. E. McGrath and P. C. Juliano, in *Block Copolymers (J. Polym. Sci. C, 26)*, J. Moacanin, G. Holden, and N. W. Tschoegl, Eds., Interscience, New York, 1969, p. 99.

17. S. L. Cooper and A. V. Tobolsky, *J. Appl. Polym. Sci.* **10**, 1837 (1966); *Textile Res. Journal*, **36**, 800 (1966).

Received August 14, 1969

Revised October 13, 1969

## NOTES

### *Sorption Behavior of Organic Pyropolymers in Aqueous Solutions*

#### INTRODUCTION

Water renovation demands the efficient removal of soluble refractory organic materials and ions from secondary effluents. This process may be carried out with activated carbon granules, the adsorption properties of which have been the subject of investigations by Morris and Weber.<sup>1,2</sup> Despite its high effectiveness, activated carbon is relatively expensive and some problems are encountered in the regeneration process.

The object of this preliminary feasibility study was to evaluate the sorption properties of selected organic pyropolymers especially with respect to organic materials and to compare the results with those obtained with activated carbons by other workers.

#### BACKGROUND

The thermal degradation of polymers follows largely free-radical-initiated chain reactions. During the degradation, two processes can take place: chain scission and/or crosslinking. Polymers in which the "backbone" undergoes mainly scission usually vaporize completely without leaving any appreciable quantity of residue when heated (pyrolyzed) for prolonged periods. This is not the case with polymers in which the formation of crosslinks occurs. These materials become stabilized due to the formation of a rigid insoluble network; the stable products are referred to as pyropolymers.

Unlike activated carbons, many pyropolymers are characterized by the presence of a large number of hetero atoms having excess electrons and/or unsaturated bonds. This property and the possibility that the microporosity of the pyropolymers might be altered by varying the preparative conditions make these systems interesting candidates for the study of sorption-desorption cycles and for the elucidation of the physicochemical parameters that enhance these processes. By understanding these phenomena it should be possible to design additional substrates for the removal of specific organic materials and/or inorganic ions from waste water.

#### APPROACH

The herbicides 2-*sec*-butyl-4,6-dinitrophenol and 2,4-dichlorophenoxyacetic acid were selected as adsorbates. These materials are among the typical organic pollutants in waste water. Furthermore, considerable previous work has been done by other workers with these herbicides with the use of activated carbon as the adsorbent.<sup>1,2</sup>

The pyropolymers were prepared from (1) poly(vinyl chloride), obtained from the Dow Chemical Company, and (2) poly[*N,N'*-(*p,p'*-oxydiphenylene)pyromellitimide], commercially available from duPont as Kapton or H-film.

Upon thermal degradation, both of these polymers leave a residue (pyropolymer), depending on the temperature and time of the pyrolysis. The mechanism of thermal degradation of the polyimide has been extensively studied by Bruck<sup>3-9</sup> and involves the cleavage of the imide groups with the elimination of carbon monoxide and the subsequent formation of a condensed polynuclear system.

## EXPERIMENTAL

## Preparation of the Adsorbent

**Vacuum Pyrolysis.** Vacuum pyrolysis was used only in the case of poly[*N,N'*-(*p,p'*-oxydiphenylene)pyromellitimide]. This material is commercially available only as a film. An accurately weighed 2-mil (0.002-in.) thickness sample of the polymer film was placed in a Pyrex glass tube which was connected to a conventional high vacuum system. The system was evacuated to approximately  $2 \times 10^{-5}$  mm Hg, then the preheated furnace was raised into position around the sample tube and the polymer pyrolyzed for predetermined periods.

**Pyrolysis in Oxygen and/or Nitrogen.** Poly(vinyl chloride) was pyrolyzed in a gaseous atmosphere in the presence of nitrogen. The pyrolyzed polymer was pulverized to a size of 40/60, that is, particles which pass through a U. S. Standard Sieve No. 40 but not through a No. 60 sieve.

Poly[*N,N'*-(*p,p'*-oxydiphenylene)pyromellitimide] was first pyrolyzed in oxygen (353 ml/min) at 450°C for 2 hr followed by pyrolysis in nitrogen (283 ml/min) at 450°C for an additional 30 min to a total weight loss of 32.4%.

## Adsorption Experiments

The adsorption studies were carried out by a simple stirred-batch-reactor technique at room temperature ( $25 \pm 2^\circ\text{C}$ ). An aqueous solution (1000 ml) of the herbicide was prepared with ion-exchange-treated water. The solution was filtered into a one-liter Pyrex round-bottomed glass bottle and was allowed to reach the desired temperature

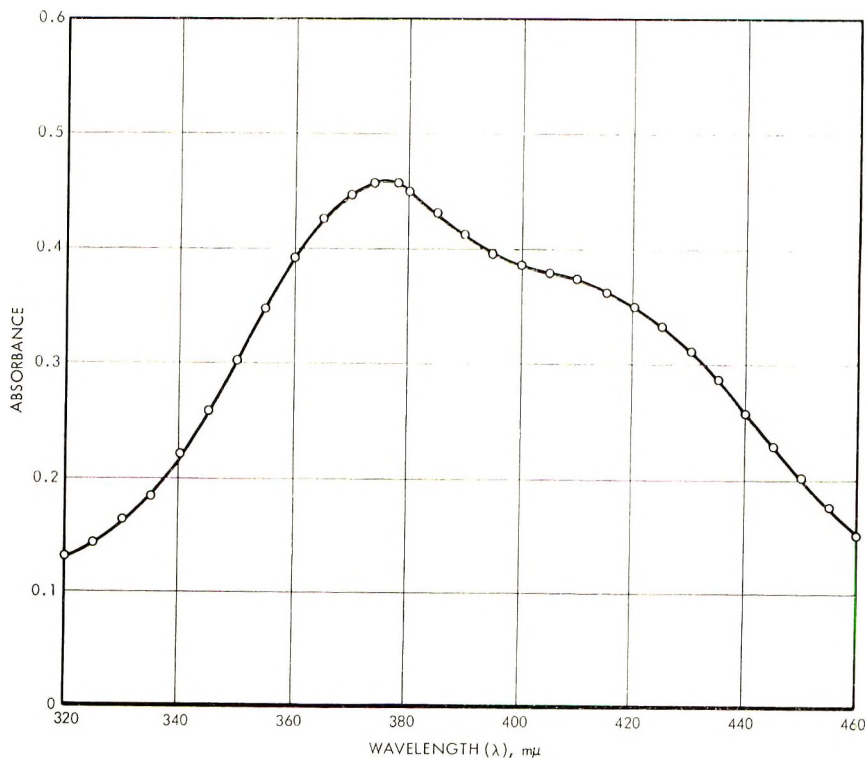


Fig. 1. Ultraviolet absorption spectrum of 2-*sec*-butyl-4,6-dinitrophenol. Cell length 1 cm, concentration = 52.5  $\mu\text{mole/l}$ .

and adsorptive equilibrium with the surface of the glass bottle. Prior to the introduction of the accurately weighed adsorbent, an initial sample was removed and its concentration determined spectrophotometrically. The adsorbent was then introduced into the aqueous solution and rapidly dispersed with a Teflon-coated magnetic stirrer. At predetermined intervals the stirring was interrupted and the adsorbent particles allowed to settle. Approximately 3 ml of the clear supernatant liquid were pipetted out for analysis. Although this resulted in a slight diminution of the solution, the estimated cumulative error was not considered significant enough to materially influence the results in this preliminary feasibility study.

### Spectrophotometry

Two spectrophotometers were used in this work: a Zeiss PMQ II single-beam instrument and a Bausch and Lomb Spectronic 505 double-beam instrument. Figure 1 shows the ultraviolet absorption spectrum of 2-*sec*-butyl-4,6-dinitrophenol.

### RESULTS AND DISCUSSION

Of the two classes of pyropolymers investigated only samples prepared from poly(vinyl chloride) showed adsorption properties. Furthermore, a selective adsorption process was observed, inasmuch as the herbicide 2-*sec*-butyl-4,6-dinitrophenol was taken up preferentially over the herbicide 2,4-dichlorophenoxyacetic acid. The pyropolymers were prepared in a nitrogen atmosphere (535 ml/min) and pyrolyzed for 30 min between 250 and 275°C. The adsorption properties of these pyropolymers were very significantly influenced by the extent of volatilization (weight loss) as shown in Table I.

With an aqueous solution of 2-*sec*-butyl-4,6-dinitrophenol having an initial concentration of 71  $\mu$ mole/l., approximately 30% of the herbicide was taken up during the first hour by samples of the pyropolymers which had been heat-treated to a weight loss of 27-28%. On the other hand, only 8% herbicide uptake was shown with another sample of the pyropolymer which had been pyrolyzed to a weight loss of 18.2%. No adsorption was observed with the other samples. Furthermore, the pyropolymers adsorbed only the herbicide 2-*sec*-butyl-4,6-dinitrophenol and not 2,4-dichlorophenoxyacetic acid. This selective adsorptive capacity of the pyropolymers is unusual inasmuch as activated carbon does not show such property.<sup>1,2</sup> This great dependence of the adsorptive power of the pyropolymers on the extent of weight loss is most likely associated with the formation of a network structure with various degrees of "tightness," the presence of hetero atoms (Cl) and the surface areas.

TABLE I  
Adsorptive Capacity of Pyropolymers (Size 40/60) of Poly(vinyl Chloride)  
with Extent of Volatilization Using 2-*sec*-butyl-4,6-dinitrophenol

Volatilization, %	Adsorption		
	Extent, %	Adsorption time, hr	Initial concn, $\mu$ mole/l.
14.3	None		
18.2	8	5	46
27.4	30	1	71
28.4	30	1	71
33.3	None		
45.0	None		
50.0	None		
Columbia activated carbon (size 40/60)	8	1	60



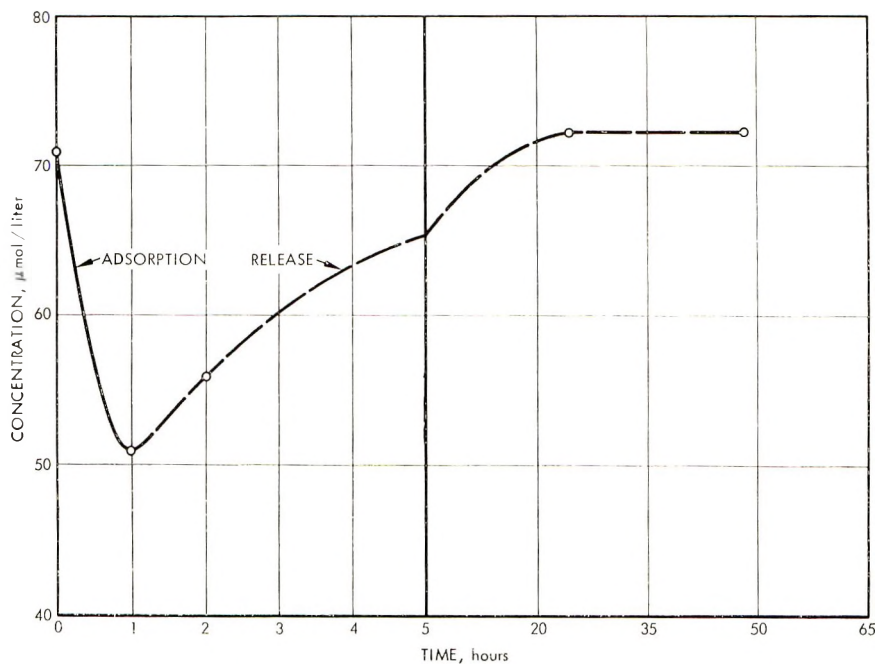


Fig. 2. Adsorption curve for 2-sec-butyl-4,6-dinitrophenol with 27.4% weight loss pyrolysis product of PVC.

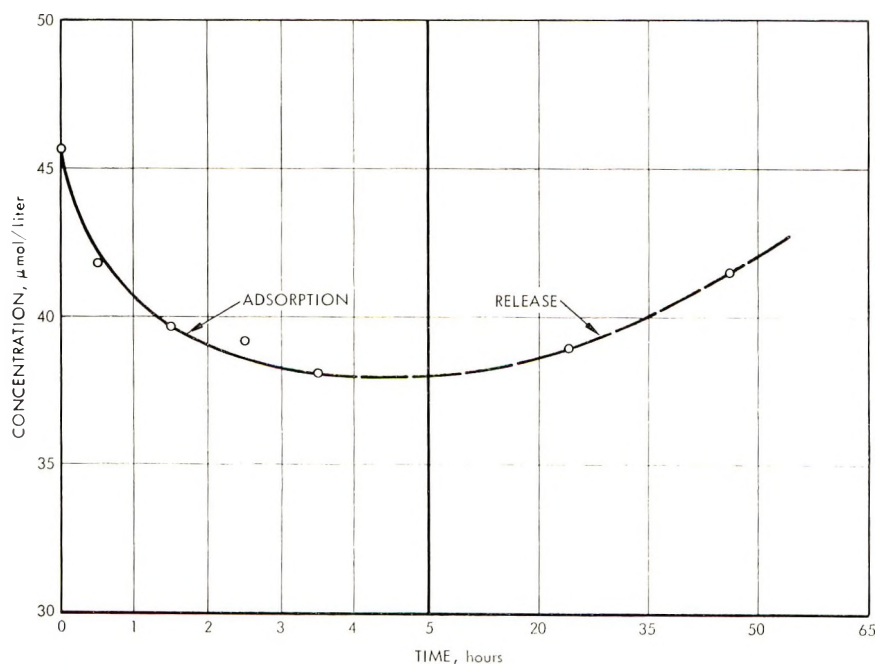


Fig. 3. Adsorption curve for 2-sec-butyl-4,6-dinitrophenol with 18.2% weight loss pyrolysis product of PVC.

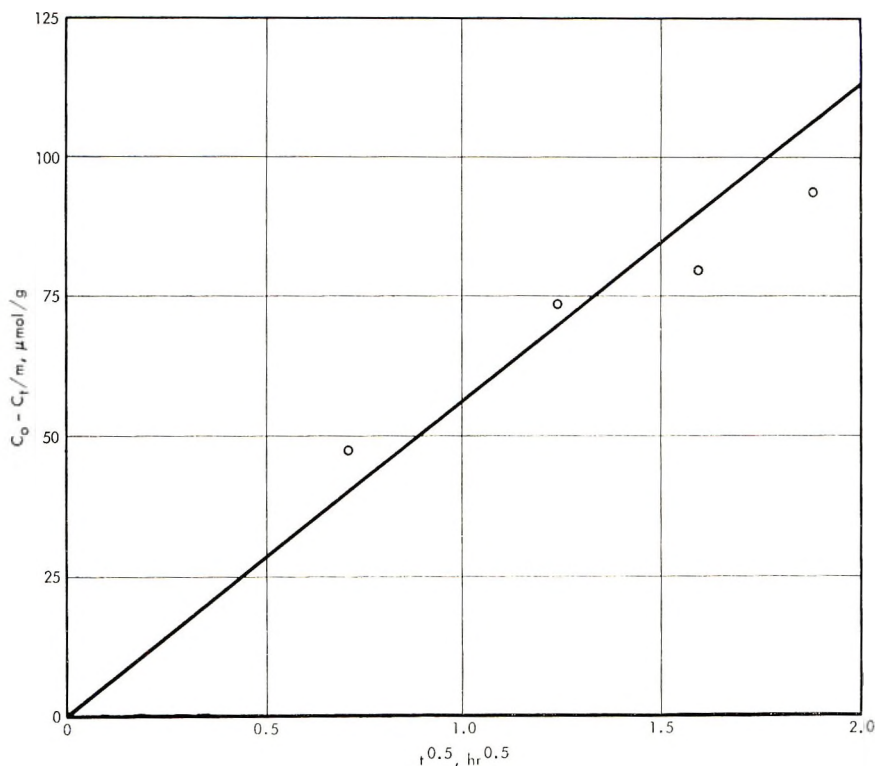


Fig. 4. Rate of adsorption of 2-*sec*-butyl-4,6-dinitrophenol on 18.2% weight loss pyrolysis product of PVC.

Figure 2 shows the adsorption curve for 2-*sec*-butyl-4,6-dinitrophenol with the pyropolymers of poly(vinyl chloride) which had been thermally degraded to a weight loss of 27.4%. An initial rapid decrease is observed in the concentration of the herbicide during the first hour. Then a gradual increase in the concentration follows. The total initial adsorption is approximately 30% and almost twice the initial rate of adsorption shown by Columbia activated carbon (particle size 40/60). A much smaller initial adsorption was observed with the pyropolymer of poly(vinyl chloride) that had been pyrolyzed to a weight loss of 18.2% as seen in Figures 3 and 4. The total adsorption after the first 5 hr was approximately 8%, followed by a gradual release of the herbicide.

Unlike the pyropolymers, activated carbon retains the adsorbent. The release of the herbicide by the pyropolymer after its initial adsorption might be due to a gradual displacement by water of the herbicide from the surface of the adsorbent.

The results underline the importance of the preparative conditions for the pyropolymers. Since very little information is known about the structure of these systems, much further work is needed (including surface area measurements) to elucidate more clearly the parameters involved in the adsorption process.

The pyropolymers prepared from poly[*N,N'*-(*p,p'*-oxydiphenylene)pyromellitimide] films (Kapton or H-film) showed no adsorptive properties toward either of the two herbicides. The pyropolymers were prepared in a vacuum and also in an oxygen/nitrogen atmosphere. The vacuum pyrolysis was carried out at 600°C ( $2 \times 10^{-5}$  mm Hg) for 2 hr to a total weight loss of 39%. The gaseous pyrolysis was first carried out in oxygen (353 ml/min.) at 450°C for 2 hr followed by further heat treatment in nitrogen (283

ml/min) at 450°C for 30 min to a total weight loss of 32.4%. The lack of adsorptive capacity of this pyropolymer is probably due not so much to its chemical structure but rather to a lack of porosity of the material (film). Present commercial preparative conditions require a two-step process which involves a diffusion controlled cyclization reaction after the precursor polyamic acid is cast as a film. The very smooth, with no apparent porosity, surface of this film is retained even after pyrolysis. Hence the lack of adsorption is likely to be associated with the surface properties of this polymer.

The author thanks the Dow Chemical Company for samples of the herbicides and for the poly(vinyl chloride) used in this work, and the duPont Company for samples of Kapton polyimide film. Thanks are also due to Dr. Leopold May and Dr. John B. Hunt, both of the Department of Chemistry, for permission to use their spectrophotometers. This work was supported by contract No. WP-01371-01A1, Department of the Interior, Federal Water Pollution Control Administration, Washington, D. C., with one of us (SDB) as the principal investigator.

### References

1. J. C. Morris and W. J. Weber, "Adsorption of Biochemically Resistant Materials from Solution. 1," AWTR-9, U. S. Department of Health, Education and Welfare, May 1964.
2. J. C. Morris and W. J. Weber, "Adsorption of Biochemically Resistant Materials from Solution. 2" AWTR-16, U. S. Department of Health, Education and Welfare, March 1966.
3. S. D. Bruck, *J. Chem. Ed.*, **42**, 18 (1965).
4. S. D. Bruck, *Polymer*, **6**, 46 (1965).
5. S. D. Bruck, *Polymer*, **5**, 435 (1964).
6. S. D. Bruck, *Polymer*, **6**, 319 (1965).
7. S. D. Bruck, in *Electrical Conduction Properties of Polymers (J. Polym. Sci. C, 17)*, A. Rembaum and R. F. Landel, Eds., Interscience, New York, **59**, 18 (1967).
8. S. D. Bruck, *Ind. Eng. Chem.*, **59**, 18 (1967).
9. *Chem. Eng. News*, **43**, 37 (July 26, 1965).

STEPHEN D. BRUCK\*  
PETER F. LIAO

Chemical Engineering Department  
The Catholic University of America  
Washington, D. C. 20017

Received July 10, 1969  
Revised August 11, 1969

\* Present address: Artificial Heart Program, National Heart and Lung Institute, National Institutes of Health, Bethesda, Maryland 20014.

## Cationic Graft Copolymerization of *N*-Vinylcarbazole onto Poly(vinyl Chloride)

### INTRODUCTION

Graft copolymerization onto polymers containing halogens takes place in only some cases.

For instance Plesch,<sup>1</sup> grafted styrene and indene by means of aluminum chloride (AlCl<sub>3</sub>) or titanium tetrachloride (TiCl<sub>4</sub>) onto PVC at 20–60°C. The solvents used were chlorobenzene and nitrobenzene. Minoura<sup>2</sup> grafted styrene onto chlorinated butyl rubber (chlorinated isoprene–isobutene copolymer) using SnCl<sub>4</sub> as catalyst.

Cationic graft copolymerization can be initiated by carbonium ions formed by reaction of Lewis acids (AlCl<sub>3</sub>, SnCl<sub>4</sub>, TiCl<sub>3</sub>, SbCl<sub>5</sub>) with a halogen contained in polymer.

If a monomer which can be polymerized by cationic mechanism is added to the medium in which these ions exist, a graft copolymer is obtained.

In this paper we report the graft copolymerization of *N*-vinylcarbazole (VCZ) onto poly(vinyl chloride) PVC in the presence of AlCl<sub>3</sub> at 20°C in nitrobenzene.

We studied the influence of catalyst concentration, of VCZ concentration, and PVC concentration on per cent grafting and grafting efficiency.

Grafting was confirmed by determination of nitrogen and infrared spectra.

### EXPERIMENTAL

#### Materials

The PVC used was dissolved in a 1:1 mixture of CS<sub>2</sub> and acetone, precipitated in methanol after removal of impurities, filtered, and well dried *in vacuo*. The intrinsic viscosity of PVC was determined with an Ubbelohde viscometer at 20°C in cyclohexanone and the molecular weight was calculated by the equations:<sup>3</sup>

$$\begin{aligned}\log M_n &= 2.10 + 1.30 \log [\eta] \\ [\eta] &= 1.136 \text{ dl/g} \\ M_v &= 50,000\end{aligned}$$

Nitrobenzene was washed well with water, separated, dried on CaCl<sub>2</sub>, distilled from P<sub>2</sub>O<sub>5</sub> at atmospheric pressure, then distilled from P<sub>2</sub>O<sub>5</sub> at reduced pressure in an inert atmosphere.

#### Polymerization

The dried PVC was dissolved completely in nitrobenzene. The solution of AlCl<sub>3</sub> in nitrobenzene was added to the PVC solution. The polymerization reaction was started by addition of a nitrobenzene solution of VCZ. The polymerization was carried out at 20°C. After 2 hr the reaction mixture was precipitated with methanol. The polymer was washed with methanol and water, filtered and extracted with boiling methanol for elimination of VCZ.

The polymer was dried *in vacuo* (35–40°C, 6–7 hr) to constant weight. The conversion of VCZ was calculated from increase in weight after drying.

The extraction of homopolyvinylcarbazole was carried out with boiling benzene (7 hr) and the insoluble portion after extraction was dried *in vacuo* (50–60°C and 6–7 hr).

Then, per cent grafting and grafting efficiency were determined. The per cent grafting is the ratio of the increase in weight of the benzene-insoluble fraction to the weight of PVC used, namely, the ratio of grafted VCZ to the PVC used.

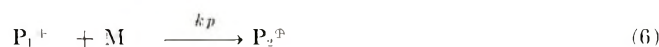
The grafting efficiency is the ratio of grafted VCZ to the total VCZ polymerized.

The viscosity of the graft copolymers was determined with an Ubbelohde viscometer at 20°C in cyclohexanone. The intrinsic viscosity was calculated by the equation:<sup>4</sup>

$$[\eta] = (\sqrt{2/c})\sqrt{\eta_{sp} - \ln \eta_{rel}}$$

## RESULTS AND DISCUSSIONS

For cationic graft copolymerization the mechanism proposed by Minoura<sup>2</sup> considered applicable:



where RCl denotes PVC; M is VCZ.

In the presence of traces of water in the reaction system, the catalyst gives two parallel reactions, (1) and (2), which determine the formation of polymerization centers.

In the first reaction a graft copolymer is obtained, and in the second one a homopolymer is obtained.

### INFLUENCE OF $\text{AlCl}_3$ CONCENTRATION ON PER CENT AND GRAFTING EFFICIENCY

The polymerization was carried at various  $\text{AlCl}_3$  concentrations. Results are shown in Table I and Figure 1.

At small concentrations of  $\text{AlCl}_3$ , graft copolymer cannot be obtained. The second reaction (2) has a much greater rate. The small slope of the curve (Fig. 1) at small concentrations of  $\text{AlCl}_3$  proves this fact (The conditions do not exclude the presence of water in the reaction system).

The increase in the slope at an  $\text{AlCl}_3$  concentration of about  $8 \times 10^{-2}$  mole/l. shows that at this point water reacted entirely with  $\text{AlCl}_3$  and any excess catalyst produces active centers on the PVC according to eq. (1).

The graft copolymerization occurred at over  $1.89 \times 10^{-2}$  mole  $\text{AlCl}_3$ /l. because the product obtained was not soluble in nitrobenzene or cyclohexanone and it could not be analyzed.

The results of viscosity of graft copolymers are also shown in Table I. An increase of intrinsic viscosity of graft copolymers was observed with the increase of catalyst concentration.

### INFLUENCE OF VCZ CONCENTRATION ON PER CENT GRAFTING AND GRAFTING EFFICIENCY

At constant  $\text{AlCl}_3$  and PVC concentrations, the graft copolymerization was carried out at various concentrations of VCZ. The results are shown in Table II and Figure 2.

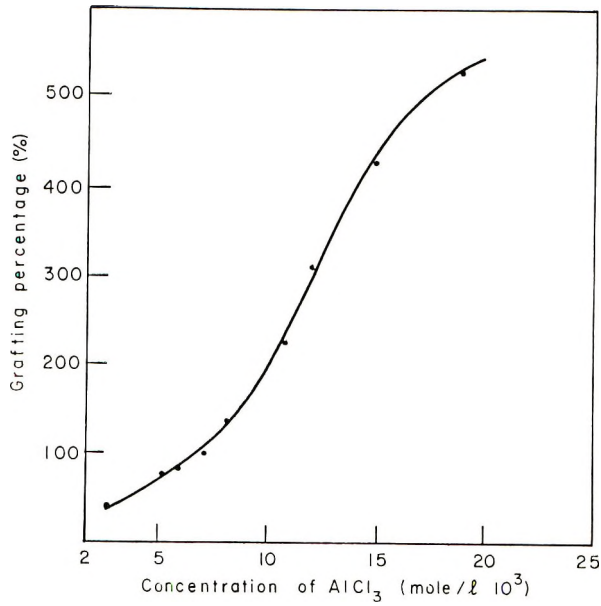


Fig. 1. Influence of  $\text{AlCl}_3$  concentration on per cent grafting.

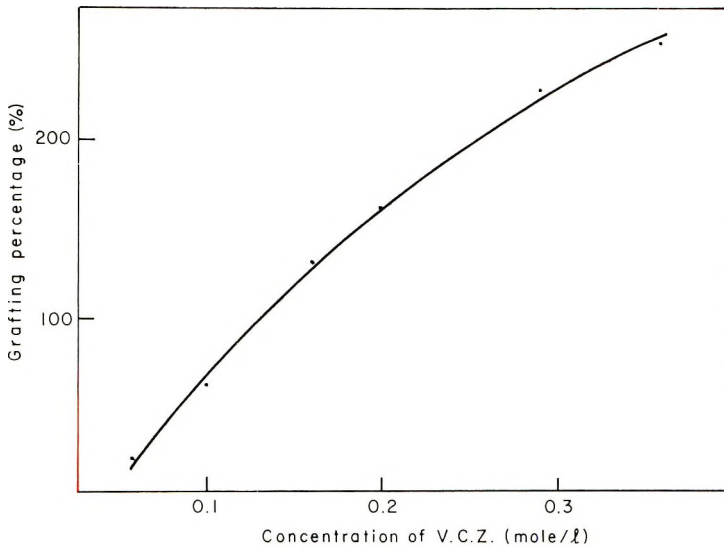


Fig. 2. Influence of VCZ concentration on per cent grafting.

Per cent grafting increases with VCZ concentration. The grafting efficiency increases with VCZ concentration up to a certain limit and then decreases.

#### INFLUENCE OF PVC CONCENTRATION ON PER CENT GRAFTING

At constant  $\text{AlCl}_3$  and VCZ concentrations, the graft copolymerization was carried out at various concentrations of PVC.

TABLE I  
Influence of  $\text{AlCl}_3$  Concentration on Per Cent Grafting and Grafting Efficiency

Expt. no.	$[\text{AlK}_3]$ , mole/l.	$[\text{PVC}]$ , g/l.	$[\text{VCZ}]$ , mole/l.	$\text{AlCl}_3/\text{PVC}$ , mole/mole	Overall yield, g/l.	Graft copolymer g/l.	Homo-polymer, g/l.	Grafting, %	Grafting efficiency, %	Content of nitrogen, %	$[\eta]$ dl/g
1	$2.96 \times 10^{-3}$	2.516	0.16	$7.29 \times 10^{-2}$	30.56	3.472	27.08	38	3.3	2	1.20
2	$5.57 \times 10^{-3}$	2.516	0.16	$1.37 \times 10^{-1}$	30.53	4.34	26.19	73.5	6.5	3.07	1.25
3	$6.17 \times 10^{-3}$	2.516	0.16	$1.52 \times 10^{-1}$	31.4	4.53	26.87	80	7	3.2	1.30
4	$7.34 \times 10^{-3}$	2.516	0.16	$1.81 \times 10^{-1}$	31.6	4.99	26.61	98.5	8.5	3.2	1.30
5	$8.52 \times 10^{-3}$	2.516	0.16	$2.1 \times 10^{-1}$	32.44	5.87	26.57	133	11.5	3.8	1.37
6	$1.1 \times 10^{-2}$	2.516	0.16	$2.71 \times 10^{-1}$	32.6	8.136	25.24	223	18.2	4.5	1.40
7	$1.22 \times 10^{-2}$	2.516	0.16	$3 \times 10^{-1}$	33	10.26	22.74	308	25.7	5	1.43
8	$1.5 \times 10^{-2}$	2.516	0.16	$3.7 \times 10^{-1}$	33	12.34	20.66	431	32.8	5.5	1.46
9	$1.89 \times 10^{-2}$	2.516	0.16	$4.66 \times 10^{-1}$	33	16.06	16.96	573	44.5	5.8	1.49
10 <sup>a</sup>	$2.23 \times 10^{-2}$	2.516	0.16	$5.5 \times 10^{-1}$	33.2	33.2	—	—	—	—	—

<sup>a</sup> The graft copolymer obtained was insoluble in cyclohexanone and nitrobenzene.

TABLE II  
Influence of VCZ Concentration on Per Cent Grafting and Grafting Efficiency

Expt. no.	[VCZ], mole/l.	[PVC], g/l.	[AlCl <sub>3</sub> ], mole/l.	AlCl <sub>3</sub> /PVC mole/mole	Overall yield, g/l.	Graft copolymer, g/l.	Homopolymer, g/l.	(Grafting, %)	Grafting efficiency, %
1	$5.68 \times 10^{-2}$	2.516	$8.52 \times 10^{-3}$	$2.1 \times 10^{-1}$	11.482	3.07	8.412	22	5.1
2	$9.94 \times 10^{-2}$	2.516	$8.52 \times 10^{-3}$	$2.1 \times 10^{-1}$	19.952	4.556	15.4	61	10.6
3	$1.59 \times 10^{-1}$	2.516	$8.52 \times 10^{-3}$	$2.1 \times 10^{-1}$	31.8	5.87	25.93	13	10.95
4	$1.99 \times 10^{-1}$	2.516	$8.52 \times 10^{-3}$	$2.1 \times 10^{-1}$	39.95	6.29	33.66	161	9.85
5	$2.9 \times 10^{-1}$	2.516	$8.52 \times 10^{-3}$	$2.1 \times 10^{-1}$	59.25	6.89	52.35	230	7.64
6	$3.6 \times 10^{-1}$	2.516	$8.52 \times 10^{-3}$	$2.1 \times 10^{-1}$	71.56	7.23	64.32	254	6.8

TABLE III  
Influence of PVC Concentration on Per Cent Grafting

Expt. no.	[PVC], mole/l.	[PVC], g/l.	AlCl <sub>3</sub> , mole/l.	AlCl <sub>3</sub> /PVC mole/mole	[VCZ], mole/l.	Overall yield, g/l.	Graft copolymer, g/l.	Homopolymer, g/l.	Grafting, %
1	$4.06 \times 10^{-2}$	2.516	$8.52 \times 10^{-3}$	$2.13 \times 10^{-1}$	$1.59 \times 10^{-1}$	31.8	5.87	25.93	133
2	$8.1 \times 10^{-2}$	5.06	$8.52 \times 10^{-3}$	$1.05 \times 10^{-1}$	$1.59 \times 10^{-1}$	34.9	11.89	23.01	135
3	$1.7 \times 10^{-1}$	10.45	$8.52 \times 10^{-3}$	$5.02 \times 10^{-1}$	$1.59 \times 10^{-1}$	40.1	24.45	15.65	134



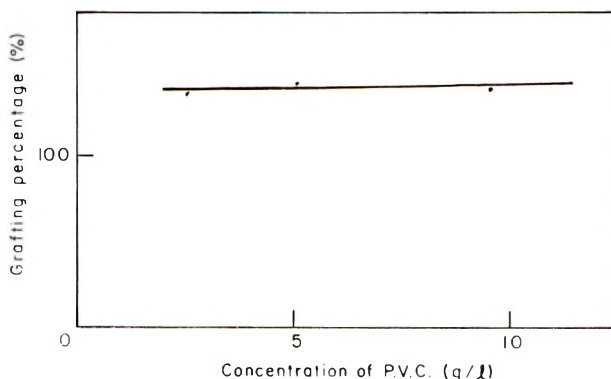


Fig. 3. Influence of PVC concentration on per cent grafting.

Results are shown in Table III and Figure 3. We observe that per cent grafting does not depend on PVC concentration since PVC and grafted polyvinylcarbazole increase at the same ratio and the grafting percentage remains at about same value.

Grafting efficiency increases with increasing PVC concentration.

The presence of PVC in the graft copolymer is verified by the determination of nitrogen in the graft copolymer (Table I). The per cent grafting was calculated gravimetrically. The per cent grafting calculated from nitrogen analysis agrees well with the value obtained gravimetrically.

#### References

1. P. H. Plesch, *Chem. Ind. (London)*, **1958**, 954.
2. Y. Minoura, T. Hanada, T. Kasabo, and Y. Uemo, *J. Polym. Sci. A-1*, **4**, 1665 (1966).
3. F. Danusso and G. Perugini, *Chim. Ind. (Milan)*, **35**, 881 (1953).
4. O. F. Solomon and I. Ciutã, *J. Appl. Polym. Sci.*, **6**, 683 (1962).

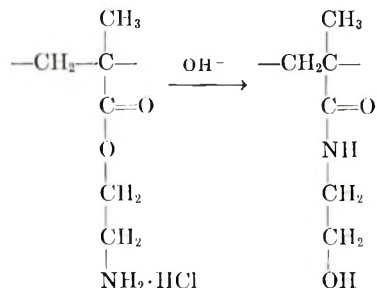
O. F. SOLOMON  
M. DIMONIE  
C. CIUCIU

Laboratory of Macromolecular Chemistry  
Polytechnic Institute  
Bucharest, Romania

Received November 25, 1968

### *Anomalous Behavior of a Polymeric Amino Ester*

Polymers containing primary amine have always been difficultly accessible, usually requiring the removal of a blocking group after the polymerization step.<sup>1,2</sup> The direct synthesis<sup>3</sup> of 2-aminoethyl methacrylate hydrochloride (I) has now made such polymers easily obtainable. In our work with polymers and copolymers of I we expected that the amine would exist only in the salt form and that deprotonation would rapidly



give the classical  $\text{O} \rightarrow \text{N}$  acyl migration. The unexpected observation that solutions of poly I still could be gelled by formaldehyde, even after days of keeping at high pH, prompted an investigation of the rearrangement reaction. Solutions of poly I and of two model compounds, 2-aminoethyl isobutyrate hydrochloride (II) and 2-aminoethyl pivalate hydrochloride (III), were treated with one equivalent of base and titrated for amine at intervals. The two models showed rapid loss of amine, whereas poly I was virtually unchanged after days.

A model of a segment of the polymer chain indicates that the degree of hindrance is greater than in the model compounds but not sufficient to prohibit the approach of amine to carbonyl. Therefore, a more important factor may be dipole-dipole interaction or hydrogen bonding between amine and its neighboring ester group, preventing formation of the cyclic intermediate.

## EXPERIMENTAL

### 2-Aminoethyl Methacrylate Hydrochloride(I)

This compound was prepared by the method of Rusting et al.<sup>3</sup> It was found advantageous to prepare and isolate ethanolamine hydrochloride before the acylation with methacryloyl chloride. The product could be recrystallized from hot acetonitrile, mp 115–117.5°C. Treatment of an aqueous solution of the monomer with Florasil removed inhibitors which were otherwise difficult to eliminate by recrystallization.

### 2-Aminoethyl Isobutyrate Hydrochloride and 2-Aminoethyl Pivalate Hydrochloride

These compounds were prepared as above; melting points were 119–121 and 192–195°C, respectively.

ANAL. Calcd for  $\text{C}_6\text{H}_{14}\text{ClNO}_2$  (167.64): C, 42.9%; H, 8.4%; N, 8.4%; Cl, 21.2%. Found: C, 42.8%; H, 8.4%; N, 8.5%; Cl, 21.4%.

ANAL. Calcd for  $\text{C}_7\text{H}_{16}\text{ClNO}_2$  (181.66): C, 46.2%; H, 8.18%; N, 7.7%; Cl, 19.5%. Found: C, 46.4%; H, 8.7%; N, 7.6%; Cl, 19.4%.

### Poly(2-aminoethyl Methacrylate Hydrochloride)

A solution of 5.0 g of I in 20 ml. of distilled water was purged with nitrogen, then heated at 60°C overnight with 0.025 g of potassium persulfate. The polymer was iso-

lated by precipitation in acetone and dried *in vacuo*. The intrinsic viscosity measured at 25°C in 0.5*M* sodium chloride was 0.11.

ANAL. Calcd for  $C_6H_{12}ClNO_2$  (165.63): N, 8.5%; Cl, 21.5%. Found: N, 8.1%; Cl, 19.9%.

### Rearrangements

Weighed samples of polymers and model compounds were dissolved in water and quickly neutralized to an endpoint with sodium hydroxide. Aliquots were removed at intervals and titrated for free amine with hydrochloric acid. In the case of the isobutyrate model the reaction was too fast for convenience, and samples were individually weighed, neutralized, and titrated. Table I summarizes the results of these experiments.

TABLE I

Sample	Amine remaining, %			
	After 5 min	After 13 min	After 1 day	After 3 days
Poly I	—	99.7	100	97.6
Compound II	33.0	20.0	0	
Compound III	45.3	3.6	0	

Several copolymers of I with acrylic acid were prepared and submitted to the same evaluation. The same retention of structure was observed as for poly I.

### References

1. D. D. Reynolds and W. O. Kenyon, *J. Amer. Chem. Soc.*, **69**, 911 (1947).
2. R. Hart, *Makromol. Chem.*, **32**, 51 (1959).
3. N. Rusting, G. G. Friebink, and G. F. VanderBeek, Dutch Pat. Appl. 6413809 (November 27, <sup>1</sup>1964).

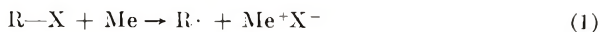
DONALD A. SMITH  
ROBERT H. CUNNINGHAM  
BARBARA COULTER

Research Laboratories  
Eastman Kodak Company  
Rochester, New York 14650

Received July 22, 1969  
Revised September 15, 1969

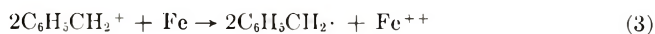
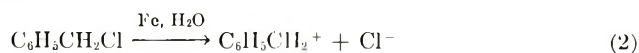
**Metal-Containing Initiator Systems. XXIII. Effect of Solvents on Radical Polymerization of Methyl Methacrylate Initiated by Metal-Alkyl Halide Systems**

It is known that various systems consisting of activated metals and organic halides can act as radical initiators of vinyl polymerizations, in which the initiating radicals are formed by an one-electron transfer reaction from halides to metals [eq. (1)].<sup>1-6</sup>



Recently we also found that the systems of reduced nickel and alkyl<sup>6</sup> or silyl<sup>7</sup> chlorides behave as selective initiators; they can initiate both radical and cationic polymerizations of vinyl monomers.

Sisido et al.<sup>8,9</sup> stated that the reaction of metallic iron with benzyl chloride in water proceeded as shown in eqs. (2)-(4)



If a radical intermediate is produced through these steps from the metal-alkyl halide systems, the ability of the systems to function as selective initiators may be understandable. The present report deals with effects of the solvent in the radical polymerization of methyl methacrylate (MMA) with systems of metals and alkyl halides in order to elucidate the initiation mechanism.

### EXPERIMENTAL

The monomer, solvents, and alkyl halides were carefully distilled prior to use. The reduced nickel composed of 50% nickel atom on kieselguhl (Nikki Chemical Co.) was used after activation treatment.<sup>5</sup> Other metals were obtained commercially and used without further treatment. The polymerization procedures were the same as described in the previous paper.<sup>5</sup>

The formation of Ni<sup>++</sup> ion from the reduced nickel-alkyl chloride systems was determined quantitatively by using dimethylglyoxime.

### RESULTS AND DISCUSSION

Table I shows the results of the MMA polymerization with the systems of various metals and ethyl bromide in solvents with different polarity. As reported previously,<sup>3</sup> commercial metals had no activity for initiation in benzene. However, in dimethylformamide (DMF) and dimethyl sulfoxide (DMSO), polymer was obtained even with the use of the commercial metals. When azobisisobutyronitrile (AIBN) was used as an initiator, the polymer yield varied slightly with the solvent used, as is shown in Table I. Therefore, it is obvious that the MMA polymerization with the metal-alkyl halide systems is influenced by the kind of the solvent used; the polymer yield increases with an increase of the solvent polarity, except for the case of acetonitrile.

When *tert*-butyl chloride, benzyl chloride, and carbon tetrachloride were used as halide components in the presence of reduced nickel, the polymerization was also influenced by solvents (Table II). The polymer yield was found to increase with the alkyl halides<sup>3</sup> in the order, C<sub>2</sub>H<sub>5</sub>Br < *tert*-C<sub>4</sub>H<sub>9</sub>Cl < C<sub>6</sub>H<sub>5</sub>CH<sub>2</sub>Cl < CCl<sub>4</sub>, with solvents in the order C<sub>6</sub>H<sub>6</sub> < DMF < DMSO. However, when *tert*-butyl chloride was used in DMSO, the polymer yield was abnormally low.

The effect of water on the polymerization in DMF was investigated. As is also shown in Table II, the polymer yield was not changed by addition of water. This

TABLE I  
 Polymer Yield in the MMA Polymerization with Various Metal-Ethyl Bromide Systems in Solvents of Different Polarity<sup>a</sup>

Solvent	Dielectric constant, $\epsilon$	Metal					AIBN <sup>d</sup>
		Reduced Ni <sup>b</sup>	Ni	Co	Cu	Mg <sup>c</sup>	
C <sub>6</sub> H <sub>6</sub>	2.3 (20°C)	6.4	0	0	0	0	20.7
CH <sub>3</sub> COOC <sub>2</sub> H <sub>5</sub>	6.0 (25°C)	9.7	0	0	0	2.1	19.5
DMF	36.7 (25°C)	14.5	3.9	2.1	0	12.1	23.8
CH <sub>3</sub> CN	37.5 (20°C)	1.8	0.6	0	0	1.5	19.3
DMSO	45 (20°C)	19.0	12.0	2.0	2.3	16.3	24.1

<sup>a</sup> MMA, 5 ml; solvent, 5 ml; metal, 0.2 g; C<sub>2</sub>H<sub>5</sub>Br, 0.15 ml; polymerization temperature 60°C; time, 6 hr.

<sup>b</sup> Reduced nickel, 0.1 g, was used.

<sup>c</sup> Mg shaving, 0.05 g, and C<sub>6</sub>H<sub>5</sub>CH<sub>2</sub>Br, 0.13 ml, were used.

<sup>d</sup> AIBN, 0.01 g, was used, and the polymerization was carried out for 2.5 hr.

TABLE II  
Effect of Solvent on the MMA Polymerization with  
Reduced Nickel and Alkyl Halide Systems at 60°C<sup>a</sup>

Alkyl halide	Time, hr.	Polymer yield, %			
		In C <sub>6</sub> H <sub>6</sub>	In DMF	In	
				DMF-H <sub>2</sub> O <sup>b</sup>	In DMSO
C <sub>2</sub> H <sub>5</sub> Br	6	6.4	14.5	15.1	19.0
<i>tert</i> -C <sub>4</sub> H <sub>9</sub> Cl	2	7.1	11.3	—	2.8
C <sub>6</sub> H <sub>5</sub> CH <sub>2</sub> Cl	1	9.0	12.0	12.4	18.5
CCl <sub>4</sub>	1	16.3	32.7	32.1	33.6

<sup>a</sup> MMA, 5 ml; solvent, 5 ml; reduced nickel, 0.1 g; alkyl halide, 0.15 ml.

<sup>b</sup> DMF/H<sub>2</sub>O, 96/4, v/v.

TABLE III  
Formation of Ni<sup>++</sup> Ion from the Reduced  
Nickel-Alkyl Halides Systems at 60°C (%)<sup>a</sup>

Alkyl halide	Ni <sup>++</sup> , %			
	C <sub>6</sub> H <sub>6</sub>	DMF	DMSO	CH <sub>3</sub> CN
<i>tert</i> -C <sub>4</sub> H <sub>9</sub> Cl	26.2	0.6	1.0	0.5
C <sub>6</sub> H <sub>5</sub> CH <sub>2</sub> Cl	22.4	2.2	2.8	6.1
CCl <sub>4</sub>	2.7	18.1	9.1	10.6

<sup>a</sup> Halide, 2 ml; reduced nickel, 0.5 g; solvent, 8 ml; time, 1 hr.

agreed with the results of the MMA polymerization with the system metallic tin-benzyl chloride in toluene,<sup>10</sup> contrary to the results of Sisido et al.<sup>9</sup>

Table III shows the amounts of Ni<sup>++</sup> ion produced from these initiator systems according to eq. (1) as a measure of the radical formation. In DMF, DMSO, and acetonitrile, the amount of Ni<sup>++</sup> ion produced was found to increase with the kind of alkyl halide in the order: *tert*-C<sub>4</sub>H<sub>9</sub>Cl < C<sub>6</sub>H<sub>5</sub>CH<sub>2</sub>Cl < CCl<sub>4</sub>.

This order agreed with that of the polymer yield mentioned above. However, in benzene, *tert*-butyl chloride and benzyl chlorides gave larger amounts of Ni<sup>++</sup> ion than in carbon tetrachloride. This might be explained by a side reaction, i.e., a Friedel-Crafts reaction between the chlorides and benzene catalyzed by nickel chloride produced according to eq. (1). A detailed investigation of this point will be described elsewhere.

The pronounced effect of solvents on Ni<sup>++</sup> ion formation was obvious from the results with carbon tetrachloride; a difference in the amount of Ni<sup>++</sup> ion produced was observed between benzene and other polar solvents. Thus, the results of Tables I and II may be explained from the difference in rate of radical formation of the various alkyl halides according to eq. (1). However, the low yield of the polymer obtained in acetonitrile can not be explained at the present time.

#### References

1. G. Henrici-Olivé and S. Olivé, *Makromol. Chem.*, **88**, 117 (1965).
2. S. Iwatsuki, H. Kasahara, and Y. Yamashita, *Makromol. Chem.*, **104**, 254 (1967).
3. T. Otsu, M. Yamaguchi, Y. Takemura, Y. Kusuki, and S. Aoki, *J. Polym. Sci. B*, **5**, 697 (1967).
4. T. Otsu, S. Aoki, M. Nishimura, M. Yamaguchi, and Y. Kusuki, *J. Polym. Sci. B*, **5**, 835 (1967).
5. T. Otsu and M. Yamaguchi, *J. Polym. Sci. A-1*, **6**, 3075 (1968).

6. S. Aoki, C. Shirafuji, and T. Otsu, paper presented at the 17th Annual Meeting of the Society of Polymer Science of Japan, Tokyo, May 1968.

7. T. Otsu, S. Aoki, M. Nishimura, M. Yamaguchi, and Y. Kusuki, *J. Polym. Sci. A-1*, in press.

8. K. Sisido, Y. Udo, and H. Nozaki, *J. Amer. Chem. Soc.*, **82**, 434 (1960).

9. K. Sisido, Y. Takeda, and Z. Kinugawa, *J. Amer. Chem. Soc.*, **83**, 438 (1961).

10. S. Aoki, C. Shirafuji, Y. Kusuki, and T. Otsu, *Makromol. Chem.*, **126**, 8 (1969).

SHUZO AOKI  
AKIRA AKIMOTO  
CHIYAKI SHIRAFUJI  
TAKAYUKI OTSU

Department of Applied Chemistry  
Faculty of Engineering  
Osaka City University  
Sumiyoshi-ku, Osaka, Japan

Received June 17, 1969

Revised September 15, 1969

### Polymerizations of *N*-Vinylcarbazole and 4-Vinylpyridine with Various Organic Halides

It has been reported that *N*-vinylcarbazole (NVC) is polymerized with carbon tetrachloride<sup>1,2</sup> and 4-vinylpyridine (4-VP) undergoes polymerization in the presence of some alkylating agents such as methyl iodide,<sup>3</sup> dimethyl sulfate,<sup>4</sup> methyl *p*-toluenesulfonate.<sup>4</sup>

In the previous paper,<sup>5,6</sup> we found that the polymerization of methyl methacrylate is induced with the binary systems of *tert*-amines such as dimethylaniline and some organic halides. When NVC was used as amine component and benzenesulfonyl chloride as halide component, a homopolymer of NVC was obtained; this suggested that this polymerization might proceed via a cationic mechanism.<sup>6</sup> To clarify this point further, the present paper will describe the results of the polymerizations of NVC and 4-VP with various organic halides.

#### EXPERIMENTAL

##### Materials

NVC was recrystallized from *n*-hexane; mp 65°C. 4-VP was purified by fractional distillation and redistilled in a stream of nitrogen prior to use, bp 65°C/15 mm Hg.

Organic halides were used after distillation of the reagent-grade materials before use.

##### Polymerization

Polymerizations and copolymerizations were carried out with shaking in a sealed glass tube without diffused light. After polymerization for a given time, the contents of the tube were poured into a large amount of precipitant (methanol for NVC and diethyl ether for 4-VP).

#### RESULTS AND DISCUSSION

##### Polymerization of NVC

Table I shows the results of the polymerization of NVC in the presence of various organic halides in benzene at 60°C. From this table, C<sub>6</sub>H<sub>5</sub>PCl<sub>2</sub>, CHBr<sub>3</sub>, *t*-BuOCl, and C<sub>6</sub>H<sub>5</sub>SO<sub>2</sub>Cl in the halides used were found to show excellent polymerization activity. An

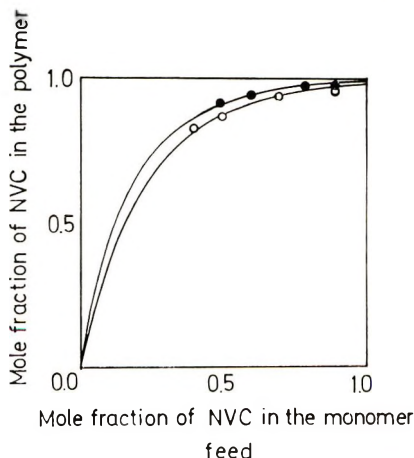


Fig. 1. Monomer-copolymer composition curves for the copolymerizations of NVC with styrene and MMA initiated by benzyl bromide at 30°C: (○) NVC-styrene; (●) NVC-MMA. The lines indicate those calculated from the reported  $r_1$ ,  $r_2$  values (Table II). [Total monomers] = 1 mole/l., [C<sub>6</sub>H<sub>5</sub>CH<sub>2</sub>Br] = 0.1 mole/l.



TABLE I  
Effects of Organic Halides on the Polymerizations of  
*N*-Vinylcarbazole (NVC) and 4-Vinylpyridine (4-VP) at 60°C<sup>a</sup>

Organic halide	NVC		4-VP	
	Conversion, %	Color in polymerization system	Conversion, %	Color in polymerization system
C <sub>6</sub> H <sub>5</sub> PCl <sub>2</sub>	83.8	Brown-black	45.2	Orange
CHBr <sub>3</sub>	43.3	Yellowish brown	3.6	Pale orange
<i>t</i> -C <sub>4</sub> H <sub>9</sub> OCl	31.4	"	7.0	Black
C <sub>6</sub> H <sub>5</sub> SO <sub>2</sub> Cl	23.3	Colorless	43.5	Brown
C <sub>6</sub> H <sub>5</sub> COCl	9.6	"	68.3	Yellow
<i>t</i> -C <sub>4</sub> H <sub>9</sub> Cl	7.4	"	Trace	Colorless
C <sub>6</sub> H <sub>5</sub> CH <sub>2</sub> Cl	6.4	"	10.9	Pale yellow
C <sub>6</sub> H <sub>5</sub> CH <sub>2</sub> Br	2.6	"	27.1	Orange
<i>n</i> -C <sub>4</sub> H <sub>9</sub> NCl <sub>2</sub>	1.9	Yellowish brown	21.8	Yellowish brown
CHCl <sub>3</sub>	1.8	Colorless	Trace	Colorless
CCl <sub>4</sub>	0.6	"	5.4	"
CH <sub>2</sub> Cl <sub>2</sub>	Trace	"	Trace	"
C <sub>6</sub> H <sub>5</sub> Cl	"	"	"	"
CH <sub>2</sub> =CHCH <sub>2</sub> Cl	"	"	3.4	Pale orange
<i>n</i> -C <sub>4</sub> H <sub>9</sub> Cl	"	"	Trace	Colorless
( <i>n</i> -C <sub>4</sub> H <sub>9</sub> ) <sub>2</sub> NCl	"	"	6.3	Yellowish brown
None	0	"	0	Colorless

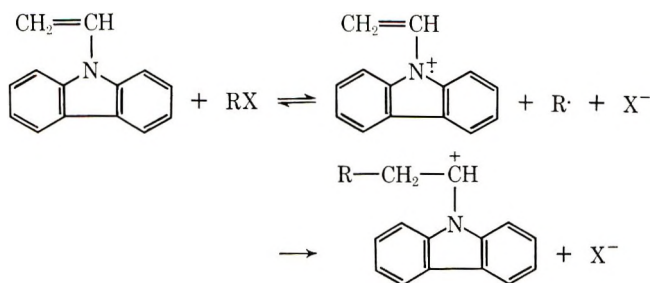
<sup>a</sup> [NVC] = 0.863 mole/l., [Halide] = 0.0863 mole/l.; [4-VP] = 3.17 mole/l., [Halide] = 0.317 mole/l. in benzene; 12 hr.

TABLE II  
Monomer Reactivity Ratios for the Copolymerizations  
of NVC (M<sub>1</sub>) with Styrene and Methyl Methacrylate (MMA)(M<sub>2</sub>)

M <sub>2</sub>	r <sub>1</sub>	r <sub>2</sub>	
Styrene	9.0	0.2	Present work
	0.012	5.5	Radical copolymerization <sup>7</sup>
	> 7	0.01	Cationic copolymerization <sup>8</sup>
MMA	> 10	0.15	Present work
	0.04	2.0	Radical copolymerization <sup>7</sup>

approximate correlation was found between the polymerization activity and the coloration of the polymerizing mixture. The polymer obtained with C<sub>6</sub>H<sub>5</sub>CH<sub>2</sub>Br contained 7.07% N, which was in agreement with that calculated for the polymer of NVC (7.25%).

To clarify the mechanism of these polymerizations, the copolymerizations of NVC (M<sub>1</sub>) with styrene and methyl methacrylate (M<sub>2</sub>) were carried out with C<sub>6</sub>H<sub>5</sub>CH<sub>2</sub>Br in benzene at 35°C. Figure 1 shows the monomer-copolymer composition curves, and the resulting monomer reactivity ratios are shown in Table II. From this table, it may be seen that the copolymerizations with C<sub>6</sub>H<sub>5</sub>CH<sub>2</sub>Br proceed via a cationic mechanism. A similar cationic mechanism was pointed out in the polymerizations of NVC with various electron acceptors<sup>9,10</sup> such as maleic anhydride, acrylonitrile, and chlorine, and with some metal salts,<sup>11,12</sup> such as Cu<sup>II</sup>, Fe<sup>III</sup>, Ce<sup>IV</sup>, and Au<sup>III</sup> salts. The reaction was also similar to the cationic polymerization of butadiene with various halides, including CCl<sub>4</sub>, C<sub>6</sub>H<sub>5</sub>CH<sub>2</sub>Br, C<sub>6</sub>H<sub>5</sub>COCl and *t*-C<sub>4</sub>H<sub>9</sub>OCl in the presence of reduced nickel.<sup>13</sup> Accordingly, the cationic polymerization of NVC with alkyl halide (RX) seems to occur by way of an intermediate NVC cation radical produced by a charge-transfer interaction.



Since NVC cation radical and R radical are produced in the initial stage of reaction, the radical polymerization of NVC would be expected to occur. However, the reactivity of the NVC monomer is much higher toward the cation than the radical (see Table II) and hence cationic polymerization may predominate.

#### Polymerization of 4-VP

The results of the polymerization of 4-VP with various organic halides are also shown in Table I. The initiating activity of halide was approximately the same as that for the NVC polymerization. However, marked coloration during polymerization was characteristic when the efficient halides were used. In these cases, the quaternary reaction was expected to occur rapidly. Actually the resulting polymers were very hygroscopic products, and the content of nitrogen in the polymer obtained with  $\text{C}_6\text{H}_5\text{CH}_2\text{Br}$  was 5.38%, indicating that this polymer contains some 4-vinylbenzylpyridinium bromide units. Accordingly, it might be assumed that this polymerization was initiated by a quaternary 4-vinylpyridinium salt, proposed by Kabanov et al.<sup>4</sup>

#### References

1. A. Chapiro and G. Hardy, *J. Chim. Phys.*, **59**, 993 (1962).
2. J. W. Breitenbach and Ch. Srna, *J. Polym. Sci. B*, **1**, 263 (1963).
3. S. Iwatsuki, T. Kokubo, K. Motomatsu, M. Tsuji, and Y. Yamashita, *Makromol. Chem.*, **120**, 154 (1968).
4. V. A. Kabanov, K. V. Aliev, and V. A. Kargin, *Vysokomol. Soedin.*, **A10**, 1618 (1968).
5. T. Otsu, T. Sato, and M. Ko, *J. Polym. Sci. A-1*, in press.
6. T. Otsu, S. Aoki, and K. Itakura, *J. Polym. Sci. A-1*, in press.
7. R. Hart, *Makromol. Chem.*, **47**, 143 (1961).
8. T. Tazuke and S. Okamura, *J. Polym. Sci. B*, **3**, 923 (1965).
9. K. Takakura, E. Kawa, K. Hayashi, and S. Okamura, *Ann. Rept. Rad. Inst. Osaka*, **6**, 205 (1964-5).
10. K. Tsuji, K. Takakura, M. Nishii, K. Hayashi, and S. Okamura, *Ann. Rept. Rad. Inst. Osaka*, **6**, 176 (1964-5).
11. S. Tazuke, T. B. Tjoa, and S. Okamura, *J. Polym. Sci. A-1*, **5**, 1911 (1967).
12. S. Tazuke, M. Asai, and S. Okamura, *J. Polym. Sci. A-1*, **6**, 1809 (1968).
13. T. Otsu and M. Yamaguchi, *J. Polym. Sci. A-1*, **7**, 387 (1969).

TAKAYUKI OTSU  
MUNAN KO  
TSUNEYUKI SATO

Department of Applied Chemistry  
Faculty of Engineering  
Osaka City University  
Sumiyoshi-ku, Osaka, Japan

Received July 14, 1969  
Revised September 20, 1969

**Mass Spectral Characteristics of *m*- and *p*-Divinylbenzene****INTRODUCTION**

The mass spectra of aromatic compounds have been studied in considerable detail,<sup>1,2</sup> but there is apparently no recorded analysis of the spectra for the pure isomeric *m*- and *p*-divinylbenzenes. Availability of carefully purified samples of these isomers and the need for the data in analysis of crosslinked polymers currently under investigation<sup>3</sup> has prompted the present study and report.

**EXPERIMENTAL**

The samples of *m*- and *p*-divinylbenzenes used for these studies were prepared by techniques previously described in detail.<sup>4-7</sup> In brief, the *meta* isomer is separated from 95% *m*-divinylbenzene supplied by the Shell Chemical Company by two consecutive preparative-scale GLC separations by using an F and M Prepmaster and Perkin-Elmer preparative column, Model 154 D, with Ucon Chromosorb W column packing. The *para* isomer is prepared by decarboxylation of phenylenediaacrylic acid and purified by GLC with a Perkin-Elmer preparative 154 D column with a Bentone packing. Both were stored under nitrogen with stabilizer at low temperature until just before use when they were distilled from potassium hydroxide. Analytical gas chromatographic analysis showed the samples to be free of all other materials and isomerically pure within the limits of accuracy of the analysis which can detect 0.01% of either isomer in the presence of the other.

The spectra were recorded by using standard procedures on a Varian M-66 mass spectrometer. The operating conditions were as follows: electron energy 70 eV (except for a series at 40 eV), electron current 30  $\mu$ A, analyzer temperature 120°C, and ionization chamber temperature 230°C, pressures of  $5-13 \times 10^{-7}$  torr. The background was examined routinely to establish absence of contamination. Care was taken to establish equilibrium conditions of temperature and pressure before recording the spectra shown in the figures and for the tabulated data. The figures were selected from many to show the characteristic spectrum. Data in the tables are averages of many redeterminations under carefully controlled conditions with reproducibility of the order of  $\pm 5\%$ . Control runs with styrene give values in accord, but not precise agreement, with those previously recorded.<sup>8</sup>

TABLE I  
Relative Peak Intensities

<i>m/e</i>	Peak intensity <sup>a</sup>	
	<i>p</i> -DVB	<i>m</i> -DVB
131	11.0	10.7
130	100.0	100.0
129	24.9	29.0
128	29.0	34.2
127	12.3	14.3
115	16.6	21.3
77	9.2	9.5
63	7.1	8.3
51	13.0	16.5
39	7.2	7.4

<sup>a</sup> The values are averages of values read from three spectra comparable to those in Figure 1 showing the entire scale at one gain setting. The deviation is  $\pm 0.1$  percentage points for the 127-131 *m/e* values and  $\pm 0.3$  percentage points for the 39-115 values for the *para* isomer and  $\pm 0.5$  for the *meta* isomer values.

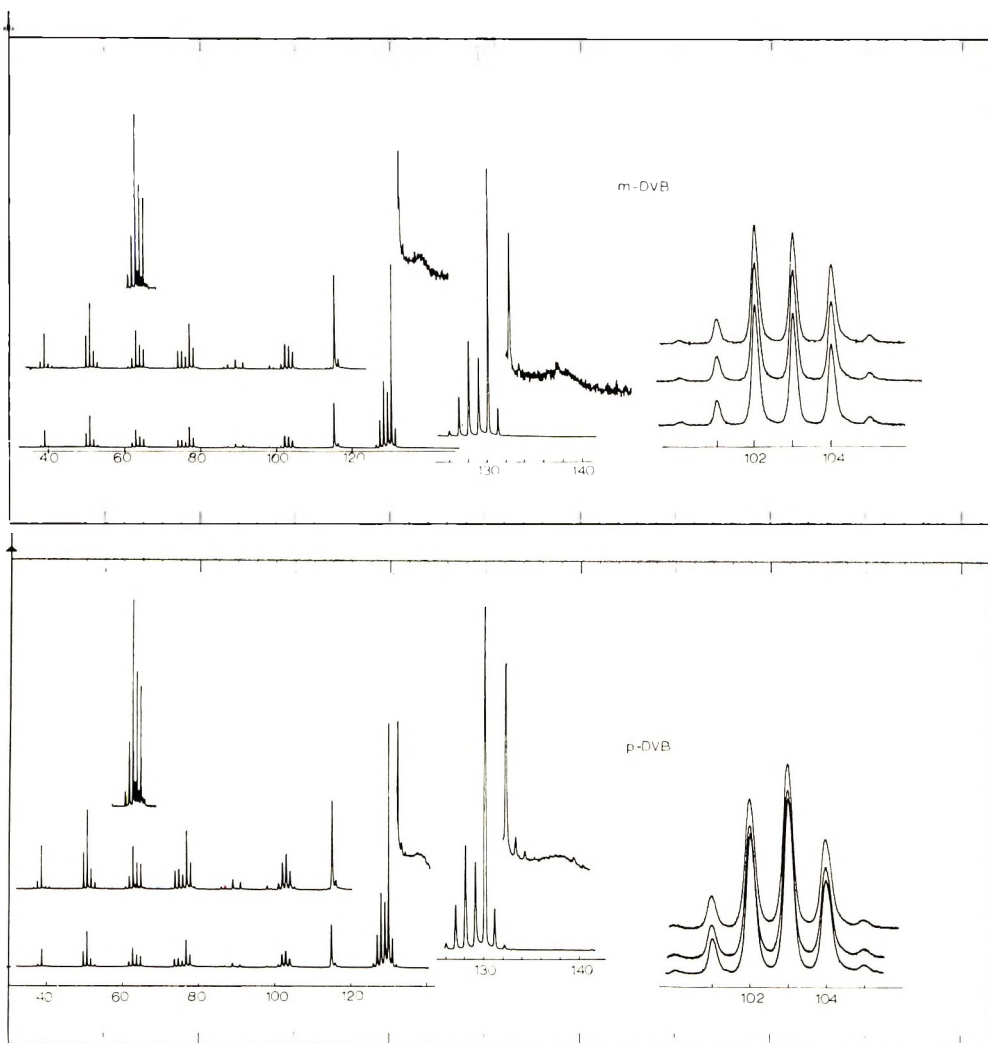


Fig. 1. Actual 70 eV Mass spectra of *m*- and *p*-divinylbenzene.

### RESULTS

The mass spectra for the isomeric *m*- and *p*-divinylbenzenes are given in Figure 1. Traces showing the complete spectra for the range from  $m/e$  20 to 140 are given and are used for the measurement of the relative intensities of the principal peaks as given in Table I. Traces at higher gain are given for the  $m/e$  ranges of 30–120 and used for measurement of the relative intensities of the low  $m/e$  peak values given in Table II. The diffuse peak at 135–140 associated with the metastable transition is shown at higher gain.

The relatively intense peaks, at 131–127, 115, 77, 63, 51, and 39, are present in the spectra of both isomers and show no major distinction in relative intensity. The molecular ion peak for the *meta* isomer is somewhat less intense than that for the *para* isomer. The 77, 63, 51 and 39 peaks and the fractional  $m/e$  peaks at 57.5, 61.5, 62.5, and 63.5, are characteristic for aromatic compounds.<sup>1,2</sup> The  $M + 1$  peak at  $m/e$  131 is

TABLE II  
Relative Peak Intensities

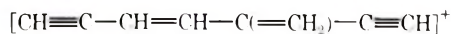
<i>m/e</i>	Peak intensity <sup>a</sup>	
	<i>p</i> -DVB	<i>m</i> -DVB
116	11.2	12.0
115	100	100.0
104	19.4	14.8
103	30.5	20.4
102	25.7	21.3
101	6.0	4.7
91	7.8	6.8
89	9.8	8.4
78	25.5	21.0
77	51.4	42.8
76	13.9	11.8
75	18.5	15.9
74	17.4	15.7
65	23.5	19.3
64	26.9	28.9
63	37.7	35.1
62	13.2	10.2
53	6.0	5.1
52	17.1	15.9
51	66.2	64.0
50	30.8	29.5
39	39.9	32.7
38	8.0	6.1

<sup>a</sup> The values are averages of values read from spectra for two different samples comparable to those in Figure 1 at the higher gain. The deviations vary from  $\pm 0.1$  to 2.0 percentage points.

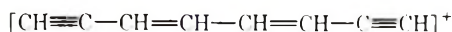
about 11% of that of the molecular ion peak at 130 *m/e* as is appropriate for the <sup>13</sup>C content of a ten-carbon compound.

## DISCUSSION

The most obvious distinction between the isomers appears at *m/e* 102 (C<sub>8</sub>H<sub>6</sub>). The 102 *m/e* peak for the *para* isomer is consistently more intense than that for the *meta* isomer. Data from fourteen spectra on five samples show relative intensities for the *meta* isomer of 101 (*m/e* 102), 100 (*m/e* 103), 71.5 (*m/e* 104) and for the *para* isomer of 81.6 (*m/e* 102), 100 (*m/e* 103), and 54 (104). The most obvious basis for the enhanced intensity for the 102 *m/e* fragment from the *meta* isomer is that of an enhanced stability of a branched, acyclic structure, such as I<sub>m</sub>, formed by the loss of H<sub>2</sub> and C<sub>2</sub>H<sub>2</sub>. The



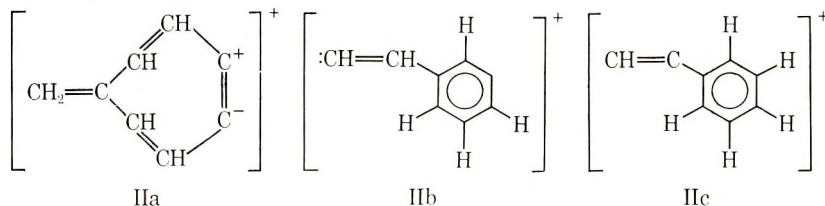
I<sub>m</sub>



I<sub>p</sub>

evidence for the acyclic character of fragments from aromatic compounds has been discussed previously<sup>2</sup> and is reasonably well established. Any cyclic structure (for example II) thus far suggested for consideration seems equally well derivable from either of the

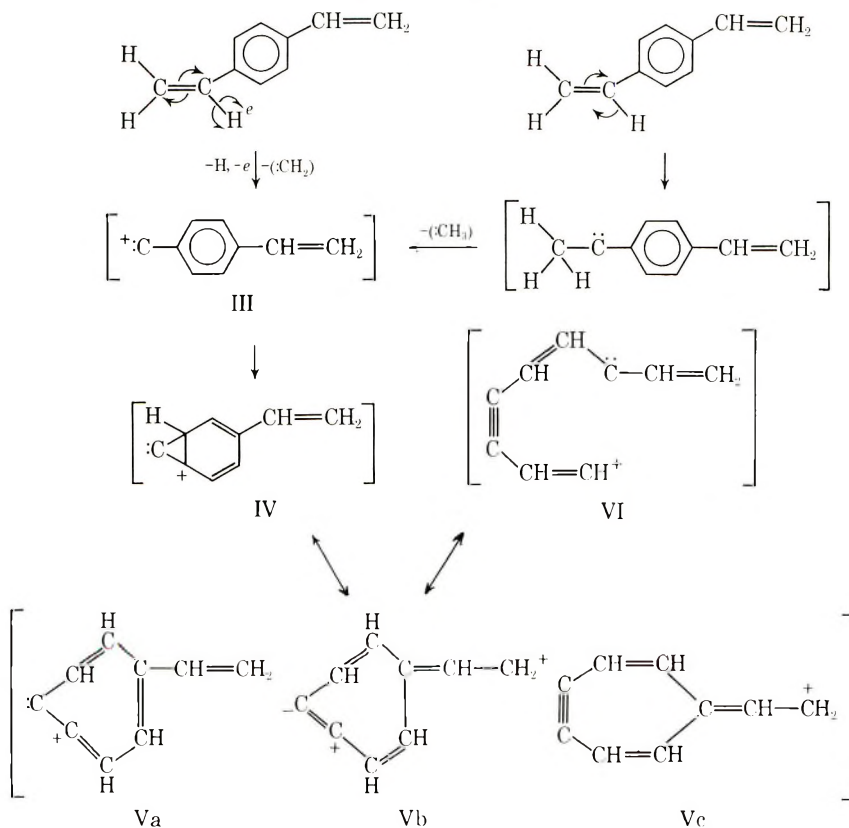
two divinyl isomers and thus offers no basis for enhancement of the 102  $m/e$  fragment from the *meta* isomer.



This can be considered further confirmation for the acyclic character of fragments from aromatic compounds.

There are evidences of metastable transitions in the spectra of both isomers.\* The peaks at 115, 104, 90, and 78 show trailing high mass edges characteristic of daughter peaks. Those at 115, 104(102), 90, and 78 seem to be associated with the usual diffuse peaks at 13  $m/e$  units higher and 26  $m/e$  units lower and are, therefore, presumably associated with the loss of  $C_2H_2$  units characteristic of aromatic degradations.

The metastable transition from 130 to 115 requires special comment. The diffuse peak at 137.5 shown in detail in Figure 1 corresponds with loss of 15  $m/e$  units in the transition from the molecular ion,  $m/e$  130, to the 115  $m/e$  ( $C_9H_7$ ) fragment. Loss of 15  $m/e$  is not common and does not appear in the styrene spectrum at all prominently.



\* Metastable transitions as observed in the cyclodial path mass spectrometer have been discussed by Benz and Brown.<sup>9</sup>

Since loss of  $\text{CH}_2$  is thought to be an unlikely transformation,<sup>2</sup> it is possible that the loss of 15  $m/e$  is a two-step process involving migration of an hydrogen followed by loss of a methyl, one step of which is rate-determining in the metastable transition.<sup>10</sup> In either process, the carbenelike cation intermediate (III), which is isomerically distinguishable as derived from each isomer is, however, stabilizable as a norcaradiene (IV), tropylium (V), or acyclic structure (VI), equally derivable from either the *meta* or *para* isomer. Such valence bond isomerizations are known in other systems. Stabilization via the tropylium ion is not possible in the styrene system and may account for the absence of the  $-15 m/e$  transformation therein.

### SUMMARY

The mass spectra of carefully purified samples of *m*- and *p*-divinylbenzene show the characteristic degradation patterns of aromatic compounds with major fragments of  $m/e$  39, 51, 63, 77, and 91. Doubly charged fragments are observed at  $m/e$  of 57.5, 63.5, and 64.5. The molecular ion peak at  $m/e$  130, an intense peak at  $m/e$  115, and a set of peaks at 102–103–104, are observed for both isomers. The 115  $m/e$  fragment is postulated to be formed by rearrangement of H and loss of  $\text{CH}_3$  and is confirmed by presence of an appropriate metastable. There is a difference in the spectra of the two isomers in the relative intensity of the 102–103–104  $m/e$  peaks. The intensity of the 102 peak is relatively greater for the *meta* isomer, and this is attributed to enhanced stabilization of the branched chain acyclic  $\text{C}_8\text{H}_6$  fragment. At lower impact voltages (40 eV/70 eV) less fragmentation is observed with no additional significant difference between the isomers.

This research was supported in part under Contract AT (30-1)-3644 between the U. S. Atomic Energy Commission and Hunter College of the City University of New York. The author is indebted to Mr. K. S. Kim for assistance in the preparation of the divinylbenzene samples.

### References

1. H. M. Grubb and S. Meyerson in *Mass Spectroscopy of Organic Ions*, F. W. McLafferty, Ed., Academic Press, New York, 1963, pp. 516–19.
2. H. Budzikiewicz, C. Djerassi, and D. H. Williams, *Mass Spectroscopy of Organic Compounds*, Holden-Day, San Francisco, 1967, pp. 72–93.
3. Richard H. Wiley and Luther H. Smithson, Jr., *J. Macromol. Sci., Chem.* **A2**, 589 (1968).
4. R. H. Wiley, G. DeVenuto, and T. K. Venkatachalam, *J. Gas Chromatog.*, **5**, 590 (1967).
5. R. H. Wiley and R. M. Dyer, *J. Polym. Sci. A*, **2**, 3153 (1964).
6. R. H. Wiley and P. H. Hobson, *J. Amer. Chem. Soc.*, **71**, 2429 (1941).
7. R. H. Wiley and E. E. Sale, *J. Polym. Sci.*, **42**, 491 (1960).
8. E. I. Quinn and F. L. Mohler, *J. Res. Nat. Bur. Stand.*, **62**, 39 (1959); see also Cat. Mass Spectral Data, No. 359.
9. H. Benz and H. Brown, *J. Chem. Phys.*, **48**, 4308 (1968).
10. M. M. Bursey and F. W. McLafferty, *J. Amer. Chem. Soc.*, **88**, 529, 4484 (1966); *ibid.*, **89**, 1 (1967).

RICHARD H. WILEY

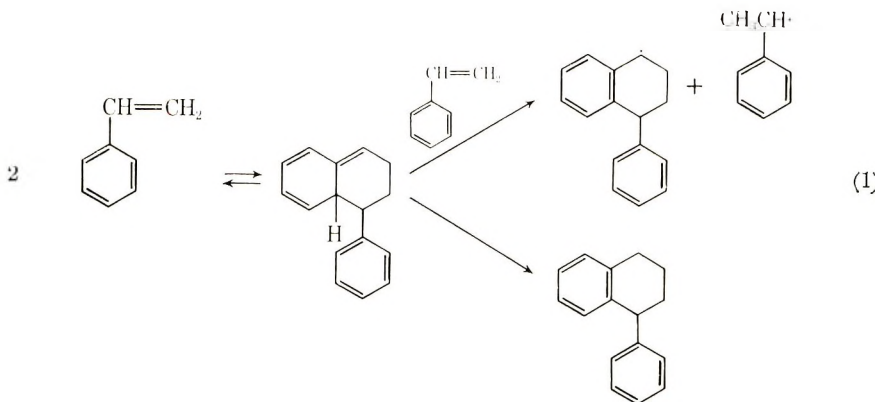
Department of Chemistry  
Hunter College  
City University of New York  
New York, New York 10021

Received August 14, 1969

Revised September 23, 1969

### Polymerization of Acrylonitrile Initiated by Hydrogen Abstraction

Recently it was shown that the thermal polymerization of styrene<sup>1,2</sup> and other vinyl-aromatic compounds<sup>3-5</sup> was initiated by hydrogen abstraction from labile Diels-Alder dimers of the monomer by a third monomer molecule as is shown, for example, by the case of styrene [eq. (1)].



Therefore, hydrocarbons with readily abstracted hydrogens would conceivably serve as initiators of the radical polymerization of vinyl monomers. In order to test this hypothesis, we carried out polymerizations of acrylonitrile in the presence of hydrocarbons which possess labile hydrogens. Triphenylmethane and fluorene were selected for this purpose, since they were known to show particularly high reactivities in chain transfer to the polystyryl radical<sup>6</sup> and in the abstraction reaction by the trichloromethyl radical.<sup>7</sup> Acrylonitrile was selected as monomer, because it does not polymerize thermally.<sup>8</sup>

The polymerization procedures were the same (vacuum system,  $10^{-4}$  mm Hg) as in the thermal polymerization of 2-vinylfuran<sup>4</sup> and 2-vinylthiophene,<sup>9</sup> except that given amounts of triphenylmethane or fluorene were added to the polymerization ampoules. These compounds were purified by repeated recrystallizations. Acrylonitrile was carefully purified by the usual method and prepolymerized thermally at  $150^{\circ}\text{C}$  for several hours in order to remove impurities which might interfere with the polymerization.

TABLE I  
Polymerization of Acrylonitrile with Triphenylmethane Initiator in Benzene

Run no.	$(\text{C}_6\text{H}_5)_3\text{CH}$ , mole/l.	Acrylonitrile, mole/l. <sup>a</sup>	Temperature, $^{\circ}\text{C}$	Time, hr:min	Conversion, %	$\bar{M}_n^b$
1	0.20	16 <sup>c</sup>	100	72:00	trace	
2	$2.43 \times 10^{-2}$	8.13	133	21:42	3.54	$21 \times 10^3$
3	$2.43 \times 10^{-2}$	7.95	141	20:14	3.59	
4	$7.96 \times 10^{-3}$	7.88	150	5:00	1.25	
5	$7.96 \times 10^{-3}$	7.88	150	32:50	5.22	$8.5 \times 10^3$
6	$2.40 \times 10^{-2}$	7.88	150	6:20	2.38	
7	$3.45 \times 10^{-2}$	7.88	150	8:25	3.71	$21 \times 10^3$

<sup>a</sup> The densities were calculated from the equations  $d_4^t = 0.9004 - 0.00109t$  for benzene<sup>10</sup> and  $d_4^t = 0.8281 - 0.001106t$  for acrylonitrile.<sup>11</sup>

<sup>b</sup> Calculated by using the relationship:<sup>9</sup>  $[\eta]_{\text{DMF}}^{30^{\circ}\text{C}} = 29.6 \times 10^{-5} M^{0.74}$

<sup>c</sup> Bulk polymerization.



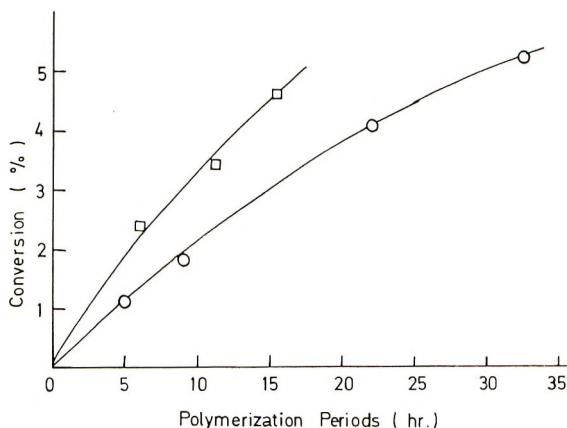


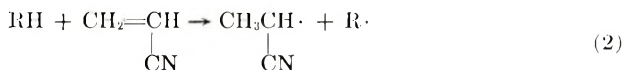
Fig. 1. Time-conversion curve at 150°C at various triphenylmethane concentrations. (○)  $7.96 \times 10^{-3}$  mole/l.; (◻)  $2.40 \times 10^{-2}$  mole/l. Monomer concentration: 7.88 mole/l.; solvent: benzene.

Given amounts of the remaining monomer were transferred to polymerization ampoules in the vacuum system. After given polymerization periods, the reaction mixture containing precipitates of polyacrylonitrile was poured into excess methanol, and the polymer (white powder) was recovered by centrifugation and dried *in vacuo*. Some of the polymerization results are given in Table I.

Although polymerization did not occur at 100°C, polymer was obtained at higher temperatures (130–150°C) in the presence of  $10^{-2}$  mole/l. of triphenylmethane. On the other hand, only a trace amount of precipitate was formed under analogous condition without triphenylmethane. Thus, it is clear that triphenylmethane initiated polymerization of acrylonitrile at 130–150°C. Similarly, the conversion was about 5% when bulk acrylonitrile was heated for 5 hr at 160°C in the presence of 0.19 mole/l. of fluorene. At a lower temperature (100°C, 72 hr), polymer was not formed, even in the presence of fluorene. Figure 1 shows the time-conversion curve at 150°C in the presence of triphenylmethane. The conversion increased with the polymerization period, and the induction period was not observed.

Polyacrylonitrile thus obtained was a white powder. The infrared spectra (KBr disk) of the polymers were similar to that of common polyacrylonitrile, including small peaks at about  $1650\text{ cm}^{-1}$ . The molecular weight ranged from 8,500 to 21,000 for the samples measured and seemed to decrease with increasing conversion.

The polymerization data described above suggest that the initiation process is a hydrogen abstraction by acrylonitrile monomer from triphenylmethane or fluorene as in eq. (2).



This process is an example of the molecule-induced homolysis in which the relative stability of the radicals produced is the driving force of the reaction.<sup>12</sup>

Although detailed discussions on the termination step are not warranted at the present time, involvement of the triphenylmethyl radical in the termination process may be inferred from the available data. Declines in the rate of polymerization were observed at conversions as low as 3–5% (Fig. 1). This decline cannot be attributed to the small concentration changes of monomer or triphenylmethane. If it is assumed that the cyanoethyl radical alone is responsible for the initiation, the relatively stable triphenyl-

methyl radical will build up in the solution and have an increasing chain-shortening effect as the reaction progresses.\*

In conclusion, some hydrocarbons which would yield stable free radicals by hydrogen abstraction were shown to initiate polymerization of acrylonitrile. This result is in accord with the mechanism proposed for the thermal polymerization of several vinyl-aromatic monomers.

The authors are grateful to Miss Reiko Ando for her capable technical assistance.

#### References

1. F. R. Mayo, *J. Amer. Chem. Soc.*, **90**, 1289 (1968).
2. K. Kirchner, *Makromol. Chem.*, **96**, 179 (1966).
3. C. Aso, T. Kunitake, and Y. Tanaka, *Bull. Chem. Soc. Japan*, **38**, 675 (1965).
4. C. Aso, T. Kunitake, Y. Tanaka, and H. Miyazaki, *Kobunshi Kagaku*, **24**, 187 (1967).
5. C. Aso, T. Kunitake, M. Shinsenji, and H. Miyazaki, *J. Polym. Sci., A-1*, **7**, 1497 (1969).
6. R. A. Gregg and F. R. Mayo, *Discussions Faraday Soc.*, **2**, 328 (1947).
7. M. Szwarc, *Chem. Ind. (London)*, **1957**, 985.
8. W. Kern and H. Fernow, *J. Prakt. Chem.*, **160**, 281 (1942).
9. J. Brandrup and E. H. Immergut Ed., *Polymer Handbook*, Interscience, New York, 1965, IV-23.
10. *Beilsteins Handbuch der Organischen Chemie*, Springer, Berlin, 1943, Vol. **E115**, p. 123.
11. K. Mizutani, Ed., *Preparations of Monomers*, Kyoritsu, Tokyo, 1957, p. 162.
12. W. A. Pryor, *Free Radicals*, McGraw-Hill, New York, 1965, p. 119.

CHUJI ASO  
TOYOKI KUNITAKE  
MASATAKE SHINSEIJI

Department of Organic Synthesis  
Faculty of Engineering  
Kyushu University  
Fukuoka, Japan

Received August 14, 1969

Revised September 24, 1969

\* The authors are very grateful to the referee for pointing out this possibility.

*Contents (continued)*

SHUZO AOKI, AKIRA AKIMOTO, CHIAKI SHIRAFUJI, and TAKAYUKI OTSU: Metal-Containing Initiator Systems. XXIII. Effect of Solvents on Radical Polymerization of Methyl Methacrylate Initiated by Metal-Alkyl Halide Systems . . .	785
TAKAYUKI OTSU, MUNAN KO, and TSUNEYUKI SATO: Polymerizations of <i>N</i> -Vinylcarbazole and 4-Vinylpyridine with Various Organic Halides . . . . .	789
RICHARD H. WILEY: Mass Spectral Characteristics of <i>m</i> - and <i>p</i> -Divinylbenzene	792
CHUJI ASO, TOYOKI KUNITAKE, and MASATAKE SHINSEnji: Polymerization of Acrylonitrile Initiated by Hydrogen Abstraction . . . . .	797

The *Journal of Polymer Science* publishes results of fundamental research in all areas of high polymer chemistry and physics. The *Journal* is selective in accepting contributions on the basis of merit and originality. It is not intended as a repository for unevaluated data. Preference is given to contributions that offer new or more comprehensive concepts, interpretations, experimental approaches, and results. Part A-1 *Polymer Chemistry* is devoted to studies in general polymer chemistry and physical organic chemistry. Contributions in physics and physical chemistry appear in Part A-2 *Polymer Physics*. Contributions may be submitted as full-length papers or as "Notes." Notes are ordinarily to be considered as complete publications of limited scope.

Three copies of every manuscript are required. They may be submitted directly to the editor: For Part A-1, to C. G. Overberger, Department of Chemistry, University of Michigan, Ann Arbor, Michigan 48104; and for Part A-2, to T. G. Fox, Mellon Institute, Pittsburgh, Pennsylvania 15213. Three copies of a short but comprehensive synopsis are required with every paper; no synopsis is needed for notes. Books for review may also be sent to the appropriate editor. Alternatively, manuscripts may be submitted through the Editorial Office, c/o H. Mark, Polytechnic Institute of Brooklyn, 333 Jay Street, Brooklyn, New York 11201. All other correspondence is to be addressed to Periodicals Division, Interscience Publishers, a Division of John Wiley & Sons, Inc., 605 Third Avenue, New York, New York 10016.

Detailed instructions in preparation of manuscripts are given frequently in Parts A-1 and A-2 and may also be obtained from the publisher.